Targeting *Chlamydia trachomatis* by eliciting CD4^{+} T cell and antibody responses through recombinant MVA expressing CTH522

Inaugural Dissertation

For the attainment of the title of doctor

in the Faculty of Mathematics and Natural Sciences

at the Heinrich Heine University in Düsseldorf

presented by

Sara Moreno Mascaraque

from Ciudad Real, Spain

Düsseldorf, January 2025

from the Institute of Virology

at the Heinrich Heine University Düsseldorf

Published by permission of the
Faculty of Mathematics and Natural Sciences at

Heinrich Heine University Düsseldorf

Supervisor: Prof. Dr. Ingo Drexler

Co-supervisor: Prof. Dr. Rainer Kalscheuer

Date of the oral examination: 23.06.2025

El destino es como un río caudaloso, nos lleva donde él quiere sin preguntar.
Destiny is like a mighty river, it takes us where it wants us to go without asking.
— Rosalía de Castro

Summary

Chlamydia trachomatis is an obligate intracellular pathogen and the major species that infects humans among the Chlamydiaeceae family. While its fourteen serovars are categorized in three biovars according to its symptoms (trachoma, genital or *lymphogranuloma venereum*), the genital biovar is the most prevalent sexually transmitted bacterial infection. C. *trachomatis* has become a burden in health worldwide, with circa 100 to 150 million new cases taking place each year globally despite the existence of a current treatment consisting of antibiotics. Many reasons have been given to explain its prevalence and the raising infection rates, including the risks of reinfection and the fact that the infection mainly presents itself as asymptomatic, making it very difficult to diagnose in the early stages and, therefore, increasing the risk of infecting others and spreading the infection. This has led the field to shift towards the search of a preventive strategy. However, even though there has been extensive research done around chlamydia and possible immunization approaches, the path for a *C. trachomatis* vaccine is still unclear, and the mechanisms necessary for a vaccine to confer protective immunity are still unknown.

CTH522 is a recombinant version of Major Outer Membrane Protein (MOMP) designed to contain four heterologous immunorepeats from the most prevalent genital serovars worldwide (D, E, F and G). Previous research on animal models proved it to be protective, and it has also shown promising results in a phase 1, first-in-human trial, where it was found to be well tolerated and immunogenic through high titers of neutralizing serum antibodies and cell-mediated immune responses. This project will be based on the use of CTH522 as an antigen in order to generate a safe and efficient vaccine against C. *trachomatis*.

The overall aim of the project is the generation of novel recombinant MVA (Modified Vaccinia Virus Ankara) expressing a variant of the *C. trachomatis* antigen CTH522. The vaccine antigen CTH522 was modified by fusing it to the transmembrane domain and cytoplasmic domain of the B7 molecule, which has been previously used to tether chimeric proteins to the surface of mammalian cells. In enhancing the surface display of CTH522 in the plasma membrane, it is theorized that an optimal cell mediated immune response will be triggered through antigen recognition by B cells.

The purpose of this recombinant MVA (named MVA-CTH522:B7) was for it to be further studied by usage in comparative *in vivo* immunization studies such as homologous

or heterologous prime/boost regimens including other vectors. Such studies necessitated to focus on both antibody and $CD4^+$ T cell antibody responses, as they have been shown to be essential for chlamydial clearance in multiple animal models. Results show that MVA-CTH522:B7 did not behave differently than the MVA-WT in terms of replication and that the chimeric protein was successfully located to the surface of mammalian cells. Furthermore, this recombinant MVA established itself as a highly promising and favorable vaccine candidate against *C. trachomatis*, as it was capable of inducing a $CD4^+$ T cell response and a very robust humoral response with a high percentage of neutralizing activity. Overall, these results encourage further research of MVA-CTH522:B7 as a vaccine against C. *trachomatis*, perhaps even able to provide bacterial clearance upon a chlamydia challenge in mice. This contributes to the current search for a *C. trachomatis* vaccine with a first-time study using MVA-CTH522:B7 and the immune response induced in a mouse model.

Zusammenfassung:

Chlamydia trachomatis ist ein obligater intrazellulärer Erreger und die wichtigste Spezies aus der Familie der Chlamydiaeceae, die Menschen infiziert. Die vierzehn Serovare des Erregers werden nach ihren Symptomen (Trachom, genitales oder *lymphogranuloma venereum*) in drei Biovare eingeteilt, wobei die genitalen Biovare die häufigsten sexuell übertragbaren bakteriellen Infektionen darstellen. *C. trachomatis* ist weltweit zu einer Belastung für die Gesundheit geworden, mit etwa 100 bis 150 Millionen neuen Fällen pro Jahr weltweit, obwohl es derzeit eine Behandlung mit Antibiotika gibt. Für die Prävalenz und den steigenden Infektionsraten werden viele Gründe angeführt, darunter das Risiko einer Reinfektion und die Tatsache, dass die Infektion meist asymptomatisch verläuft, was eine Diagnose im Frühstadium sehr schwierig macht und somit das Risiko einer Ansteckung und Verbreitung der Infektion erhöht. Dies hat dazu geführt, dass sich die Forschung auf die Suche nach einer Präventionsstrategie verlagert hat. Trotz umfangreicher Forschungsarbeiten zu Chlamydien und möglichen Immunisierungsansätzen ist der Weg für einen Impfstoff gegen *C. trachomatis* noch unbestimmt, und die Mechanismen, die ein Impfstoff benötigt, um eine schützende Immunität zu verleihen, sind noch unbekannt.

CTH522 ist eine rekombinante Version des Major Outer Membrane Protein (MOMP), das vier heterologe Immunrepeats der weltweit am häufigsten vorkommenden genitalen Serovare (D, E, F und G) enthält. Frühere Impfstoffforschungen in Tiermodellen haben gezeigt, dass es als Protein schützend wirkt, und es hat auch vielversprechende Ergebnisse in einer Phase-1-Studie beim Menschen gezeigt, wo es sich als gut verträglich und immunogen erwiesen hat, da es hohe Titer neutralisierender Serumantikörper und zellvermittelter Immunreaktionen aufwies. Dieses Projekt basiert auf der Verwendung von CTH522 als Antigen, um einen sicheren und effizienten viralen Vektor-basierten Impfstoff gegen *C. trachomatis* zu entwickeln.

Das übergeordnete Ziel des Projekts ist die Herstellung eines neuartigen rekombinanten MVA (Modified Vaccinia virus Ankara), der eine Variante des *C. trachomatis* Antigens CTH522 exprimiert. Das Impfstoff-Antigen CTH522 wurde modifiziert, indem es mit der Transmembrandomäne und der zytoplasmatischen Domäne des B7-Moleküls fusioniert wurde, welches bereits früher zur Bindung chimärer Proteine an die Oberfläche von Säugetierzellen verwendet wurde. Es wird erwartet, dass eine optimale zellvermittelte Immunantwort durch Antigenerkennung durch B-Zellen

ausgelöst wird, indem die Oberflächenpräsentation von CTH522 auf der Plasmamembran verbessert wird.

Dieser rekombinante MVA (MVA-CTH522:B7) soll in vergleichenden *in-vivo* Immunisierungsstudien, wie z. B. unter Anwendung von homologen oder heterologen Prime/Boost-Schemata unter Einbeziehung anderer Vektoren, weiter untersucht werden. Solche Studien müssen sich sowohl auf die Antikörper- als auch auf die $CD4^+$ T-Zell-Antworten konzentrieren, da sich diese in mehreren Tiermodellen als wesentlich für die Chlamydien-Clearance erwiesen haben. Die Ergebnisse zeigen, dass sich MVA-CTH522:B7 in Bezug auf die Replikation nicht anders verhielt als MVA-WT und dass das chimäre Protein erfolgreich auf der Oberfläche von Säugetierzellen transportiert wurde. Darüber hinaus erwies sich dieser rekombinante MVA Vektor als vielversprechender und günstiger Impfstoffkandidat gegen *C. trachomatis*, da er in der Lage war, eine $CD4^+$ T-Zell-Antwort und eine sehr robuste humorale Antwort mit einem hohen Prozentsatz an neutralisierender Aktivität zu induzieren. Insgesamt ermutigen diese Ergebnisse zur weiteren Erforschung von MVA-CTH522:B7 als Impfstoff gegen *C. trachomatis*, der vielleicht sogar in der Lage ist, die Chlamydien nach einer Belastung von Mäusen mit diesen Erregern zu beseitigen.

ABBREVIATIONS:

(NH4)2SO4: Ammonium Sulfate

AH: Aluminum Hydroxide

APC: antigen presenting cell

APS: Alkaline phosphatase buffer

BAC: Bacterial Artificial Chromosome

BFA: Brefeldin A

BMDCs: Bone Marrow-Derived Dendritic Cells

bp: basepair

BSA: Bovine serum albumin

C. trachomatis: Chlamydia trachomatis

CAM: chloramphenicol

CDC: Center for Disease Control and Prevention

CEB: Crude Extraction Buffer

CM cells: cloudman cells

CMV: citomegalovirus

col.: colonic

COPII: coatomer complex II

CPAF: Chlamydia Protease-like Activity Factor

CPE: cytophatic effect

CPXV: cow poxvirus

CVA: Chorioallantois vaccinia virus Ankara

DAPI: 4′,6-diamidino-2-phenylindole

DC: Dendritic Cells

Del: deletion

DNV: Dengue Virus

DMEM: Dulbecco's Modified Eagle Medium

DMSO: dimethyl sulfoxide

DTT: Diiodotyrosine

dVI: deletion VI

EB: Elementary Bodies

ECL: enhanced chemiluminescence

EDTA: Ethylenediaminetetraacetic acid

eGFP: enhanced green fluorescent protein

ELISA: enzyme-linked immunosorbent assay

EMA: Ethidium Monazide Bromide

ER: Endoplasmic Reticulum

FACS: Fluorescence-activated cell sorting

fwd: forward

GFP: Green Fluorescent Protein

GPI: Glycosylphosphatidylinositol

HaK cells: Hamster Kidney cells

HCV: Hepatitis C Virus

HeLa cells: Henrietta Lacks cells

HIV: Human Immunodeficiency Virus

i.d.: intradermally.

i.m.: intramuscular

i.n.: intranasal

i.p. intraperitoneally

i.u.: intrauterine

i.vag.: intravaginally

IFN: interferon

IRF: Interferon Regulatory Factor

KCl: Potassium azide

KH3PO4: Monopotassium phosphate

LGV: *lymphogranuloma venereum*

mAb: monoclonal antibodies

MCS: Multiple Cloning Site

MFI: Mean Fluorescence Intensity

MgCl2: Magnesium dichloride

MHC: Major Histocompability complex

mLi: mouse invariant chain

MOI: multiplicity of infection

MOMP: Major Outer Membrane Protein

MSM: Men who have Sex with Men

MVA: Modified Vaccinia virus Ankara

NaCl: Sodium Chloride

NaN3: Sodium azide

NHI: National Institute of Health

NHP: Nonhuman Primate

NP: Nucleocapsid protein

PAGE: polyacrylamide gel electrophoresi

PBS: Phosphate Buffered Saline

PCR: Polymerase Chain Reaction

PFA: Paraformaldehyde

PID: Pelvic Inflammatory Disease

PMPs: Polymorphic Membrane Proteins

recMVA: recombinant MVA

rev: reverse

RFV: Rabbit Fibroma Virus

RPMI: Roswell Park Memorial Institute

s.c.: subcutaneous

SAFE: Surgery for trichiasis, Antibiotics, Facial cleanliness and Environmental improvement

SDS: sodium dodecyl sulfate

SFV: Semliki Forest Virus

SLA: second-generation lipid adjuvant

SPG: Sucrose-Phosphate-Glutamate

STI: sexually transmitted infections

TBE: Tris-Borate-EDTA

TBS-T: tris-buffered saline-Tween

TEMED: Tetramethylethylenediamine

TRIC: Trachoma/Inclusion Conjunctivitis

TTFC: Toxin Tetanus Fragment C

VACV: Vaccinia Virus

VDIV: variable sequence domain IV

WGA: wheat germ agglutinin

WHO: World Health Organization

wt: wild-type

1. INTRODUCTION

1.1. Chlamydia

Chlamydia is a pathogen that has historically persisted for thousands of years. It is thought that trachoma as a disease first developed in China and Mesopotamia around 2.700 B.C. before reaching the Mediterranean area through the Middle East (De La Maza et al., 2017). However, the first description of an actual pathogen as related to Chlamydia itself would not surface until many centuries later when, in 1907, two associates of the German physician Albert Neisser first saw intracytoplasmic inclusions in conjunctival scrapings of orangutans infected with material from patients suffering with trachoma (De La Maza et al., 2017; Kane et al., 1984). Despite its initial mislabeling as a protozoa and a virus, they were able to identify the presence of an infectious agent and labelled it Chlamydia after the Greek word chlamys (χλαμύς), a type of cloak (Taylor-Robinson, 2017) that resembled the draping of the intracytoplasmic inclusions they observed around the nucleus, describing it as a "mantled animal" (Kane et al., 1984).

It is irrefutable that the research landscape framing chlamydia has improved radically and wildly in the last decades. Nowadays, modern technological developments in genetics and proteomics have the potential to untangle the molecular mechanisms and pathways that lie beneath the interactions between these pathogens and their hosts. This allows us to bridge the gap between the currently established concepts and the prospective future findings that will be discovered down the chlamydia road, opening up many different possibilities of research for its future clinical approaches.

1.1.1. Chlamydia as a pathogen

Chlamydia are a highly diverse phylum of gram-negative obligate intracellular pathogens that include symbionts affecting unicellular eukaryotes, parasites of invertebrate organisms and bacteria affecting humans and animals (Sixt & Valdivia, 2016; Wan et al., 2023). These pathogens replicate in a specialized membrane compartment called reticulate bodies and are able to survive in the host's intracellular environment by using a wide range of secreted effectors. The most studied group in the *Chlamydiota* phylum is the *Chlamydiaceae* family, which contains a total of eleven species found to be pathogenic to vertebrates (Elwell et al., 2016). Despite the apparent diversity within this group of organisms, the species are highly similar to each other, as their disease pathology

and the site of infection has been found to remain analogous, with the major difference between the species being the diverse range of hosts that each species can selectively infect (Phillips et al., 2019). Within this family, the main species that are able to infect humans are *C. pneumoniae*, which predominately infects humans' upper and lower respiratory tracts leading to pneumonia or bronchitis and is associated to asthma exacerbation in children (Bayramova et al., 2018), atherosclerosis and neurological diseases (Sixt & Valdivia, 2016) such as Alzheimer's disease (Phillips et al., 2019); *C. psittaci*, which mainly infects animals but can also cause intense zoonotic infections in humans (Sixt & Valdivia, 2016) such as zoonotic avian chlamydiosis, a disease characterized by a wide range of symptoms that affect organs like the liver, heart and gastro-intestinal tract (Bayramova et al., 2018); and *C. trachomatis*, which has the largest impact on human health and can cause trachoma, the leading cause of preventable blindness in developing countries (Wan et al., 2023).

The strains of *C. trachomatis* can be categorized into three biovars that are additionally subtyped by serovars. Serovars A, B and C comprise the trachoma biovar; serovars D, E, F, G, H, J and K comprehend the genital biovar; and serovars L1, L2 and L3 form the *lymphogranuloma venereum* (LGV) biovar (Elwell et al., 2016) (**Figure 1**). The trachoma biovar causes primarily ocular infections that can eventually lead to trachoma, an infection of the inner area of the eyelids which is one of the major causes of preventable non-congenital blindness worldwide, especially in developing countries (Elwell et al., 2016; Sixt & Valdivia, 2016). The genital biovar includes the most prevalent

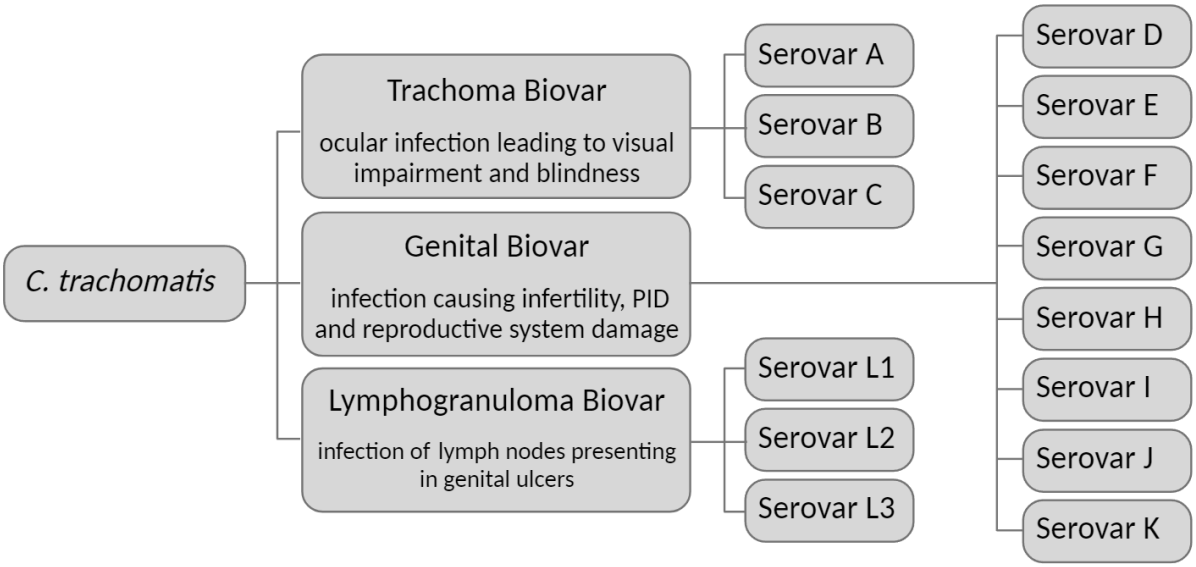

Figure 1. Schematic of *C. trachomatis* classification. The *C. trachomatis* species is divided into three biovars which are then further subdivided into their corresponding serovars, names from A-K and L1-L3. Image designed with biorender.com software.

sexually transmitted bacterium (Elwell et al., 2016) which leads to infertility, ectopic pregnancy, pelvic inflammatory disease (PID) and miscarriages (Elwell et al., 2016; Bayramova et al., 2018). In men, the most severe complication of *C. trachomatis* is epididymitis, with infertility not having been reported; reactive arthritis has also been associated with Chlamydia infection (De La Maza et al., 2017). On the other hand, the LGV biovar is the less frequent form of a sexually transmitted infection (STI) (Panzetta et al., 2018); it spreads to regional lymph nodes through the lymphatic vessels (Bayramova et al., 2018) and causes invasive anorectal or urogenital infections (Elwell et al., 2016), presenting inguinal lymphadenopathy or proctitis (Panzetta et al., 2018). LGV has also been connected to cervical cancer, with its incidence in the last decade having risen in HIV infected men who have sex with men (MSM) through the fact that it has been proven that *C. trachomatis* infection eases the transmission of HIV (Elwell et al., 2016).

C. trachomatis infection is most commonly asymptomatic, with up to 70-90% of the infections not presenting any symptomatology and being long-lasting (Panzetta et al., 2018), which in turn causes a delay in treatment and leads to possible serious complications in the patient's future.

1.1.2. Epidemiology

Because *C. trachomatis* has been found to be asymptomatic in most of cases in women (De La Maza et al., 2017), there are scarce population-based prevalence estimates or wide-ranging epidemiology studies available. It has been widely established as the most common sexually transmitted bacterial infection to the point of becoming a burden in health around the globe. In fact, according to the World Health Organization (WHO), in 2020 there was an estimate of 128.5 million new chlamydia infections from people between 15 and 49 years of age worldwide (World Health Organization, 2023) and approximately 125 million people live in trachoma endemic areas at risk of trachoma blindness as of 2022, presenting as a public health problem in over 40 countries. *C. trachomatis* is specifically more common in adolescents between the ages of 15 and 19 and young adults between 20 and 25 years of age, with a prevalence of 1.804/100.000 and 2.485/100.000 respectively (Lane & Decker, 2016)Back in 1996, the WHO implemented the SAFE (Surgery for trichiasis, Antibiotics, Facial cleanliness and Environmental improvement) strategy and 3 years later launched the WHO Alliance in order to eliminate trachoma as a blinding disease worldwide by 2020. However, regardless of the efforts, *C. trachomatis* has become the world's leading cause of

preventable blindness, with a prevalence of 60-90% in endemic areas (World Health Organization, 2022).

The progressive growth in chlamydia infection rates reveals the raising prevalence and the progress in detection through the screening of asymptomatic individuals thanks to the increasingly sensitive molecular testing. As of 2021, the antibiotic coverage worldwide for trachoma was 44% (World Health Organization, 2022), a testament to the efforts of the WHO to fight the epidemic of *C. trachomatis* that plagues the globe. Nevertheless, it is undeniable that over the past twenty years, public health programs such as antibiotic treatment, infected individual's partner identification or screening for individuals at risk have had a limited success in controlling the increasing prevalence of *C. trachomatis* infections worldwide.

1.1.3. Prevention

While there is a definite success in reducing the infection rate, the large number of efforts and investments in the last decade in order to attempt to control genital and ocular chlamydial infections are unfortunately falling short of ideal in order to eliminate *C. trachomatis* as a public health problem. While the approaches to genital infections have focused on enhanced detection and treatment, the strategies to approach ocular infections have been focused on a better access to water, sanitation, hygiene and mass drug administration in communities that have been vastly affected by the pathogen (Woodhall et al., 2018). Precisely because there has been a continued lack of success in controlling the incidence of *C. trachomatis* infections, it has become vital to develop effective prevention strategies. The road towards the effective control of Chlamydia comes across its first standstill when it encounters the staggering percentage of asymptomatic patients, with the previously mentioned statistic of 70-90% of women not showing any apparent symptomatology (Panzetta et al., 2018). Due to this, periodic screening of high-risk populations has been decided as the best approach for prevention for decades now. The Centers for Disease Control and Prevention (CDC) has recommended for all sexually active women under 25 years of age and those that are exposed to a higher risk of infection to get tested regularly. Although they have stated that evidence has been insufficient to endorse routine screenings of active young men, they advise for men who are sexually active and for groups with a higher risk of infection such as men who have sex with men to be screened on a regular basis (Centers for Disease Control and Prevention, 2021). Screening programs have been shown to be effective in a number of studies, and they have been defined as the backbone of spread prevention in chlamydial infections, using

such tool to identify and treat those individuals who are asymptomatic (Lane & Decker, 2016).

However, finding factual and consistent estimates of incidence and prevalence is a challenge in itself, as most of the cases are asymptomatic and, therefore, most people do not follow the CDC guidelines of routine screening if they do have access to said testing. Because of this, most screenings are centered on case-based reporting, which incidentally leads to an underestimate of the true incidence of *C. trachomatis* in the population (Woodhall et al., 2018).

1.1.4. Treatment

In order to treat genital and urinary *C. trachomatis* infections, the recommended antibiotic treatment is azithromycin or doxycycline (Lane & Decker, 2016). Doxycycline has been used for non-specific genital infections and it was thought to have a better patient adherence (Kane et al., 1984) but it has been recently shown that azithromycin might be better tolerated and it can be directly observed in order to ensure compliance to treatment (Lane & Decker, 2016). At the same time, even though doxycycline was previously the treatment of choice for children and pregnant women (Kane et al., 1984), it was later decided to be avoided and replaced by a single dose of azithromycin. Furthermore, there was an ongoing debate regarding the efficacy of single-dose azithromycin to tend to rectal infections of *C. trachomatis*, as a few studies had informed of potential reduced efficacy (Lane & Decker, 2016). As a matter of fact, it has been recently been proven that a single dose of azithromycin is not the desired treatment for chlamydial infections as opposed to a week-long course of doxycycline, which was reported to have a higher microbiological cure rate in both men who have sex with men (Lau et al., 2021) and women (Peuchant et al., 2022). Other treatments include ofloxacin, levofloxacin, erythromycin or fluoroquinolone, but these last ones have proven to cause gastrointestinal secondary effects, as well as being less cost effective when compared to the others (Lane & Decker, 2016).

While therapeutic treatment such as antibiotics has proved to be effective in clearing chlamydial infections, continuous clinical treatment failures have led researchers to investigate the issue of antibiotic resistance (S. A. Wang et al., 2005), as it has shown that it is a significant issue within global health involving chlamydial infections (Borel et al., 2016). The range of treatment failure varies widely depending on the patient population that was examined, with a 8% failure rate in women with no re-infection risk or a high

23% in men with non-gonococcal urethritis (Horner, 2012). Further studies show a staggering 22% treatment failure in rectal infections to azithromycin and 13.7% treatment failure in *C. trachomatis* genital infection where the patient population reported full medical compliance and no post-treatment sexual contact of any kind (Borel et al., 2016). Heterotypic resistance, the replication of a heterogenous resistant population from a single organism that has been incubated in an antimicrobial medium (S. A. Wang et al., 2005), has been described as a possible explanation to clinical failure to antibiotic treatment (Borel et al., 2016; Horner, 2012).

Because these kinds of treatment failures ensure the continuous transmission of chlamydia, a short-term solution could be the repetition of tests and improving the understanding of microbial resistance (Horner, 2012). Nowadays there have been plenty of studies to develop the most effective treatment against *C. trachomatis* and, in spite of this, it is undeniable that they have not been entirely successful when controlling the increasing prevalence of infections over the past two decades, raising the question of whether the approach to *C. trachomatis* should be therapeutic, preventive or both.

1.1.5. Vaccines against Chlamydia

The STI vaccine roadmap assessed by the WHO and the National Institute of Health (NIH) has previously stated the need for an effective vaccine against *C. trachomatis* (Woodhall et al., 2018). Vaccine development is an arduous road, but a much necessary one when considering the limits that the world faces when trying to reduce the incidence and prevalence rates of chlamydial infections. Not only is it highly difficult to develop an effective screening program with an infection that mainly presents itself as asymptomatic, but it has been shown that they have not resulted in an actual reduction of sexual transmissions when they are accompanied by partner treatment (Gottlieb et al., 2013). At the same time, there is a consistent risk of antimicrobial resistance and a concern in regards to antibiotic shortages that highlight the overall agreement in chlamydia research: more needs to be done.

The early approaches to Chlamydia vaccine development were back in 1957 after the first isolation of the pathogen, and the research efforts revolved around the use of live or inactivated Chlamydia. However, these studies soon proved to not only be inconclusive but also detrimental to the test subjects, as several immunized patients developed more severe symptoms than the groups treated with the placebo (De La Maza et al., 2017). Ten years later, several studies were published regarding inflammatory reactions in non-human primates after chlamydia challenges. One of them cautioned against the use of live

trachoma vaccines in humans due to the chlamydia pathogen (previously referred to as Trachoma/Inclusion Conjunctivitis or TRIC) being able to disseminate after a subcutaneous injection in clinical subjects (Collier & Smith, 1967). At the same time, immunized individuals that weren't fully protected by the vaccination developed a severe autoimmune reaction when they were exposed to the organism again, making it clear that using the whole organism as a vaccine was no longer an acceptable option (Pal et al., 2003). Hence, the landscape of chlamydia vaccines inherently shifted towards the identification and study of antigens in order to develop vaccine candidates that are able to safely elicit protective humoral and cell-mediated responses (Paes et al., 2016).

The many different approaches to an effective *C. trachomatis* vaccine development have allowed for a wide variety of vaccine studies, some of which are described on **Table 1**.

Type of Vaccine	Description	Route of Inoculation	Results	References
Whole Cell	Elementary Bodies (EB) of the *Chlamydia trachomatis* mous e pneumonitis biovar	i.n.	Three different mice strains showed protection against a genital challenge with fertility rates equal to those of unchallenged animals	(Pal et al., 2003)
Plasmid Vector	*Ct* pgp3 DNA plasmid	i.d.	Over half of the mice were shown to prevent salpinx infection. All mice were resistant to re-infection.	(Donati et al., 2003)
Viral Vector	Recombinant Adenovirus vector expressing cPAF and a recombinant cPAF prime/boost (adjuvants: CpG oligodeoxynucleo	i.n.	Mice immunized with a single dose of AdCPAF had a robust antibody response but a weak cellular immune response. Homologous prime/boost regimen	(Brown et al., 2012)

	tides and/or peptide HH2)		elicited weak antibody responses but robust cellular immunity (Th1/Th17)	
Subunit	rCPAFep fusion protein containing 5 epitopes presented by the HLA-DR4 complex	i.n. and s.c.	Mice exhibited a significant cell-mediated immune response and a fast resolution of genital and pulmonary infection	(W. Li et al., 2013)
Multisubunit	Recombinant protein including four PMPs (PmpEFGH) with/without MOMP with Th1 polarizing adjuvant	s.c.	Mice vaccinated with PmpEFGH+MOMP showed a higher cellular immune response than those vaccinated with individual antigens.	(Yu et al., 2014)
Subunit	*Chlamydia muridarum* MOMP, (adjuvants: Montanide+CpG or Alum+CpG)	i.m. and s.c.	Mice vaccinated with adjuvants favoring Th1 response were protected against chlamydial challenge whereas those vaccinated with adjuvants favoring Th2 were not.	(Pal et al., 2015)
Inactivated Pathogen	UV-inactivated *C. trachomatis* (adjuvant: nanocarriers)	i.u., s.c., i.vag. and i.n.	Mice exhibited systemic memory T-cells but limited effector T-cells	(Stary et al., 2015)
Subunit	*Ct* rPmpD (adjuvant: TLR4 agonistic SLA)	s.c.	Mice exhibited a strong protection against urogenital *Ct*	(Paes et al., 2016)

			infection and reduced bacterial burden.	
Subunit	MOMP variable segments 2 and 4 (adjuvant: cholera toxin)	i.n. and i.vag.	Mice showed systemic and local specific antibody responses (IgG and IgA) and primed T cells producing IFN-γ, IL-13 and IL-17	(Hadad et al., 2016)
Subunit	Recombinant protein CTH522 prime/boost (adjuvant: CAF01 liposomes or AH)	i.m. and i.n.	Protein was found to be safe and immunogenic with CTH522:CAF01 showing a more robust response than CTH522:AH	(Abraham et al., 2019) [1]
Subunit	Recombinant MOMP (Adjuvant: CpG+Montanide SLA 720)	i.n., col., i.m., and s.c	Mice showed robust cellular and humoral immune responses for 180 days post-immunization and showed a decline then	(Pal et al., 2020)
Subunit/Viral Vector	CTH522 antigen (adjuvant: CAF01/AH), MOMP DNA, HuAd5 MOMP, MVA MOMP	i.m., i.n., i.d., i.m.	A specific cell mediated response and neutralizing activity against SvD, SvE and SvF was observed. Clearance of the SvD infection was observed in several groups.	(Lorenzen et al., 2022)[2]
Monoclonal Antibodies	mAb against MOMP VDIV	i.m. and i.p.	mAb only induced a neutralization activity of 38%	(Degn et al., 2023)

Table 1. Summary of some of the Chlamydia vaccine research performed in the last two decades. Examples include but are not limited to those which advanced the search of an effective vaccine candidate or were within the purview of this dissertation. MOMP: Major Outer Membrane Protein. EB: Elementary Bodies. i.n.: intranasal. col.: colonic. i.m.: intramuscular. s.c.: subcutaneous. i.vag.: intravaginally. i.u.: intrauterine. i.d.: intradermally. i.p. intraperitoneally. PMPs: Polymorphic Membrane Proteins. SLA: second-generation lipid adjuvant. AH: Aluminum Hydroxide. Sv: serovar. pgp: plasmid glycoprotein.
[1] phase 1 human clinical trial
[2] study with nonhuman primates (NHP)

The Major Outer Membrane Protein (MOMP) was the first subunit vaccine that was tested in animal models (Yu et al., 2014) and it is considered as the reason behind the positive results obtained in the whole cell trials from the last century by DNA sequencing and computational analysis. It contains five genetically conserved domains (CD) and four variable domains (VD) that determine the species-specific serovar and that encode multiple B-cell and T-cell epitopes that have previously elicited specific T-cell immunity as well as neutralizing activity (Phillips et al., 2019). Recent studies suggest that not only the outer membrane localization might play a role in antigen presentation, but abundance rate of the antigen of interest might as well, with MOMP constituting 60% of the total outer membrane protein abundance (Karunakaran et al., 2015). While the MOMP is highly antigenic and surface exposed, studies performed with the objective of inducing protection with recombinant MOMP, with DNA plasmids containing the MOMP gene or with peptides found within the protein have shown poor results in different animal models. This has led scientists to believe that the conformation of the MOMP might be vital for a proper immune response or that additional antigens are needed if protection from the infection is desired (Pal et al., 2005).

Another potential antigenic target in the search for a Chlamydia vaccine is polymorphic membrane proteins (PMPs), a series of proteins that are surface exposed and that contain highly conserved regions, which are able to be recognized across serovars. PMPs are involved in early chlamydial infection processes (Phillips et al., 2019) and are capable of presenting to the immune system of the host through multiple Major Histocompatibility Complex (MHC) binding epitopes (Karunakaran et al., 2015).

Additionally, a recent study investigating monoclonal antibodies (mAb) against a surface-exposed MOMP variable sequence domain IV (VDIV) epitope as an immunization strategy showed a neutralization activity of just 38%, failing to reduce the infectivity and provide protection against the pathogen (Degn et al., 2023).

In regards to immunization strategies, vaccine vectors have always been considered as potential vaccine delivery systems against infectious diseases, with several studies including Chlamydia as the target pathogen. Among them, DNA and viral vectors have

been widely proven to induce an effective immune response against the pathogen of interest. Immunization with the gene encoding the plasmid glycoprotein (pgp) 3 hoped to prove advantageous as it had been shown to compete with other major chlamydial antigens as a serology marker, and it did indeed induce a strong IgG and IgA antibody response, but it failed to prevent salpinx infection in 44% of the tested animals (Donati et al., 2003). A study immunizing mice with a recombinant adenoviral-based vaccine encoding Chlamydia Protease-like Activity Factor (cPAF) antigen in a single dose showed limited protection when challenged with a genital *C. muridarum* infection with a strong antibody response despite the lacking cellular response. However, a heterologous regimen where mice were primed with the recombinant adenoviral vaccine and boosted with a CPAF subunit vaccine proved to induce a robust cellular and antibody response (Brown et al., 2012). Moreover, a recent study analyzed the immune response in different prime/boost strategies, where mice were primed with either the vaccine antigen CTH522, DNA-, MVA- or adenovirus-based vectors encoding MOMP and boosted with CTH522. They succeeded in showing clearance of chlamydial infection in several groups through the neutralizing activity, as well as eliciting a specific cell mediated response (Lorenzen et al., 2022).

Interestingly, there is little research that unites chlamydial research to that of viral vectors in vaccine development, despite them having proven to be a safe, immunogenic and cost-effective approach. Examples of such viral vectors include but are not limited to: adenovirus vectors, double-stranded non-enveloped viruses with a safe profile; rhabdovirus vectors, membrane-enveloped single-stranded RNA viruses with safe genetically-engineered attenuated strains; poxvirus vectors, enveloped double-stranded DNA viruses that represent the first and most common viral vectors used for gene delivery. Within poxvirus vectors, Modified Vaccinia virus Ankara (MVA) is of note, an attenuated vaccine with a safe and immunogenic profile that has been widely used as a recombinant vaccine candidate to different infectious diseases (Sasso et al., 2020).

1.2. Vaccinia virus

Vaccinia Virus (VACV) is a double-stranded DNA orthopoxvirus that belongs to the subfamily *Chordopoxvirinae* within the *Poxviridae* family. VACV had an essential contribution to the smallpox eradiation back in 1979 (Y. Wang, 2023), with Variola virus (VARV) being the pathogen behind this fatal disease, considered to be the deadliest poxvirus with a staggering 30% of deaths among those infected and more than 3.500 years

of existence. The initial attempts to fight smallpox included the use of the pathogen itself, inoculating small amounts of VARV as the immunization agent in what was called *variolation*, a practice that aimed to prevent the natural infection and that stemmed from Asia before being introduced into Europe in the early 1700s. By the end of the century, Edward Jenner established what would later on be known as *vaccination* by using a cow-infecting poxvirus to prevent human infections (Sánchez-Sampedro et al., 2015). Several strains of VACV were developed and used for its eradication, with the New York City Board of Health (NYCBH), Tian Tan (VTT), Lister and Modified Vaccinia virus Ankara (MVA) being among them. Despite the eradication of smallpox, VACV and its strains have remained vectors of interest within the vaccine development field, with a wide variety of studies using it in order to generate recombinant vaccines against infectious, oncolytic or neurological diseases (Kaynarcalidan et al., 2021).

Because of the highly successful use of VACV in the eradication of smallpox, the use of VACV as vectors of foreign antigens was put under the spotlight and deemed of interest for further preclinical and clinical research. However, there were concerns in regards to the inoculation of recombinant VACV into human vaccine regimens, as certain side-effects had been observed through the smallpox eradication campaign. In order to solve this issue, studies focused on virus attenuation by deleting or inserting DNA sequences and inactivating single virulence genes (Meyer et al., 1991).

1.2.1. MVA

MVA is a virus strain derived from Chorioallantois Vaccinia virus Ankara (CVA) that underwent over 570 serial sub-passages in chicken embryo fibroblast (CEF) cells in an attempt at finding attenuated alternatives to the injection of VACV itself into human patients. This series of passages led to an overall loss of large fragments of its genome, amounting to about 30 kb, which contributed to its conversion into that of an attenuated phenotype without the ability of replicating in most mammalian cells. (Wyatt et al., 1998). Overall, the original CVA genome developed a total of six deletions within the 572 passages in the process of becoming MVA (**Figure 2**). Specifically, during the initial 382 passages, the so-called variant CVA 382 had an attenuated phenotype very similar to MVA's itself, as it showed deletions in the terminal fragments. The next 190 passages led to MVA, and exhibited two additional deletions which did not seem to augment the virus' attenuation. After performing a rescue with the corresponding DNA from the wild-type strand, researchers were able to allow both CVA 382 and MVA strains to replicate in non-

permissive tissue cultures, ensuring that the attenuated virulence and the growth behavior of the viruses were not altered (Meyer et al., 1991).

Nevertheless, the modifications that MVA underwent through the 572 passages resulted in the two out of five classical host range genes being deleted or truncated in the MVA genome as opposed to the VACV genome, contributing to its limited host range and rendering it unable to replicate in most mammalian cell lines, including human cells. This was shown not to be only due to the six major deletions formed during the attenuation process, but most likely because of a combination between said deletions and other genetic alterations (Meisinger-Henschel et al., 2010). Furthermore, its inability to replicate in most mammalian cells is what allows for it to be used under biosafety level 1 laboratory conditions (Staib et al., 2005). Despite the fact that MVA is indeed unable to generate infectious progeny virus in most mammalian cell lines, it does produce early, intermediate and late proteins in most cells, forming immature virions (García-Arriaza & Esteban, 2014; Sutter & Moss, 1992) (García-Arriaza & Esteban, 2014). Since MVA is part of the poxvirus family, it shares the same unique characteristics when it comes to replication, as it replicates in the cytoplasm of the cell instead of the nucleus. Specifically, poxviruses replicate in what are referred to as *viral factories*, organelles that form after infection in the cytoplasm of the host cell. Because the replication does not occur in the nucleus, there is an unquestionably reduced possibility of genomic integration in the host cell (Kaynarcalidan et al., 2021). MVA has shown to be an excellent candidate as a vaccine vector, not just because it is easy to produce and manipulate as well as cost-effective, but because it offers a highly safe profile as a killed virus vaccine with an impaired replication ability but also a highly immunogenic profile as a live virus vaccine. The immunogenicity of MVA, able to induce both cellular and humoral responses, stems from its capacity to express the antigens of interest in cells that are consequently efficiently presented through pathways of both major histocompatibility complex (MHC) class I and II, thereby activating the antigen-specific $CD8^+$ and $CD4^+$ T cells as well as the production of the antigen-specific antibodies (García-Arriaza & Esteban, 2014).

Overall, MVA is an excellent vaccine candidate that had been previously studied in several clinical trials in order to ascertain its safety profile prior to its use as a smallpox vaccine by the Bavarian State Vaccine Institute in Germany at the end of the 20^{th} century. Several trials were reported with no severe adverse reactions, with patients exhibiting subtle scarring, mild pustule appearance at the vaccination site or, at worst, a mild fever (Mahnel & Mayr, 1994; Schröter et al., 1980; H. Stickl et al., 1974; H. A. Stickl, 1974), effectively establishing MVA as a safe vector within the vaccine development field.

1.2.2. Strategies of improving MVA-based vaccines

While MVA has been thoroughly proven to be a safe and immunogenic vector, the research around its use as a vaccine vector is far from over. In fact, strenuous studies have been and are currently underway to test for ways to improve its immunogenicity in an attempt of enhancing immune characteristics such as polyfunctionality, magnitude, durability, scope and others.

1.2.2.1. Genetic manipulation

One of the strategies that continues to be of interest to this day in the search for immunogenicity enhancement is the deletion of viral immunomodulatory genes found within the MVA genome. An example that has been systematically studied is C6, a non-essential protein that is expressed during early stages of infection that encodes an IFN-β inhibitor that prevents the activation of the Interferon Regulatory Factors 3 and 7 (IRF 3, IRF 7) (Marín et al., 2018). Deletion of the C6L gene in a recombinant vector expressing HIV antigens did not display any detrimental differences in growth kinetics, proving its futility in virus replication, but showed an enhancement in $CD4^+$ and $CD8^+$ T cell responses, as well as increasing the antibody concentration as opposed to a recombinant MVA with the intact C6L gene (García-Arriaza et al., 2011). A following study showed an enhanced magnitude and quality in HIV-specific cell responses in mice immunized with a recombinant MVA with a C6L and K7R double deletion when compared to both the MVA-wild type and the MVA with the sole C6L deletion (García-Arriaza et al., 2013). Studies have also been performed with a recombinant MVA exhibiting the simultaneous deletions of A44L (associated with steroid hormone metabolism), A46R (an inhibitor of Toll-like Receptor-signaling) and C12L (coding for IL-18 binding protein) that described the enhanced immunogenicity when compared to the MVA-wt (wild-type), with not only a higher $CD4^+$ and $CD8^+$ T-cell response but also an increased anti-VACV cellular response (Holgado et al., 2016). Interestingly, early studies reported a comparable $CD8^+$ T cell response in BALB/c mice immunized with MVA coding for deletions in genes C12L, A44L, A46R and B7R (chemokine binding protein), with only a statistically significant difference on $CD8^+$ T cell responses in mice immunized with a recombinant MVA with a B15R (IL-1β binding protein) deletion, although this was reportedly not as pronounced as a previous experiment on HHD mice (Cottingham et al., 2008). Other gene deletions that have been successfully proven to improve MVA's immunogenicity include

the N2L gene (coding for an IRF3 inhibitor), a study that proved to enhance the antibody levels against the antigen of interest, as well as the innate immunity against HIV-1 (García-Arriaza et al., 2014) the A41L gene (thought to have an immunomodulatory role), with research showing its deletion provided a higher level of protection against VACV WR challenge (Clark et al., 2006) and an increased polyfunctionality and magnitude in HIV-specific cellular response with antibody levels comparable to that of the wild-type as part of a double deletion along gene B16R (García-Arriaza et al., 2010); the A40R (encoding a protein with an unknown function related to immunogenicity), where the study showed an increased magnitude of $CD4^+$ and $CD8^+$ T cell responses (Pérez et al., 2020); the A35R (a virulence factor in the mouse model, unnecessary for viral replication), which showed that its deletion increased the virus-specific IFN-γ splenocytes and an immunoglobulin production (Rehm & Roper, 2011). Additionally, an example of another strategy used to optimize the immune response elicited by MVA immunization through genetic manipulation is the replacement of MVA fragmented genes 181R/182R (with an anti-apoptotic function) with a functional B13R obtained from VACV, where they showed an enhanced antibody response in mice (Chea et al., 2019). Promoters have also been the focus of comparative studies aiming to optimize vaccine regimens with recombinant vaccinia virus LC16m8Δ strain under moderate or strong promoters, resulting in both recombinant strains displaying antigen-specific immunity with the strong promoter recombinant strain inducing a more robust cytotoxic T cell response (Isshiki et al., 2014). Recently, chimeric poxviral promoters have been used as a strategy to increase the different immunogenic characteristics of recombinant MVAs aiming for a protective vaccine against IAV, and proved to induce circulating serum antibodies and a robust $CD8^+$ T cell response (Langenmayer et al., 2023).

1.2.2.2. Prime-Boost Protocols

MVA had already been used in heterologous prime-boost protocols in the 1970s, where priming, referred to as pre-vaccination, was performed with MVA in order to induce an immune response without the risks that the conventional vaccination carried then. Boosting, then referred to as the vaccination itself, was performed with the conventional VACV (H. Stickl et al., 1974). Research around heterologous prime-boost protocols involving virus vaccines would continue in the later years, with the certainty that using different live vectors in a sequential immunization regimen would have a synergistic effect on the immune response (S. Li et al., 1993a). There have been plenty of

studies in the last thirty years to not only establish those findings, but further investigate the mechanisms behind them.

Priming the clinical subject must induce a specific T-cell response with a percentage of memory cells that are specific to the antigen of interest and that will then go through a swift population growth when the antigen of interest is exposed to the system again with the following boosting (Dunachie & Hill, 2003). The notion of the immune response being dependent on which vectors are used as priming agents and which as boosting agents has been known for decades, but the concept continues to stand up to this day (Richert et al., 2022). While many vector agents have shown to be successful at eliciting an immune response when priming, there are not many vectors that have proven to be able to efficiently boost that same response (Dunachie & Hill, 2003). Excellent priming agents include DNA plasmids encoding the antigen of interest, lipopeptides and virus-like particles, but they have proven to be poor boosting candidates. On the other hand, recombinant viruses have shown to be strong boosting agents (Dunachie & Hill, 2003). While MVA as a vector candidate has shown to be a worse priming option when compared to other vector candidates such as adenovirus, it has proved to efficiently boost both cellular and humoral responses against a wide variety of pathogens (Sasso et al., 2020). A comparative study performed in NHPs researching the different immune responses elicited by three Hepatitis C Virus (HCV) heterologous prime/boost vaccine protocols, including priming with DNA and Semliki Forest Virus (SFV), and boosting with MVA and human serotype 5 adenovirus. Even though there wasn't a statistically significant difference after priming with either DNA or SFV, once animals were boosted with MVA, the group that had been primed with SFV had a higher cytokine production. Interestingly, despite the slightly higher proliferation in groups boosted with MVA when compared to groups boosted with the human adenovirus vector, and a subtle increased trend in IFN-γ response in the human adenovirus group, these differences were not statistically significant. However, the researchers urged caution when considering one vector superior to another, as they have both been shown to induce robust immune responses to different antigens (Rollier et al., 2016). Heterologous DNA-priming/MVA-boosting immunization protocols have proven numerous times to induce an enhanced immune response when compared to homologous vaccinations. A study analyzing two therapeutic vaccines against HCV showed that the heterologous DNA-priming/MVA-boosting regimen not only provided significant protection against a challenge while the single-vaccine-regimens did not, but also increased the polyfunctionality and magnitude of the T-cell response (Fournillier et al., 2013). A heterologous DNA-priming/MVA-boosting regimen

against Zika virus (ZIKV) induced a significantly higher ZIKV-specific T cell response and increased levels of neutralizing antibodies as opposed to the homologous DNA-priming/DNA-boosting or MVA-priming/MVA-boosting vaccination regimens (Pérez et al., 2021).

MVA has also been included in several clinical trials, which have analyzed the safety or immunogenic profile of the viral vector in heterologous prime/boost protocol. A phase I/II multi-arm trial analyzed the safety, gene expression profile and T cell immunogenicity induced by heterologous protocols that included MVA, lipopeptides or DNA against HIV, showing changes in whole-blood gene expression in groups that had been primed or boosted with MVA and an increase in the rate of ELISPOT responders in groups boosted with MVA. Results also indicated that the frequency of polyfunctional $CD4^+$ T cells specific to the vaccine was long-lasting, sustained up to 6 months after the last boost in groups that included priming or boosting with MVA (Richert et al., 2022). Additionally, a recent first-in-human study against Ebola virus disease, Sudan ebolavirus and Marburg Disease was performed by immunizing healthy adults with either MVA or human adenovirus in both MVA-priming/Adenovirus-boosting and Adenovirus-priming/MVA boosting, finding that both regimens were safe, well-tolerated and immunogenic for the patients but being unable to draw any conclusions as to the protection against the pathogens it was targeting (Bockstal et al., 2022). Overall, this is an essential notion to keep in mind as the research around MVA as a vaccine candidate moves forward, because any desired immune response will highly depend on the variables attributed to the immunization itself, and a prime/boost protocol, be it heterologous or homologous, is just one part of the whole.

1.2.2.3. Adjuvants

One of the earliest definitions of adjuvants was published in 1974, and it described them as components added to vaccine antigens in order to increase their immunogenicity (O'Hagan & De Gregorio, 2009). Nowadays, adjuvants are still an important aspect when designing vaccine regimens (Buonaguro et al., 2011a), as they have significantly contributed to the success of currently available vaccines (O'Hagan & De Gregorio, 2009).

Aluminum salts (referred to as alum) are adjuvants that have been in use for over eighty years in a wide range of vaccine candidates in infectious diseases such as Tetanus, Diphteria and HPV. They have been shown to be safe and to increase the immunogenicity of the antigen that is adsorbed into the particulates by increasing antigen uptake and

stability (Mbow et al., 2010). Alum has been used in studies related to MVA, with one comparing the immunogenicity of a DNA-priming/MVA-boosting vaccine regimen with or without the addition of an HIV protein in alum or said protein expressed by MVA itself. They found that the protein in alum increased $CD4^+$ T cell responses and induced an earlier response, while the MVA-expressed protein induced a long-lasting antibody response (Shen et al., 2017). A recent study researched the effect of incorporating a protein in alum as a boost to an adenovirus/MVA vaccination regimen, and found no significant difference in the immune responses among the groups that had been administered the boost or not (Ventura et al., 2022).

Additionally, adjuvants MF59 and AS03 have been licensed in Europe for their use in influenza vaccines. They are oil in water emulsions vaccines with an adjuvant effect that was shown to be superior to that of alum in clinical trials targeting Influenza A virus subtype H5N1 vaccines (Mbow et al., 2010). Furthermore, MF59 was used in a study using prime/boost vaccination regimens against *C. trachomatis* using DNA plasmid, Human Adenovirus 5 and MVA vectors coding for consensus MOMP with or without MF59. They showed that those regimens with MOMP-MF59 induced a bigger IgG1 response, but did not enhance the T cell response elicited by a homologous DNA-priming/DNA-boosting/DNA-boosting and a heterologous Adenovirus-priming/MVA-boosting regimens (Badamchi-Zadeh et al., 2016).

Many other adjuvants have been studied in the search of vaccine optimization. Among them, AS04, a TLR-4 agonist in alum has been licensed for HBV and HPV in Europe and the United States, but it does not seem as if its effect has been studied along with MVA vector vaccines. AS01 has been studied against Malaria (Walker et al., 2015) and Tuberculosis, with the latter including a study analyzing the safety and immunogenicity of a peptide-based vaccine and an MVA vector vaccine (Ullah et al., 2020). Additional adjuvants include liposomes, immunostimulatory complexes and virosomes, which have been licensed for Influenza vaccines (Buonaguro et al., 2011b).

1.2.2.4. Fusion Antigens

Fusion agents have been used to optimize heterologous antigens expressed by MVA for decades. Among them, protein 14K has been fused to HIV-1 envelope glycoprotein encoded by MVA in an attempt at improving the antigen's immunogenicity by increasing the oligomerization of the protein (Raman et al., 2019). 14K is a protein encoded by the A27L gene that is related to the entry of vaccinia virus into the cell (Vázquez & Esteban, 1999) and that is composed of 110 amino acid residues. It has been shown to have an

effect similar to that of an adjuvant, effectively increasing the immune response when fused to antigens in heterologous prime/boost protocols (Vijayan et al., 2015).

The MHC class II invariant chain (Ii) has been used in studies aiming to increase T cell immune responses in both mice and humans. Also called CD74, Ii is expressed in a large range of immune cell types and is highly conserved across species, with studies showing that it increases the breadth and magnitude of cellular immune responses when fused to the antigen of interest, as it is known to be involved in the MHC class II antigen presentation pathway (Esposito et al., 2020). Studies have also shown that Ii enhances the $CD8^+$ T cell response when fused to antigens encoded by plasmid DNA plasmids or human adenovirus 5 vectors (Spencer et al., 2014).

Because cytotoxic T-cell activation requires of co-stimulatory molecules B7-1 or B7-2, they have also been used when devising vaccination regimens. Among them, B7-1 is essential for the response to intracellular pathogens, and it has been shown to increase the immune response to an antigen of interest after vaccination with a vector coding both said antigen and B7-1. A study showed an immunostimulatory effect and reported no detrimental inferences in B-cell proliferation and natural killer cell functions after immunizing mice with a recombinant vaccinia virus encoding B7-1 (Freund et al., 2000). B7 was used in a phase I study as part of a triad of human T-cell costimulatory molecules along LFA-3 and ICAM-1 encoded by both MVA as the priming agent and by a fowlpox virus acting as a boosting agent. The vaccine was deemed as well-tolerated, and positive results concluded that it was of clinical benefit (Collins et al., 2020).

1.2.3. MVA vaccines against Chlamydia

MVA has been thoroughly used in immunology in the search of a vaccine capable of inducing a broad, long-lasting and robust immunogenicity encompassing both cellular and humoral responses that would hopefully contribute to protection against the targeted pathogen. In regards to bacterial agents, MVA has shown to be a remarkable vaccine candidate against tuberculosis, able to induce $CD4^+$ and $CD8^+$ T cell responses in non-human primates (Leung-Theung-Long et al., 2015) and protective immunity in guinea pigs (Nangpal et al., 2017).

There are few studies using MVA against *C. trachomatis*, but those that have been completed have shown promising results. Previous research has always used MVA as part of vaccination regimens that included other vectors, providing limited information on homologous MVA vaccinations or simple heterologous prime/boost regimens (as opposed to the prime/boost/boost protocols already evaluated).

One of the firsts studies against Chlamydia with an MVA vector taking part of the immunization regimens additionally used DNA plasmid, HuAd5 coding MOMP and the MOMP protein adjuvanted with the monophosphoryl Lipid A adjuvant and the previously mentioned MF59. They found that the group immunized with three doses of the adjuvanted protein elicited the highest ocular IgG concentrations, while the group immunized with two doses of DNA and two successive protein doses had the lowest levels. Mice immunized with an Adenovirus priming dose, an MVA boosting dose and two protein boosting doses also induced MOMP-specific IgG antibodies, but IgA was undetected in all of the experimental groups. While authors reported neutralizing activity, they also mentioned that the protective immunity against ocular infections caused by *C. trachomatis* may not provide cross-protection across the different serovars (Badamchi-Zadeh et al., 2015). While that specific study did not focus on cellular response, a very similar experimental system was used in a following study that chose to center around T-cell immunity that would be capable of eliciting cross-serovar protection. They found the DNA/HuAd5/MVA/Protein immunization protocol not only induced significant levels of serum and vaginal antibodies specific to MOMP, but also a robust cellular response, both of which contributed to a $CD4^+$ T cell dependent chlamydial clearance in the study subjects. Researchers hypothesized that a superior infection clearance would be obtained in other study models, such as humans, NHPs and transcervical infection models (Badamchi-Zadeh et al., 2016). A new study was recently completed that analyzed the effect of a similar vaccination regimen in Cynomolgus macaques, a NHP model. Test subjects were immunized with vaccination regimens combining DNA plasmid, MVA and HuAd5 vectors encoding a consensus MOMP antigen with the synthetic fusion protein CTH522 with either adjuvant AlOH or adjuvant CAF01. All groups displayed a robust antibody response but only three groups displayed chlamydial clearance: the one consisting of a triple dose of CTH22-CAF01 followed by a double dose of CTH422, the group immunized with DNA-MOMP thrice and then boosted with CTH522:CAF01, and the vector vaccine group where subjects were immunized with DNA-MOMP, HuAd5-MOMP, MVA-MOMP and CTH522:CAF01. Despite the fact that they all did induce a $CD4^+$ T cell response, only those groups that had been immunized with the DNA plasmid or the vector vaccines were able to elicit a significant $CD8^+$ T cell response (Lorenzen et al., 2022). Overall, results from these past studies strongly point in the direction of the use of a heterologous prime/boost protocol in order to elicit a broad, long-lasting and robust immune response including both cellular and humoral responses that would hopefully lead to cross-serovar protection against the targeted pathogen.

1.3. Scope of the thesis

1.3.1. The immune needs of a Chlamydia vaccine

While researchers have worked towards the development of a *C. trachomatis* vaccine for over fifty years, there is not a current vaccine candidate capable of eliciting a robust and broad immune response that would be able to protect the subject against infection.

Even though $CD8^+$ T cells are typically essential in eliciting immune responses against intracellular pathogens, early studies already showed the unimportance of a $CD8^+$ T cell response when clearing chlamydial infection in mice. While $CD8^+$ T cells were shown to be involved in the host response to the infection, this role was deemed as "modest" when compared to that of $CD4^+$ T cells. Not only was the depletion of $CD8^+$ T cells in the organism not leading to a statistically significant higher mortality, but those mice were still able to clear the infection despite the lack of functional $CD8^+$ T cells (Magee et al., 1995). While some studies have managed to prove CTL cytotoxicity *in vitro*, results are consistently failing to provide *in vivo* protection against chlamydia, further stablishing the fact that a $CD8^+$ T cell response is insignificant for the murine subject to acquire protective immunity (Morrison et al., 2000). This evidence led to the overall believe that $CD4^+$ T cells were vital in clearing the infection, while $CD8^+$ T cells were of importance in the disease resolution, as well as burden reduction. Possibly because of the limitations of studying *C. trachomatis*, a human pathogen, in murine models, or perhaps merely due to further scientific elucidation, more recent studies have attempted to resolve the unanswered questions rising over the T cell immune responses elicited by chlamydial infections (Murray & McKay, 2021). Interestingly, immunization with a plasmid-deficient live-attenuated trachoma vaccine in macaques found that both $CD4^+$ and $CD8^+$ T cell responses conferred protective immunity to the experimental subjects (Olivares-Zavaleta et al., 2014). Additionally, while $CD8^+$ T cells are not stimulated by a natural *C. trachomatis* genital infection, intranasal priming was reported to elicit an immune response mediated by both $CD4^+$ and $CD8^+$ T cells that confers cross-mucosal protection in mice genital tract (Nogueira et al., 2015). Further recent studies performed in murine models have reaffirmed the notion of the $CD4^+$ T cell immune response being essential in providing protective activity against the infection, while $CD8^+$ T cells are not, as depletion of $CD4^+$ T cell populations in $CD8^+$ T cell-deficient mice

increased chlamydial infection (Yu et al., 2019). Nonetheless, the current understanding is clear: $CD4^+$ T cells are essential for protection against *C. trachomatis* and, as such, should be one of the main objectives of vaccine development against Chlamydia.

While it was initially believed that immunity upon reinfection would be solely acquired through a cellular response, antibodies have shown to exert a protective role against *C. trachomatis* (Farris et al., 2010; Morrison & Morrison, 2005). In order to achieve chlamydial clearance, B cells are responsible for priming $CD4^+$ T cells by presenting the antigen of interest on the cell surface, as well as antibody-dependent cell-mediated cytotoxicity and neutralization (Murray & McKay, 2021). While $CD4^+$ T cells are involved in crucial mechanisms that elicit protection, studies have shown that the humoral response does play a role in the immune response elicited by *C. trachomatis* genital reinfection. Mice that were only depleted of $CD4^+$ T cells were immune to a secondary chlamydial infection, unlike antibody-deficient mice that were depleted of $CD4^+$ T cells (Morrison & Morrison, 2005). Additional studies showed that immunization did not protect B-cell deficient mice from infection and that these mice showed a similar profile to the negative control groups, but anti-MOMP serum transfer provided them with slightly protective immunity (Farris et al., 2010). Supporting the notion that antibodies do indeed play a role in bacterial neutralization, a study administered antibodies specific to a vaccine construct to knockout mice that produced neither mature T cells nor mature B cells. After three days, 48% of mice were uninfected, and 83% of those mice displayed an entirely controlled infection, indicating the possibility of the humoral response neutralizing *C. trachomatis* on its own (Olsen et al., 2017).

It is indisputable that many of the mechanisms of protection against *C. trachomatis* infection have yet to be elucidated. However, ultimately, researchers have repeatedly and consistently shown how indispensable it is for a potential vaccine candidate against *C. trachomatis* to induce a $CD4^+$ T cell and antibody immune response in order to confer protection against infection.

1.3.2. CTH522 as a vaccine antigen

MOMP has been the center of different approaches in *C. trachomatis* vaccine development and, despite its immunogenicity and the fact that it is surface exposed, there aren't any vaccines encoding MOMP that have been able to move past *in vivo* studies into clinical trials. This may be due to the fact that, despite the robust neutralizing activity

these vaccine candidates are capable of eliciting, they only provide homotypic protection (Rose et al., 2018).

CTH522 has recently emerged as a promising novel vaccine antigen as the main point of study in a phase 1, first-in-human, double-blind, parallel, randomized, placebo-controlled trial recently completed in London in order to ascertain the safety of the vaccine candidate (Abraham et al., 2019). CTH522 was genetically designed by fusing a truncated MOMP encompassing amino acids 34 to 259 (henceforth referred to as rMOMP) to heterologous immunorepeats from 4 variable domains from serovars D, E, F and G (Figure 3). MOMP's variable domains determine the serovar of the bacteria, and contain multiple epitopes that have previously been found to confer neutralizing immunity. The four variable domains found in CTH522 all contain the LNPTIAG epitope, a highly conserved sequence that is species-specific with flanking regions specific to each of those four serovars. Further modifications within the antigen include the replacement of all cysteine residues with serine residues in an attempt at controlling possible disulfide bond formations (Rose et al., 2018)., that could lead to stability issues or changes in the antigen conformation.

CTH522 as a vaccine antigen had already been evaluated in animal models such as mice, guinea pigs and non-human primates before being tested in a human clinical trial where a total of 35 healthy women between the ages of 19 and 45 were administered one of the two adjuvanted vaccines (either CTH522:CAF01 or CTH522:AH) or mere saline solution as placebo. Both vaccines were proven to be immunogenic and safe, without reporting any severe adverse effects and with the patients solely displaying slight local reactions to the immunization. CTH522:CAF01 showed an increased immunogenicity when compared to CTH522:AH in both cellular and humoral immune profiles, although both vaccines provided patients with a robust concentration of neutralization antibodies (Abraham et al., 2019). An additional phase I, double-blind, parallel, randomised, and placebo-controlled clinical trial was performed between 2019 and 2022 where 65 healthy adults were immunized with two different vaccine formulations (CTH522:CAF01, CTH522:CAF09b) and tested for the safety and immunogenicity of the vaccines. Groups had analysis of their cellular immune response and were also tested for CTH522-specific memory B cells and neutralizing antibodies against serovars D, E, F and G in order to evaluate the humoral immune response (Borges et al., n.d.). As of November 2023, no results of said clinical trial have been published.

Recent studies have continued to use CTH522 as part of their vaccine strategies against *C. trachomatis* in animal models in order to ascertain further clarification in the

mechanisms of the immune response necessary to fight the pathogen. B6C3F1 mice immunized with a homologous prime/boost protocol of CTH511/CAF01 displayed protection against an initial chlamydial infection and long-lived Th1/Th17 T cells after challenge with *C. trachomatis* (Nguyen et al., 2021). Another study proposes enhancing the breadth of the humoral immune response and extending to serovars other than the ones CTH522 targets, suggesting to do so by supplementing the vaccine with additional constructs such as one based on the VD1 region of MOMP, which they showed to induce not only neutralizing antibodies but also protection against chlamydial infection (Olsen et al., 2021). Nonetheless, CTH522 as a vaccine antigen has shown to be sufficient in clearing the infection when adjuvanted with CAF01 in NHPs. As previously mentioned, a recent study showed that test subjects immunized with vectors encoding CTH522 were able to display antibodies and a robust $CD4^+$ T cell response. Moreover, those groups vaccinated with vector delivery systems (including DNA plasmids and viral vectors such as MVA) also elicited a $CD8^+$ T cell response (Lorenzen et al., 2022).

Overall, CTH522 has proven to be a promising vaccine antigen that is slowly but steadily gaining traction in the search for a vaccine against *C. trachomatis* on account of the encouraging results in both preclinical animal studies and clinical trials.

1.3.3. B7 as a vaccine modification

The display of chimeric proteins on mammalian cell surfaces has been theorized to be a useful and favorable approach to vaccine development, as it has been shown that antibody concentrations were enhanced upon the surface expression of antigens of choice in previous studies (Chou W. et al., 1999). The transmembrane domain and cytosolic tail of murine B7-1 have proven to display a high surface expression when compared to other approaches such as the transmembrane domains of the H1 subunit of the human asialoglycoprotein receptor or the decay-accelerating factor (Liao et al., 2001). Nowadays, the use of B7-1 as a fusion antigen is considered to be favorable as opposed to other approaches such as using a glycosylphosphatidylinositol (GPI) anchor for the expression of proteins on the plasma membrane, as proteins using GPI anchors have spontaneously released from the cell membrane through proteolytic cleavage or shedding (Pan et al., 2012).

There is still a vast amount of research to be done in regards to the exact mechanisms involved with the cytoplasmic tail of B7 and its interactions with the cell itself. Nonetheless, the fact is that the cytoplasmic domain of the B7-1 protein has been shown to not only enhance the mammalian cell surface display of antigens but also their intracellular transport. Furthermore, certain requisites have been proposed for the use of cytoplasmic tails in mammalian surface display enhancement strategies, such as a minimum of five amino acids and a length appropriate for a swift active transport to the golgi apparatus (Lin et al., 2013). This further establishes the rationale behind the expectations and methodology when using B7-1 (henceforth referred to as B7) in combination with vaccine antigens such as CTH522 (**Figure 3**) in order to induce an optimal cell-mediated immune response against the pathogen of interest.

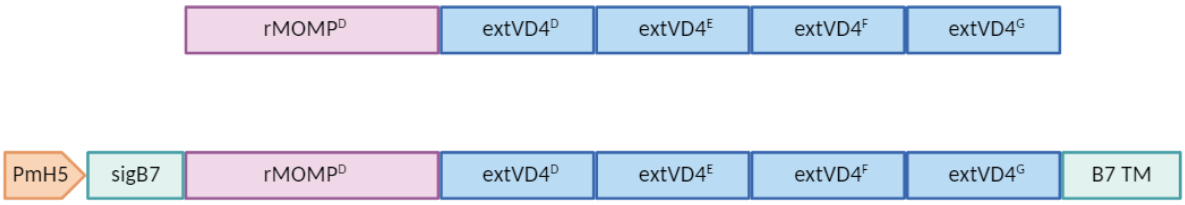

Figure 3. Schematic representation of CTH522 and CTH522:B7 antigens. CTH522 (above) contains a cysteine-free truncated MOMP (rMOMP) fused to 4 heterologous immunorepeats of variable domains from serovars D, E, F and G (extCD4^{D-G} respectively). CTH522:B7 (below) is the construct of study in this work and encompasses the PmH5 promoter (PmH5), a signal sequence of the B7-1 molecule (sigB7) and the transmembrane domain and cytoplasmic tail of the B7-1 molecule (B7 TM). Additionally, the CTH522:B7 gene has two further modifications: codon optimization for eukariotic expression and codon optimization (first 50 bp) for ribosomal binding. Fragment sizes are relative.

1.3.4. Final aim of this study

An approximate 128.5 million new cases of C. *trachomatis* emerged in 2020 around the globe (World Health Organization, 2023), making it responsible for the majority of sexually transmitted diseases caused by a bacterium (Sturd & Rucks, 2023). Despite the fact that it is a treatable infection through the use of antibiotics, C. *trachomatis* continues to impose a great threat to the wellbeing and welfare of people worldwide, specially to those living in endemic areas, where approximately 125 million people were at risk of trachoma in 2022 (World Health Organization, 2022). Because *C. trachomatis* infection presents as mostly asymptomatic, with 70-90% of women (Panzetta et al., 2018) and 40-

50% of men (Sturd & Rucks, 2023) showing no symptoms, this inevitably delays the treatment and increases the prevalence of the disease.

Following previous research centered around the immune response to chlamydial infection, this study proposes a novel vaccine candidate targeting a $CD4^+$ T cell and antibody response that could potentially lead to protection from the infection in order to develop a preventive strategy against the increasing infection rates. While many different approaches have been studied, it is of note that recombinant viral vectors have been used for decades in both vaccination strategies to eradicate infectious pathogens and immunology literature in the search for vaccine candidates against ailments such as cancer or neurological and infectious diseases. Among them, MVA is a VACV strain that was derived from CVA after going through 572 serial sub-passages in CEF cells, which attributed MVA with an attenuated phenotype that rendered it unable to replicate in most mammalian cells (Wyatt et al., 1998). MVA has emerged as a promising viral vector because of its immunogenicity and safe profile and it is the delivery system of choice used within this framework to investigate the potential of a vaccine candidate encoding CTH522. CTH522 is a recombinant vaccine antigen modeled after a truncated version of MOMP that is fused to immunorepeats from the variable domain of four different serovars. This antigen has been previously tested in both animal models and a phase 1, first-in-human, double-blind, parallel, randomized, placebo-controlled trial (Abraham et al., 2019) where it was deemed safe and immunogenic. Due to these favorable results, this study aims to elicit a robust and broad immune response against C. *trachomatis* by generating and characterizing a recombinant MVA viral vector expressing CTH522 in a codon optimized version for eukaryotic expression and ribosomal binding. Moreover, because the immune responses that have previously been shown to be essential for bacterial clearance are not only based on a strong $CD4^+$ T cell response but also an antibody-specific response, the CTH522 antigen was further modified with a n-terminal Ig□ signal peptide sequence and a c-terminal transmembrane domain and cytoplasmic tail of the B7-1 molecule, which has been shown to increase surface display of chimeric molecules (Pan et al., 2012). With these modifications, it is expected that CTH522 expression on the plasma membrane will induce an optimal B-cell response, as antibodies play a crucial role in chlamydial clearance (Olsen et al., 2017).

Overall, this work proposes the recombinant MVA vector expressing CTH522 with the genetic modifications outlined above (henceforth referred to as MVA-CTH522:B7) as a vaccine candidate against C. *trachomatis* in hopes to develop a promising preventive strategy against this bacterium.

2. MATERIALS

2.1. Cells

2.1.1. Bacterial cells

Name	Description	Source
E. coli XL-1-Blue	chemical-competent cells. incubated at 37 ºC.	Stratagene
E. Coli GS1783 #22	Derivative of DH10B cells containing Red recombination genes and I-*Sce*I endonuclease. It carries pMVAF-DX (an MVA-BAC clone), where the modified BAC is self-excising and allows for insertion of target genes in deletion VI. Incubated at 32 ºC.	Gift from Matthew G.Cottingham modified by Karsten Tischer
MAX Efficiency™ Stbl2™	Chemical-competent cells. Incubated at 30 ºC.	Thermo Fisher Scientific

2.1.2. Mammalian cells

Name	Description	Source
DF-1	immortalized chicken (Gallus gallus) fibroblasts	ATCC (CRL-12203)
Cloudman S91	melanocyte-derived epithelial mouse melanoma cell	ATCC (CCL-53.1)
HeLa	human cervical carcinoma cells	ATCC (CCL-2)
BMDCs	Bone Marrow-Derived Dendritic Cells	C57BL/6 mice
DC 2.4	immortalized murine dendritic cells	SCC142
HaK	Syrian golden male hamster (mesocricetus auratus) kidney cells	ATCC (CCL-15)

2.2. Mice

Mice were used for BMDC generation (described below in 3.2.8) or for splenocyte isolation or blood collection after vaccination regimens were performed (as extensively described in 3.2.12).

Name	Description	Source
C57BL/6	Class I : H2-K^b and H2-D^b Class II: I-A^b	http://jaxmice.jax.org/strain/000664.html

2.3. Virus

All viruses used in the study are derived from the parental MVA-BAC strain. At the same time, they were all purified with a sucrose cushion assay and titrated using standard methods as described on 3.2.5. and 3.2.7 accordingly.

MVA-CTH522: recMVA virus expressing CTH522 antigen that was inserted in the deletion VI of the MVA genome, generated by Giuseppe Andreacchio.

MVA-CTH522:B7: recMVA virus expressing CTH522:B7 antigen that was inserted in the deletion VI of the MVA genome.

MVA-mLi:CTH522: recMVA virus expressing mLi:CTH522 antigen that was inserted in the deletion VI of the MVA genome.

MVA-WT (SB): BAC-produced virus that corresponds . to the non-recombinant MVA-BAC and was used as a wild-type control in this study for growth kinetics, FACS and immunization studies.

Rabbit Fibroma Virus (RFV): helper virus used for recMVA generation as it does not replicate in DF-1 cells but it contains the initial transcription machinery able to trigger the rescue of MVA from the BAC by initiating recMVA replication (Kugler et al., 2019).

MVA-WT (F6): wild type MVA strain that was derived from the Ankara strain of the Vaccinia Virus after over 586 serial passages in chicken Embryonic Fibroblast cells, grown from the F6 clone. Used in this study for initial Western Blot experiments.

2.4. Nucleic Acids

2.4.1. Plasmids

pcDNA3.3TOPO-CTH522: plasmid that worked as a delivery vector encoding gene CTH522 used for cloning purposes of recMVA viruses (ThermoFisher GENEART). The plasmid contains a kanamycin resistance gene for selection.

pEP-MVA-dVI-PmH5: plasmid containing a Multiple Cloning Site (MCS) under control of the PmH5 promoter used for cloning purposes of recMVA viruses where CTH522:B7, mLi:CTH522 or CTH522 were inserted (generated by L. Dai).

pEP-MVA-dVI-CTH522: plasmid with the CTH522 antigen inserted under the PmH5 promoter used for transfection of DF-1 cells with the objective of generating a recombinant MVA expressing CTH522 (termed MVA-CTH522).

pUC57-CTH522:B7: plasmid encoding antigen CTH522:B7 used for cloning purposes. (kindly provided by Matia Ciancaglini at Basel University)

pEP-MVA-dVI-CTH522:B7: plasmid containing the CTH522 antigen with the B7 optimization (consisting of a signal sequence upstream of the CTH522 gene and the B7opt cytoplasmic tail downstream of the CTH522 gene) inserted in the MCS under control of the PmH5 promoter used for transfection of DF-1 cells in order to generate MVA-CTH522:B7.

pEP-MVA-dVI-mLi:CTH522: plasmid with the CTH522 antigen along with the mouse invariant chain (mLi) optimization (containing a linker sequence and the mLi sequence (kindly provided by Emanuele Nolfi at Utrecht University) upstream of the CTH522 gene) inserted in the MCS under control of the PmH5 promoter used for transfection of DF-1 cells aiming to generate MVA-mLi:CTH522.

pEP-MVA-dVI-PK1L: template plasmid for BAC selection encoding a *Sce*I-Kanamycin cassette and containing the GFP cassette but lacking CTH522 used as a negative control for screening PCR (generated by L. Dai).

cDNA-SP:CTH522: plasmid encoding the CTH522 gene and containing a toxic tetanus fragment C (TTFC) upstream of the CTH522 gene which was used for heterologous vaccination regimens (generated and provided by M. Sc. Emanuele Nolfi, Utrecht University).

pVAX1: mammalian expression vector used for heterologous vaccination regimens (kindly provided by Emanuele Nolfi at Utrecht University). The plasmid encodes a MCS

under control of the cytomegalovirus (CMV) promoter, as well as a resistance gene to kanamycin, neomycin and G418.

2.4.2. Primers

Primers were all purchased from Eurofins Genomics.

Name	Sequence (5'- 3')	Application
MVA Del VI 3′ new	CTCCGCATCTAGTTGATATTCCAA CCTCTT	sequencing, colony PCR
MVA Del VI 5′	CCTGGACATTTAGTTTGAGTGTTC CTGAAT	sequencing, colony PCR
RT_CTH522-1_fwd	GCACTTTGGGAGCAACTTCTG	sequencing, colony PCR
RT_CTH522-2_fwd	GAGCTGAAGGACAATTGGGAG	sequencing
RT_CTH522-3_rev	TCCTTCAGTGTTGGCTCCAG	sequencing, colony PCR
RT_CTH522-4_rev	ACATTCCCACAAAGCAGCCC	sequencing
RT_CTH522-5_rev	GCAGCATCAGTTCCAGCAGT	sequencing
GFP F.P	TTGTACAGCTCGTCCATGCCGAG	control PCR
GFP R.P	GCAAGGCCGGATCTGGGAATTC	control PCR
RFV fwd	AAAGATGCGTACATTGGACCC	control PCR
RFV rev	GTTCGAGACTAGAAAAGCGCC	control PCR
RT_S5aph_fwd-out	CCTATGGAACTGCCTCGGTG	sequencing
RL_S1aph_rev_in	ATTCGTGATTGCGCCTGAGC	sequencing, colony PCR
RL_S2aph_fwd_in	CGTACTCCTGATGATGCATG	sequencing, colony PCR
RL_S3aph_rev_out	CATCAGAGATTTTGAGACAC	sequencing, colony PCR

RL_S4aph_fwd_out	TGGTATTGATAATCCTGATATG	sequencing, colony PCR
mLi XbaI Fwd	CTAGAGGATCGGCCACC ATGGATGACCAACGCGACCTC	cloning, sequencing
mIi linker_fwd	AGGTTGACTCTAGAGGATCGC TAGCATGGATGACCAAC	cloning
mIi linker_rev	CAAGCAAAAGTTGTGTCAGT ATTCAACAACAGATTGATCAAAA G	cloning
reverse BamHI	GGATCCGAATTCGCACAGGGTG ACTTGACCCA	cloning

2.5. Proteins

2.5.1. Antibodies

Antibody	**Clone / (Reference number)**	**Host**	**Application**	**Manufacturer**
Anti-mouse β-actin	AC-15	Mouse	Western Blot	Sigma-Aldrich
Anti-VACV	(9503-2057)	Rabbit	Western Blot	BioRad
CT602: anti-*C. trachomatis* species -specific MOMP monoclonal antibody	MAb6ciii	Mouse	Western Blot, Flow Cytometry, ELISA	Chlamydia Biobank, University of Southampton
Anti-Mouse CD16/CD32, purified	Clone: 93 (14-0161-82)	Rat	Flow Cytometry	Thermo Fisher Scientific
Anti-Mouse CD16/CD32, purified	Clone: 93 (101301)	Rat	Flow Cytometry	Biolegend
Anti-Mouse CD28	(557393)	Syrian Hamster	Flow Cytometry	BD Pharmingen

Anti-Mouse IgG (H+L) Alexa Fluor 647	(115-605-003)	Goat	Confocal Microscopy	Jackson Immunoresearch
Anti-Mouse IgG (H+L) Alkaline Phosphatase-conjugate	(115-055-003)	Goat	ELISA	Jackson Immunoresearch
Anti-Mouse IgG (H+L) Peroxidase-conjugate	(115-035-146)	Goat	Western Blot	Jackson Immunoresearch
Anti-Rabbit IgG (H+L) Peroxidase-conjugate	(115-035-003)	Goat	Western Blot	Jackson Immunoresearch
Anti-Rabbit IgG (H+L) Alexa Fluor 488	(A-11008)	Goat	Neutralization Assay	Thermo Fisher Scientific
Anti-Mouse CD11c APC- Cy™7	(561241)	Armenian Hamster	Flow Cytometry	BD Pharmingen
Anti-Mouse CD4 eFluor™ 450	(48-0041-82)	Rat	Flow Cytometry	eBioScience
Anti-Mouse CD4 PE-Cyanine7	(100528)	Rat	Flow Cytometry	Biolegend
Anti-Mouse CD62L FITC	(104405)	Rat	Flow Cytometry	Biolegend
Anti-Mouse CD62L PE	(12-0621-82)	Rat	Flow Cytometry	eBioScience
Anti-Mouse CD62L PE-Cyanine7	(25-0621-82)	Rat	Flow Cytometry	Invitrogen
Anti- Mouse CD8 PB	(558106)	Rat	Flow Cytometry	BD Pharmingen
Anti-Mouse CD8a eFluor™ 450	(48-0081-82)	Rat	Flow Cytometry	Invitrogen

Anti- Chlamydia specific LPS	CT403	Rabbit	Neutralization Assay	Statens Serum Institute
Fragment Goat Anti-Mouse IgG, Fcγ fragment specific R-PE	(115-116-071)	Goat	Flow Cytometry	Jackson Immunoresearch
Anti-Mouse IFN-γ FITC	(554411)	Rat	Flow Cytometry	BD Pharmingen
Anti-Mouse/Rat IL-17A (eBio17B7) PE	(12-7177-81)	Rat	Flow Cytometry	eBioScience
Anti-Mouse IL-17A PE	(559502)	Rat	Flow Cytometry	BD Pharmingen
Anti-Mouse IL-2 (JES6-5H4) FITC	(12-7021-82)	Rat	Flow Cytometry	eBioScience
Anti-Mouse IL-4 PerCP-Cy™5.5	(560700)	Rat	Flow Cytometry	BD Pharmingen
Anti-Mouse/Human IL-5 (TRFK5) PE	(12-7052-81)	Rat	Flow Cytometry	eBioScience
Anti-Mouse TNF APC-Cy™7	(560658)	Rat	Flow Cytometry	BD Pharmingen
Anti-Mouse TNF-α-APC/Cyanine7	(506344)	Rat	Flow Cytometry	Biolegend

2.5.2. Synthetic Peptides

The 138 overlapping peptides designed by Giuseppe Andreacchio in accordance to the CTH522 sequence tested as described in 3.4.3 can be found in **Supplementary Table 1**. Peptides were produced by peptides & elephants GmbH (Hennigsdorf, Germany) and dissolved in dimethyl sulfoxide (DMSO) at a stock concentration of 1 ug/uL unless otherwise specified.

Name	Sequence	Origin	MHC-II Restriction
B5R (46-60)	FTCDQGYHSSDPNAV	MVA/VACV	I-Ab
OVA (265-280)	TEWTSSNVMEERKIKV	Chicken Ovalbumin	I-Ab
49	DTTFAWSVGARAALW	CTH522	I-Ab
69	DYHEWQASLALSYRL	CTH522	I-Ab
NP	QVYSLIRPNENPAHK	Flu-derived nucleoprotein (NP)	I-Ab

2.5.3. Enzymes

Name	Manufacturer
*Afl*II	New England Biolabs
*Bam*HI-HF	New England Biolabs
*Bsr*GI-HF	New England Biolabs
DreamTaq DNA Polymerase	Thermo Fisher Scientific
*Pac*I	New England Biolabs
Proteinase K	AG Scientific
Quick Ligase	New England Biolabs
RNAse A	Qiagen
T4-DNA-Ligase	Roche
*XBa*I	New England Biolabs

2.6. Reagents and chemicals

Name	Manufacturer
100 bp DNA Ladder	New England Biolabs
Acetic Acid	Merck
Acrylamid	Sigma-Aldrich
Agarose	Biozym
Ammonium Sulfate	Sigma-Aldrich
Ammoniumperoxidsulfat (APS)	Sigma-Aldrich
Ampicilin	Carl Roth
Bacteriological Agar	Sigma-Aldrich
BD Cytofix/Cytoperm™ solution	BD Biosciences
BD Perm/Wash™ solution	BD Biosciences
BD Pharm Lyse™ Lysing Buffer	BD Biosciences
Bovine Serum Albumin (BSA)	Thermo Scientific
Brefeldin A (BFA)	Sigma Aldrich
Bromophenol blue	Merck
Calcium Chloride	Merck
Chloramphenicol	Sigma-Aldrich
Chocolate agar PolyViteX	Biomérieux
CutSmart® Buffer	New England BioLabs
Cycloheximide	Thermo Fisher Scientific
D-(+)-Glucose solution	Sigma-Aldrich
DAPI	Thermo Fisher Scientific
Dimethyl sulfoxide (DMSO)	Sigma-Aldrich
di-Sodium hydrogen phosphate dodecahydrate	Sigma-Aldrich

DMEM	Gibco
DreamTaq Green PCR Master Mix (2X)	Thermo Fisher Scientific
DTT (0,1 M)	Invitrogen
Dulbecco’s phosphate buffered saline (DPBS)	Gibco
Dulbecco's Modified Eagle Medium (DMEM)	Gibco
Enzyme buffers (10X)	New England Biolabs
Epoxomycin	Sigma-Aldrich
Ethanol	Merck
Ethidium Monazide Bromide (EMA)	Sigma-Aldrich
EZ-Vision® In-Gel Solution, 10000X	VWR
Fixable Viability Dye eFlour 660	eBioscience
Gel loading dye, Purple (6X)	New England Biolabs
Gentamicin	Sigma-Aldrich
Glycerol	Carl Roth
Glycine	Carl Roth
HEPES (1M)	Gibco
Hydrochloric acid (32%)	Carl Roth
HyperLadder™ 1kb	Bioline
Isoflurane	Piramal
Isopropanol	Merck
Kanamycin	Sigma-Aldrich
L-(+)-arabinose	Sigma-Aldrich
LB-Broth (Lennox)	Carl Roth
LE Agarose	Biozym
Lipofectamine™ 2000	Thermo Fisher Scientific
Magnesium Chloride	Merck
Methanol	Merck

Opti-MEM™	Gibco
P1, P2, P3 buffers (DNA isolation)	Qiagen
PageRuler™ Prestained Protein Ladder, 10 to 180 kDa	Thermo Fisher Scientific
Paraformaldehyde (PFA)	Merck
Pierce ECL Substrate	Thermo Fisher Scientific
Ponceau S	Sigma-Aldrich
Potassium Chloride	Sigma-Aldrich
Potassium Hydrogen Phosphate	Sigma-Aldrich
ProLong Glass Antifade Mountant	Thermo Fisher Scientific
Propidium Iodide	Invitrogen
Quick Ligase Reaction Buffer (2X)	New England Biolabs
Roth Skimmed milk powder	Sufocin
ROTI®Phenol/Chloroform/Isoamyl alcohol	Carl Roth
RPMI 1640	Sigma-Aldrich
Sodium Azide	Merck
Sodium Chloride	Sigma-Aldrich
Sodium Dihydrogen Phosphate	Sigma-Aldrich
Sodium dodecyl sulfate (SDS), ultrapure	Carl Roth
South America origin Fetal Bovine Serum (FBS) Supreme	PAN-Biotech
Succinic Acid	Sigma-Aldrich
SYBR™ Select Master Mix	Thermo Fisher Scientific
TEMED	VWR
TRIS	Carl Roth
Tris-Borate-EDTA (TBE) buffer, 10X	VWR
Triton™ X-100	Sigma-Aldrich
Trypan Blue Solution, 0.4%	Gibco

Trypsin-EDTA (0.05%), phenol red	Gibco
TurboFect Transfection Reagent	Thermo Fisher Scientific
Tween® 20	Merck
UltraPure™ DNase/RNase-Free Distilled Water	Invitrogen
Wheat Germ Agglutinin, Alexa Fluor™ 488 Conjugate (W11261)	Thermo Fisher Scientific
β-mercaptoethanol	Carl Roth

2.7. Media

Name	**Composition**
Culture medium	RPMI 1640 / DMEM
Freezing medium	FBS + 10% 2 um filtered DMSO
Growth medium	RPMI/DMEM + 10% inactivated FBS
Infection medium (MVA)	RPMI/DMEM + 2% inactivated FBS
Infection medium (C.t.)	McCoy media 5% Glucose 1:1000 Cycloheximide
Pre-infection medium (C.t)	McCoy media 5% Glucose
LB-Agar	35 g bacterial agar / L H_2O (1.5 % w/v)
LB-medium	20 g LB-Broth (Lennox) / L H_2O
M2 medium	RPMI 1640 10% inactivated FBS 28 µl 80% (v/v) β-mercaptoethanol

2.8. Buffers

Name	Composition	Application
10% Separating gel	10.5 ml 2 M Tris pH 8.8 22 ml H2O 19.8 ml Acrylamide 249 µl 20% SDS 597 µl 10 % APS 99.5 µl TEMED	Western Blot
10X Laemmli Running Buffer	250 mM Tris 2 M Glycine 1% SDS (w/v)	Western Blot
10X TBS-T	0.1 M Tris pH 8.0 1.5 M NaCl 0.5% Tween 20 (v/v)	Western Blot
10X transfer buffer (stock)	0.5 M Tris 0.4 M Glycine	Western Blot
1X transfer buffer (experimental use)	700 ml H2O 200 ml Methanol 100 ml 10X transfer buffer	Western Blot
5X sample loading buffer	250 mM Tris pH 6.8 30% Glycerol (100%) 12.5% β-mercaptoethanol 10% SDS 0.05% Bromophenol blue	Western Blot
Blocking buffer	3% BSA (w/v) 0.05% Tween 20 (v/v) in PBS	ELISA
Blocking buffer	5% milk powder (w/v) in TBS-T	Western Blot
CEB-Proteinase K (1 ml)	100 µl CEB 100 µl Proteinase K	DNA isolation

	25 µl 20% Tween 20 775 µl H2O	
Coating buffer	0.2 M carbonate/bicarbonate pH 9.4 in PBS	ELISA
Crude extraction buffer (CEB)	750 mM Tris 200 mM (NH4)2SO4 12 mM MgCl2 pH 8.8	DNA isolation
FACS buffer	5% BSA 0.02% NaN_3 in PBS	FACS
Fixing buffer	2% PFA	FACS
SPG Buffer	125 mL 1M sucrose 10 mL 0.5 M Na_2PO_4 pH 7.2 12.5 mL 0.2 L glutamic acid 352.5 mL H_2O	Neutralization Assay
Stacking gel	2.4 ml 0,5 M Tris/HCl pH 6.8 12.6 ml H2O 3 ml Acrylamide 90 µl 20% SDS 240 µl 10% APS 24 µl TEMED	Western Blot
Transfection Mixture	400 uL DMEM 5 ug BAC DNA 6 uL Turbofect	Transfection-Infection
Tyr-lysis buffer	50 mM Tris pH 8.0 150 mM NaCl 1% Triton X-100 0.02% NaN3	Protein sample storage
Wash buffer (ELISA)	8.1 mM NA2HPO4X12XH20 2.7 mM KCl 137 mM NaCl 1.47 mM KH3PO4	ELISA

	0.05% Tween20 in H_2O	
Dilution Buffer	1% BSA (w/v) 0.05% Tween 20 (v/v) In PBS	ELISA

2.9. Kits

Name	Manufacturer
Anti mouse Ig K/Negative control compensation particles set BD (552843)	Thermo FisherScientific
BD Cytofix/Cytoperm™ Fixation/Permeabilization Kit	BD Pharmingen
NucleoSpin™ Gel and PCR Clean-up Kit	Macherey-NageL
Phusion High-fidelity PCR kit	New England Biolabs
Phusion® High-Fidelity PCR Kit	New England Biolabs
Pierce BCA Protein Assay Kit	Thermo Fisher Scientific
QIAamp DNA Mini Kit	QIAGEN
QIAGEN® Plasmid Maxi Kit	QIAGEN
QIAprep Spin Miniprep	QIAGEN
QIAquick Gel Extraction Kit	QIAGEN
QIAquick PCR purification Kit	QIAGEN
Quick Ligation™ Kit	New England Biolabs
RNase-free DNase Kit	QIAGEN

2.10. Technical Equipment

Name	Manufacturer
AMG EVOS fl fluorescence microscope	Thermo Fisher Scientific
Analytical Balance ABJ 220-4NM	Kern & Sohn GmbH
Basic meter PB-11	Sartorius
Biometra TRIO - Triple Powered PCR thermal cycler	Analytik Jenna
Centrifuge: 5424R	Eppendorf
Centrifuge: 5810 R (microcentrifuge)	Eppendorf
Centrifuge: Fresco 21 (microcentrifuge)	Heraeus
Centrifuge: Heraeus Megafuge 16R	Thermo Fisher Scientific
Centrifuge: Heraeus Pico^{TM} 21	Thermo Fisher Scientific
CHEMOSTAR Touch ECL & Fluorescence Imager	Intas
CKX41 Inverted Microscope	Olympus Life Sciences
Comb 1 mm, 10 teeth, 5.3 mm wide, vol. 65 µl	neolab
Eporator	Eppendorf
FACSCanto II Diva	BD Biosciences
FiveEasy pH meter F20-Std-Kit	Mettler Toledo
Gammacell 1000 Elite	Nordion international
Gel chamber Midi arge vertical HIO, complete	NewoLab

Gel electrophoresis chamber Maxi vertical HIO, complete	NewoLab
Gel electrophoresis chamber Mini vertical, complete	neolab
Heating plate MR Hei-Tec	Neolab
Heracell™ 150i CO2 incubator with stainless steel chamber, TCD sensor, 230 V	Thermo Fisher Scientific
Ice Flaker AF124	Scotsman
M-20 Microplate Swinging Bucket Rotor (75003624)	Thermo Fisher Scientific
Magnetic shaker St. 5	Neolab
MaxQ™ 4000 Bench orbital shaker	Thermo Fisher Scientific
Mr Hei-Tec Heidelberg Hot Plate	Neolab
MTS 4 MTP Microplate Shaker Mixer	IKA
Multiskan GO	Thermo Scientific
NanoDrop™ 2000/2000c Spectrophotometers	Thermo Scientific
Neolab 1 2503 Neoblock Heater Mono I with no pad	NeoLab
Power supply MP 3AP	Major science
Power Unit I	Cheyenne
Precision Balance EW 4200 2NM	Kern & Sohn GmbH
Scanlaf Mars Class 2 Safety Cabinet	Labogene
Semidry Blot – Complete System	neolab
Shaking Water Bath 1083	GFL
Sharp forceps HSC 801-11 115 mm	Hammacher

SHKE4000: MaxQ™ 4000 Benchtop Orbital Shaker	Thermo Fisher Scientific
Sonopuls HD 2200	Bandelin
ST 5 rocking shaker	CAT
ThermoMixer C (comfort)	Eppendorf
TX-400 4 x 400mL Swinging Bucket Rotor (75003629)	Thermo Fisher Scientific
ULE 400 Incubator	Memmert
Vortex-Genie 2	Scientific Industries

2.11. Consumables

Name	**Manufacturer**
12-well plates	VWR
12-well tissue culture treated nonpyrogenic polystyrene plate	Corning
15 mL Centrifuge Tubes	Corning
24-well plates	VWR
24-well tissue culture treated nonpyrogenic polystyrene plate	Corning
48-well tissue culture treated nonpyrogenic polystyrene plate	Corning
50 mL Centrifuge Tubes	Corning
60 mm Surface Treated Tissue Culture Dishes	VWR
6-well plate	VWR
6-well tissue culture treated nonpyrogenic polystyrene plate	Corning

96-well cell culture cluster Flat Bottom with lid tissue culture treated nonpyrogenic polystyrene plate	Corning
96-well plate	VWR
BD Microlance™ 3 Needle	BD
BD Plastipak Syringe 1 ml	BD
Cell scraper (medium)	TPP
Cell scraper (small)	TPP
Cell strainer 70 µm	VWR
DeckWorks Reload Systems	Corning
Falcon tube (15 ml)	Cellstar
Falcon tube (50 ml)	Cellstar
Filter 0.2 µm	GE Healthcare Life Sciences
Filter 0.45 µm	GE Healthcare Life Sciences
Filter tip 1000 µL XL Graduated	TipOne, Starlab
Filter tip 20 µL Bevelled	TipOne, Starlab
MiniCollect® TUBE 0.8 ml CAT Serum Separator	greiner bio-one
Nitrocellulose blotting membrane 0.45 µm	GE Healthcare Life Science
Nunc EasYFlask 175 cm^2 Nunclon Delta Surface	Thermo Fisher Scientific
Nunc EasYFlask 25 cm^2 Nunclon Delta Surface	Thermo Fisher Scientific
Nunc EasYFlask 75 cm^2 Nunclon Delta Surface	Thermo Fisher Scientific

PCR tubes 0.2 ml 8-Strip	Starlab
Petri Dish 100 mm	Thermo Fisher Scientific
Serological pipette 10 ml	Sarstedt
Serological pipette 2 ml	Sarstedt
Serological pipette 25 ml	Sarstedt
Serological pipette 5 ml	Sarstedt
Stripette® 10 ml	Costar
Stripette® 25 ml	Costar
Stripette® 5 ml	Costar
Syringe 0.5 ml 0.3 mm gauge	BD Plastipak
Syringe 5 mL	BD
Tissue culture dish 100 mm (sterile)	TPP
Tissue culture dish 60 mm (sterile)	VWR
Titertube® Micro Test Tubes	Bio-Rad
Tube 1.5 ml	Sarstedt
Tubes 2.0 ml	Eppendorf
Universal Fit 1000 µL Pipet Tips	Corning
Universal Fit 1-30 µL Pipet Tips	Corning
Universal Fit 200 µL Pipet Tips	Corning
Whatman paper	GE Healthcare Life Sciences

3. METHODS

3.1. Molecular Biological Methods

3.1.1. DNA Restriction digestion

In order to clone the sequence of CTH522:B7 into the plasmid pEP-MVAdVI-PmH5, New England Biolabs (NEB) restriction enzymes were used according to the manufacturer's instructions. Firstly, 5 ug of the plasmid pEP-MVAdVI-PmH5, 10 uL of CutSmart buffer, 2 uL of *Bam*HI (High-Fidelity) and 2 uL of *Afl*II were mixed on a tube before reaching 100 uL of final volume with water. At the same time, 5 ug of the plasmid pUC57-CTH522-B7opt (kindly provided by Matias Ciancaglini, Basel University), 10 uL of CutSmart buffer, 2 uL of *Bam*HI (High-Fidelity) and 2 uL of *Afl*II were transferred to a tube before reaching 100 uL of final volume with water. Tubes were left to incubate for 1 hour at 37 ºC before proceeding to their detection in an agarose gel under UV light.

With the objective of preparing pEP-MVAdVI-CTH522:B7 for bacterial electroporation, *Pac*I was used as a restriction enzyme using the same procedure as just described.

3.1.2. Agarose gel electrophoresis

In order to visualize the DNA fragments, a 0.8 % (w/v) agarose-TBE gel was prepared by adding the agarose onto 1X TBE and boiling the solution until the powder was completely dissolved. A drop of EZ vision in-gel solution was added per 100 mL of agarose-TBE mixture for visualization purposes and the solution was then poured onto a chamber where it was allowed to cool for 1 hour. Once solidified, 6X DNA-loading buffer was added to digests and the samples were then transferred onto the gel pockets along with a 1kb HyperLadder as a size marker to measure the DNA fragments during analysis. The gel then ran for 1 hour at 130 V or until the loading buffer was visible at the bottom of the gel. Next, the DNA digests were visualized with a UV-transilluminator and carefully cut out with a sterile scalpel.

3.1.3. DNA purification

DNA purification and PCR clean-up were performed following the protocol of Macherey-Nagel™ NucleoSpin™ Gel and PCR Clean-up Kit. Fragments were weighed

in a 1.5 mL tube and 200 uL buffer NTI were added for every 100 mg of the agarose gel slice. Samples were then incubated between five and ten minutes at 50 ºC, vortexing the tubes every 2 minutes until the gel was completely dissolved in the buffer. A Nucleospin Gel and PCR Clean-up column were then placed into a collection tube and up to 700 uL of the sample were loaded onto it before both the column and the collection tube were centrifuged for 30 seconds at 16000 rcf. The flow-through was then discarded and the column was placed back onto the collection tube for an additional 700 uL of the sample to be added. This step was repeated as necessary and, once all the entire sample volume had run through the column, 700 uL of Buffer NT3 was added to the column and centrifuged for 30 seconds at 16000 rcf. Flowthrough was discarded and this step was repeated in order to avoid chaotropic salt carry-on and achieve a higher purity. Samples were then centrifuged for 1 minute at 16000 g in order to remove the Buffer NT3 completely and the column was then placed into a clean 1.5 mL tube to incubate for 5 minutes at 70 ºC before and after elution with pre-warmed buffer NE in order to increase DNA concentration. After centrifuging for 1 minute at 16000 rcf, the volume in the 1.5 mL tube was collected and placed on top of the column. Samples were incubated at 70 ºC for five minutes and centrifuged for 1 minute at 50 g and for 1 minute at 16000 g. This step was repeated thrice and samples were then stored at 4 ºC before measuring their concentration with NanoDrop 2000 photometer. Then, samples were stored at -20 ºC.

3.1.4. DNA ligation

With the objective of inserting the CTH522:B7 fragment into pEP-MVAdVI-PmH5, a vector:insert molecular ratio of 1:3 was used in the ligation and the method was performed according to the Quick Ligation kit from New England biolabs. Shortly, vector and insert volumes were mixed with 10 uL 2X QuickLig buffer and 1 uL Quick ligase. Water was then added to attain a final volume of 20 uL and the mixture was left to incubate for 10 minutes at 25 ºC and immediately used in bacterial transformation.

3.1.5. Transformation

A 50 uL aliquot of chemically competent XL-1 Blue *Escherichia coli* bacteria was thawed on ice for ten minutes before adding the ligation reaction previously prepared and stirring carefully with a pipetting tip. After a 30-minute incubation on ice, the bacteria were heat-shocked by transferring them to 42 ºC for 1 minute and 900 uL of pre-warmed SOC medium were added. Tubes were then placed on a shaking apparatus and left to

incubate at 37 ºC for one hour. Due to the lack of data in reference to the cell concentration in the tubes and with the intention of accounting for an overgrowth or undergrowth possibility, two lysogeny broth (LB) agar plates plate supplemented with antibiotics (kanamycin in the case of the pEP-MVAdVI-CTH522) for positive colony selection were usually prepared; one with a higher concentration and one with a lower concentration of bacteria. For this, 100 uL of the solution were streaked on an LB agar plate and the rest was centrifuged at 1500 g for 2 minutes at room temperature. The pellet was resuspended in 100 uL of LB medium which were consequently streaked into another LB agar plate. LB agar plates were left at 37 ºC overnight or until colony growth became apparent. The following day, a dozen colonies were picked from the plates and left to incubate in 4 mL LB medium supplemented with the corresponding antibiotics overnight at 37 ºC in a shaking apparatus at 1.6 g. Next, DNA would be isolated from the bacteria as described below.

3.1.6. DNA isolation from bacteria

In case of BAC DNA being isolated, tips with cut ends should be used to avoid shearing because of the large size of the DNA itself.

Bacteria were cultured overnight at 37 ºC on a subtle agitation The following day, the tubes were centrifuged at 6000 g for 4 minutes at 4 ºC before discarding the supernatant and carefully removing the remaining liquid from the pellets. From then on, all steps were completed on ice. The pellets were resuspended in 250 uL P1 buffer (with RNAse) from Qiagen NucleoSpin® Gel and PCR Clean-up kit. Next, 350 uL of P2 buffer were added and the tubes were inverted five times, leaving the samples to incubate on ice for 4 minutes before adding 350 uL of P3 buffer and inverting the tubes another 5 times. The mixture was left to incubate for 15 minutes on ice and then centrifuged for 5 minutes at 18500 g. Then, 700 uL were transferred to a clear 1.5 mL tube and 700 uL of phenol-chloroform-isoamyl alcohol were very carefully added before gently mixing the two liquids. After a new centrifugation of 18500 g for 2 minutes, three layers were immediately visible, and 500 uL of the clear upper phase were transferred to another 1.5 mL tube, where 450 uL of isopropanol were added. Tubes were then vortexed and left to incubate on ice for 1 hour. Subsequently, in order to precipitate the DNA, tubes were centrifuged at 18500 g for 30 minutes at 4 ªC and the supernatants were discarded. To get rid of any residual isopropanol, 500 uL of 70% EtOH was added to each sample, and tubes were centrifuged at 18500 g for 10 minutes before discarding the supernatants and letting the pellet to dry for one hour at room temperature.

Pellets were then resuspended in 50 uL of TE buffer and left at 4 ºC for at least 1 hour in order to ensure the DNA has completely dissolved before or until their concentration was to be analyzed with NanoDrop 2000 photometer.

3.1.7. DNA Recombination

With the objective of generating the MVA vector MVA-CTH522:B7, *en passant* BAC mutagenesis was performed between the transfer DNA vector pEP-MVAdVI-CTH522:B7 (containing two homologous regions to the deletion VI of the MVA genome) and the viral genome itself. In order to achieve this, the MVA genome had been previously inserted in electrocompetent E. Coli GS1783 #22, a bacterial artificial chromosome (BAC), which would allow for the homologous recombination of the DNA vector into the viral genome found within the bacteria. (Karsten Tischer et al., 2010). Furthermore, within the deletion III locus of MVA, a self-exicing BAC cassette contained a GFP gene for the correct monitoring of infected cells throughout MVA generation and to confirm the self-exicion of the cassette itself (Cottingham & Gilbert, 2010).

For this first recombination, a 50 uL aliquot of the GS1783 #22 bacteria was thawed on ice for 10 minutes before 100 ng of the purified single stranded DNA vector (which, as mentioned before, included two homologous regions to the deletion VI of the MVA genome as well as an I-*Sce*I-kanamycin cassette for positive colony selection and the PmH5 promoter) was added to it and gently stirred with cut ends tips (used for the remaining of the method). The mixture was then moved to a 1 mm cuvette that had been chilled on ice for 10 minutes before it was pulsed at 1.5kV, 200 Ω, 25 μF. Immediately following the pulsing, 1 mL of pre-warmed LB medium was added and the mixture was then transferred into a 1.5 mL tube to be incubated at 32 ºC for 2 hours on a shaking apparatus. Just as previously described, two LB agar plates (this time containing 30 uL/mL of chloramphenicol (CAM) and 30 ug/mL kanamycin (KAN)) were used; 100 uL of the undiluted bacterial mixture was plated on one of them before the tube was centrifuged at 90 g for 3 minutes at room temperature for the pellet to be resuspended in 100 uL of fresh LB medium that was then plated on the second LB agar plate. Both plates were incubated for 48 hours at 32 ºC.

After the two days had passed, sixteen colonies were picked and transferred to 15 uL of PCR grade water in 1.5 mL tubes that were then flicked for them to dissolve. Once the colony was completely dissolved, 2 uL of each of the mixtures were then plated on an LB agar plate (supplemented with CAM and kanamycin just as described above) and left to grow at 32 ºC between 24 and 48 hours to use in the following second recombination.

In order to test that the colonies positively included the vector, the rest of the mixture was incubated at 95 ºC for 10 minutes to lysate the DNA to perform a colony PCR. Primers annealing in the flanking region and the CTH522 sequence were used in order to confirm the presence of the insert; an empty transfer plasmid and the DNA vector pEP-MVAdVI-CTH522:B7 were both used as a negative and positive control respectively.

Once positive colonies had been identified, a colony was selected to continue on with the second recombination. This colony was picked from the plate that had been left to incubate and transferred to 1 mL LB supplemented with 30 ug/mL CAM and left to incubate for four hours at 32 ºC in a shaking apparatus. Then, 1 mL LB containing 30 ug/mL CAM and 2% L-arabinose (since the I-*Sce*I endonuclease gene is found under the control of a promoter inducible by arabinose) was added to the tube which was then incubated in a shaking apparatus for one hour at 32 ºC (which would trigger the I-*Sce*I endonuclease induction in order to eliminate the kanamycin resistance gene from the MVA BAC), 30 minutes at 42 ºC (to induce the homologous recombination of the sequences present at both sides of the kanamycin cassette) and an additional 2 hours at 32 ºC. Afterwards, optical density (OD) at wavelength 600 nm was measured with Multiskan GO and 10 uL were taken out of a 1:100 dilution (if OD600 was found to be $\leq$ 0.5) or out of a 1:1000 (if OD600 was found to be > 0.5) to be plated on LB agar plates containing 30 ug/mL CAM and 1% L-arabinose at 32 ºC for 24 to 48 hours depending on colony growth.

Colonies were picked and treated as previously described for the first recombination. When plated, a 30 ug/mL CAM and 1% L-arabinose supplemented LB agar plate was used. For the colony PCR, primers annealing in the flanking region and the CTH522 sequence were used in order to confirm the presence of the insert; an empty transfer plasmid was used as a negative control and the DNA vector pEP-MVAdVI-CTH522:B7 was used as both a positive control and to check for the proper excision of the kanamycin cassette in the positive colonies due to the difference in size.

Positive colonies were picked from the agar plate that had been left incubating and they were then cultured in 5mL LB supplemented with 30 ug/mL CAM in a shaking apparatus between 24 and 48 hours. Once it had grown, 1mL was transferred to a tube containing 1mL 100% sterile glycerol and stored at -80 ºC. The remaining 4 mL were used as previously described for DNA isolation before moving on to the viral progeny rescue (described in cytological methods).

3.1.8. Isolation of viral DNA

In order to isolate DNA from cell cultures, crude extraction buffer was prepared with the addition of proteinase K (CEB-PK). Cells were centrifuged at 15000 rpm for 2 min at room temperature and the supernatant was removed in order to resuspend the pellet in 20 uL of CEB-PK. Samples were then incubated at 56 ºC for 3 hours before inactivating the proteinase K by incubating the samples at 96 ºC for 12 minutes. Samples were stored at -20 ºC for short term and -80 ºC for long term.

3.1.9. Polymerase Chain Reaction (PCR)

PCR was performed according to manufacturer's instructions from Phusion high-fidelity PCR kit (used for general cloning purposes) or DreamTaq Green PCR master mix (used for analysis such as colony PCR).

The PCR program used for the so-called colony PCR was as follows: 5 minutes at 94 ºC, 1 minute at 94 ºC for the initial denaturation, 1 minute at 62 ºC for the annealing step, 30 cycles of 1.5 minutes at 72 ºC for elongation, 5 minutes at 72 ºC for the final elongation. The primers used to test whether or not the GFP cassette had been efficiently removed were GFP F.P (TTGTACAGCTCGTCCATGCCGAG) and GFP R.P (GCAAGGCCGGATCTGGGAATTC). The primers used to check if the RFV was found in the sample were RFV fwd (AAAGATGCGTACATTGGACCC) and RFV rev (GTTCGAGACTAGAAAAGCGCC). The primers used to ensure the proper insertion of CTH522:B7 or mLi:CTH522 were RT_CTH522-1_fwd and RT_CTH522-3_rev.

3.1.10. DNA sequencing

In order to confirm the correct insertion and genomic engineering of different DNA sequences, including plasmid DNA and purified DNA products, samples were sent to be sequenced at Eurofins Genomics Germany GmbH according to the instructions of their TubeSeq service.

3.2. Cytological Methods

3.2.1. Cell Culture

Unless otherwise specified, all cells were cultured in RPMI medium with 10% heat-inactivated Fetal Bovine Serum (FBS) in an incubator containing 5% CO_2 at 37 ºC.

BMDCs were cultured in M2 medium Medium (RPMI 1640 with 10% inactivated FBS and 50 uM β-mercaptoethanol) and 10% GM-CSF (supernatant from B16 cells expressing GM-CSF now used as conditioned medium). Cells were passaged every two to three days depending on when they had reached 80-90% confluency. For this, the supernatant of the flasks was removed and discarded, and cells were briefly washed with PBS to remove any residual medium before adding 0.05% Trypsin-EDTA in order to efficiently detach the cell monolayer from the cell culture flask. Flasks were left in the incubator at 37 ºC for five minutes before visually confirming that the cells had successfully detached. Then, trypsin was neutralized by adding pre-warmed RPMI medium in a ratio of 1:3 Trypsin-EDTA:RPMI to the flask and the cell mixture was transferred over to a tube to centrifuge at 1500 rpm for 5 minutes at room temperature. After discarding the supernatant, the pellet was resuspended in fresh RPMI and split in a ratio according to the experimental requirements before being left at 37 ºC. When cell counting was required, a sample of the cell suspension after its centrifugation was mixed with Trypan Blue in a 1:5 ratio to count the living cells with the use of a Neubauer chamber.

3.2.2. Transfection and recMVA BAC-rescue

Due to the use of BAC-DNA in the transfection, tips with cut ends were used throughout the process. In order to account for technical error, two or more duplicates were performed each time. DF-1 cells were seeded on 6-well plates at 80% confluency and left to incubate at 37 ºC while the transfection mixture was prepared and incubated for 20 minutes at room temperature. The supernatant from the cells was removed and discarded and the transfection mixture was carefully added drop by drop onto the cell monolayer. After a 3-hour incubation at 37 ºC, the supernatant was removed once again and infection with Rabbit Fibroma Virus (RFV) at multiplicity of infection (MOI) = 1 was performed by diluting the virus in 100 uL DMEM 10% FBS that was slowly added onto the well. The plate was manually rotated for the inoculum to thoroughly cover the entirety of the DF-1 monolayer and it was then incubated for 1 hour at 37 ºC; every 15 minutes, the plate was manually rotated for approximately 10 seconds before being put back in the incubator. Then, 2.5 mL DMEM 10% FBS was added into each well and the plate was left to incubate for 48 to 96 hours at 37 ºC. Cells were checked on a daily basis in order to find Green Fluorescent Protein (GFP) positive plaques covering over 50% of the monolayer. When this was the case, cells were harvested by scraping and transferred to a 15 mL Falcon in order to be centrifuged at 4000 rpm for 10 minutes at 4 ºC. The supernatant was discarded and the pellet was resuspended in 500 uL DMEM and taken

through 3 cycles of freezing and thawing before being sonicated for 1 minute a total of 3 times. The transfected cells were stored at -80 ºC until further use.

3.2.3. Selection of infected monolayers with GFP- and CPE+ cells (plaques)

With the purpose of allowing the virus to naturally lose the GFP cassette, fresh DF-1 cells were plated at approximately 80% confluency and a serial dilution (10^{-1} to 10^{-5}) was prepared with the culture of the previously transfected cells. Then, 200 uL of each dilution was transferred to a different well on top of the uninfected cells. This was considered to be the first passage, as it was left to incubate at 37 ºC for four to seven days according to when the cells displayed the most cytopathic effect (CPE). Once one of the higher dilutions (usually 10^{-4} or 10^{-5}) would show cell monolayers with high CPE (and, additionally, a lower green brightness as the virus loses the GFP cassette), it would be harvested via gentle scraping and centrifuged for five minutes at 1500 rpm. The pellet was resuspended in 500 uL of RPMI and taken through 3 cycles of freezing and thawing before being sonicated for 1 minute a total of 3 times. This step was repeated a minimum total of three times (namely, three passages) or until the GFP was no longer visible through light microscopy.

Next, intending to select a single viral clone from that last passage, DF-1 cells were seeded in 96-well plates at 80% confluency. Serial dilutions (10^{-1} to 10^{-9} at least) were prepared with the aliquot from the last passage and each of the last four dilutions (10^{-6} to 10^{-9}) were transferred onto each plate by adding 100 uL per well. Plates were then incubated at 37 ºC and evaluated daily after the fourth day in order to check for GFP^- and CPE^+ cells (plaques) in each well. Seven days after the initial infection, twelve wells were selected and harvested based on those criteria. Half of each aliquot was frozen at -80 ºC for further use and the other half was transferred to a different aliquot in order for the viral DNA to be extracted as previously described in 3.1.8. The viral DNA was then used for a PCR in order to test for samples that were GFP- and RFV^- all the while showing that CTH522 was properly inserted. Proper controls such as RFV material for the PCR testing for residual RFV content in the culture, a recMVA not containing CTH522 and material from the second recombination of CTH522:B7 (containing the GFP cassette) were used.

3.2.4. recMVA amplification and crude stock generation

Based on the PCR results, one of the colonies was chosen in order to continue with the amplification process and subsequent purification. Therefore, 50 uL of the viral

aliquot stored at -80 ºC was used to infect previously seeded DF-1 cells at 80% confluency in a 6-well plate. The plate was then left to incubate at 37 ºC for 48 hours or until CPE was observed, at which point the cells were harvested via scraping and centrifuged at 1500 g for 10 min. The pellet was resuspended in 1 mL and underwent sonication for three minutes before three cycles of freezing and thawing. The viral aliquot was stored at -80 ºC before 500 uL (in 10 mL 2% FBS RPMI) were used to infect 1 182.5 cm^2 flask (T-182.5) of DF-1 cells previously seeded. The infection was left to incubate at 37 ºC undergoing subtle agitation every fifteen minutes for an hour before 15 mL prewarmed 2% FBS RPMI was added. Flask was then left to incubate at 37 ºC for 48 hours or until CPE was observed, at which point the cells were harvested via scraping and centrifuged at 1500 g for 10 min. The pellet was resuspended in 1 mL and underwent sonication for three minutes before three cycles of freezing and thawing. The aliquot was stored at -80 ºC before 500 uL were used to infect 10 T-182.5 flasks of DF-1 cells as just described. In order to harvest this infection as what was termed as the "crude stock" of MVA-CTH522:B7 (as it is the unpurified stock that will not be used for future experimentation), cells were harvested as just described but the pellet was resuspended in 6 mL 10 mM Tris Buffer pH = 9. The crude stock was stored at -80 ºC until further use.

3.2.5. Working stock generation and purification

With the objective of generating what was termed as the "working stock" (as it will be purified and therefore used for further experimentation), 40 T-182.5 flasks were seeded with DF-1 cells at 80% confluency and infected at MOI = 1 with the crude stock. After approximately 72 to 96 hours or when the monolayers exhibited sufficient CPE (determined as when 70-80% of the cells showed CPE), cells were harvested by scraping. The supernatants were then transferred into ultracentrifuge buckets that were balanced with each other using 10 mM Tris Buffer pH = 9 in order to centrifuge them with a previously chilled ultracentrifuge rotor (A-621) at 16000 rpm for 90 minutes at 4 ºC. Then, the supernatant was carefully discarded and the pellets were resuspended in 10 mL 10 mM Tris Buffer pH = 9 a total of three times in order to ensure the maximum possible collection of the virus material. Samples were sonicated for three minutes and underwent three cycles of freezing and thawing before being stored at -80 ºC for its future purification.

An ultrasonic needle was disinfected with 80% ethanol and 20 minutes under UV light in order to be used for the sonication of the virus containing material previously harvested. After three 15-second cycles of sonication at 76% power on ice, the sample

was centrifuged at 1500 g for 5 minutes at 4 ºC and the supernatant was transferred to a new 50 mL Falcon tube. The pellet was then resuspended with 10 mL 10 mM Tris Buffer pH = 9 before undergoing another three rounds of sonication as just described and the supernatant was pooled with the one from the previous round. Samples were kept on ice through the viral purification.

Ultracentrifuge tubes for rotors AH 626-17 and 626-36 had been placed at 4 ºC the previous night in order to chill before their use, and they were then placed under UV light for 20 minutes to ensure their sterilization. Then, 25 mL of 36% sucrose solution were placed on each of four 36 mL polyallomer (PA) vials that had already been autoclaved. The virus supernatant was gently placed on top of the four sucrose cushions (equally transferred among them with approximately 5 mL per tube). The PA vials were then placed inside the ultracentrifuge tubes corresponding to the AH 626-36 rotor before being filled within millimeters of the brim and balanced with 10 mM Tris Buffer pH = 9. Samples were then centrifuged at 13500 rpm for 1 hour at 4 ºC and the supernatant was discarded (gently removed by initially pipetting the most of it and decanting any leftover fluid by placing the PA vials down on paper towels that had been saturated with 80% EtOH for 5 minutes). Pellets were resuspended with 5 mL of 10 mM Tris Buffer pH = 9 and transferred into a clean 50 mL Falcon tube. An additional 5 mL of 10 mM Tris Buffer pH = 9 was used to wash any remains of the pellet in order to ensure the maximum possible collection of the virus material. Next, 12 mL of 36% sucrose solution were placed on each of four 17 mL PA vials that had also been autoclaved before. The supernatant from the initial centrifugation was carefully transferred to the four sucrose cushions and the vials were placed within tubes for the AH 626-17 rotor before being filled and balanced with 10 mM Tris Buffer pH = 9 as just described. Tubes were then centrifuged at 13500 rpm for 1 hour at 4 ºC before removing the supernatant as just described and resuspending the pellets with 500 uL 1 mM Tris Buffer pH = 9 twice. This purified virus stock was considered to be the working stock and would be titrated, aliquoted and kept at -80 ºC for its further use.

In order to guarantee that the working stocks of recMVAs were free of any contamination, three different tests were completed. First of all, a small amount of the working stock (2-5 uL) was placed on chocolate agar plates that were kept at 37 ºC for a maximum of five days, after which, if the plate had remained clear, the stock was marked as fungi free. At the same time, another small amount of the working stock (2-5 uL) was plated on a LB agar plate without any antibiotics and kept at 37 ºC for a maximum of two days, after which, if the plate had remained clear, the stock was labelled as bacteria free.

Lastly, to determine whether or not there was mycoplasma contamination, the supernatant from cells that had been infected with the working stock for two days was tested with PCR.

3.2.6. Infection of cells with MVA

All viruses were kept at -80 ºC and thawed in a water bath at room temperature moments prior to their use. Once thawed, they were vortexed and sonicated three times in a cycle of 10 second sonication and 10 second pause.

Adherent cells (such as DF-1, HeLa or Cloudman cells) were cultured and seeded as previously described in 3.2.1. for infection. At the point of infection, supernatant was removed and the virus material was added in a small amount of RPMI medium without FBS (in the case of 6-well plates, as most infections were performed in them, 500 uL of the inoculum were used). Cells were then left to incubate at room temperature for 1 hour for the adsorption of the virus to the surface of the cells, during which the plates were gently rotated every fifteen minutes for the homogenous distribution of the virus among the monolayer. Afterwards, the fluid was carefully removed by pipetting and 5% FBS RPMI was added and removed in order to gently wash out any remnants of the viral inoculum. Finally, 5% FBS RPMI was added, systematically marking this as the 0 hour timepoint of the infection (0 hpi). Cells were kept at 37 ºC for the desired time of infection and would be then harvested via scraping or by EDTA addition.

Semi-adherent cells (such as BMDCs) were cultured as described in 3.2.8. and would be harvested by gentle scraping of the plates before transferring them over to 50 mL falcons and centrifuging them at 200 g for 5 minutes. The supernatant was discarded and the pellet was resuspended for cell counting as previously described. For infection, cells were transferred to 15 mL Falcon tubes (1 million cells per 200 uL medium with a maximum of 400 uL per Falcon tube to avoid clumping of the cells that would lead to an inefficient infection). Cells were then left to incubate at room temperature for 1 hour for the adsorption of the virus to the surface of the cells, during which the Falcon tubes were gently shaken every fifteen minutes to maintain them in suspension and allow the homogenous distribution of the virus between the cells. Afterwards, 1 mL M2 was added and samples were centrifuged at 1500 RPMI for 5 minutes in order to wash out the inoculum. The medium was then discarded and the infected cells were seeded in a 6-well plate before placing them in the incubator at 37 ºC for the duration of the infection.

3.2.7. Viral growth kinetics and titration

To characterize the recMVAs and ensure that the inclusion of a foreign antigen had not negatively impacted the replication behavior and capacity of the virus, growth kinetics were performed in a permissive cell line (DF-1), a semi-permissive cell line (HeLa) and a non-permissive cell line (Cloudman or BMDCs).

In the case of the replication capacity study (termed one-step growth kinetics), cells were infected at MOI = 5 as previously described and harvested at 0, 4, 8 and 24 hours post infection (hpi) by scraping. Samples were centrifuged at 200 g for 5 minutes and the supernatant was discarded for the pellet to be resuspended in 500 uL RPMI. Samples were kept at -80 ºC for further use.

On the other hand, in the case of the replication behavior study (termed multi-step growth kinetics), cells were infected at MOI = 0.01 as previously described and harvested at 0, 24, 48 and 72 hpi by scraping. Samples were centrifuged at 200 g for 5 minutes and the supernatant was discarded for the pellet to be resuspended in 500 uL RPMI. Samples were kept at -80 ºC for further use.

In order to titer any viral material, the 50% tissue culture infectious dose ($TCID_{50}$) assay was used, a series of endpoint dilutions used to determine the infectious viral titer within samples. For this, a 96-well plate was seeded with DF-1 cells at 80% confluency with 100 uL 5% FBS RPMI. In order to account for the future calculations for the titer, six serial dilutions (10-fold) were prepared for each titer, ranging from 10^{-1} to 10^{-6} (for samples infected with non-permissive cell lines), 10^{-3} to 10^{-8} (for samples infected with replicative cell lines), 10^{-6} to 10^{-11} (for samples infected with the working stock), or others depending on the predicted infectious dose of the sample. The initial dilution (10^{-1}) was prepared by adding 60 uL of the sample to 540 uL of 2% FBS RPMI and vortexing before preparing the following dilution by taking 500 uL of this first dilution and adding them to 4.5 mL 2% FBS RPMI, vortexing once again. From then on, serial dilutions were carried out by taking 500 uL of the previous dilution and adding them to 4.5 mL 2% FBS RPMI to prepare the next dilution, vortexing in between steps to properly dilute the viral material within the medium. Once the serial dilutions were prepared, 100 uL of the first dilution to be used were transferred to the wells in the first column of the 96-well plate; 100 uL of the second dilution to be used were transferred to the second and third column; 100 uL of the third dilution to be used were transferred to the fourth and fifth column; 100 uL of the fourth dilution to be used were transferred to the sixth and seventh column; 100 uL of the fifth dilution to be used were transferred to the eight and nineth column; 100 uL of the sixth dilution to be used were transferred to the tenth and eleventh column.

In the end, 100 uL of 2% FBS RPMI was added to wells acting as mock controls to the infection. Plates were then left to incubate at 37 ºC for a total of 7 days before visually studying the number of wells exhibiting viral plaques under light microscopy. In order to calculate the viral titer, the Spearman-Kärber method was used by introducing the noted data into the following formula in order to calculate the 50% end point:

$$\text{viral particles/mL} = 10^{\,a + 0.5 + \sum (b/n)} \times 10$$

a = the highest dilution exhibiting CPE in all wells

b = number of wells with CPE in the next dilutions

n = number of wells per dilution (in the case of this dissertation, 8 wells was the number chosen for the study, and the number of wells noted down for a and be were divided in half to account for this)

3.2.8. Bone Marrow Derived Dendritic Cells (BMDCs) preparation

BMDCs were isolated from 12-16 weeks old female C57BL/6 mice after their sacrifice via cervical dislocation. Femurs and tibiae from the mice were severed and the skin and muscle tissue around the bones was carefully removed before briefly dipping the bones into 70% EtOH and placing them in a 6 cm dish with 10 mL M2 medium. Both ends of the bone were cut off and discarded, and then the bone marrow was flushed with a 1 mL sterile syringe loaded with fresh M2 medium. The bone marrow was flushed a minimum of three times or until the bone ends appeared white, having lost the reddish color indicative of the bone marrow presence. The bone marrow was then transferred into a 50 mL falcon and the dish where it had been flushed into was washed twice with 5 mL M2 medium and transferred to the falcon in order to collect any residual bone marrow. Cells were centrifuged at 1500 rpmi for 5 minutes and the medium was discarded by carefully decanting. Erythrocytes were lysed by quickly resuspending the pellet in 5 mL lysis buffer (dH2O + 10x BD Erythrolysis buffer, diluted 1:10 in deionized H_2O) and incubating at room temperature for a maximum of 1 minute. The cell suspension was filled up to 40 mL with M2 medium to neutralize the lysis buffer and filtered through a 0.75 um nylon filter before centrifuging at 200 g for 5 minutes. The supernatant was discarded and the pellet was resuspended in 5 mL M2 medium in order to be counted as previously described with a Neubauer cell counting chamber. A total of 5 x 10^6 cells were seeded per 94x16 mm dish with 10 mL M2 medium and 10% GM-CSF. Plates were left to incubate at 37 ºC with this effectively serving as day 0 of the BMDC culturing. On day 3, 10 mL of M2 medium with 10% GM-CSF were added to each dish. On day 6, 10 mL

of the supernatant is removed and replaced with 10 mL of fresh M2 medium containing 10% GM-CSF. On day 7, cells are collected and used for further experiments.

3.2.9. Isolation of Splenocytes

Spleens were isolated from 10-12 weeks old C57BL/6 mice after their sacrifice via cervical dislocation. An incision of approximately 2 cm is made on the left side of the mouse parallel to the midline with fine scissors previously sterilized. With the aid of smooth round small forceps, the spleen is held up away from the incision, and the scissors are used to detach it from the body, as well as to separate the omentum from its side. The spleen is then transferred on top of a metal grid previously placed in a 6 cm dish with 5 mL M2 medium in order to break the organ apart by mechanically crushing it against the grid with the use of a plastic plunger. The splenocyte suspension is transferred into a 50 mL falcon through a 75 um nylon cell strainer and the 6 cm dish is washed twice with 10 mL M2 medium in order to collect any residual splenocytes. Cells are centrifuged at 200 g for 5 minutes and the supernatant is discarded before quickly resuspending the pellet in 5 mL lysis buffer and incubating the resuspended cells at room temperature for a maximum of 1 minute in order to lysate erythrocytes. The cell suspension was filled to 40 mL with M2 medium and centrifuged at 200 g for 5 minutes. After discarding the supernatant, the pellet was resuspended in 5 mL M2 medium and cells were counted using a Neubauer chamber and adjusted to a concentration of 4×10^7 cells/mL unless otherwise specified.

3.2.10. Mice serum isolation

Blood after the vaccinations in MVA homologous prime-boost vaccination regimens was collected from the venous sinus in what is referred to as peri-orbital venous sinus bleeding. Mice were under general anesthesia (with isoflurane in an induction chamber) when they were restrained and held by the neck, pulling the skin taut in order for their eye to bulge so a capillary tube could be very gently inserted laterally in a 30º angle into the medial canthus. Once the sinus was punctured, blood would flow through the capillary tube into a 1.5 mL tube and kept at room temperature for 1 hour. Blood flow would be visually monitored in order to collect an approximate maximum 170 uL of blood before the capillary tube was then removed from the mouse and soft pressure applied to the eye in order to stop the bleeding.

Mice would be monitored for possible periorbital lesions and postoperative behavior one hour after the blood collection and the following day in order to ensure their welfare.

Blood after the vaccinations in DNA-MVA homologous prime-boost vaccination regimens (in collaboration with the university of Utrecht, Netherlands) was collected from the submandibular vein. Mice were under general anesthesia (with the use of isoflurane in an induction chamber) when they were restrained and held by the neck and ears, pulling the skin taut over the mandible. A 25 gauge needle was then used below the ear canal and right next to the mandible to very gently puncture the vein by a mere 1-2 mm and allow for the blood to be transferred with a pipette into a 1.5 mL tube. About 170 uL of blood were collected before the needle was retrieved and gentle pressure was applied to the blood collection site with gauze until the bleeding subsided.

Mice would be evaluated for possible adverse effects, such as hematoma formation or ear canal hemorrhage the day after blood collection to confirm their wellbeing. In both cases, after a room temperature incubation of 1 hour, blood would be centrifuged at 13500 g for 15 minutes in order to separate the blood in three layers; the plasma, a mixture of platelets and white blood cells, and red blood cells. Plasma would be the higher layer, as it is less dense than the other two groups, and it would be transferred to a clean 1.5 mL tube by pipetting. The rest of the blood would be discarded and the plasma would be kept at -80 ºC until further use.

3.2.11. Neutralization Assay

HaK cells (cells isolated from the kidney of a Syrian golden male hamster, kindly provided by Statens Serum Institute) were seeded into a 96-well plate with a concentration of 0.5 x 10^6 cells/mL in McCoy Media with 5 % glucose and left to incubate overnight at 37 ºC. The following day, the serum samples were heat-inactivated for 30 minutes at 56 ºC and a dilution series was performed in SPG buffer (previously filtered through a 0.22 um filter) ranging from 1:12.5 to 1:200. The serial dilution was kept at 37 ºC until further use and *Chlamydia trachomatis Sv. D* (kindly provided by Statens Serum Institute) was diluted in SPG buffer to the suitable concentration of the assay (MOI = 2). Then, 75 uL of bacteria was added to 75 uL of each of the serum dilutions in a 96-well plate which was left to incubate for 45 minutes at 37 ºC. Afterwards, 50 uL of this serum:bacteria mix was transferred to the previously seeded HaK cells after discarding the supernatant. After plates were left to incubate at 37 ºC for 2 hours on a rocking apparatus, supernatant was discarded and cells were washed with 100 uL RPMI per well. Once the RPMI was

removed as well, 100 uL infection medium (McCoy media with 5% Glucose and 1:1000 Cycloheximide) was transferred to the cells. Plates were allowed to incubate for 24 hours at 37 ºC.

The following day, the supernatant was removed and 135 uL EtOh 96% was placed on the wells for 15 minutes at room temperature in order to fix the cells. EtOh was carefully removed by pipetting and 100 uL PBS was added. Plates were left at 4 ºC until staining.

For the staining, all steps were performed at room temperature and on dim lighting conditions unless otherwise specified. First, PBS was removed from the cells and the nucleus was stained with 70 uL DAPI (diluted 1:1000 in PBS) for 5 minutes in the dark. In order to stain for chlamydia inclusion bodies, the supernatant was removed and the antibody CT043 rabbit (kindly provided by Statens Serum Institute) was diluted 1:1000 in PBS with 0.1% BSA (previously diluted from 2% BSA) to add 85 uL per well. Plates were incubated at room temperature for 1 hour in the dark. The antibody was discarded and the plates were washed thrice by adding 135 uL PBS to each well. The secondary antibody Alexa Fluor 488 goat α rabbit IgG (H+L) was diluted with a concentration 1:1000 in PBS with 0.1% BSA (2% BSA) to add 35 uL per well. Plates were left to incubate for 1 hour in the dark before removing the supernatant and adding 200 uL PBS. Plastic seals were placed on top of the plates and they were kept at 4 ºC until further use.

Counting of the plates was performed by visually monitoring 10 different fields of view (with a diameter of 707 um) per well in a EVOS fl fluorescence microscope (AMG) with the 20x objective and mechanically counting each inclusion body found within the field of view.

3.2.12. Animal vaccination

The animals to be vaccinated were 8-10 weeks old female C57BL/6 mice purchased from Janvier.

In the case of MVA vaccination, mice were always immunized with 100 uL PBS containing 10^7 infectious unit for the priming and 10^8 infectious units for the boosting (or without any infectious dose in the case of the PBS group that acted as a negative control). Mice were restrained without anesthesia by pulling the neck back and the immunization doses were slowly applied intraperitoneally with a 0.5 mL sterile syringe. The puncture site was gently rubbed with gentle finger pressure before the mouse was returned to its cage.

In the case of DNA vaccination, mice legs were shaved the day prior to the vaccination while they were under general anesthesia (with isoflurane in an induction chamber), and the immunization was performed via intradermal tattooing. Mice were restrained under anesthesia just as described and a 9-needle bar mounted on a tattoo rotary device (Cheyenne) at 100 Hz was pressed onto the skin at 1mm depth for a maximum of 1 minute, injecting 15 uL cDNA (2 ug/uL) diluted in Tris-EDTA buffer.

In order to evaluate the T cell response from immunized animals, animals were sacrificed by cervical dislocation after 7 days in the prime only protocol. For the homologous MVA-MVA prime-boost protocol, animals were immunized with PBS, MVA-WT, MVA-CTH522 or MVA-CTH522:B7 and they were primed on day 0, boosted on day 5 and sacrificed on day 13. For the heterologous DNA-MVA prime-boost regimen performed at the University of Utrecht, animals were immunized with cDNA-Ø or MVA-WT (as controls), DNA-SP:CTH522 or MVA-CTH522:B7 and they were primed with MVA on day 0 (in the case of the homologous MVA-CTH522:B7/MVA-CTH522:B7 experimental group) or with DNA thrice on days 0, 3 and 6 (in the cases of the homologous DNA-SP:CTH522/DNA-SP:CTH522 or the heterologous DNA-SP:CTH522/MVA-CTH522:B7 and cDNA-Ø/MVA-WT experimental groups); then, they were boosted on day 28 (a single dose immunization for all groups involved) and sacrificed on day 35 via cervical dislocation.

On the other hand, with the objective of analyzing the antibody response after immunization, different regimens were carried out. In the case of homologous MVA-MVA prime-boost regimens, blood collection was performed on day 20 after the priming with MVA as previously described. Animals were boosted with MVA on day 30 and blood collection was performed again when the animal was sacrificed on day 44. In the case of heterologous DNA-MVA regimen, the initial blood collection was carried out on day 16 after the priming and animals were boosted with MVA or DNA on day 26 before their sacrifice on day 36. The experimental groups were the same as those just described for the regimen decided upon to study the T cell response.

The animal studies hereby described were performed in accordance with the recommendations of the European Health Law of the Federation of Laboratory Animal Science Associations (FELASA). The homologous vaccination regimens were approved by the North Rhine-Westphalia State Agency for Nature, Environment and Consumer Protection (LANUV), Germany. Permit Number: 2024-135 Grundantrag. The heterologous vaccination regimens performed in the Netherlands were approved by the Utrecht University Animal Ethics Committee, permit number: AVD1080020198224.

3.3. Protein Biochemical methods

3.3.1. Protein isolation

Infected cells were harvested by 5 mM EDTA or scraping and transferred into 1.5 mL tubes before being centrifuged at 5000 rpm for 7 min at 4 ºC. After discarding the supernatant and while keeping the tubes on ice, the cell pellet was washed with cold PBS. Tubes were then centrifuged in the same manner as before and pellets were resuspended in 80 uL Tyr lysis buffer. Tubes were then subjected to three cycles of freeze-thaw before undergoing three cycles of 1-min sonication. After centrifugation at 2000 g for 10 minutes at 4 ºC, supernatants were transferred into new 1.5 mL tubes in order to eliminate any debris from the final product. Protein lysates were stored at -80 ºC until needed.

3.3.2. SDS-PAGE

Sodium dodecyl sulfate polyacrylamide gel electrophoresis (SDS-PAGE) was used with the intention of separating proteins according to their molecular masses in order to study the expression of certain proteins. Firstly, protein denaturation was achieved by incubating the samples at 90 ºC for 10 minutes or 95 ºC for 5 minutes after being mixed with 5X sample loading buffer (containing both SDS, in order to coat the proteins and prevent the gel electrophoresis from being affected by the samples' properties, and β-mercaptoethanol, to reduce the disulfide bridges within the protein and prevent protein oligomerization, therefore breaking it down into its corresponding subunits). The samples were then transferred to a polyacrylamide gel formed by two gel solutions (differing in pore size, ionic strength and pH) where samples would first be loaded onto the upper stacking gel and then they would settle according to their molecular weight along the separation gel. A protein size ladder was used as a marker in all gels. The size of the gel would vary according to the number of samples to be included in the experiment and so would the electrophoresis itself (120 V for 1.5 hour if it was less than or 10 samples and 230 V for 2.5 hours if it was more than 10 samples; electrophoresis time is an approximation, gels would generally run for that amount of time but it could be reduced or extended accordingly).

3.3.3. Western blot

Once the electrophoresis was through, the separating gel was carefully transferred from its glass chamber where it was polymerized to a nitrocellulose membrane in order

to transfer the proteins onto it through the method of semi-dry blotting. Therefore, both the membrane and the gel were flanked on each side by three pieces of Whatman paper previously soaked in transfer buffer and the proteins were transferred on the nitrocellulose membrane in the presence of an electric field at 15 V for 1 hour. Afterwards, the membrane was blocked by soaking in 5% skimmed milk (milk powder dissolved in 1X TBS-T) for one hour at room temperature with subtle agitation on a rocking apparatus in order to avoid unspecific binding of the antibody. In order to detect the protein of interest, the membrane was then left overnight at 4 ºC on a rocking apparatus in the presence of the primary antibody (diluted in the same blocking solution as previously described). The following morning, the membrane was washed three times with TBS-T for 15 minutes each before being soaked in the secondary antibody (horseradish peroxidase (HRP) coupled antibody diluted in blocking solution) for one hour at room temperature on a rocking apparatus. The membrane was washed three times in the same manner as before and carefully handled to let as much TBS-T as possible drip out before placing it on a film and adding enhanced chemiluminescence (ECL) substrate (1:1 substrate mixture as indicated by manufacturer). It was then immediately detected with ChemoStar Touch ECL Imager from Intas in order to digitally detect the different protein bands.

3.3.4. Confocal microscopy imaging

In order to obtain images of the expression of CTH522 in cells, confocal microscopy imaging analysis was performed. For this, Cloudman cells were seeded at 80% confluency on top of microscope cover slips previously placed in a 12-well plate. Then, cells were left uninfected to serve as a mock group or infected with MVA-CTH522, MVA-CTH522:B7, MVA-WT or left uninfected as a control. All infection groups had a MOI=5 and were subtly shaken every 10 minutes at room temperature for the first hour of infection (which, when finished, effectively served as the 0 hour time point). The supernatant was then discarded and cells were carefully washed with PBS before fresh medium was added to them. Cell were left incubating at 37 ºC until their end time point (0, 8 and 24hpi) when their supernatant was discarded and they were fixed with 97% EtOH for 15 minutes. After the EtOH was discarded cells were washed once with PBS and they were left at 4 ªC in fresh PBS until their staining.

All staining was performed at room temperature in dim lighting. Once all the groups had been fixed, the PBS was discarded and the cells were stained with 20 uL DAPI (1:1000 concentration in 1% BSA PBS) for 5 min. With the objective of characterizing the co-localization of CTH522 and the cellular membrane, cells were stained for

glycoproteins of the cell membrane through the use of Wheat Germ Agglutinin (WGA) molecular probe. This was performed by adding 5.0 ug/mL WGA conjugate to the wells and letting them incubate for 10 minutes before discarding the supernatant and washing once with PBS. To stain for CTH522, cells were stained with *C. trachomatis* species-specific MOMP monoclonal antibody and incubated for one hour in the dark. Since this antibody is not conjugated to a fluorescent dye, cells were then stained with anti-mouse IgG Alexa Fluor 647 for 40 min in the dark before being washed again with PBS.

The microscopy cover slips were then carefully taken off the plate wells and the PBS was allowed to drip off in order for them to dry slightly before they were transferred onto the glass base were 7uL of ProLong Glass Antifade Mountant had been previously added. The slides were allowed to dry for 2 hours at room temperature and then kept at room temperature in the dark until imaging. They were detected with a LEICA SPE-II confocal microscope at the Center for Cell Imaging in Utrecht University and visualized by LAS AF lite software.

3.4. Immunological methods

3.4.1. Flow Cytometry

All steps were performed on ice. Plates were centrifuged at 1400 rpm for 2 minutes at 4 ºC and washed with 180 uL FACs buffer in between steps unless otherwise specified. Cells were plated in 96-well plates according to the needs and specificities of the experiment and centrifuged at 1400 rpm for 2 minutes at 4 ºC. Plates were then washed with 180 uL PBS before staining in order to differentiate live/dead cells by resuspending the cells in 100 uL of viability dye (1:2000) and leaving them to incubate for 20 minutes in the dark. Blocking of the Fc-receptors was performed by resuspending the cells in 50 uL of anti-mouse CD16/CD32 (1:300) (in order to block the fc receptors) and letting them incubate for 20 minutes in the dark. If applicable, surface markers' staining was performed (such as $CD4^+$ T cell staining with a dilution of 1:300). In the case of any CTH522 staining on the cell surface, cells were resuspended in 100 uL of 1:5000 *C. trachomatis* species-specific MOMP monoclonal antibody and incubated for one hour in the dark. Cells were then resuspended in 200 uL of 1:200 secondary antibody anti-mouse – PE and left incubating for 40 minutes in the dark. Pellets were resuspended in 150 uL 2% PFA and transferred into FACS tubes already containing 150 uL of FACS buffer

before being stored at 4 ºC until flow cytometry analysis was completed for a maximum of 5 days.

The samples' fluorescent signal was measured with FACS Canto II Diva and its analysis was completed through FlowJo software.

3.4.2. Intracellular Staining

All steps were performed on ice. Plates were centrifuged at 1400 rpm (for 2 minutes at 4 ºC and washed with 180 uL FACs buffer in between steps unless otherwise specified. Cells were plated in 96-well plates according to the needs and specificities of the experiment and centrifuged at 1400 rpm for 2 minutes at 4 ºC. Following the viability staining (performed as previously described), cells were permeabilized by resuspending them in BD Cytofix/Cytoperm^{TM} solution and incubating them in the dark for 15 minutes. Cells were then stained with the antibodies corresponding to the cytokines of interest (1:300 for CD4, IFN-γ, IL-17, IL-2 or TNFα) and incubated in the dark for 30 minutes. In the case of intracellular staining of CTH522, cells were resuspended in 100 uL of 1:5000 *C. trachomatis* species-specific MOMP monoclonal antibody and incubated for one hour in the dark. Cells were then resuspended in 200 uL of 1:200 secondary antibody anti-mouse – PE and left incubating for 40 minutes in the dark. Pellets were resuspended in 150 uL 2% PFA and transferred into FACS tubes already containing 150 uL of FACS buffer before being stored at 4 ºC until flow cytometry analysis was completed for a maximum of 5 days.

3.4.3. Peptide Pulsing

In order to find an immunogenic epitope within CTH522 for further study, a total of 138 15-mer overlapping peptides were designed by Giuseppe Andreacchio according to the CTH522 sequence. These peptides were grouped into 14 different so-called "pools" of 8-10 peptides each. All samples were diluted in M2 medium to achieve a final overall peptide concentration of 10^{-8} M (g/l). Protein complex CD3 or a mixture of CD3 and CD28 were used as an activation control, the MVA late gene product B5 was used as an MVA control and the Influenza nucleocapsid protein NP was used as a negative control.

Splenocytes were isolated from immunized mice (as previously described) and prepared with a concentration of $40x10^6$ cells/mL to transfer 100 uL per well to a 96-well plate. Next, 50 uL of the solution of each peptide pool, single peptide or control sample were added to the corresponding wells before adding 50 uL BFA (1:5000) as a golgi-

transport inhibitor in order to prevent protein transport from the endoplasmic reticulum. Plates are then incubated at 37 ºC for 15 hours.

Staining was performed as previously described for the markers of interest (mainly, $CD4^+$ IFN-γ^+ cells) and cell populations were analyzed through FACS Canto II Diva.

3.4.4. ELISA

The enzyme-linked immunosorbent assay (ELISA) was performed with the intention of detecting and quantifying antibodies from mouse serum. Therefore, a 96-well polystyrene plate was coated with 50 ug of purified CTH522 protein (kindly provided by Huynh Dung at Abera Bioscience) in 100 uL of coating buffer by overnight incubation at 4 ºC. After its incubation, the plate was washed three times with washing buffer before 200 uL of blocking buffer was added per well. The plate was left to incubate at room temperature for one hour and then washed three times with washing buffer. Then, 50 uL of the previously made serial dilutions of mice serum in dilution buffer were added to the plate for one hour. The plate was then washed a total of four times before 50 uL of a dilution of 1:1000 of the Alkaline Phosphatase-conjugated secondary antibody were added per well. Plate was left to incubate for one hour at room temperature in the dark. Then, plate was washed four times and 100 uL of the substrate solution (2 PNPP tablets, 2 mL diethanolamine and 8 mL water thoroughly vortexed) were added per well and the plate was left to incubate for 30 minutes at room temperature in the dark. Values were measured with the Multiscan 60 at 405 nm.

3.5. Statistical Analysis

Statistical values were calculated using GraphPad Prism software applying 1-way ANOVA or unpaired two-tailed student's t-test with error bars representing SD or SEM of at least three independent experiments (further specified in the results) with $p < 0.05$ considered as significant where one star * indicates $p < 0.05$, two stars ** indicate $p < 0.01$ and three stars *** indicate $p < 0.001$.

4. RESULTS

4.1. Generation of recombinant MVA containing antigen CTH522:B7

4.1.1. Red-mediated two-step recombination yields MVA-CTH522 progeny virus

With the aim of generating a recombinant MVA efficiently expressing the CTH522:B7 vaccine antigen for its *in vivo* testing, after the transfer vector pEP-MVAdVI-CTH522:B7 was cloned by restriction digestion as previously described in 3.1.1, the proper insertion of the CTH522:B7 antigen into the plasmid pEP-MVAdVI-PmH5 was confirmed by a screening PCR. DNA was purified from a selected dozen bacterial colonies grown in the presence of kanamycin and DreamTaq Green PCR master mix was used to prepare the samples for the amplification. Out of the twelve samples, CTH522:B7 was confirmed to be properly inserted in five of them by using primers RT_CTH522-1_fwd and RT_CTH522-3_rev (**Figure 4**). Samples 3 and 9 were sent for sequences to Eurofins Genomics (using primers MVA Del VI 5´, RL_S4aph_fwd_out, RT_CTH522-1_fwd and RT_CTH522-3_rev) in order to ensure a lack of endpoint mutations.

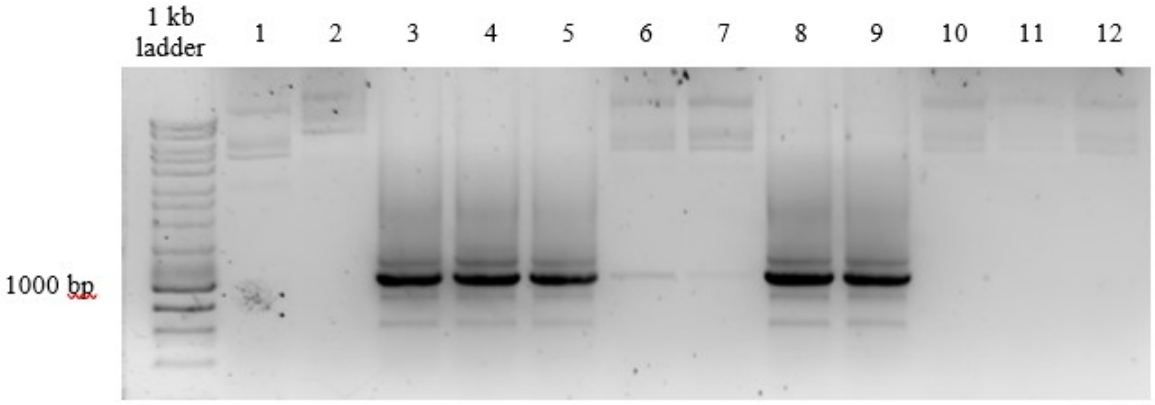

Figure 4. CTH522:B7 sequence is correctly inserted in the transfer vector in five out of twelve bacterial colonies containing pEP-MVAdVI-CTH522:B7. An agarose gel containing the DNA fragments amplified from a screening PCR with the purified DNA from bacterial colonies after restriction digestion of pEP-MVAdVI and CTH522:B7. Primers annealing within CTH522:B7 were used and offered an expected size of 1012 bp. The marker ladder of 1 kb can be found on the left.

Once the correct sequencing had been verified, the transfer vector pEP-MVAdVI-CTH522:B7 was prepared for bacterial electroporation by cleaving at the *Pac*I site between both flanks (Fl1 and Fl2). The transfer vector consisted of the two flanking regions homologous to those of the MCS found at deletion VI of the MVA genome, a I-*Sec*I homing endonuclease recognition site, an adjacent kanamycin cassette (still found within the vector for its previous use for bacterial colony selection) located between two

sequence repeats, the PmH5 promoter (a very strong MVA early/late promoter modified from the original promoter of the H5 gene of western reserve (WR) (Wyatt et al., 1998) and the CTH522 vaccine antigen with a short signal sequence upstream of the antigen and the B7-optimization cytoplasmic tail downstream of the antigen (**Figure 5**). The I-*Sce*I homing endonuclease recognition site will induce cleavage of the adjacent kanamycin cassette via *en passant* mutagenesis, a process using *E. coli* derived from DH10B and termed GS1783. This GS1783 *E. coli* strain contains a BAC-MVA genome harboring a cassette for temperature-dependent expression of the red recombinase gene and a cassette for arabinose-dependent expression of the I-*Sce*I endonuclease gene.

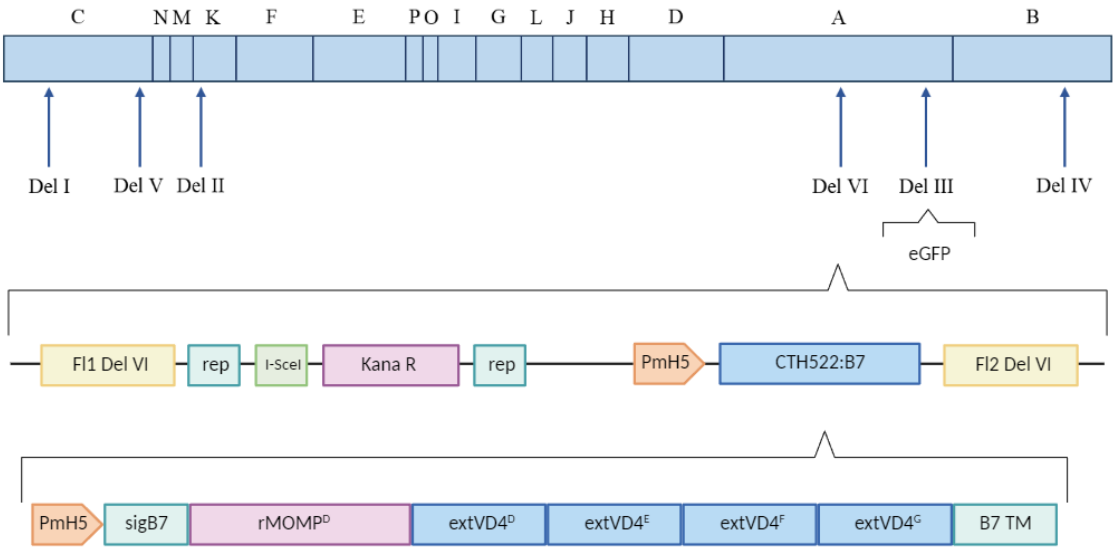

Figure 5. Schematic of the first recombination step from the red-mediated two-step MVA-BAC recombination. The pEP-MVAdVI-CTH522:B7 transfer vector is inserted into the deletion VI of the MVA genome via homologous recombination in what is the first step of the red-mediated recombination. Insert contains two flanking regions (Fl1 Del VI, Fl2 Del VI), the *I-SceI* endonuclease (*I-SceI)* and kanamycin marker gene (Kana) between two homologous sequences (rep), the PmH5 promoter and the CTH522:B7 antigen.

For the first recombination step, the linearized pEP-MVAdVI-CTH522:B7 from colonies 3 and 9 were used in the transformation of the GS1783 bacteria by electroporation at 1500 V and grown for 2 hours at 32 ºC before being transferred to plates containing CAM and KAN and incubated at 32 ºC. After 48 hours, 16 colonies were picked out of each plate (termed 3.1, 3.2, 3.3, etc., and 9.1, 9.2, 9.3, etc., respectively and accordingly to the original colony they were derived from) and their DNA was purified for another screening PCR in order to verify the presence of CTH522:B7 by using primers RT_CTH522-1_fwd and RT_CTH522-3_rev (**Figure 6**). Colonies 3.1 and 9.2 were sent to Eurofins for sequencing and further used for the following steps.

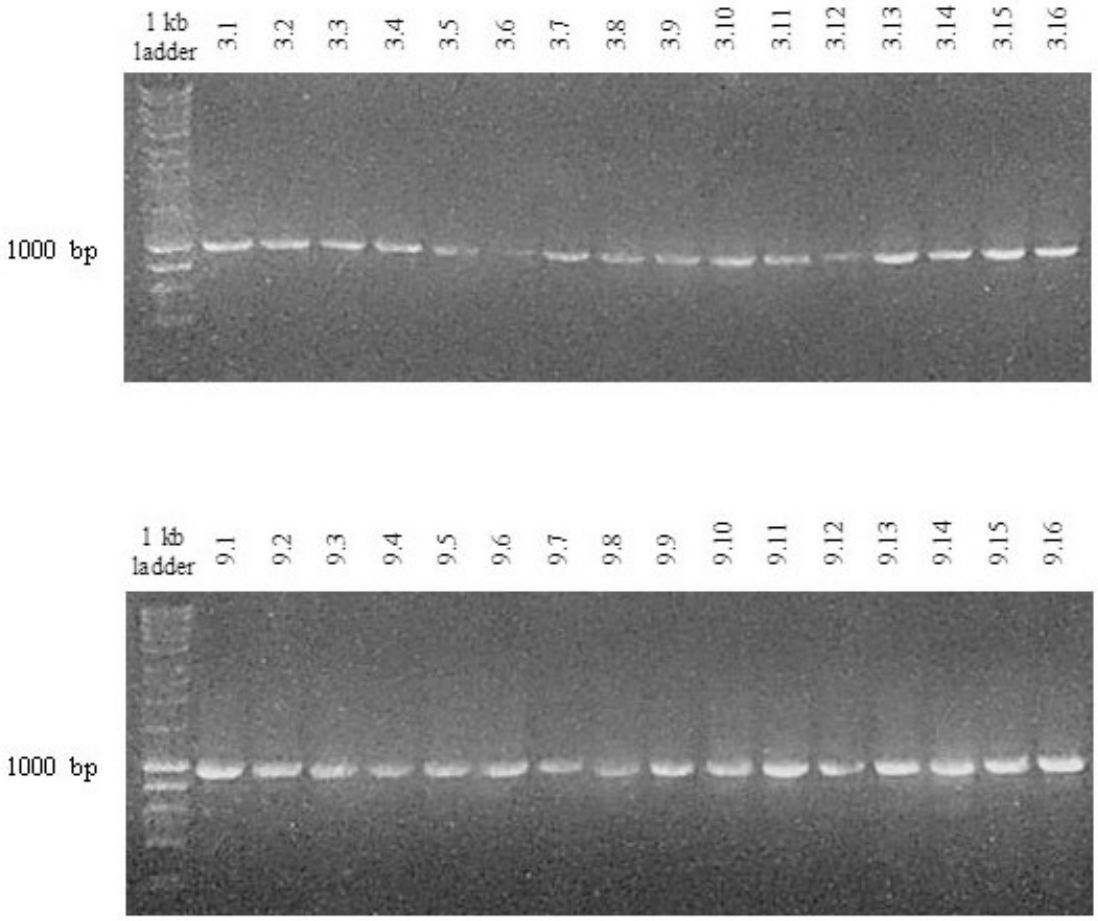

Figure 6. PCR analysis of the first recombination step from the red-mediated two-step MVA-BAC recombination. An agarose gel containing the DNA fragments amplified from a screening PCR with the purified DNA from bacterial colonies after electroporation at 1500 V of pEP-MVAdVI-CTH522:B7 into BS1873 *E. coli* strain bacteria with a BAC-MVA genome containing a temperature and arabinose-dependent cassette for the red recombinase gene and the I-*Sce*I endonuclease gene respectively. Primers annealing within CTH522:B7 were used with an expected size of 1012 bp. The marker ladder of 1 kb is on the left.

For the second recombination step, colonies 3.1 and 9.2 containing the CTH522:B7 antigen were incubated at 32 ºC for 4 hours in LB medium containing 30 ug/mL CAM before adding 1 mL medium containing 30 ug/mL CAM and 2% L-arabinose in order to induce the homologous recombination between the two sequence repeats and therefore cleaving the I-*Sce*I endonuclease and the kanamycin cassette from the final product. Next, the lambda red enzymes catalyzed the homologous recombination of pEP-MVAdVI-CTH522:B7 DNA (previously electroporated into the GS1783 bacteria) with the MVA-BAC DNA by incubating the samples at 32 ºC for 1 hour and immediately rising the temperature to 42 ºC for 30 minutes before going back down to 31 ºC for an additional 32 ºC. The optical density (OD) of the samples was measured then at 600 nm; clone 3.1 measured 0.5473 and clone 9.2 measured 0.3067, so they were both diluted in LB medium 1:100 and streaked on LB agar plates containing 30 ug/mL CAM and 2% L-arabinose.

After 48 hours, plates were visually monitored for bacterial growth and 7 colonies (termed 3.1.1, 3.1.2, 3.1.3, etc., and 9.2.1, 9.2.2, 9.2.3, etc., respectively and accordingly to the original colony they were derived from) out of each plate were picked out for a colony PCR screening in order to verify the presence of CTH522:B7 in the same manner as for the first recombination step. Five out of seven colonies from 3.1 and all colonies from 9.4 were verified via this PCR using primers Fwd-1 and Rev-3 (**Figure 7**).

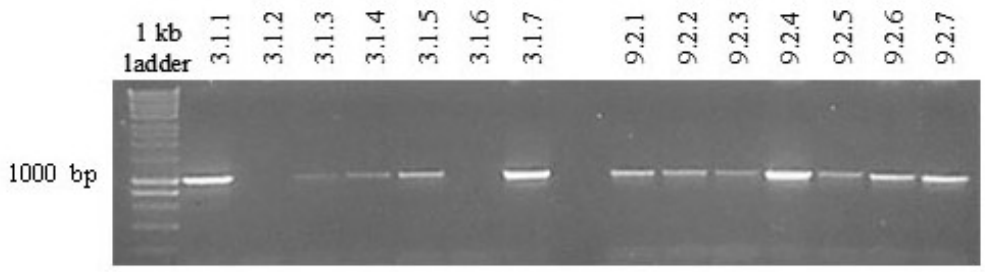

Figure 7. Second recombination step from the red-mediated two-step MVA-BAC recombination. An agarose gel containing the DNA fragments amplified from a screening PCR with the purified DNA from bacterial colonies after heat and arabinose induction for the I-*Sce*I endonuclease gene and the red recombinase gene respectively. Bacterial colonies were grown under selective antibiotic pressure for CAM and with 2% arabinose. Primers annealing within CTH522:B7 were used with an expected size of 1012 bp. The marker ladder of 1 kb can be found on the left.

Out of the 13 colonies where the presence of CTH522:B7 was confirmed, 3.1.1, 3.1.7 and 9.2.4 were sent to Eurofins (using primers MVA Del VI 3´ new, RT_CTH522-3_rev, RT_CTH522-5_rev and MVA Del VI 5´) for sequencing. Results verified that all three sequences were correct, lacked the kanamycin cassette and aligned properly to the original sequence (alignment confirmed by the use of CloneManager software).

4.1.2. Rescue of progeny virus and single clone selection of MVA-CTH522:B7

In order to rescue the progeny virus MVA-CTH522:B7, a transfection-infection process was performed where permissive DF-1 cells were transfected with the purified DNA obtained from bacterial colonies grown after the second recombination step. Because BAC-MVA-CTH522:B7 at this step lacked the necessary early transcription factors that would induce its life cycle, RFV (MOI=1) was used as a helper virus. This process finalized with a recombinant MVA harboring not only the vaccine antigen CTH52:B7, but also the BAC cassette and residual RFV material. In order to clear the RFV from the sample and for the GFP cassette to self-excise from the rec-MVA thanks to its own intended design, three sub-passages were performed on DF-1 cells until fluorescent green plaques were no longer found through visual monitoring of the plates

despite the CPE found within the cell monolayers. At this stage, a series of limiting dilutions stemming from the viral sample from the last passage was completed and plated onto 96-well plates in order to subsequently screen for GFP^-, RFV^- and $CTH522:B7^+$ recombinant MVA single clones. A total of 12 clones were harvested by scraping and their DNA was purified before carrying out three different PCR amplifications (**Figure 8**). Firstly, in order to check that any residual RFV had been cleared, primers RFV fwd and RFV rev were used, and RFV material was used as a positive control while the negative control was recombinant pEP-PK1L-DelVI, a plasmid lacking CTH522:B7 used for BAC selection. To confirm that the BAC cassette had excised from the recombinant MVAs, primers GFP F.P and GFP R.P. were used in a PCR amplification were DNA purified from a bacterial colony after both the first and the second recombination (and, therefore, containing the BAC cassette) were used as positive controls, and water was used as a negative control. To verify the integrity of CTH522:B7 within the recombinant MVA, a third PCR was performed with primers RT_CTH522-1_fwd and RT_CTH522-3_rev; the positive control was DNA purified after the second recombination and before viral rescue and the negative control was pEP-PK1L-DelVI. Lastly, with the aim of further confirming that CTH522:B7 was found in the proper MCS a fourth PCR was performed with primers MVA Del VI 3' new and MVA Del VI 5' annealing in the flanks of deletion VI of the MVA genome and therefore amplifying the whole expression cassette (**Supplementary Figure 1**).

Clone 4 was selected to be sent to Eurofins for sequencing and once it was further verified, it underwent amplification to generate viral stocks and purification for its *in vitro* and *in vivo* testing. After purification, it was labeled as MVA-CTH522:B7, titered and tested negative for fungi, bacteria and mycoplasma contamination.

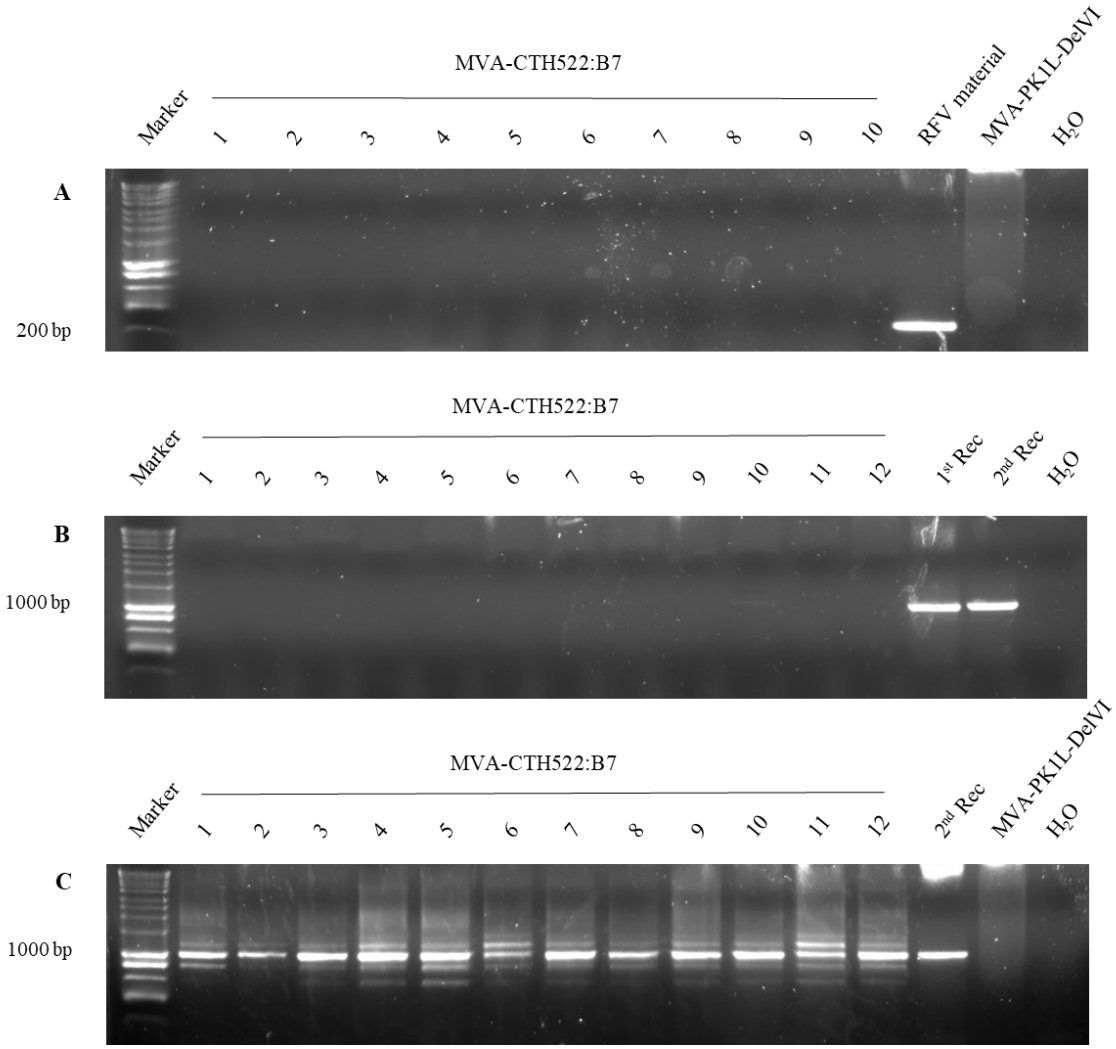

Figure 8. Single MVA-CTH522:B7 clones generated after viral progeny rescue and by limiting dilution. Three agarose gels containing PCR-amplified DNA fragments obtained by a screening PCR performed with purified DNA generated from single viral clones obtained after limiting dilution. **(A)** Verification of the RFV material being lost after three sub-passages in DF-1 cells. Positive control was RFV material previously harvested, negative control was recombinant MVA-PK1L-DelVI. Primers annealed within the RFV sequence. Ten clones were tested. **(B)** Verification of the BAC cassette being excised after three sub-passages in DF-1 cells. Positive control was DNA obtained after the first and second recombination, negative control was RNAse-free H_2O as primer control. Primers annealed within the BAC cassette sequence. Twelve clones were tested (**C)** Verification of the integrity of CTH522:B7 after three sub-passages in DF-1 cells. Positive control was DNA obtained after the second recombination, negative controls were RNAse-free H_2O as primer control and recombinant MVA-PK1L-DelVI. Primers annealed within the CTH522:B7 sequence. Twelve clones were tested. The marker ladder of 1 kb ison the left.

4.2. *In vitro* characterization of MVA-CTH522

4.2.1. Stability of MVA-CTH522:B7 recombinant virus confirmed via PCR testing and Western Blot analysis after successive passages.

In order to confirm the genomic stability and functionality of the vaccine antigen CTH522:B7 expressed by recombinant MVA-CTH522:B7 for its future use as a vaccine candidate, several successive virus passages in DF-1 cells were performed. More specifically, 1.0 x 10^6 DF-1 cells at 80% confluency were infected with the crude stock of MVA-CTH522:B7 at an undefined MOI. When general CPE was observed on the cell monolayer after an approximate 48 h post-infection, cells were harvested by scraping, lysed by three vortex-freeze-thaw cycles in order to release the virus from within the cells and sonicated. The supernatant containing the virus was used as an inoculum for the first round of the so-called "stability passages" and the process was repeated for a total of ten

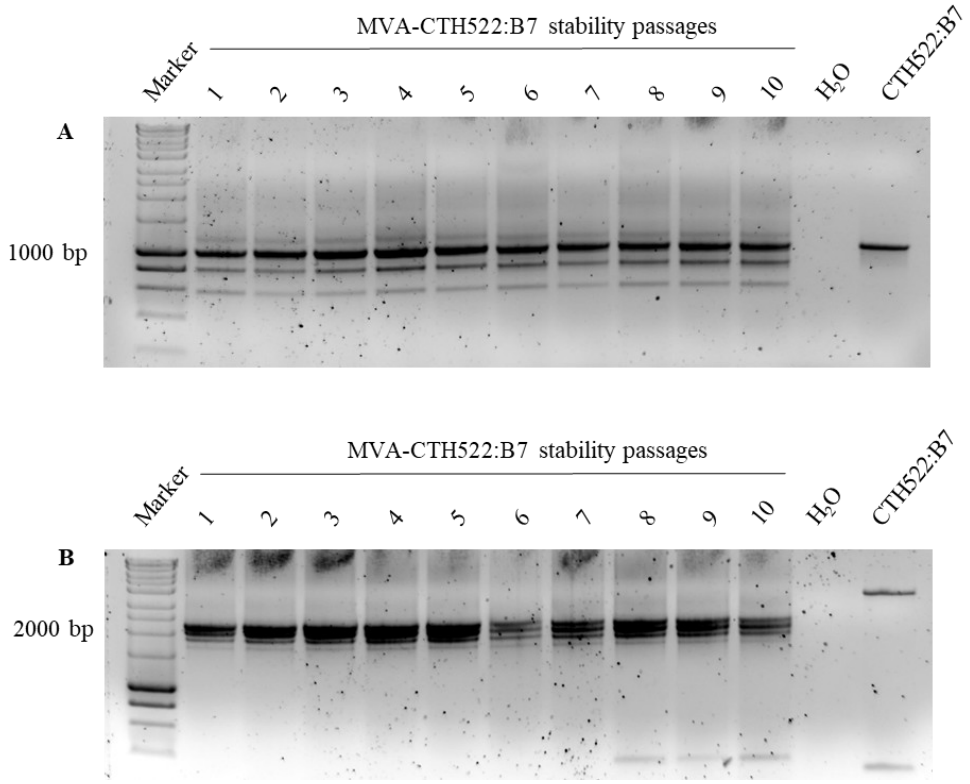

Figure 9. Genomic stability analysis via PCR of 10 successive infection cycles of MVA-CTH522:B7 on DF-1 cells. An agarose gel containing amplified DNA from a PCR with the purified DNA from 10 successive sub-passages on replicative cell line DF-1. DNA purified after the first recombination was used as a positive control. **(A)** Primers annealing within CTH522:B7 were used with an expected size of 1012 bp. **(B)** Primers annealing in the flanking region of MVA deletion VI and CTH522:B7 were used with an expected size of 2320. Positive control displayed a bigger fragment size due to the presence of the kanamycin cassette within the sequence. The marker ladder of 1 kb can be found on the left.

times. Once the ten stability passages were completed, the genomic stability was tested through PCR amplification (**Figure 9**) using primers RT_CTH522-1_fwd and RT_CTH522-3_rev annealing within the CTH522:B7 antigen (with an expected size of 1010 bp) and MVA Del VI 3' and RT_CTH522-3_rev annealing at the flanking region of deletion VI of MVA and CTH522:B7 (with an expected size of 2320 bp). The laddering shown in the figure was due to non-specific product formation, possibly because of a high template concentration. DNA purified from clone 3.1.1. after the first recombination was used as positive control, displaying a bigger sequence size due to the kanamycin cassette still contained within the plasmid (with an expected size of 3311 bp) The genomic functionality of CTH522:B7 was monitored through protein synthesis in western blot with an infection performed with MVA-WT serving as the negative control (**Figure 10**). Both the PCR and the western blot analysis showed that CTH522:B7 remains stably integrated and functional despite multiple infectious sub-passages on permissive cells.

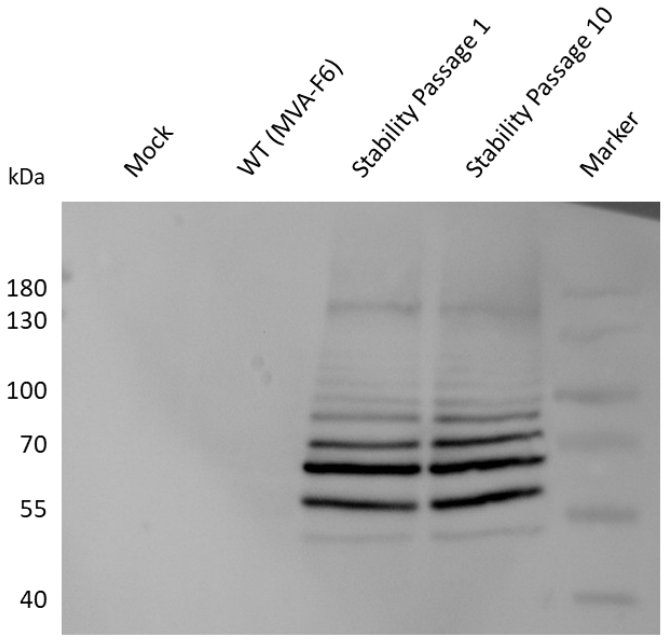

Figure 10. Stable expression of the target gene after 10 successive infection rounds of MVA-CTH522:B7 on DF-1 cells by western blot analysis. A 10% SDS-PAGE gel containing purified protein from 10 successive sub-passages on replicative cell line DF-1. Shown is the 1st (Stability Passage 1) and 10th passage (Stability Passage 10). DF1 cells infected with MVA-WT at MOI=1 were used as a negative infection control., DF-1 cells were left uninfected (mock) and used as negative control. The marker ladder can be found on the right.

4.2.2. Western Blot analysis confirms the correct synthesis of CTH522:B7 by MVA-CTH522:B7 in different cell lines at different time points

Despite the fact that it had already been proved that MVA-CTH522:B7 was able to express the vaccine antigen CTH522:B7 in a stable manner after ten successive passages, it became of interest to analyze the correct synthesis of the antigen upon MVA infection within a short and long timeframe in order to check for the minimum time required for western blot detection and an estimation of the stability of the protein respectively. Therefore, with this objective in mind, permissive cell line DF-1 was infected with a MOI=1 by both MVA-CTH522:B7 and MVA-WT (in order to serve as a negative infection control) and samples were harvested at the 0 timepoint and progressively after 4, 8 and 24 hours. These samples were lysed and the protein extracts were denatured before being fractioned by a 10% SDS-PAGE (**Figure 11**). Protein purified from an independent infection in DF-1 cells at MOI=1 was used as a positive control, and samples were exposed to three different antibodies; *C. trachomatis* species-specific MOMP monoclonal antibody to detect CTH522:B7, rabbit α H3L, an antibody for anlate vaccinia protein as an infection control for MVA, and an antibody for β-actin in order to serve as a loading control.

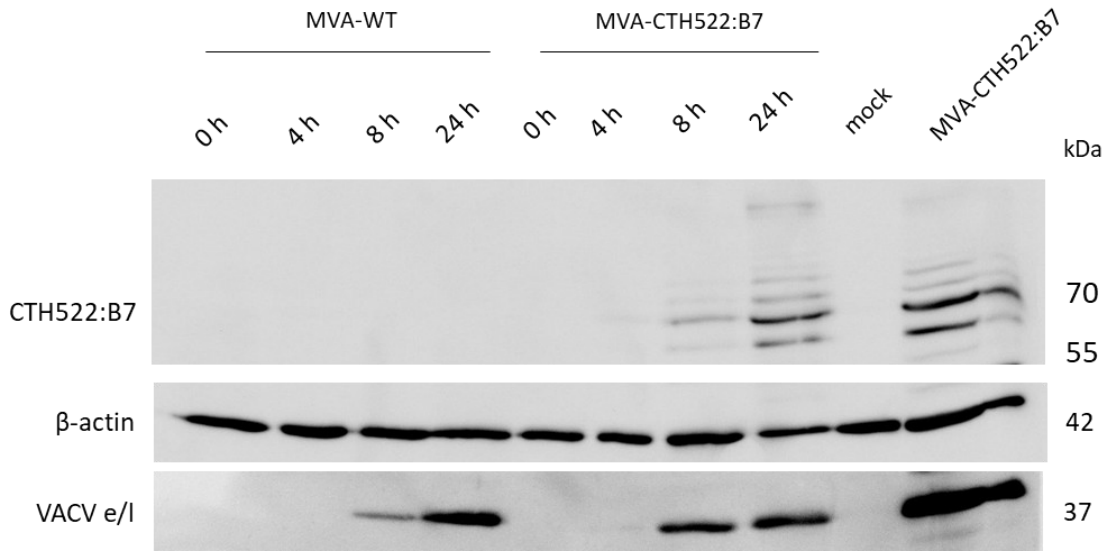

Figure 11. Antigen CTH522:B7 is detectable from 8 to 24 hours post infection using MVA-CTH522:B7 in permissive cell line DF-1. A 10% SDS-PAGE gel containing purified protein from 4 different timepoints after infection on replicative cell line DF-1 at MOI=1. An infection with MVA-WT was used as a negative infection control, DF-1 cells were left uninfected (mock) and used as negative control. VACV e/l is an early/late vaccinia protein used as an infection control. Recombinant target antigen CTH522:B7. B-actin was used as a loading control.

Results showed that MVA-CTH522:B7 was synthesized and observed by western blots early as 8 hours, even though the protein band was faint.

Furthermore, the same study was performed on a semi-permissive human cell line (HeLa cells) and non-permissive murine cell line (Cloudman cells) in the same manner as described above. (**Figure 12**). Results were similar to those found in the permissive cell line DF-1.

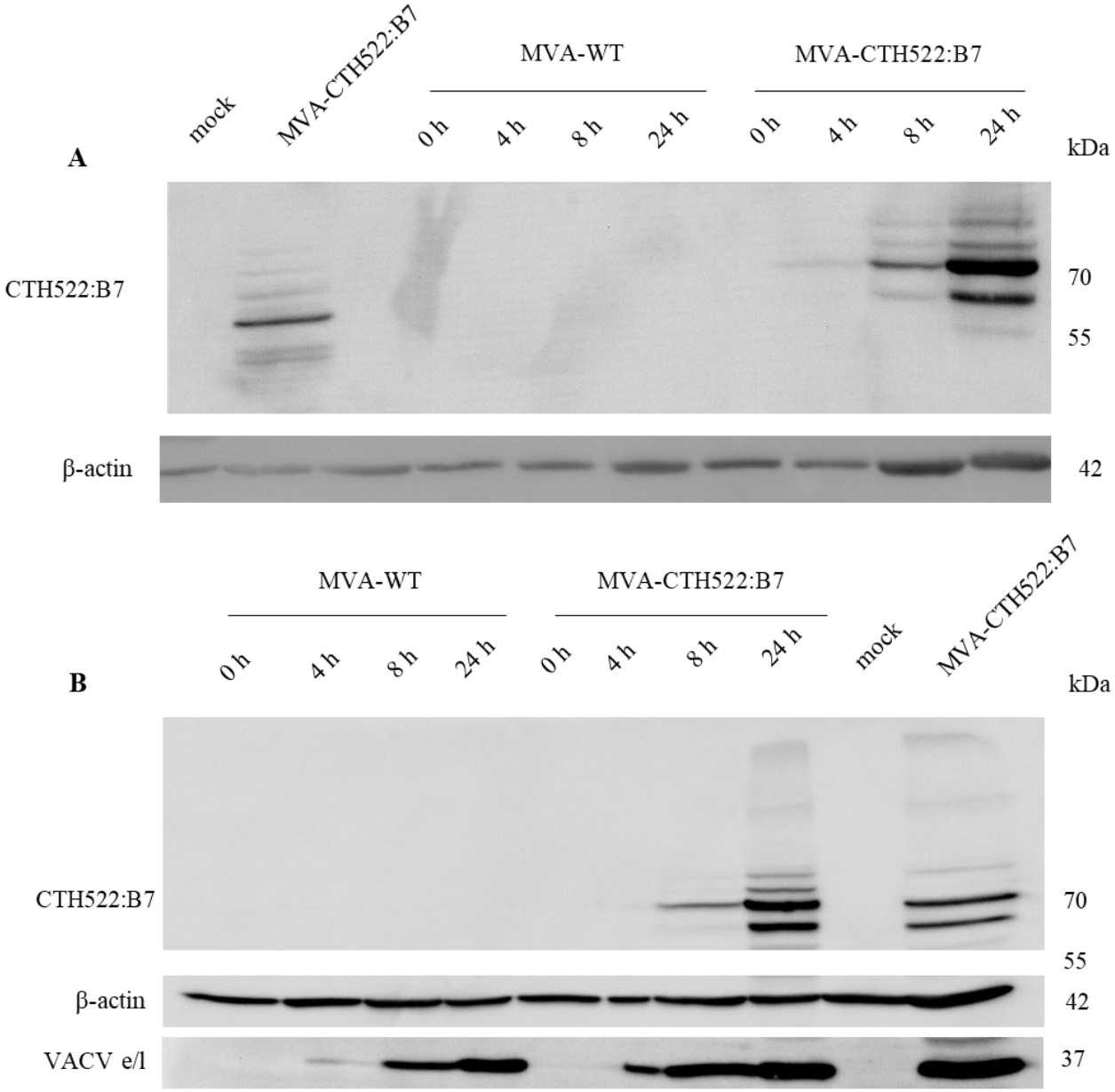

Figure 12. Kinetic analysis of antigen CTH522:B7 expression after infection using virus MVA-CTH522:B7. A 10% SDS-PAGE gel containing purified protein from 4 different timepoints after infection with a MOI=1. Infection with MVA-WT was used as a negative infection control, DF-1 cells were left uninfected (mock) and used as negative control. **(A)** Infection on semi-permissive HeLa cells. **(B)** Infection on non-permissive Cloudman cells. VACV e/l is an early/late vaccinia protein used as an infection control for detection of CTH522:B7. B-actin is protein used as a loading control.

In order to study whether or not the protein levels of CTH522:B7 would change with later time points, three additional experiments were performed where DF-1, HeLa and Cloudman cells were infected at MOI = 5. Samples were harvested and treated as just described above, and the same controls were kept for all three experimental set-ups (**Figure 13**). The sample of the 48 hour MVA- WT infection was mistakenly used in the 48 hour MVA-CTH522:B7 infection sample, leading to a missing band in the western blot. However, both bands at 24 and 72 hours display a positive protein production. In any case, the band at 72 hours showed to be slightly fainter than the one at 24 hours. Whereas the samples from HeLa cells showed a comparative synthesis between the initial 24-hour timepoint and the 72 hour one, Cloudman cells exhibited a stark difference between both of them. Nevertheless, samples were not quantified.

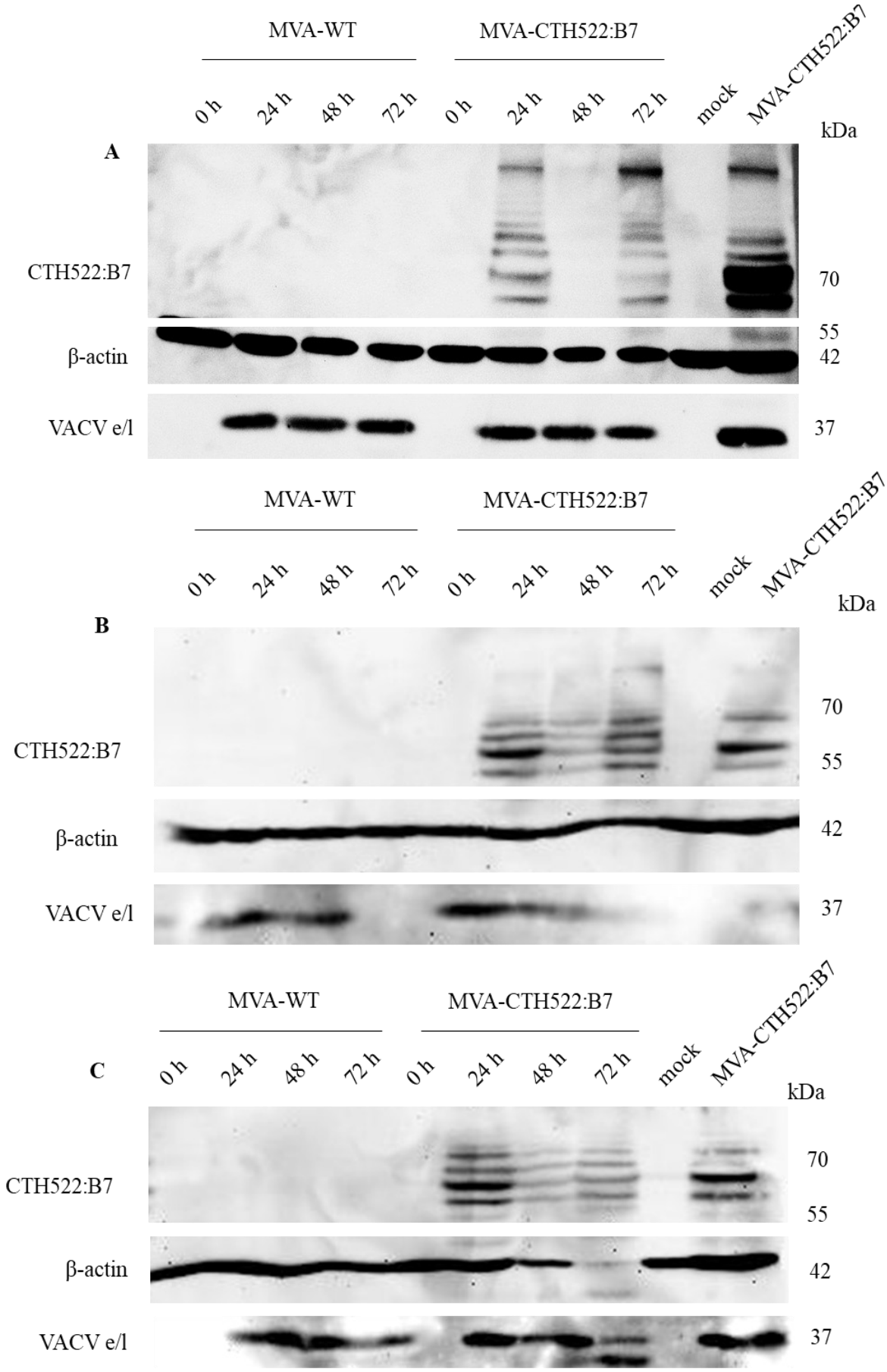
MVA-WT
MVA-CTH522:B7
0 h
24 h
48 h
72 h
0 h
24 h
48 h
72 h
mock
MVA-CTH522:B7
kDa
A
CTH522:B7
β-actin
VACV e/l
70
55
42
37
MVA-WT
MVA-CTH522:B7
0 h
24 h
48 h
72 h
0 h
24 h
48 h
72 h
mock
MVA-CTH522:B7
kDa
B
CTH522:B7
β-actin
VACV e/l
70
55
42
37
MVA-WT
MVA-CTH522:B7
C
0 h
24 h
48 h
72 h
0 h
24 h
48 h
72 h
mock
MVA-CTH522:B7
kDa
CTH522:B7
β-actin
VACV e/l
70
55
42
37

Figure 13. Kinetic analysis of antigen CTH522:B7 expression after infection using virus MVA-CTH522:B7. A 10% SDS-PAGE gel containing purified protein from 4 different timepoints after infection with a MOI=5. Infection with MVA-WT was used as a negative infection control, DF-1 cells were left uninfected (mock) and used as negative control. **(A)** Infection on permissive DF-1 cells (**B)** Infection on semi-permissive HeLa cells. **(C)** Infection on non-permissive Cloudman cells. VACV e/l is an early/late vaccinia protein used as an infection control for detection of CTH522:B7. B-actin is protein used as a loading control.

4.2.3. Virus growth and replication

As any kind of genetic modification, the insertion of the expression cassette coding for the CTH522:B7 antigen into the MVA genome can have different sorts of effects on the growth and replication behavior of the virus itself, be it beneficial or detrimental. In order to determine whether or not MVA-CTH522:B7 exhibited different replication characteristics when compared to the parental strain MVA-WT, a growth kinetics analysis was performed.

In order to test the replication capacity of MVA-CTH522:B7, growth kinetics were performed on the permissive DF-1 cell line, the semi-permissive HeLa cell-line and on non-permissive primary BMDCs isolated from C57BL/6 mice. Cells were infected with a MOI = 5 and harvested at 0, 4, 8 and 24 hours post-infection. Samples were then subjected to three freeze-thaw cycles and limiting dilutions were carried out and tested on DF-1 cells in order to ascertain the viral titer (TCID50/mL) of each sample. The results show a comparable growth to that of the parental strain (**Figure 14**), where it can be observed that the insertion of CTH522:B7 did not have any kind of impact on the overall replication behavior of MVA.

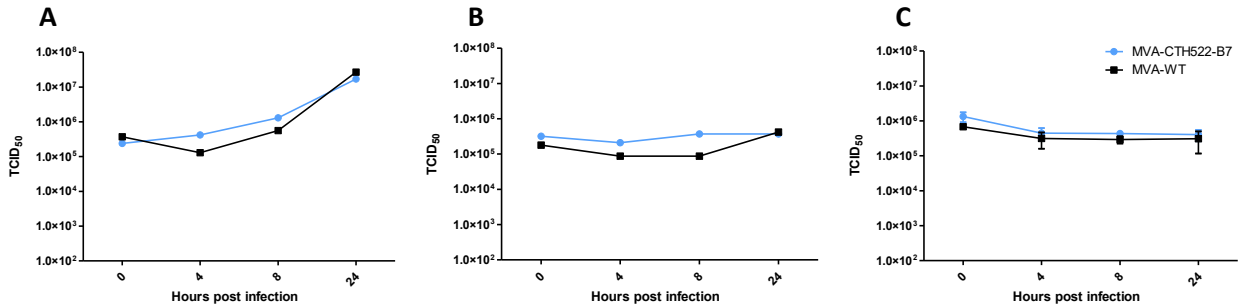

Figure 14. MVA-CTH522:B7 shows a comparable growth capacity to MVA-WT in different cell lines. Growth kinetics of MVA-CTH522:B7 and MVA-WT. Cells were infected at MOI = 5 with MVA-CTH522:B7 or MVA-WT and harvested via scraping after 0, 4, 8 and 24 hpi (hours post infection). Viral titers determined for $TCID_{50}$ were calculated using the Spearman-Kärber method. **(A)** DF-1 cells. **(B)** HeLa cells. (**C).** BMDCs. Results show the Log $TCID_{50}$ viral titer (TCID50/mL) and represent the mean of 2 (A, B) or 3 (C) independent experiments shown with means ±SD.

While this previous growth kinetics was done under a high MOI during a short period of time to analyze the replication behavior of MVA-CTH522:B7 in a single round of infection since most cells in the monolayer were infected. Additionally, a longer time frame with a lower MOI was necessary to analyze the replication behavior MVA-CTH522:B7 when multiple rounds of replication cycles are allowed because not all cells were infected, thus mimicking more an *in vivo* infection. While both DF-1 and HeLa cells were still used to analyze the difference between MVA-CTH522:B7 and MVA-WT in both permissive and semi-permissive cell lines, since the last time point when cells were to be harvested was 72 hpi, Cloudman cells also were used to study the difference in non-permissive cell lines. As described, cells were infected with a MOI = 5 and harvested at 0, 24, 48 and 72 hours post infection. Samples were subjected to three freeze-thaw cycles before performing limiting dilutions on DF-1 cells in order to determine the viral titer. Once again, MVA-CTH522:B7 showed a comparable growthto that of the parental strain in all three cell lines (**Figure 15**).

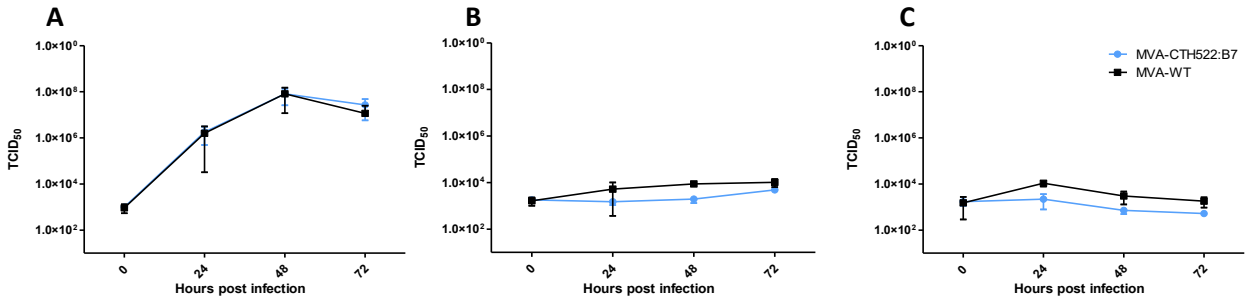

Figure 15. MVA-CTH522:B7 shows a comparable growth behavior to MVA-WT in different cell lines. Growth kinetics of MVA-CTH522:B7 and MVA-WT. Cells were infected at MOI = 0.01 with MVA-CTH522:B7 or MVA-WT and harvested via scraping after 0, 24, 48 and 72 hpi (hours post infection). Viral titers determined for $TCID_{50}$ were calculated using the Spearman-Kärber method. **(A)** DF-1 cells. **(B)** HeLa cells. **(C)** Cloudman. Results show the Log $TCID_{50}$ viral titer (TCID50/mL) and represent the mean of 2 independent experiments shown with means ±SD.

4.2.4. FACS analysis confirms the localisation of CTH522:B7 both intracellularly and on the surface of mammalian cells

Since the purpose of fusing the B7 cytoplasmic tail at the end of the CTH522 sequence was to enhance the intracellular transport and the cell surface display of CTH522 by tethering the antigen to the surface of mammalian cells, it became necessary to carry out a study that would confirm or refute the theoretical increase of CTH522 surface expression in those mammalian cells that had been infected with MVA-CTH522:B7 as opposed to those that had been infected with MVA-CTH522 without the

B7 sequence (kindly provided by Giuseppe Andreacchio). Cloudman and HeLa cells were initially used to test the intracellular and surface localisation in mammalian cells (**Figure 16**). BMDCs were later included in the study with the aim of analysing the CTH522:B7

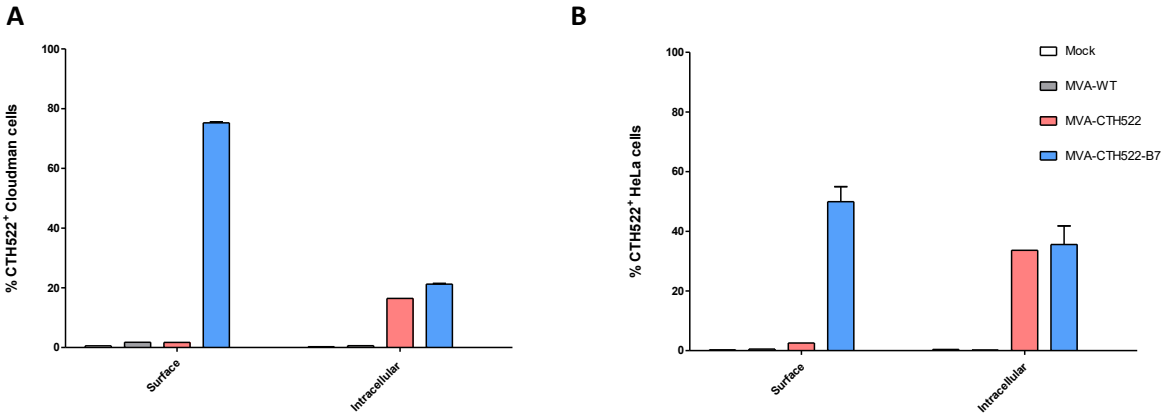

Figure 16. CTH522:B7 poduced by MVA-CTH522:B7 exhibits an enhancement on the surface rather than intracellular accumulation in mammalian cells. FACS analysis of CTH522 expression. Cells were infected at MOI=5 overnight and harvested via scraping. Samples stained for living or dead cells with Fixable Visability Dye eFluor 660, for CTH522:B7 with C. *trachomatis* species-specific MOMP mononuclear primary antibody and fragment Goat Anti-Mouse IgG-PE secondary antibody. **(A)** Cloudman cells and **(B)** HeLa cells. Results represent 2 independent experiments shown with means ±SD.

localisation in antigen presenting cells (APCs). However, as BMDCs showed to be less than ideal for such study, DC2.4 cells were included in the experiments to test whether or not the low CTH522:B7 production in BMDCs was due to their primary nature or to them being APCs (**Figure 17**). The Mean Fluorescence Intensity (MFI) of the FACS was also analyzed (**Supplemental Figure 2**), with results supporting the percentage populations

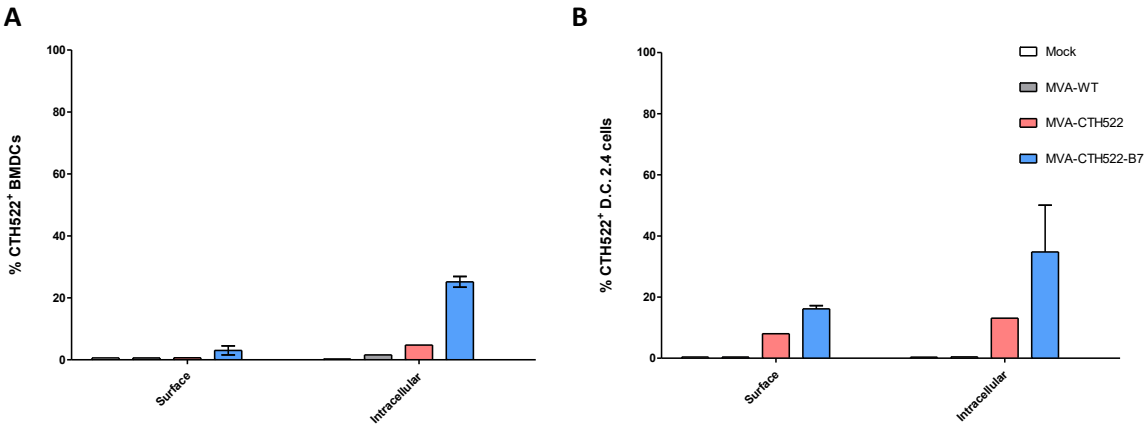

Figure 17. CTH522:B7 poduced by MVA-CTH522:B7 exhibits an enhancement on the surface rather than intracellular accumulation in dendritic cells. FACS analysis of CTH522 expression. Cells were infected at MOI=5 overnight and harvested via scraping. Samples stained for living or dead cells with Fixable Visability Dye eFluor 660, for CTH522:B7 with C. *trachomatis* species-specific MOMP mononuclear primary antibody and fragment Goat Anti-Mouse IgG-PE secondary antibody. **(A)** BMDCs and **(B)** DC2.4 cells infected at MOI = 5 overnight. Results represent 2 **(B)** or 3 **(A)** independent experiments shown with means ±SD.

of CTH522 positive cells found in both cloudman and HeLa cells, with a significant difference in both MVA-CTH522:B7 infected cloudman and HeLa cells where CTH522 was detected at the surface of the cell, as well as in MVA-CTH522 and MVA-CTH522:B7 infected HeLa cells where CTH522 was detected intracellularly. Cells were infected at MOI = 5 and harvested after an overnight infection with EDTA treatment before being immediately stained for living or dead cells with Fixable Viability Dye eFlour 660 and for CTH522:B7 with *C. trachomatis* species-specific MOMP monoclonal primary antibody and fragment Goat Anti-Mouse IgG-PE secondary antibody. As a note, a MOI = 5 showed to be exceedingly high for the dendritic cells, as even after 14 hpi a high percentage of the cells was observed to be apoptotic or dead already. The MFI analyzed from this experiment failed to show a difference in BMDCs where CTH522 was detected on the surface, but did display an increase in both BMDcs and DC2.4 cells infected with both MVA-CTH522 and MVA-CTH522:B7 where CTH522 was detected intracellularly (**Supplemental Figure 3**). Moreover, everything was kept the same for all four experiments. Uninfected cells for each experiment were used as the mock control.

Overall, cells infected with MVA-CTH522:B7 showed an increase in CTH522 surface expression as opposed to those infected with MVA-CTH522. At the same time, while cells such as HeLa and Cloudman displayed an enhancement in the surface expression when compared to the intracellular one, both BMDCs and Dc2.4 cells showed a higher intracellular synthesis rate rather than a surface one. Nevertheless, both BMDCs and DC2.4 cells exhibited a higher CTH522 concentration in cells infected with MVA-CTH522:B7 than in those infected with MVA-CTH522.

4.2.5. Time-course study of CTH522:B7 synthesis in dendritic cells

Because the previous results exhibited such a low yield of surface expression in BMDCs after an overnight infection, a time course study was carried out in a similar manner to the experiment analysing the surface and intracellular antigen localisation **(Figure 18)**. Briefly, cells were infected at MOI = 5 and harvested with EDTA after 0, 4, 8 and 24 hours. Cells were stained immediately at time of harvesting, and samples were stored at 4 ºC until their analysis. As previously observed, there was a high percentage of dead cells at 24 hpi, which would most likely be the reason for the low percentage. Additionally, the MFI of these two experiments seemed to follow seen in Figure 18, where the only significant difference in CTH522 positive populations detected on the surface of the cell was found at 8 hours in MVA-CTH522:B7 infected BMDcs (**Supplemental**

Figure 4). Within the intracellular analysis, MVA-CTH522 infected BMDCs had a significantly higher MFI than MVA-CTH522:B7 infected cells.

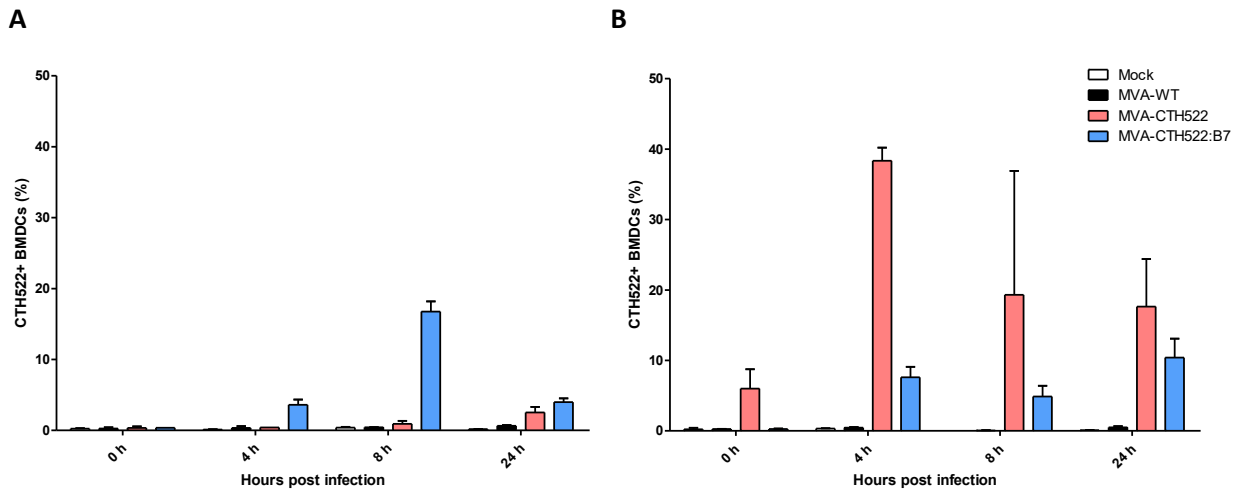

Figure 18. Time course analysis of CTH522:B7 distribution in BMDCs. FACS analysis of CTH522 and CTH522:B7 localisation in BMDCs **(A)** at the surface or (**B)** intracellularly. Cells were infected at MOI=5 for 0, 4, 8 and 24 hours and harvested via Ethylenediaminetetraacetic acid (EDTA) treatment. Samples were stained for living or dead cells with Fixable Visability Dye eFluor 660, for CTH522:B7 with C. *trachomatis* species-specific MOMP mononuclear primary antibody and fragment Goat Anti-Mouse IgG-PE secondary antibody. Results represent 3 independent experiments shown with means ±SEM.

In order to ensure that the low presence of CTH522:B7 on the surface level as well as intracellularly was due to the primary nature of the BMDCs and not because of their nature as dendritic cells, the same experiment was carried out on DC2.4 cells (**Figure 19**).

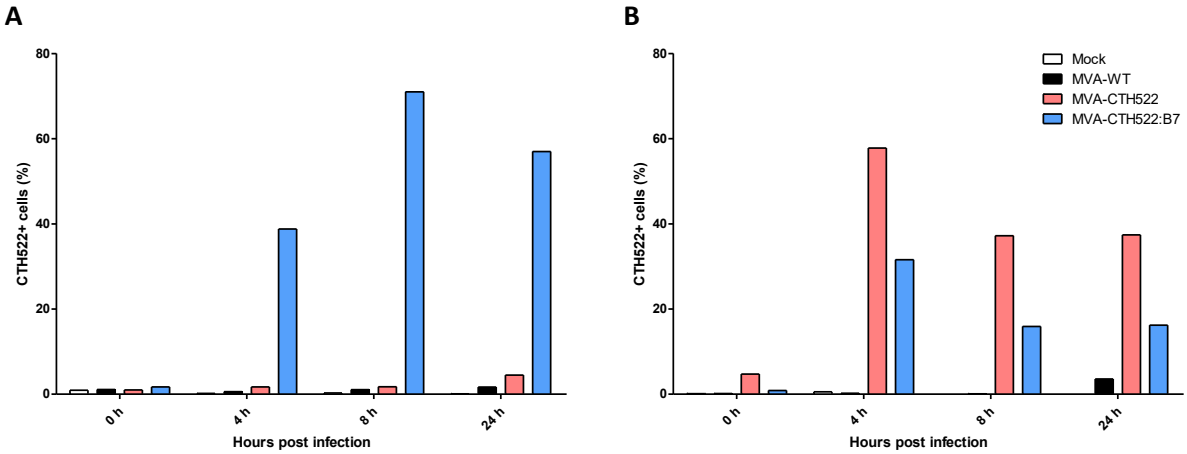

Figure 19. Time course analysis of CTH522:B7 on DC2.4. FACS analysis of CTH522 expression on DC2.4 cells analyzing the **(A)** surface and **(B)** intracellular synthesis. Samples were stained for living or dead cells with Fixable Visability Dye eFluor 660, for CTH522:B7 with C. *trachomatis* species-specific MOMP mononuclear primary antibody and fragment Goat Anti-Mouse IgG-PE secondary antibody. Results represent 1 independent experiment.

Again, cells were infected with MVA-CTH522:B7, MVA-CTH522, MVA-WT with a MOI = 5 or left uninfected to act as a mock control. Samples were harvested at 0, 4, 8 and

24 hpi with EDTA and stained immediately for CTH522 both on the surface and intracellularly. Results showed a significantly higher expression of CTH522 on the surface of the cells infected with MVA-CTH522:B7 as opposed to those infected with MVA-CTH522, which showed close to no surface expression at all. At the same time, the strongest surface accumulation seemed to be at 8 hours. In regards to the intracellular level, cells infected with MVA-CTH522 were approximately two times more frequent when compared to those cells infected with MVA-CTH522:B7, and the peak of detection seemed to be at 4 hours as opposed to the 8 of the surface level. Further analysis of the MFI for this experiment supported the findings, as the MFI for MVA-CTH522:B7 infected DC2.4 in the surface study yielded a significantly high MFI at 4, 8 and 24 hpi, while DC2.4 infected with MVA-CTH522 only had a significant MFI in the intracellular analysis with the highest MFI found at 4 hpi (**Supplemental Figure 5**).

4.2.6. Confocal analysis displays the subcellular localization of CTH522:B7 in Cloudman cells

As an additional step to characterize the recombinant MVA-CTH522:B7 and confirm the colocalization of CTH522:B7 on the cell surface of mammalian cells infected with MVA-CTH522:B7, the subcellular localization of the antigen was analyzed through confocal microscopy. Cloudman cells previously seeded on microscope cover slips were infected with MVA-CTH522:B7. MVA-CTH522 served as a control to assess any changes the fused B7 exerts on the antigen localization, MVA-WT as an infection control and uninfected cells as a mock control. As such, cells were infected with a MOI=5 and fixed with EtOh after 0, 8 or 24 hpi to study the progression of the antigen localization at different timepoints. Cells were stained with DAPI for visualizing the nucleus and viral factories, Wheat Germ Agglutinin for the cell surface and *C. trachomatis* species-specific MOMP mouse monoclonal antibody followed by anti-mouse IgG Alexa Fluor 647 for CTH522. Cells were analyzed with a LEICA SPE-II confocal microscope at the Center for Cell Imaging in Utrecht University and images were visualized and edited by LAS AF lite software.

Results show a CTH522 positive signal in both, cells infected by MVA-CTH522:B7 or MVA-CTH522 as early as 0 hpi, which, as described in 5.2.6. infection with MVA, is actually one hour where the virus inoculum is placed on the cells at room temperature, allowing the virus to attach to the surface of the cell (**Figure 20**). CTH522:B7 can be seen at 8 hpi, when cells display CTH522 fluorescence within the cell in those infected with MVA-CTH522:B7 or MVA-CTH522 (**Figure 21**). In the case of the cells infected with

MVA-CTH522:B7, a cell expressing CTH522 at the cell surface can also be observed in the image, as the fluorescent signal for WGA and CTH522 colocalize in the right bottom corner.

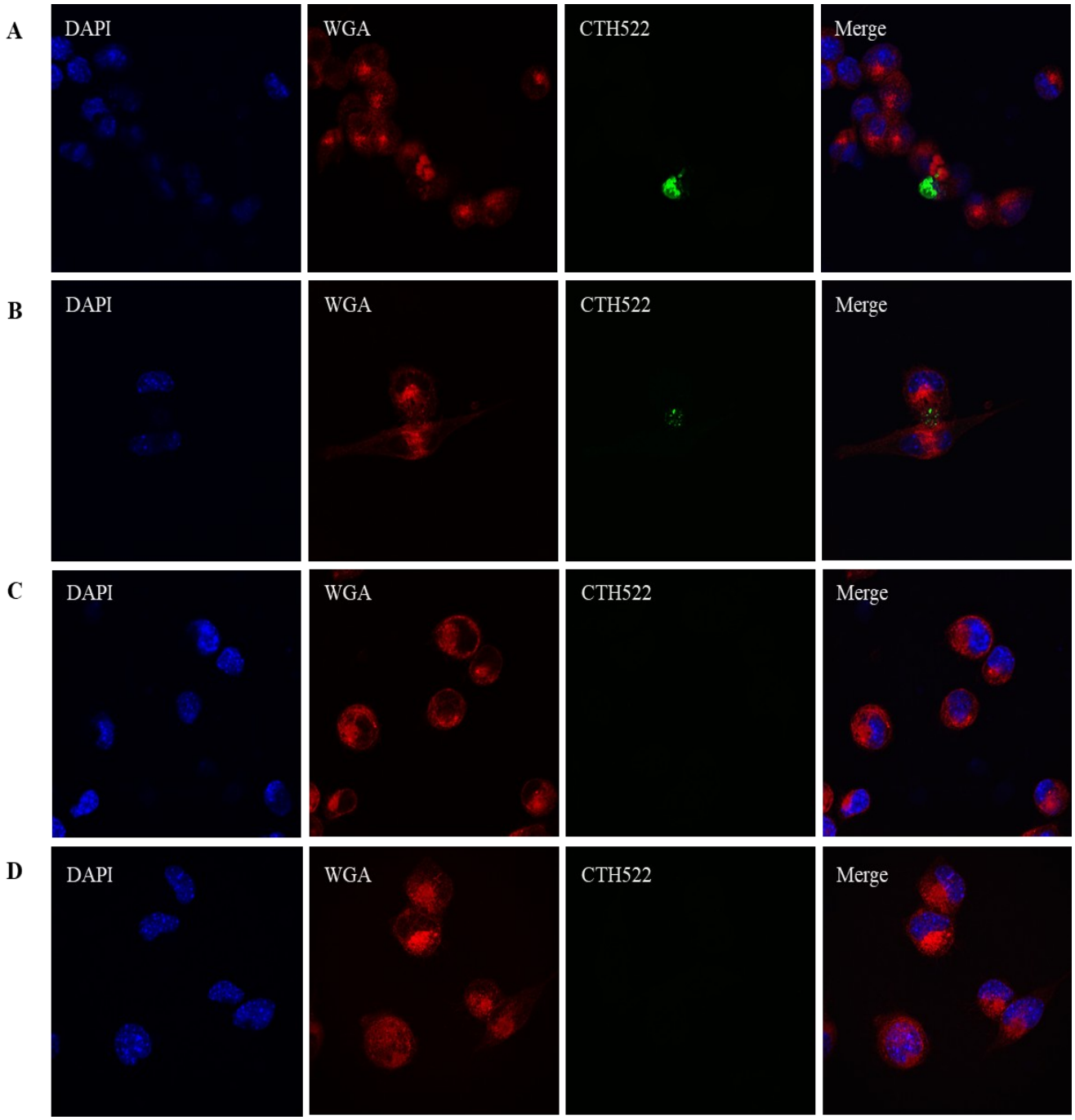

Figure 20. CTH522 is not detected at 0 hpi in cells infected with MVA-CTH522:B7 or MVA-CTH522. Confocal microscopy imaging showing Cloudman cells infected with **A.** MVA-CTH522:B7. **B.** MVA-CTH522. **C.** MVA-WT. **D.** Mock. Cells were fixed at 0 hpi (1 hour after inoculum was placed on cells at room temperature) after an infection at MOI=5 and stained with DAPI for visualizing the nucleus and viral factories, WGA for the cell surface, *C. trachomatis* species-specific MOMP mouse monoclonal 1st antibody and anti-mouse IgG Alexa Fluor 647 2nd antibody. Multiple images were taken and results display the best representatives of each group (n = 3)

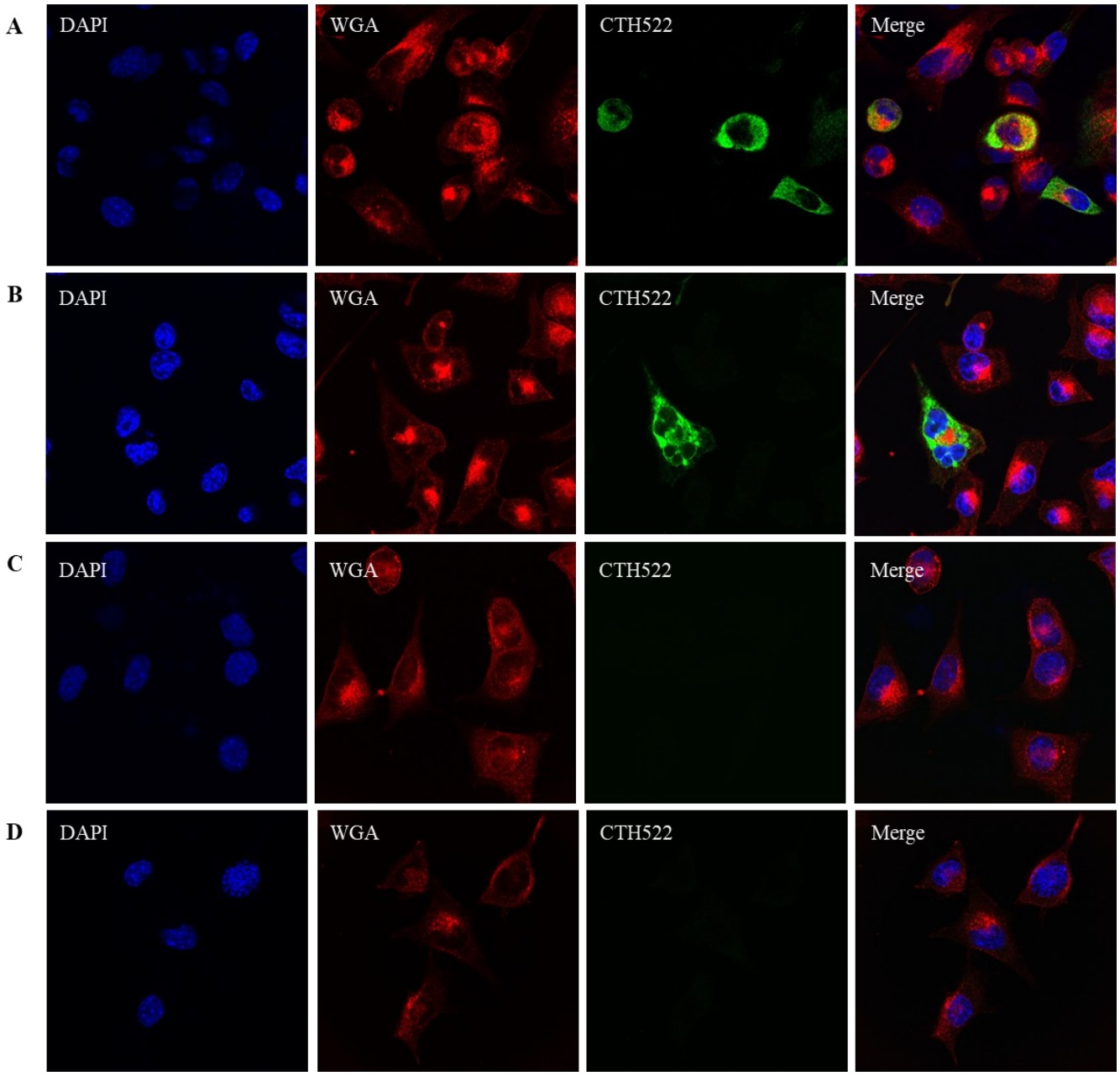

Figure 21. CTH522 is found both within the cell and on the cell surface in cells infected with MVA-CTH522:B7 at 8 hpi. Confocal microscopy imaging showing Cloudman cells infected with **A.** MVA-CTH522:B7. **B.** MVA-CTH522. **C.** MVA-WT. **D.** Mock. Cells were fixed at 8 hpi after an infection at MOI=5 and stained with DAPI for the nucleus and viral factories, WGA for the cell surface, *C. trachomatis* species-specific MOMP mouse monoclonal 1st antibody and anti-mouse IgG Alexa Fluor 647 2nd antibody. Multiple images were taken and results display the best representatives of each group (n = 3)

Any CTH522 signal to be found on cells infected with MVA-CTH522 is lost at 24 hours or, at the very least, extremely faint for the microscope to perform a proper readout (**Figure 22**). However, this is not the case for those cells infected with MVA-CTH522:B7, where a strong fluorescence is detected at 24hpi, positively colocalizing with the WGA signal and, therefore, confirming that MVA-CTH522:B7 successfully expresses CTH522:B7 on the cell surface at 24 hpi.

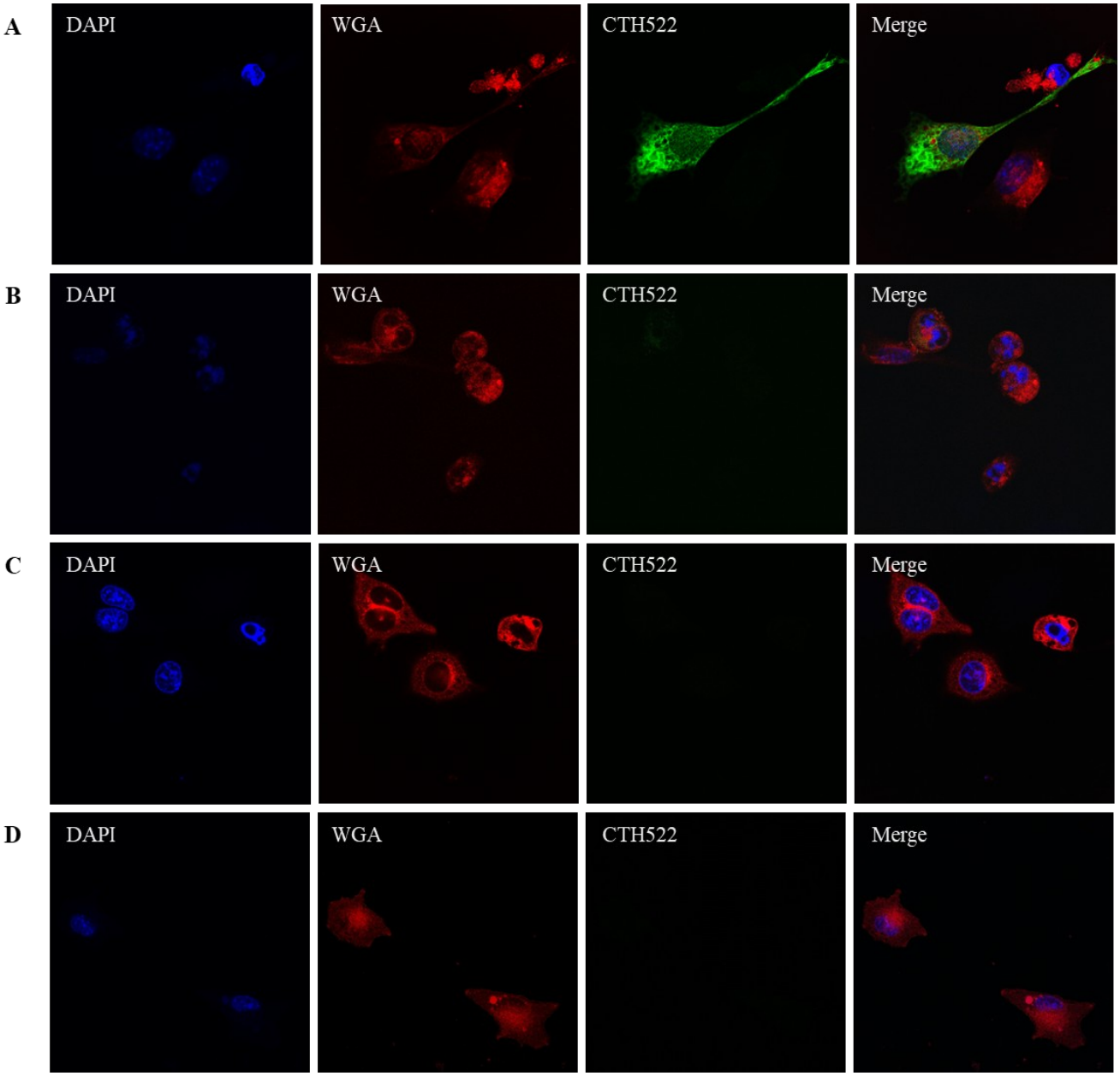

Figure 22. CTH522:B7 is found within and on the cell surface of cells infected with MVA-CTH522:B7 at 24 hpi. Confocal microscopy imaging showing Cloudman cells infected with **A.** MVA-CTH522:B7. **B.** MVA-CTH522. **C.** MVA-WT. **D.** Mock. Cells were fixed at 24 hpi after an infection at MOI=5 and stained with DAPI for the nucleus and viral factories, WGA for the cell surface, *C. trachomatis* species-specific MOMP mouse monoclonal 1st antibody and anti-mouse IgG Alexa Fluor 647 2nd antibody. Multiple images were taken and results display the best representatives of each group (n = 3)

4.3. *Ex vivo* testing of the purified MVA-CTH522:B7 administered to mice in homologous or heterologous immunization regimens

4.3.1. Immunological evaluation of CTH522 peptide candidates by flow cytometry

In order to determine immunological relevant T cell epitopes within the CTH522 sequence, a total of 138 15-mer overlapping peptides were designed according to the CTH522 protein sequence. To test the immunogenicity of all 138 peptides at once would be too arduous a task and, consequently, they were grouped into 14 different groups (hereby called "pools") of 8-10 peptides each (further described in **Supplemental Material Table 2**) to be tested accordingly. Initially, C57BL/6J mice were vaccinated once with MVA-WT, MVA-CTH522 and MVA-CTH522:B7 and sacrificed 7 days later. Splenocytes were isolated and incubated for 15 hours with the corresponding peptide pools in the presence of Brefeldin A to inhibit the protein transport to the golgi complex. Pool 12 proved to be the most promising group with a value of 1.58% IFN-γ^+ CD62L$^-$ CD4$^+$ T cells in comparison to the 0.48% IFN-γ^+ CD62L$^-$ CD4$^+$ T cells pulsed with NP as a negative control (**Figure 23 A**). At the same time, pool 6, with a value of 1.13% IFN-γ^+ CD62L$^-$ CD4$^+$ T cells and pool 5, with a value of 0.99% IFN-γ^+ CD62L$^-$ CD4$^+$ T cells, were also marked as candidates to move forward with.

With the objective of testing the peptide pools with a homologous prime/boost regimen, C57BL/6J mice were vaccinated once again with MVA-WT, MVA-CTH522 and MVA-CTH522:B7. However, in this case, mice were boosted on day 5 with a higher dose immunization and sacrificed on day 13. Just as before, splenocytes were isolated and incubated with the corresponding peptide pool in the presence of Brefeldin A for 15 hours. In this case, the most promising groups were pools 5 and 6, with values of 1.62% IFN-γ^+ CD62L$^-$ CD4$^+$ T cells and 1.55% IFN-γ^+ CD62L- CD4$^+$ T cells correspondingly, in comparison to the 0.50% IFN-γ^+ CD62L$^-$ CD4$^+$ T cells of the NP-pulsed splenocytes. Overall, groups 5, 6 and 12 were determined to be the most immunogenic ones out of the 14 initial groups.

Once the most immunogenic pools had been determined, in order to test the single peptides within those groups and analyze the immune response the single peptides recalled, pools 6 and 12 were chosen for further studies. Mice were immunized in the same manner as described above for a homologous prime/boost regimen; boosted on day 5 and sacrificed on day 13. Splenocytes were then isolated and incubated with the

corresponding peptide for 15 hours in the presence of brefeldin A before staining for IFN-γ^+ $CD62L^-$ $CD4^+$ T cells to be analyzed through FACS.

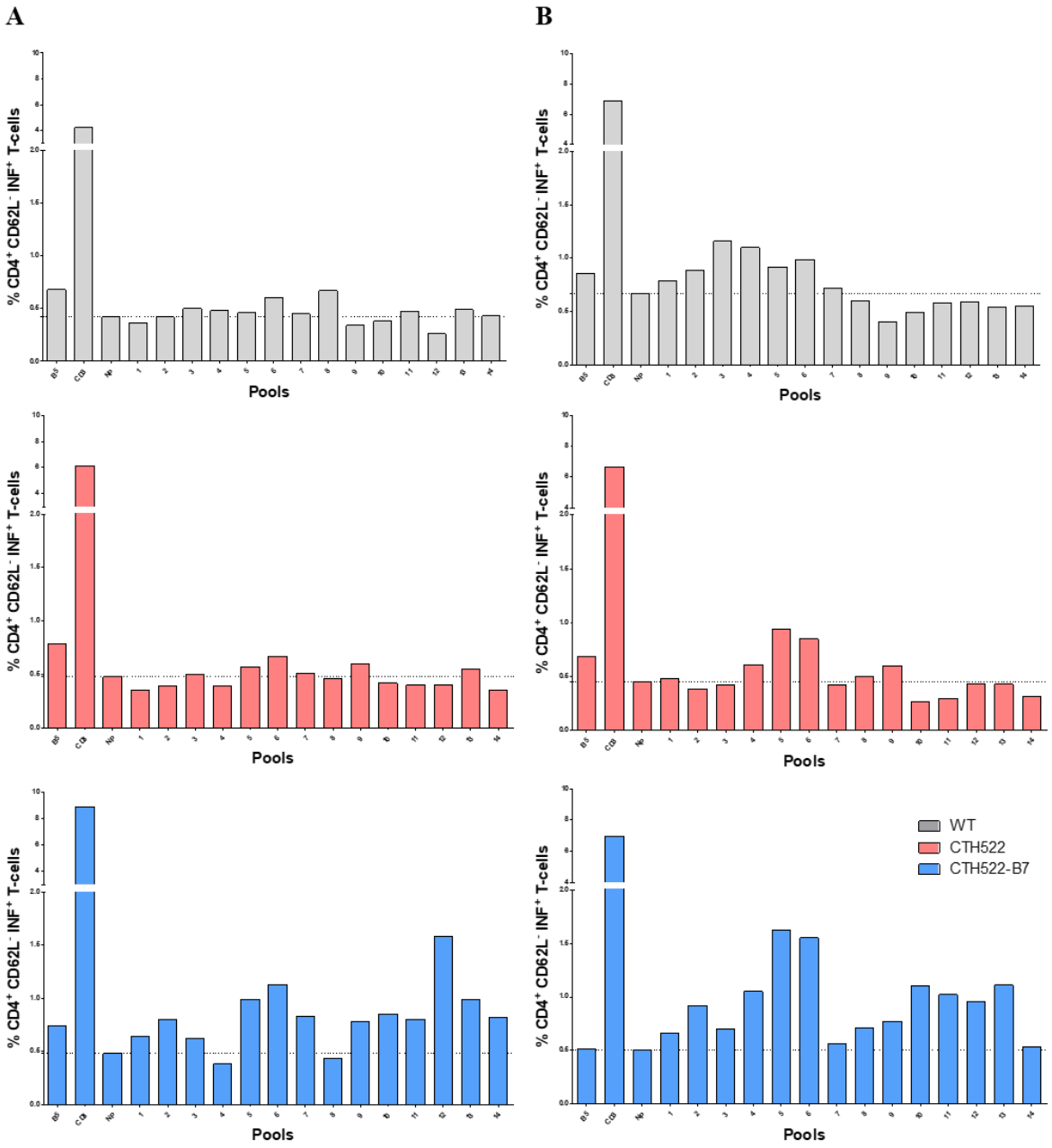

Figure 23. Peptide pools exhibit different ranges of CTH522-specific IFN-γ expression within CD4+ T cell population after vaccination. A total of 138 15-mer overlapping peptides were designed after the CTH522 sequence and grouped into 14 different "pools" of 8-10 peptides each. C57BL/6J mice were vaccinated with MVA-WT, MVA-CTH522 and MVA-CTH522:B7 in **(A)** a single priming regimen where mice were sacrificed 7 days after priming with 10^8 TCID/mL and **(B)** a homologous prime/boost regimen where animals were primed on day 0 at 10^7 TCID/mL and boosted on day 5 at 10^8 TCID/mL before being sacrificed on day 13. Splenocytes were pulsed with the CTH522 peptide pools for 15 hours with Brefeldin A. 15 hours after peptide pulsing, the splenocytes were stained for living or dead cells with Fixable Visability Dye EMA PerCP/PE, anti-mouse IFN-γ-APC, anti-mouse CD62L-PeC7 and anti-mouse CD4-Pacific Blue. Controls were used as follows; B5 45-60, an MVA late gene product that serves as a MVA control. Purified Hamster Anti-Mouse CD3e: protein complex that serves as an activation control. NP 311-325: influenza virus nucleocapsid peptide that serves as a negative control. Thresholds were determined as the corresponding NP value. n=1

Results conclusively showed two peptides displaying a significantly high reactivation level through all three independent experiments: peptide #49 (**Figure 24**), which was previously referred to as peptide 6-4, and showed a significant difference when compared to the NP peptide control (* $p < 0.5$); and peptide #69 (**Figure 25**), which was referred to as peptide 12-5 and displayed a significantly higher response when compared to the NP peptide control (** $p < 0.01$). Splenocytes pulsed with either of these peptides consistently displayed high percentages of IFN-γ^+ CD62L$^-$ CD4$^+$ T cell populations, indicating their possible value as immunogenic peptides for future *in vivo* studies.

Peptide 6-4 and peptide 12-5 will be referred to as peptide 49 and peptide 69 for the remainder of the study.

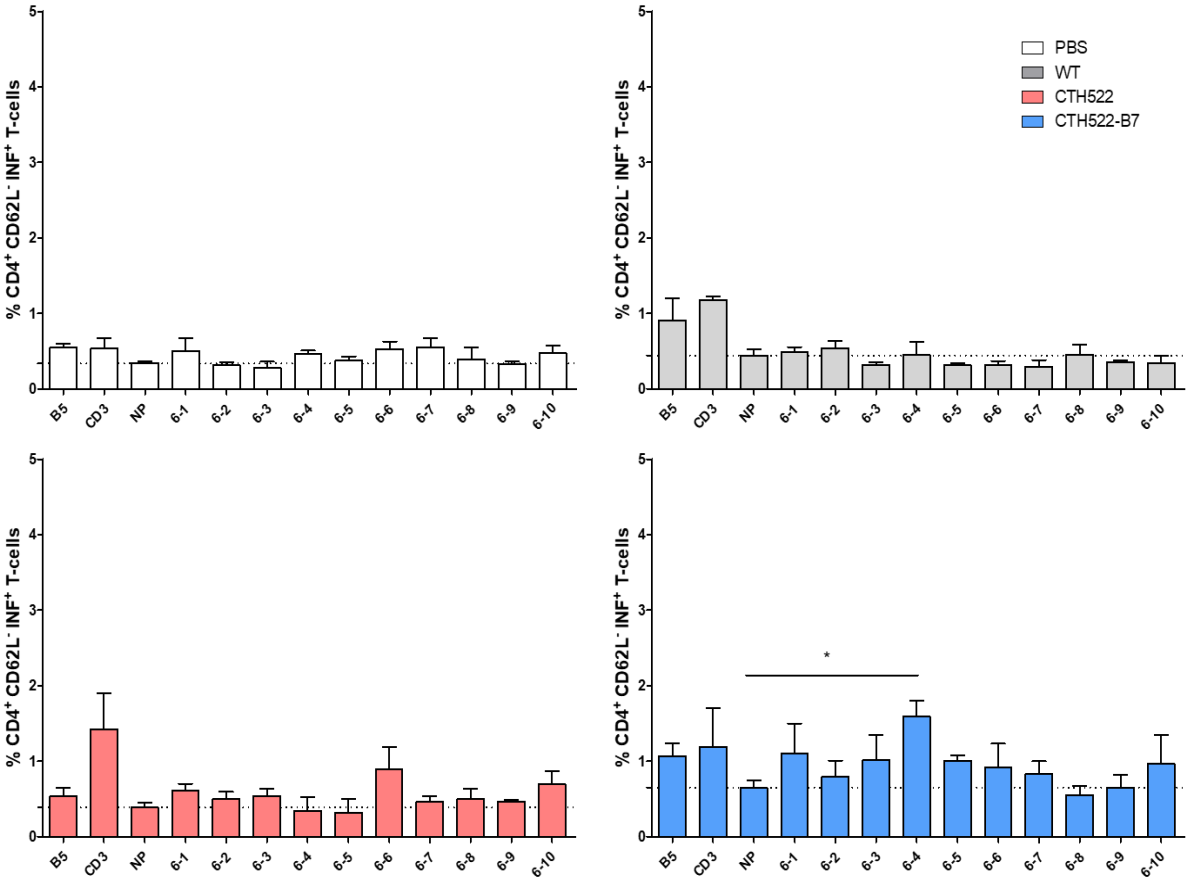

Figure 24. *Ex vivo* analysis of single peptides from pool 6 resulting in CTH522-specific IFN-γ production within CD4+ T cell population after prime/boost vaccination. C57BL/6J mice were immunized with PBS, MVA-WT, MVA-CTH522 and MVA-CTH522:B7 in a homologous prime/boost regimen where animals were primed on day 0, boosted on day 5 and sacrificed on day 13. Splenocytes were pulsed with the corresponding peptide for 15 hours with Brefeldin A. 15 hours after peptide pulsing, the splenocytes were stained for living or dead cells with Fixable Visability Dye APC, anti-mouse CD62L-PE, anti-mouse CD4-Pacific Blue and anti-mouse IFN-γ-FITC by intracellular cytokine staining followed by FACS analysis. Thresholds were determined by the corresponding NP value. Results represent 3 independent experiments shown with means ±SEM. Controls were used as follows; B5 45-60, an MVA late gene product that serves as a MVA control. Purified Hamster Anti-Mouse CD3e: protein complex that serves as an activation control. NP 311-325: influenza virus nucleocapsid peptide that serves as a negative control. Statistical analysis was done by two-tailed student's t-test were one star * indicates $p < 0.05$ and two stars ** indicate $p < 0.01$.

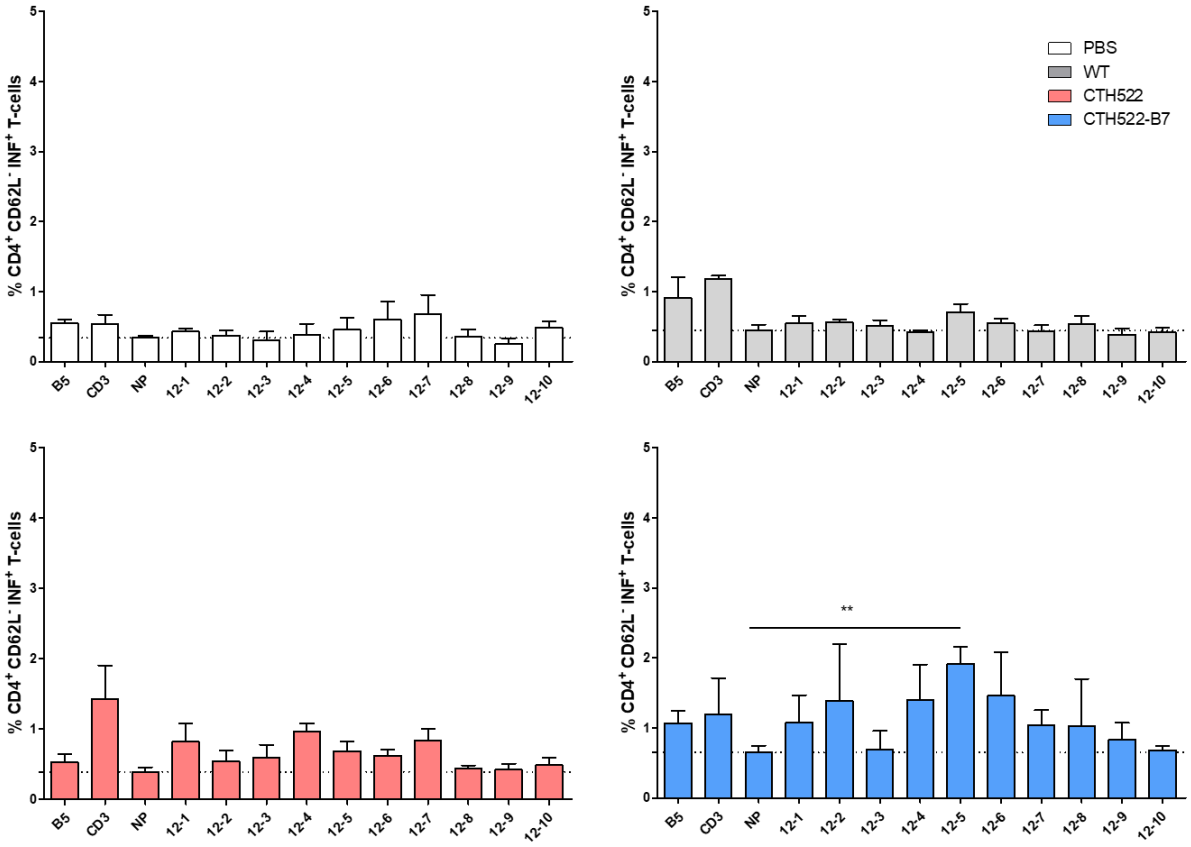

Figure 25. *In vivo* analysis of single peptides from pool 12 expressing high IFN-γ activation concentration within CD4+ T cell population after prime/boost vaccination. C57BL/6J mice were immunized with PBS, MVA-WT, MVA-CTH522 and MVA-CTH522:B7 in a homologous prime/boost regimen where animals were primed on day 0, boosted on day 5 and sacrificed on day 13. Splenocytes were pulsed with the corresponding peptide for 15 hours with Brefeldin A. 15 hours after peptide pulsing, the splenocytes were stained for living or dead cells with Fixable Visability Dye APC, anti-mouse CD62L-PE, anti-mouse CD4-Pacific Blue and anti-mouse IFN-γ-FITC. Thresholds were determined as the corresponding NP value. Results represent 3 independent experiments shown with means ±SEM. Controls were used as follows; B5 45-60, an MVA late gene product that serves as a MVA control. Purified Hamster Anti-Mouse CD3e: protein complex that serves as an activation control. NP 311-325: influenza virus nucleocapsid peptide that serves as a negative control. NP: influenza nucleocapsid. Statistical analysis was done by two-tailed student's t-test were one star * indicates $p < 0.05$ and two stars ** indicate $p < 0.01$.

4.3.2. Analysis of CD4+ T cells in heterologous immunization regimen in combination with a DNA vector expressing CTH522

It has been previously shown that in vaccination regimens involving MVA, priming with a DNA-based vector and boosting with the recombinant MVA increases the specific cellular response when opposed to priming and boosting in a homologous MVA-MVA regimen (Chapman et al., 2017; Chege et al., 2017). With the objective of determining whether or not this remained true for the CTH522-specific $CD4^+$ T cell responses, a study was designed accordingly in order to compare the $CD4^+$ T cell responses of a homologous MVA-MA prime/boost immunization response to that of a heterologous DNA-MVA prime/boost regimen (**Figure 26**).

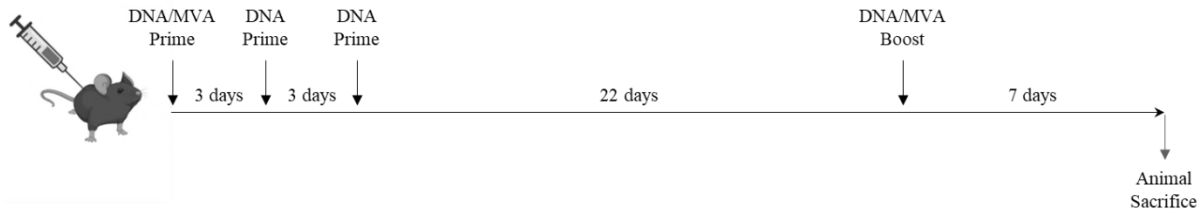

Prime	Boost
DNA-φ	MVA-WT
DNA-SP:CTH522	DNA-SP:CTH522
DNA-SP:CTH522	MVA-CTH522:B7
MVA-CTH522:B7	MVA-CTH522:B7

Figure 26. Immunization scheme followed for the *ex vivo* analysis of $CD4^+$ T cell responses comparing a MVA-MVA homologous prime/boost regimen to a DNA-MVA heterologous prime/boost regimen. C57BL/6J mice were immunized with the groups on the table above with DNA immunizations administered intradermally and MVA immunizations intramuscularly. Five mice were used per group.

Five animals per group were immunized according to the timeline displayed in Figure 26 with DNA vaccines being administered by intradermal tattooing and MVA vaccines being administered intramuscularly. All animals were sacrificed on day 35 and their spleens were harvested with the intention of determining the CTH522-specific CD4 T cell response. Splenocytes were pulsed with the peptide of choice (peptides 49 and 69, as well as a combination of both were analyzed in the study), the corresponding controls (a combination of CD3 and CD28 for unspecific activation, B5 peptide as an MVA control and NPxx peptide as a negative peptide control) or the purified CTH522 protein.

Results show that the group immunized with a heterologous DNA-MVA prime/boost vaccination regimen showed a higher IFN-γ activation profile when

compared to the homologous DNA-DNA prime/boost vaccination regimen or the homologous MVA-MVA prime/boost vaccination (**Figure 27**). Interestingly, while those splenocytes pulsed with peptide 69 showed a significant difference between the

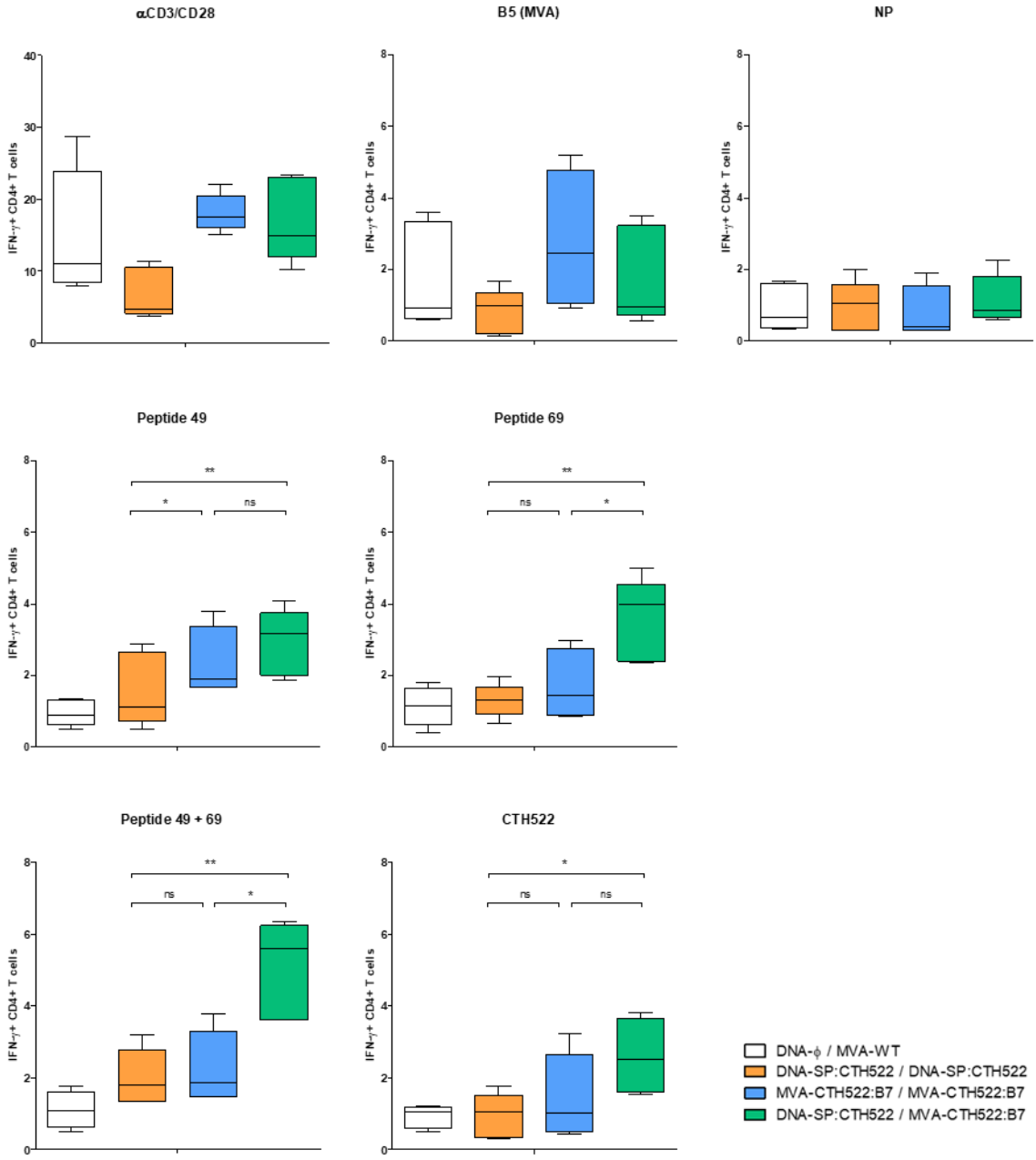

Figure 27. CTH522-specific IFN-γ+ CD4 T cell responses in homologous MVA-MVA, homologous DNA-DNA and heterologous DNA-MVA immunization regimens measured 7 days post boost. C57BL/6J mice were immunized with DNA plasmid administered intradermally and MVA immunizations administered intramuscularly. Splenocytes were isolated inmediately following animal sacrifice and pulsed with each individual peptide for 6 hours beforeintracellular staining andFACS analysis. Samples were stained for living or dead cells with Fixable Visability Dye eFluor 660, anti-mouse CD4-Pacific Blue and anti-mouse IFN-γ-FITC. Controls were used as follows; B5 45-60, an MVA late gene product that serves as a MVA control. Purified Hamster Anti-Mouse CD3e: protein complex that serves as an activation control. NP 311-325: influenza virus nucleocapsid peptide that serves as a negative control. n = 5 shown by box and whiskers; min to max. Statistical analysis was done by two-tailed student's t-test were one star * indicates $p < 0.05$ and two stars ** indicate $p < 0.01$.

heterologous DNA/MVA and the MVA/MVA (** $p < 0.01$) in a very similar manner to that of the splenocytes pulsed with the combined 49 and 69 peptides, those pulsed with peptide 49 did not display a significant difference between the groups, but did exhibit a significant increase when compared to the homologous DNA/DNA (* $p < 0.05$). Cells pulsed with the purified CTH522 protein also lacked a significant difference between the different regimens, merely displaying a significant difference (* $p < 0.05$) between the heterologous DNA/MVA and the homologous DNA/DNA regimen.

4.3.3. Mice immunized with MVA-CTH522:B7 show a higher antibody response as opposed to mice vaccinated with MVA-CTH522 after a 13-day prime/boost protocol

Despite the fact that a 13-day regimen is not considered to be ideal for a proper study of antibody responses elicited from MVA immunizations, one was conducted in spite of this with the objective of ensuring the thorough use of the animals sacrificed for cellular immune response analysis. Therefore, blood was collected from mice immunized in a short prime/boost vaccination regimen. Mice were primed intramuscularly with PBS, MVA-WT, MVA-CTH522 and MVA-CTH522:B7 on day 0, boosted on day 5 and sacrificed on day 13. Serum was separated from blood by centrifugation after allowing the sample to clot for an hour at room temperature. Samples were analyzed with Multiskan GO at wavelength 405. The threshold for what was determined to be a specific antibody response (both IgG and IgM) was defined as twice the mean of the values obtained from PBS immunized mice. Results show a definitive difference in those mice vaccinated with MVA-CTH522:B7, which displayed a consistent CTH522-specific antibody response defined over the determined threshold even at endpoint titer 1:200, and those mice immunized with MVA-CTH522, which failed to show CTH522-specific antibody responses and were comparable to that of the controls MVA-WT and PBS (**Figure 28**). While the experimental setup itself was not modelled after MVA antibody responses but after cellular responses, results proved that there was B cell activation thirteen days after MVA priming and within five days of MVA boosting in those animals immunized with MVA-CTH522:B7.

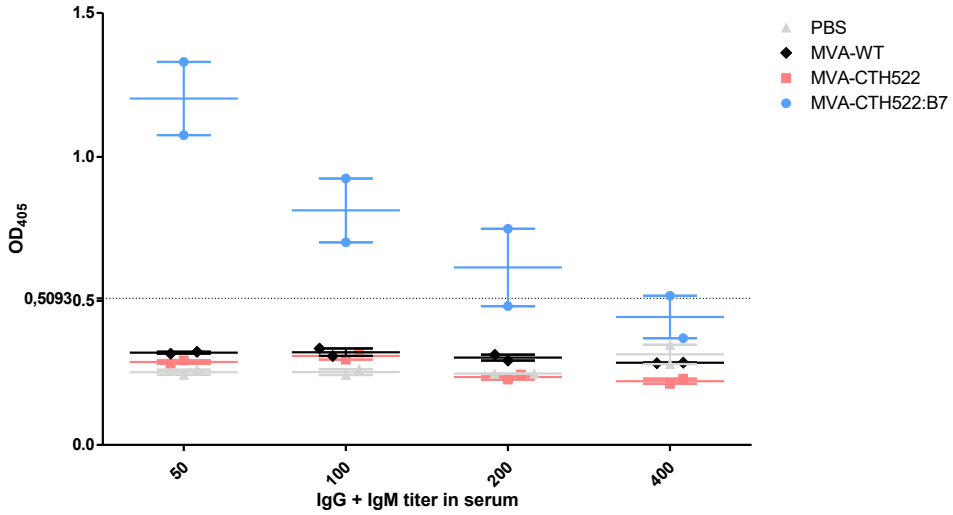

Figure 28. Only mice immunized twice with MVA-CTH522:B7 show a CTH522-specific antibody response already at day 13 following a prime/boost protocol. Antibody endpoint titers determined by ELISA analysis of serum collected on day 13 after vaccination of C57BL/6J mice with PBS, MVA-WT, MVA-CTH522 and MVA-CTH522:B7 on day 0 and day 5. Plates were coated with the purified CTH522 protein, followed by the serum and then with a secondary antibody binding to IgG and IgM. Threshold was determined as the median of the PBS group values multiplied by two. Results represent n = 2 shown with means ±SEM

4.3.4. Antibody evaluation after a 44-day prime/boost regimen by ELISA displays a higher antibody response against CTH522 after boosting with MVA-CTH522:B7

Once it had been confirmed that mice vaccinated with MVA-CTH522:B7 elicited an antibody response against CTH522, a proper study with an agenda that adjusted to the optimal conditions for MVA immunizations was performed. For this, mice were primed intramuscularly with PBS, MVA-WT, MVA-CTH522 and MVA-CTH522:B7 on day zero. Blood was collected 20 days after priming and serum was separated by centrifugation. A total of 30 days after priming, animals were boosted with a higher viral dose compared to priming. Mice were sacrificed on day 44 after priming, which was 14 days after the boost. Sera were analyzed by ELISA for the presence of CTH522-specific IgG and IgM, but failed to show any kind of specific antibody response to CTH522 after the priming **(Figure 29)**. However, there was a drastic difference in the results obtained with the samples collected after the boosting, with a highly significant response (*** $p < 0.001$) in those mice immunized with MVA-CTH522:B7 even in the higher serum endpoint dilutions such as 1:800. While at this point the significance started to gradually decrease, it still displayed a definitive difference at endpoint titer 1:3200 (* $p < 0.05$) until it finally

became not significant at endpoint titer 1:6400. Mice vaccinated with MVA-CTH522 did not display significant CTH522-specific response after priming nor after boosting.

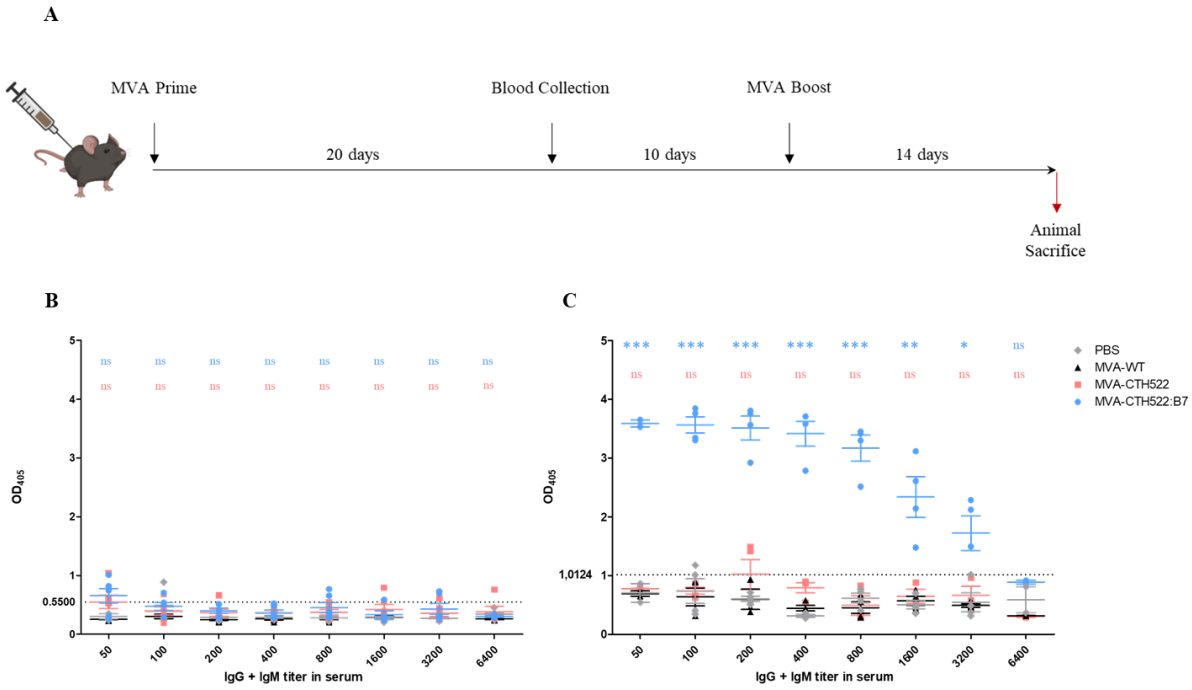

Figure 29. Mice exhibit a significant IgG and IgM response against CTH522 only after boosting with MVA-CTH522:B7. (A) Schematic of the timetable used for antibody analysis of homologous MVA-MVA immunization regimens **(B)** Antibody endpoint titers by ELISA analysis of serum collected from C57BL/6J mice on day 20 after priming with PBS, MVA-WT, MVA-CTH522 and MVA-CTH522:B7. **(C)** Antibody endpoint titers by ELISA analysis of serum collected on day 44 from C57BL/6J mice boosted with PBS, MVA-WT, MVA-CTH522 and MVA-CTH522:B7. Results represent n = 3 shown with means ±SEM. Statistical analysis was done by two-tailed student's t-test were one star * indicates $p < 0.05$ and two stars ** indicate $p < 0.01$.

With the intention of further studying the antibody responses from mice immunized with MVA-CTH522, the same samples were analyzed by ELISA for CTH522-specific IgG only concentrations (**Figure 30**). Results showed a significant response after the priming only at the lowest endpoint titer, corresponding to a serum dilution of 1:50 and, therefore, the highest serum concentration of all the analyzed samples. Interestingly, significant difference was seen in those groups vaccinated with either MVA-CTH522 or MVA-CTH522:B7 but it is of note that those vaccinated with MVA-CTH522:B7 displayed a higher significance (*** $p < 0.001$) than those vaccinated with MVA-CTH522 (** $p < 0.01$). Once again, there was a stark contrast to the results obtained from the samples taken after the boosting, with IgG responses increasing drastically. The group immunized with MVA-CTH522 had a significant difference as opposed to the controls with a slight response at endpoint titer 1:50 (* $p > 0.05$) but it fell short when compared to those mice immunized with MVA-CTH522:B7 and exhibiting a higher significant

difference (*** p > 0.001) at the same endpoint titer. While mice immunized with MVA-CTH522 failed to show any significant results after the endpoint titer 1:50, the group immunized with MVA-CTH522:B7 continued to display the highest statistical significance (*** p > 0.001) all the way to endpoint titer 1:800, when it decreased (** p > 0.01) before resulting in a not significant response at endpoint titer 1:1600. Overall, it can be concluded that vaccinating with MVA-CTH522:B7 seems vital in order to elicit any humoral response against CTH522.

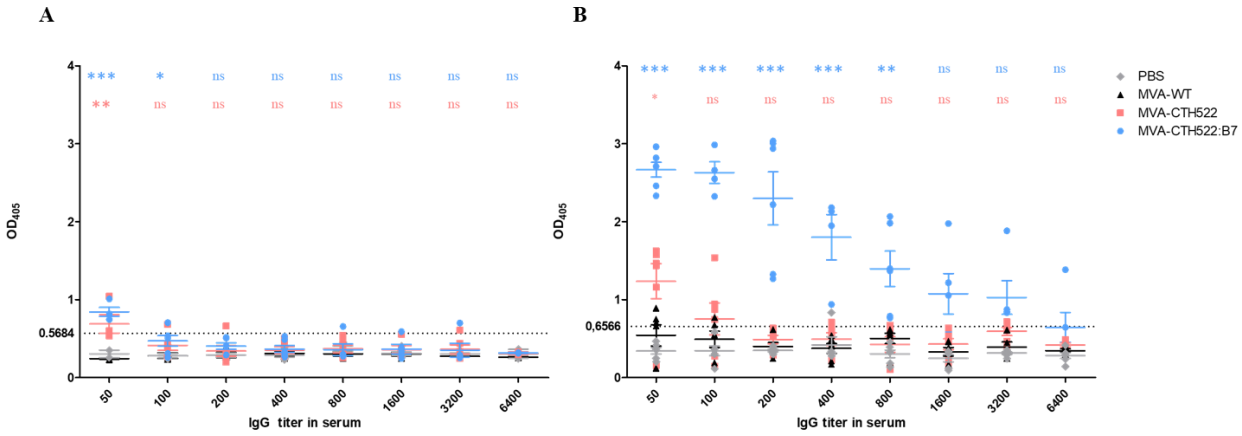

Figure 30. Mice display a highly significant specific IgG response against CTH522 after priming and boosting with MVA-CTH522:B7. (A) Antibody endpoint titers by ELISA analysis of serum collected on day 20 from C57BL/6J mice primed with PBS, MVA-WT, MVA-CTH522 and MVA-CTH522:B7. **(B)** Antibody endpoint titers by ELISA analysis of serum collected on day 44 from C57BL/6J mice boosted with PBS, MVA-WT, MVA-CTH522 or MVA-CTH522:B7. Results represent n = 3 shown with means ±SEM. Statistical analysis was done by two-tailed student's t-test were one star * indicates $p < 0.05$ and two stars ** indicate $p < 0.01$.

4.3.5. Mice immunized with MVA-CTH522:B7 exhibit a significantly increased neutralization activity against C. trachomatis when compared to MVA-CTH522

In order to continue the evaluation of MVA-CTH522:B7 as a vaccine candidate against *C. trachomatis*, it is vital to determine whether or not the antibody activity previously displayed in mice immunized with a homologous MVA-CTH522:B7/MVA-CTH522:B7 was neutralizing and would, therefore, counteract or reduce the bacterial infection. For this, a neutralization assay was performed. HaK cells were incubated with an inoculum formed by a 1:1 ratio of *Chlamydia trachomatis* Sv. D in SPG buffer and serum obtained from mice that had been immunized intramuscularly with PBS, MVA-WT, MVA-CTH522 and MVA-CTH522:B7 in homologous vaccination regimens with the same priming and boosting schedule as depicted in **Figure 29A**. After washing the inoculum from the cells and incubating them at 37 ºC for 4 hours, cells were fixed with EtOH and stained with DAPI in order to display the nuclei and with CT043 monoclonal

rabbit Ab as 1st Ab and Alexa Flour 488 goat anti-rabbit IgG (H+L) as 2nd Ab to stain the inclusion bodies that would form from the bacterial infection.

A sample image of the neutralization activity of sera from homologous MVA-CTH522:B7/MVA-CTH522:B7 prime/boost immunization in comparison to the MVA-WT/MVA-WT immunization regimen (**Figure 31**) displayed a large number of inclusion bodies in those samples that were incubated with serum from mice vaccinated with MVA-WT/MVA-WT. These control samples where no neutralization activity was to be expected showed approximately fourteen inclusion bodies in the optical field as opposed to those samples incubated with serum obtained from mice vaccinated with MVA-

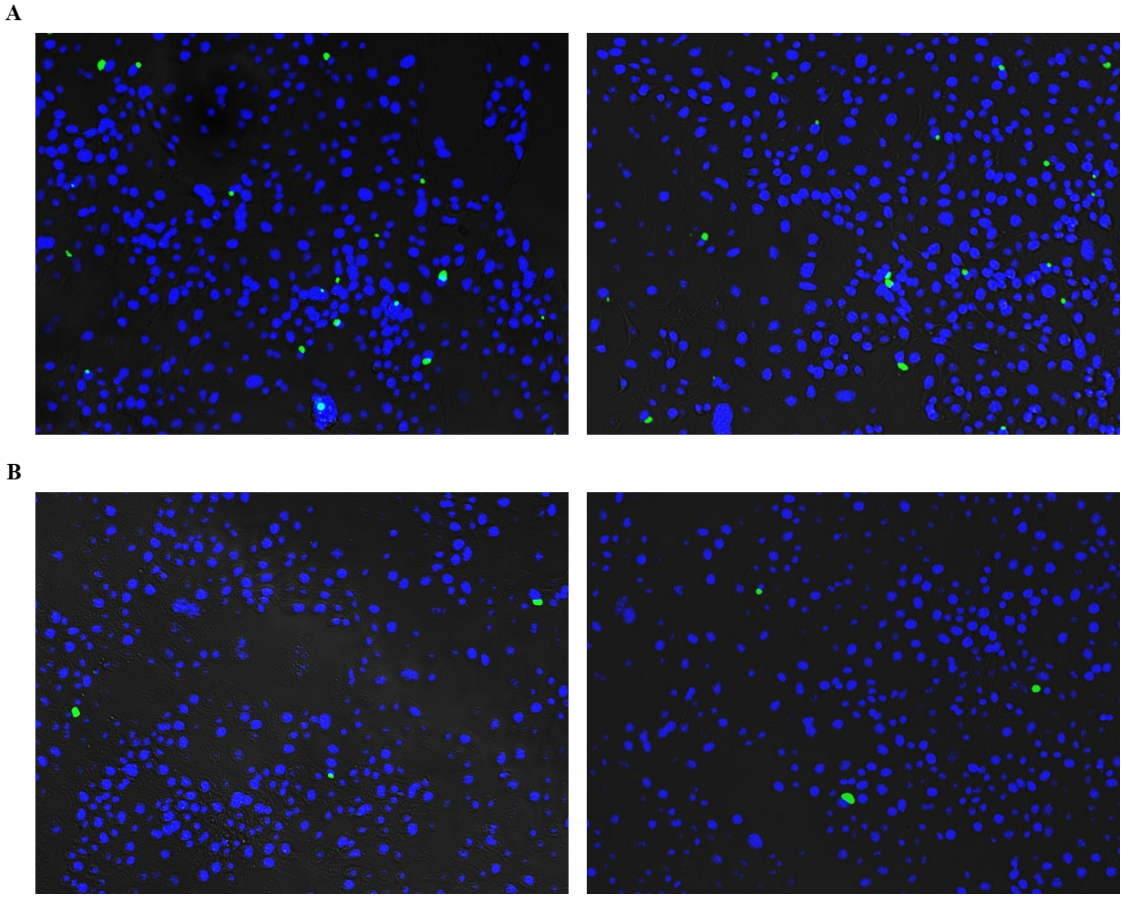

Figure 31. Sample images of *C. trachomatis* neutralization assay. Images depict HaK cells after a 2 hour co-incubation with an 1:1 inoculum of serum:bacteria. *Chlamydia trachomatis Sv. D* bacteria and serum obtained from mice immunized with **(A)** a homologous MVA-WT/MVA-WT regimen and **(B)** a homologous MVA-CTH522:B7/MVA-CTH522:B7 regimen were used. After a 24 hour incubation, cells were fixed and stained with DAPI, CT043 anti-rabbit monoclonal antibody as 1st antibody and Alexa Flour 488 goat anti-rabbit IgG (H+L) as 2nd antibody. The blue immunofluorescence indicates DAPI-stained nuclei and the green immunofluorescent indicates inclusion bodies formed from the Chlamydia infection. Images were obtained through AMG EVOS fl fluorescence microscope and their brightness was increased to improve the quality. Images depict the best representative from each group (n = 3). Ten optical fields were evaluated for each sample with AMG EVOS fl fluorescence microscope.

CTH522:B7/MVA-CTH522:B7, which displayed about three inclusion bodies in the optical field. Ten optical fields were evaluated for all samples.

Results conclusively showed a neutralization activity in those samples incubated with serum obtained from mice that had been previously immunizedwith a homologous MVA-CTH522:B7/MVA-CTH522:B7 regimen (**Figure 32**), with an average

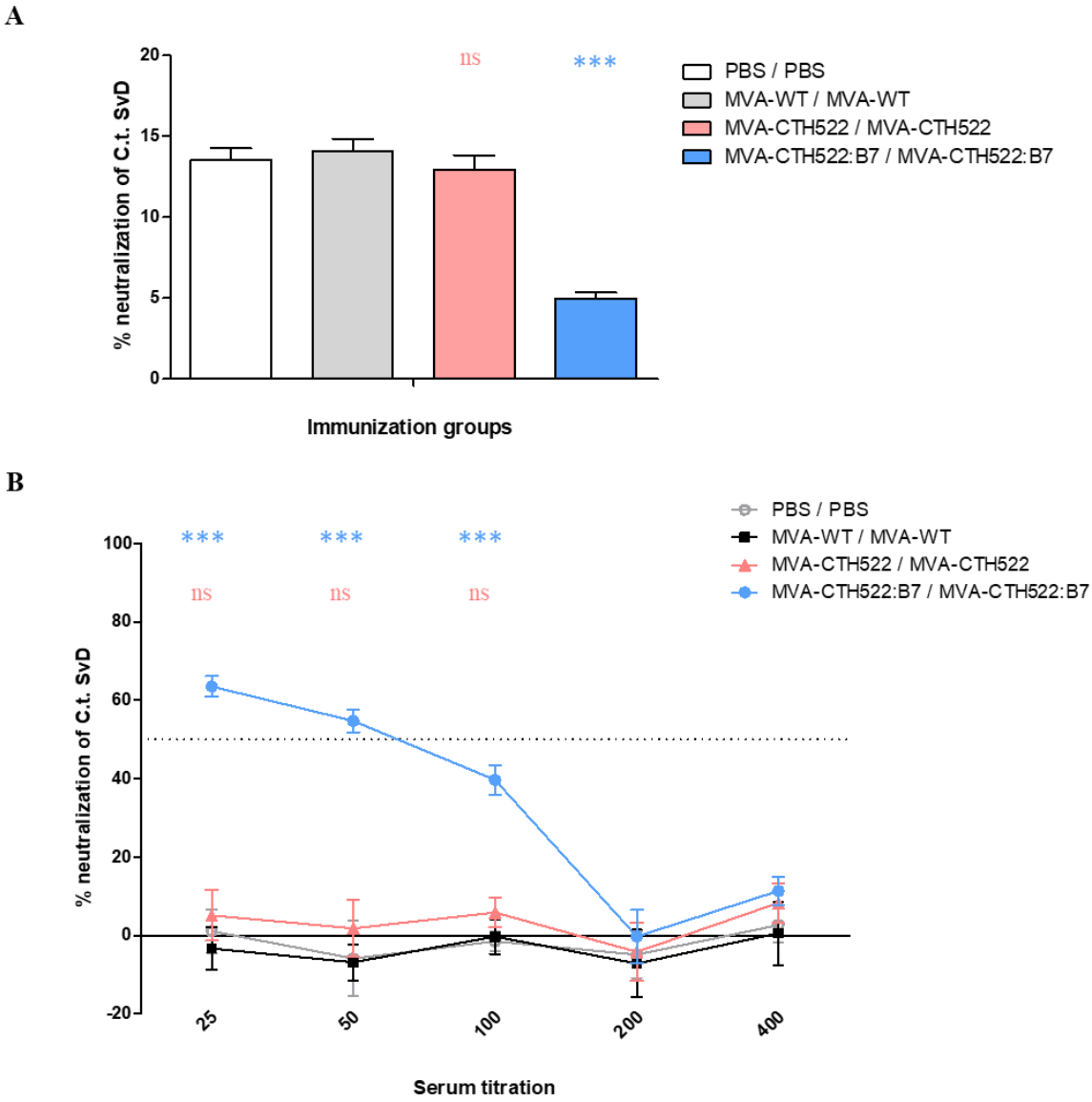

Figure 32. CTH522-specific neutralization activity in sera from immunized mice. HaK cells were co-incubated for 2 hours with an inoculum of serum:bacteria with *Chlamydia trachomatis Sv. D* bacteria and serum obtained from mice immunized with homologous regimens of PBS, MVA-WT, MVA-CTH522 and MVA-CTH522:B7. After a 24 hour incubation, cells were fixed and stained with DAPI, CT043 anti-rabbit monoclonal antibody as 1st antibody and Alexa Flour 488 goat anti-rabbit IgG (H+L) as 2nd antibody **(A)** Bar graph shows the inclusion body count from each group with a serum dilution of 1:25 **(B)** Graph depicting the neutralization capacity of the different immunization groups as percentage deviating from the baseline defined by the median of the inclusion bodies found in the PBS/PBS group. Threshold was established at 50% neutralization activity. Results represent n = 3 with 2 technical replicates each shown with means ±SEM. Statistical analysis was done by two-tailed student's t-test were one star * indicates $p < 0.05$ and two stars ** indicate $p < 0.01$. Ten optical fields were evaluated for each sample with the use of AMG EVOS fl fluorescence microscope.

neutralization activity of 63.5% at serum endpoint titer 1:25. The baseline of 0% neutralization activity had been defined as the median of the inclusion body count found in the group with serum from mice immunized with PBS as a mock control. The neutralization activity percentage of the MVA-CTH522:B7/MVA-CTH522:B7 group decreased in an exponential curve as the serum dilution increases, reaching the threshold of 50% neutralization activity between the 1:50 and the 1:100 dilutions, at which point it was no longer considered to be an ideal neutralization capacity against the bacterial infection. Nevertheless, the neutralization activity shown by the MVA-CTH522:B7/MVA-CTH522:B7 group continued to be highly statistically significant (*** $p > 0.001$) while the neutralization from the MVA-CTH522/MVA-CTH522 was not significant at any dilution tested.

4.3.6. Mice immunized following a homologous MVA-MVA regimen show a higher antibody response than those immunized using a heterologous DNA-MVA regimen

After calculating the difference in CD4 T cell responses between a homologous prime/boost MVA-CTH522:B7/MVA-CTH522:B7 and a heterologous prime/boost DNA-SP:CTH522/MVA.CTH522:B7 and finding a higher CD4 T cell response in those mice immunized according to the heterologous protocol, an antibody study was performed with the aim of determining which protocol allows for a higher humoral immune response. For this, an immunization scheme that was a compromise for both

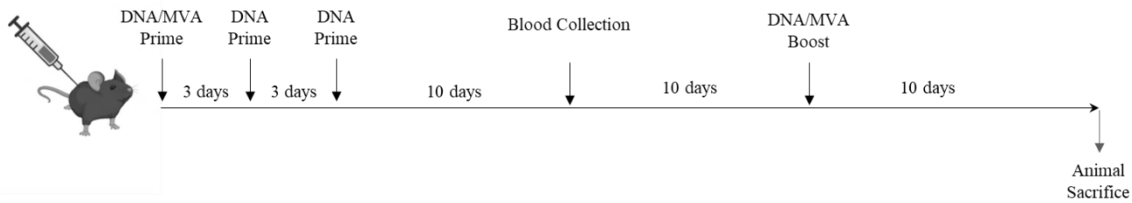

Prime	Boost
DNA-φ	MVA-WT
DNA-SP:CTH522	DNA-SP:CTH522
DNA-SP:CTH522	MVA-CTH522:B7
MVA-CTH522:B7	MVA-CTH522:B7

Figure 33. Immunization scheme and experimental groups for the *ex vivo* analysis of antibody responses comparing a MVA-MVA homologous prime/boost regimen to a DNA-MVA heterologous prime/boost regimen. C57BL/6J mice were immunized accordingly as described on the table above with DNA immunizations administered intradermally and MVA immunizations intramuscularly. Blood was collected by submandibular vein puncture at day 16 and by peri-orbital venous sinus bleeding at the time of animal sacrifice. Six mice were used per group.

DNA- and MVA-based vaccines in regards to antibody responses was decided upon (**Figure 33**). Therefore, mice were primed at day 0 with DNA- or MVA-based vaccines, and primed again at day 3 and 6 with DNA-based vaccines. Blood was collected 16 days after the priming and at the time of animal sacrifice, 10 days after boosting with DNA or MVA depending on the experimental group. DNA vaccines were administered by intradermal tattooing and MVA vaccines were administered intramuscularly. Mice serum was separated from blood by centrifugation after allowing the sample to clot for one hour at room temperature. After coating an ELISA plate with the purified CTH522 protein, the plate was washed and serial dilutions of mice serum were added to the plate for an hour before washing again and placing a dilution of alkaline phosphatase-conjugated IgG secondary antibody. After an incubation of one hour, the plate was washed and a substrate solution was added for thirty minutes before samples' optical density was measured with Multiskan GO at wavelength 405. The threshold for what was determined to be a positive antibody response was defined as twice the mean of the optical density values measured in the PBS group.

Results do not show any kind of significant response after the priming (**Figure 34**) despite the presence of a slight peak from the mice immunized with the homologous DNA/DNA protocol at endpoint titer 1:50. However, as it has been previously shown, antibody responses in the MVA-MVA group drastically increased in those samples collected after mice were boosted.. Specifically, antibody responses from mice vaccinated with the MVA-CTH522:B7/MVA-CTH522:B7 regimen were significantly (*** $p > 0.001$) higher when compared to the control groups. Antibody responses in mice vaccinated with the heterologous DNA-SP:CTH522/MVA-CTH522:B7 regimen were

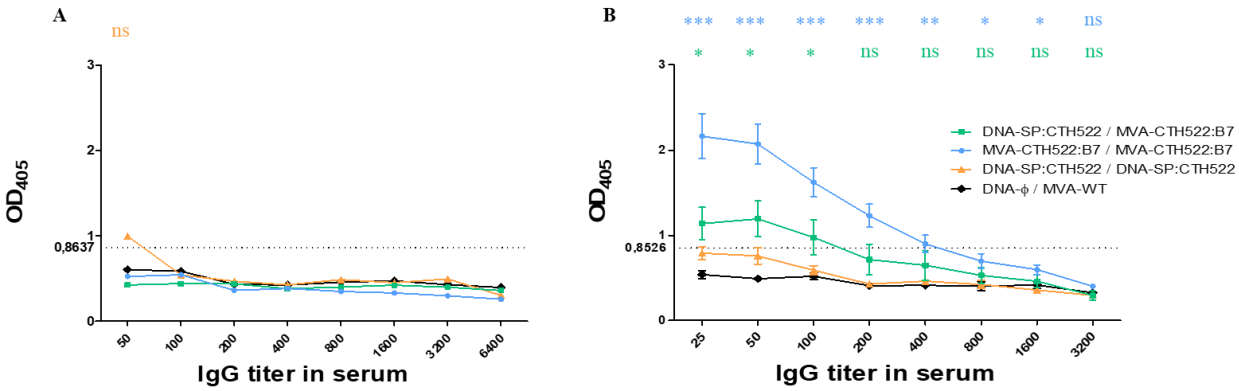

Figure 34. Mice exhibit a significantly higher IgG response against CTH522 after homologous MVA-CTH522:B7/MVA-CTH522:B7 prime/boost immunization. Antibody endpoint titers calculated after ELISA analysis of sera collected on day 36 from C57BL/6J mice after **(A)** priming with MVA-CTH522:B7, DNA-SP:CTH522 or pVAX1 (hereby referred to as DNA-Ø) **(B)** boosting with MVA-CTH522:B7, DNA-SP:CTH522 or MVA-WT. Results represent n = 6 shown with means ±SEM

less increased (* $p > 0.05$) when compared to the control groups. While mice vaccinated with the homologous DNA-DNA regimen failed to show statistical significance at any serum dilution, mice vaccinated with the homologous MVA-MVA regimen continuously showed a significant difference all the way up to endpoint titer 1:200, and gradually started to lower but continued to show a significant difference with the control even when they fell under the established threshold until finally becoming not-significant at endpoint titer 1:3200.

5. DISCUSSION

There might be many reasons behind the obvious unsuccess in reducing the infection rate of *C. trachomatis*, but the conclusion remains constant: something has to be done if a decrease in prevalence and infection rate is to be observed. The fact remains that chlamydia is the pathogen behind the most common sexually transmitted disease caused by a bacterium and, among its species, *C. trachomatis* has the greatest burden on world health even today (Wan et al., 2023). The question of whether to approach infectious pathogens with a preventive or therapeutic strategy always arises when considering measures to control the incidence of an infectious disease. There are current antibiotic options available that make the infection curable and, in spite of them, approximately 128.5 million cases emerged in 2020 (World Health Organization, 2023). Not only is this treatment unsuccessful in controlling the infection rate of Chlamydia worldwide, but it also does not offer protective immunity and is of no use when trying to decrease the incidence in asymptomatic individuals (Murray & McKay, 2021). Because C. *trachomatis* presents most commonly asymptomatically (with a staggering 70-90% of infections) (Panzetta et al., 2018), individuals are not aware that they are infected until severe symptoms do present and develop, leading to serious complications in the patient that can no longer be mitigated by bacterial clearance through antibiotics. Current preventive strategies are aimed at increased routine screening of high-risk populations (Centers for Disease Control and Prevention, 2021), access to better hygiene and sanitation and mass antibiotic administration in affected communities (Woodhall et al., 2018). Therefore, while the preventive approach seems to be the most favorable one when aiming to decrease *C. trachomatis* incidence, current strategies are failing to do so, pointing in the direction of vaccine development in the hope of reducing the infection rate.

While there is little research targeting C. *trachomatis* through the use of viral vectors, they have shown to generally be a valuable choice when aiming to elicit a robust immune response against infectious pathogens. Specifically, MVA is a poxvirus vector that has been thoroughly used in the field of vaccine research and development because of its attenuated profile, conferring it the characteristic of being replication-incompetent in most mammalian cells. Not only is MVA cost-effective in terms of generation and development, but it has also proven to have a safe profile and to be able to elicit a robust humoral and cellular immune response, making it an ideal candidate for gene delivery (Sasso et al., 2020).

Therefore, with the objective of generating a promising vaccine candidate against C. *trachomatis*, this study proposes a novel recombinant MVA vector encoding the vaccine antigen CTH522 fused to the signal sequence and cytoplasmic domain of the B7.1 molecule.

5.1. recMVA-CTH522:B7 is successfully generated through the BAC system

CTH522 is a recombinant vaccine antigen originally designed by fusing a truncated MOMP to immunorepeats from the variable domains of four different serovars. This antigen has been previously studied as a protein vaccine in both, animal models and clinical trials, proving to have a safe and immunogenic profile against *C. trachomatis* (Abraham et al., 2019). With the objective of targeting a robust two-arm response involving both humoral and cellular immunogenicity, the vaccine antigen CTH522 that had been codon-optimized for eukaryotic expression was inserted into the MVA genome via the so-called BAC system.

As opposed to the more traditional marker-based system, which consists of homologous recombination led by a shuttle vector in infected cells and a consequent optical selection of solid plaques detected by expression of reporter genes, the BAC system relies on a self-excising variant of MVA-BAC where the selection marker is encoded within the BAC cassette which is deleted after reconstitution of viral progeny. This makes the identification of positive clones considerably less demanding and ensures the insertion of the antigen of interest at an earlier stage than the marker-based system (Kugler et al., 2019).

In order to generate the recombinant MVA-CTH522:B7, the vaccine antigen CTH522:B7 was cloned into pEP-MVA-dVI-PmH5, a shuttle vector that contains homologous regions to the deletion VI of the MVA genome and that would later on allow the homologous recombination into the deletion VI locus of the MVA genome, while the deletion III acts as an integration site for the BAC (**Figure 5**). The plasmid contained PmH5, a strong early/late vaccinia virus promoter that has been shown to overexpress the antigen of interest, inducing an increased immune response when compared to other vaccinia virus promoters (Kugler et al., 2019). A Kanamycin resistance gene (*AphAI*) was also found within the transfer plasmid for positive selection in bacterial agar plates. Despite the fact that the *Aph*AI gene can remain in the recombinant virus without eliciting any detrimental effects on the immune response in murine models or deterring viral

replication (Cottingham & Gilbert, 2010), it was nonetheless excised in this work in order to ease its use in future clinical applications. After the first stage of the two-step Red-mediated BAC system where the CTH522:B7 antigen was inserted into the plasmid (**Figure 6**), the deletion of the *AphAI* gene was achieved in the GS1783 *E. coli* strain, where *en passant* recombineering occurs via *in vivo* I-*Sce*I cleavage (Karsten Tischer et al., 2010) that was triggered by L-arabinose, therefore leading to what is referred to as a markerless construct (Tischer et al., 2006).

The next step in the generation of a recombinant MVA was to rescue the recombinant progeny virus, which was easily achieved through a transient co-transfection-infection assay performed with Rabbit Fibroma Virus acting as a helper virus, as it is unable to replicate in DF-1 cells, where the rescue was performed, but it provides the initial transcription machinery that will trigger the recombinant MVA replication. In contrast to the previously mentioned marker system for recMVA generation, where eliminating the wild-type virus from the viral culture involves several rounds of tedious plaque isolation and plaque purification (Kugler et al., 2019), the BAC system was shown to eliminate the helper virus RFV in merely three rounds of serial sub-passaging in this study. Another group using the MVA-BAC system found it took approximately 1-2 weeks for the subpassing step to be completed successfully, although they did not mention the number of passages they had to perform. They also used an attenuated strain of fowlpox as a helper virus instead of RFV, and performed the titrations in CEF cells instead of DF-1, as it was done for this work (Cottingham & Gilbert, 2010). The proper excision of the BAC cassette and the thorough elimination of RFV in the culture while maintaining the integrity of the CTH522:B7 antigen (**Figure 8**) proved the successful generation of the recombinant MVA-CTH522:B7.

5.2. MVA host range and stability is not impaired after insertion of CTH522:B7 antigen

In order to ensure that MVA-CTH522:B7 could be safely passaged without partially or completely losing the foreign antigen, the genomic stability and functionality were verified after ten serial sub-passages in DF-1 cells. A PCR analysis of the ten passages with primers annealing within CTH522 revealed that the antigen CTH522:B7 was found in its complete integrity throughout the ten passages, and a further PCR analysis with primers annealing within CTH522 and a flanking region of the MVA deletion VI proved that the antigen was indeed stably located within its intended insertion site, therefore

revealing that CTH522:B7 was genetically stable within MVA (**Figure 9**). The functionality was checked through protein expression by western blot analysis, showing that MVA-CTH522:B7 efficiently expresses CTH522:B7 after prolonged serial sub-passages in avian cells (**Figure 10**).

Since it had already been proven that MVA-CTH522:B7 efficiently expressed the antigen of interest, additional Western Blot analyses were able to further elucidate the protein synthesis by MVA-CTH522:B7 in a wide variety of cell lines at different time points post-infection. The current standard in avian cell lines used for MVA studies are the primary Chicken Embryo Fibroblasts (CEF), and spontaneously-immortalized DF-1 cells, derived from CEF. Because CEF cells have displayed certain limitations such as reproducibility issues because of mild batch differences, a high production cost and a lengthy and strenuous generation (Giotis et al., 2019), DF-1 were the cell line of choice in these studies. Expression of CTH522 by MVA-CTH522:B7 was analyzed in DF-1 cells at 0, 4, 8 and 24 hpi via Western Blot analysis following viral inoculum isolation. A faint band was slightly visible at 4 hours post infection, consistent with the concept of what is referred to as viral eclipse; a phase as early as 2 hours after the initial infection (Garber et al., 2009), and even reported to last 4 to 6 hours post infection, where an absence of infectivity can be observed through lowered viral titers, and that is quickly followed by an increase in viral production at 7 to 8 hours post infection (Postlethwaite & Maitland, 1960). This can also be observed with the growing strength in band intensity at 8 and 24 hours post infection (**Figure 11**).

Aiming to study the antigen expression in human cells, HeLa cells were infected with MVA-CTH522:B7 or MVA-WT and harvested at 0, 4, 8 and 24 hours post infection before performing a Western Blot analysis. Multiple studies have analyzed the viral replication and infectivity rate of MVA in HeLa cells, with consistent results indicating that MVA is unable to replicate in them (Sutter & Moss, 1992). It is of note that MVA does lead to viral protein synthesis in non-permissive human cells, an essential characteristic of MVA within the vaccinology field. Research indicated that late protein processing in MVA-infected HeLa cells was inhibited and it was then theorized that it was due to the inability of MVA to form mature virions in HeLa cells (Sutter & Moss, 1992). Nonetheless, a study found a subtle increase in MVA titer between the 0 and 24 hour post infection time point (Carroll & Moss, 1997), which can also be observed in the progressive band strength of the Western Blot comparing the different time points after infection of HeLa cells with MVA-CTH522:B7 (**Figure 12**). Overall, both experiments proved that CTH522:B7 is stably integrated after 24 hours of infection at MOI = 5. Future

characterization studies should include the quantification of western blot bands in order to provide a more accurate analysis of the changing band strength among the different samples.

While there are some studies analyzing the non-replicative behavior of MVA in murine cell lines such as L-929 (Moss et al., 1996) and NMuLi (Okeke et al., 2006), there are seemingly no available research characterizing the behavior of MVA in Cloudman S-91 mouse melanoma cell line. S-91 cells are more commonly and presently referred to as "Cloudman cells" because they were derived from the Cloudman S-91 mouse melanoma culture from the DBA mouse strain. They are epithelial cells described to behave in a manner similar to that of cells derived from the Harding-Passey melanoma when in culture (Barishak et al., 1961). Preliminary unpublished data from Prof. Dr. Drexler's group had indicated a similar non-permissive nature to murine cell lines infected with MVA and, thus, the same experiment previously described was performed to analyze the protein synthesis in MVA-CTH522:B7 infected cells by western blot analysis. Results indicate an increase in expression when comparing the 0 and the 24 hour post infection time point in a similar manner to the HeLa cells (**Figure 12**), indicating that MVA is capable of infecting Cloudman cells, but not quite demonstrating whether or not the virus is able to replicate within the mouse melanoma cell line, therefore requiring further experiments (shown in later figures) before drawing any conclusions.

In order to accomplish this, a study was designed following the same pattern as the previous ones, but lengthening the duration of the harvesting time points. Whereas, the previous experiment (termed one-step growth) had samples from cells infected at high MOI collected at 0, 4, 8 and 24 hours post-infection, this one (namely, multiple-step growth) had the samples gathered at 0, 24, 48 and 72 hours post infection at low MOI in order to analyze the long-term functionality of CTH522-B7. The 48-hour sample of MVA-WT infected cells was mistakenly used in place of the 48 h MVA-CTH522:B7 infected cells' sample, leading to a missing band in the western blot when detecting CTH522 but displaying both bands at the cellular and viral controls. However, both bands at 24 and 72 hours display a positive expression. In any case, the band at 72 hours shows to be slightly fainter than the one at 24 hours. The reasons behind this are unclear, but one hypothesis points to a delayed degradation of CTH522:B7 mediated by the proteosome, as it has been shown that CTH522 without the B7 modification is degraded as early as 4 hours post infection through the ubiquitin-proteasome system (unpublished data by Giuseppe Andreacchio). Nevertheless, results were conclusive and in accordance with the established literature stating that DF-1 are fully permissive for MVA replication (Lohr et

al., 2009). Whereas the samples from semi-permissive HeLa cells show a comparative protein production between the initial 24-hour timepoint and the 72 hour one, the samples from non-permissive Cloudman cells exhibit a clear decrease in CTH522 synthesis past the 24 hour timepoint (**Figure 13**). However, it is of note that samples were not quantified and, therefore, any comparisons are based on mere visual monitoring, leading to a more specific and mathematical analysis of the replication behavior of MVA-CTH522:B7 through the study of growth kinetics.

While DF-1 and HeLa cells were excellent choices for functionality characterization of the recombinant virus, little to nothing has been previously published about MVA characterization on non-permissive Cloudman cells, indicating that perhaps future studies should be performed to deepen the understanding in this field. Another possibility would have been to characterize MVA synthesis in other murine cell lines. The same experimental setup as previously described was also performed on BMDCs (data not shown), *ex vivo* primary cells isolated from C57BL/6 mice that were used in later studies to characterize the viral replication capacity. However, through careful monitoring of the cell monolayer throughout the timeline of the experiment, the assay was terminated after observing that most of the cells had undergone apoptosis in the later time points, rendering any conclusions drawn from possible band strength as meaningless.

5.3. Insertion of CTH522:B7 has no detrimental nor beneficial effects on viral growth and replication

In order to test whether or not the insertion of antigen CTH522:B7 had any sort of effect on the virus multiplication of the novel MVA-CTH522:B7, so-called one-step growth kinetics was performed to compare the virus growth profile of MVA-CTH522:B7 to that of MVA-wt. Cells were infected with a high MOI and samples were harvested at 0, 4, 8 and 24 hours post infection.

DF-1 cells were analyzed once again to study how differently the recombinant virus would behave when compared to the wild type in a permissive line. The behavior of MVA in DF-1 cells has already been described as permissive, with an infection rate comparable to those known from primary CEF and BHK-21 cells. Moreover, studies have already shown the growth pattern of MVA-WT in DF-1 cells after the initial 24 hours of infection, displaying a sudden growth between the 0 and 24 hour time points (Garber et al., 2009). This study presents a more detailed analysis, showing the titer differences in DF-1 cells at four different timepoints within the first 24 hours of infection (**Figure 14 A**). The

previous work also showed an abrupt increase after 24 hours of infection at MOI = 3 when comparing DF-1 and CEF, supporting the growth kinetics of MVA-CTH522:B7 in permissive DF-1 cells. Both viruses show a comparative initial viral titer at 0 hours post infection, and MVA-WT exhibits a decreased titer at 4 hours post infection consistent with the previously described viral eclipse that MVA undergoes through the initial hours after viral infection. There seems to be a slight difference at the 4 and 8 hour post infection timepoint, it is marginal and insignificant, with the importance residing in the first and last timepoints of the experiment, which are nearly identical in both viruses.

Previous studies analyzing the growth behavior of MVA-WT in HeLa cells show a slight decrease between the 0 and 24 hour timepoints (Sutter & Moss, 1992) that is not exactly mirrored in this work (**Figure 14 B**). There is a subtle increase of viral titer along the first 24 hours of infection following viral adsorption, although the raise is indeed minimal. This disparity might be due to the difference in MOI, since the previous article used ten times less the amount chosen for the experiment in this study, infecting at MOI = 0.05 whereas HeLa cells were infected at MOI = 5 for this work. At the same time, it is of worth to note that this analysis has taken a look at four different time points where one can see the slight decrease in viral titer at the four hour time point, something consistent with previous literature and other results, and the consequent raise after 24 hours of infection, while the previously mentioned work limited itself to a direct comparison between 0 and 24 hours, without considering the slight curve that can be observed during the viral eclipse of MVA between the 4 and 8 hours post infection. Other studies have shown a slight increase in antigen production after 24 hours of a recombinant MVA infection in HeLa cells (Moss et al., 1996; X. Zhang et al., 2007), further supporting the results found within this work.

With the objective of analyzing the replication of MVA in a primary murine cell line, BMDCs isolated from C57BL/6 as described above (3.2.8) were infected with the same MOI of 5 and samples were also harvested at 0, 4, 8 and 24 hours. Dendritic Cells (DCs) have previously been described as non-permissive for MVA, with a regressive growth pattern where the viral titer decreases along four different time points within the initial 24 hours of infection (Drexler et al., 1998). Similarly, results in this work also indicate decrease in viral infection at four hours but, unlike with HeLa and DF-1 cells, there isn't a subtle or abrupt increase in viral titer, with the curve reaching a low but stable plateau after 8 hours that is maintained until 24 hours post infection (**Figure 14 C**). The experimental results from this work show that MVA-CTH522:B7 exhibits a comparable

growth to that of MVA-WT, with a significant similitude at the 0 hour time point after the adsorption period and after 24 hours of infection in all cell lines.

There are plenty of studies that have analyzed the replication capacity of MVA in DF-1 in longer timepoints than the previously mentioned 24-hour window. Results seem to be consistent in showing a sudden growth in the initial 24 hours of infection following the adsorption period, followed by a progressive viral growth until viral replication rate finally stabilizes at around 48-72 hours post infection (García-Arriaza et al., 2011, 2014, 2020; Pérez et al., 2019). These results are consistent with those found in this work (**Figure 15 A**), although the growth seemed to occur in a slightly steeper proportion and the stabilization of the infection rate between 48 and 72 hours post infection presented itself in a decrease of viral titers at 72 hours post infection.

Previous works have also studied the replication capacity of recombinant MVA vectors in HeLa cells. Interestingly, a study observed plasma membrane protrusions when HeLa cells were infected with a high MOI or with a low MOI for a long period of time, claiming a change of phenotype necessary for virus entry caused by the MVA infection (Gallego-Gómez et al., 2003). A study performed with a MOI = 0.05 found the viral titer virtually unchanged throughout four different timepoints, with a very subtle increase after the total 72 hours after the initial adsorption time (Moss et al., 1996). The study mentioned beforehand that described a slight decrease after 24 hours of infection was also able to observe an increase in virus yield as soon as 48 hours post infection (Sutter & Moss, 1992). Results in this work show a progressive increase in MVA-WT even after 24 hours, while MVA-CTH522:B7 seems to increase only after 48 hours post infection, remaining with stable viral titers until then (**Figure 15 B**). It has been proven that MVA does undergo a certain maturation stage in HeLa cells, leading to the formation of intracellular mature virions, which are the first infectious form of the virus, and intracellular envelope virus. The presence of both of these kinds of virions even in a semi-permissive cell line such as HeLa could, in turn, be potentially responsible for surrounding cell infection (Gallego-Gómez et al., 2003). This could theoretically explain why a certain degree of viral replication can be seen in a seemingly non-permissive cell line, something that is not replicated in other kinds of non-permissive lines, such as Cloudman cells. While there certainly is a slight increase in the infectivity rate 24 hours after the adsorption period, it is quickly followed by a gradual but constant decrease in infectious units all the way to 72 hours post infection, indicating that the virus is not replicating, but that cells are slowly undergoing apoptosis and, therefore, still regarded as infected (**Figure 15 C**). Since there does not seem to be any published data available on the replication behavior or capacity

of MVA on Cloudman cells, there are certain limitations in drawing definitive conclusions from the results in this work.

Nonetheless, it is expected for the virus to behave differently among a variety of hosts and cell types. The crucial conclusion from this study is the comparison between MVA-WT and MVA-CTH522:B7 within each isolated cell type or host, and MVA-CTH522:B7 has displayed a comparable pattern and behavior to MVA-WT in terms of viral growth. Therefore, the kinetic studies conclusively show that the insertion of CTH522:B7 into the MVA-WT genome had no effect on virus growth and replication. This was an essential step in virus characterization, as the insertion of a foreign antigen into the viral genome could have had a detrimental effect on its replication, which could have proven to be disadvantageous for further analysis, as well as *in vivo* studies. Moreover, the fact that MVA-CTH522:B7 behaved in the same pattern as the wild-type strain in several cell lines that force a different replicative capacity on the virus means that the recombinant MVA-CTH522:B7 can be further analyzed before moving on to preclinical studies.

5.4. MVA-CTH522:B7 successfully expresses CTH522:B7 intracellularly and on the surface of the cell

Once it had been ensured that the insertion of the vaccine antigen did not change the replication behavior or capacity of the recombinant virus, it was crucial to determine whether or not MVA-CTH522:B7 produced a chimeric protein that was found both intracellularly and on the surface of the infected cells. Since one of the objectives of the present study was to induce a robust humoral response, it was theorized that this could be achieved through the expression of CTH522:B7 on the surface of the cell. Mammalian surface display proteins have been studied since last century in biotechnology and medical fields alike (Lin et al., 2013). Among them, B7-1 has proven to be the ideal choice for tethering fusion antigens to the surface of the cell, displaying a higher target protein concentration on the cell membrane when compared to other candidates such as the C-terminal extension of decay-accelerating factor, the transmembrane domain of the human platelet-derived growth factor receptor, the transmembrane domain of the H1 subunit of the human asialoglycoprotein receptor (Liao et al., 2001) or the GPI anchor (Pan et al., 2012).

B7.1 corresponds to the murine CD80 receptor, consisting of an extracellular domain, a transmembrane domain and an entire cytoplasmic tail (Chuang et al., 2014),

considered as a type-II integral protein, with the N-terminal oriented towards the cytosol and the C-terminal found outside the plasma membrane (Chou W. et al., 1999). Research has previously shown that the fusion of B7 to the antigen of interest not only facilitates their cellular transport to the surface of the cell membrane, but also lengthens the half-life of the proteins anchored to said membrane (Chuang et al., 2014). This is something that had been suggested when a study proved that the transmembrane domain of choice to enhance protein surface display would affect the half-life, sorting rate and surface retention of the fusion protein which would, in turn, highly impact the surface expression (Liao et al., 2001).

Previous results showed a correlation between the secreted antibodies and the concentration of proteins fused to the B7 antigen that were anchored to the plasma membrane (Chuang et al., 2014), and other studies have shown what was described as an ineffective antibody response following a decreased expression of surface antigens (Han et al., 2023). Precisely because this work aimed to induce an enhanced antibody response through a theorized increase in CTH522 expression on the plasma membrane, it was crucial to prove that MVA-CTH522:B7 did indeed allow for an enhanced CTH522 surface expression, especially when compared to a recombinant MVA-CTH522 lacking the B7 transmembrane domain and cytoplasmic tail. Therefore, a study was performed with both murine and human cell lines where Cloudman and HeLa cells were infected with a MOI of 5 with MVA-CTH522:B7 to analyze its surface protein expression. MVA-CTH522 lacking the B7 transmembrane domain and cytoplasmic tail was used as a control to ensure that the protein expression in the surface of the cell, if any, was due to the presence of B7 and not to the CTH522 vaccine antigen itself. Results showed a staggering difference in the CTH522 localization on the surface of the plasma membrane, where MVA-CTH522:B7 infected cells had an eighty-fold increase in the percentage of the surface CTH522 positive population in Cloudman cells and fifty-fold percentage increase in HeLa cells when compared to CTH522 without the B7 sequence (**Figure 16**). This conclusively shows that MVA-CTH522:B7 infection does indeed lead to an increased CTH522 surface expression in mammalian cells due to the enhanced intracellular transport including the Ig*k* signal peptide and mammalian surface display characteristics of the B7 transmembrane domain. Additionally, the extracellular-transmembrane domain of the B7 sequence is believed to be glycosylated, further stabilizing the expression of the fusion proteins on the surface of the cell (Chuang et al., 2014). Interestingly, further analysis in antigen presenting cells revealed that, while there still was an increase in synthesisof CTH522 by MVA-CTH522:B7 when compared to

MVA-CTH522, the difference was not only found in the surface of both BMDCs and DC2.4, but also displayed in the intracellular analysis (**Figure 17**). It is not the first time that a study shows the lack of internalization of a chimeric protein fused to B7 (June et al., 1994), and researchers have previously reported a lower concentration of the chimeric protein fused to B7 when compared to a chimeric protein fused to another cell surface targeting domain, suggesting protein degradation because of conformational restraints mediated by the B7 transmembrane domain in the protein folding (Chou W. et al., 1999). However, the low levels of intracellular protein synthesis in dendritic cells might be due to the CTH522 antigen in itself, as both cells infected with MVA-CTH522:B7 or MVA-CTH522 display lower protein levels than Cloudman or HeLa cells. This overnight infection yielded a higher CTH522 amount in both intracellular and surface analysis of BMDCs infected with MVA-CTH22:B7 but a time course analysis of CTH522 synthesis where infected BMDCs were harvested at 0, 4, 8 and 24 hours post infection showed different results (**Figure 18**). While the surface expression was indeed enhanced when cells were infected by MVA-CTH522:B7, reaching a peak of twenty-fold at eight hours post infection, this was not the case for the intracellular analysis. BMDCs infected with MVA-CTH522 lacking the B7 transmembrane domain and cytoplasmic tail displayed a higher number of cells with intracellular CTH522; the highest frequency was measured at 4 hours post infection with a subsequent exponential decline. CTH522 synthesis in BMDCs infected with MVA-CTH522:B7, however, seemed to remain more or less stable at 4, 8 and 24 hours post infection. Additionally, similar results were obtained in the same time course analysis performed with DC 2.4 infected cells (**Figure 19**). In this case, following the pattern of the overnight infection, there was an enhanced surface expression of CTH522 in those cells infected with MVA-CTH522:B7, albeit it was a much higher percentagein the time course study than in the single overnight infection. Surface expression of CTH522 peaked at 8 hours in cells infected with MVA-CTH522:B7, showing percentagelevels almost seventy-times higher than cells infected with MVA-CTH522 lacking the B7 domain. Moreover, as it had proven with BMDCs, intracellular CTH522 synthesisin cells infected with MVA-CTH522:B7 was slightly lower than those infected with MVA-CTH522. This might be due to the uniqueness of dendritic cells as antigen-presenting cells capable of presenting antigens to effector $CD8^+$ T cells (Barnowski et al., 2020; Dai et al., 2014). It has been previously reported that proteins fused to the B7 cytoplasmic domain are transported through the coatomer complex II (COPII) pathway, a selective transport process exporting proteins out from the ER (Lin et al., 2013). Interestingly, previous research showed that this facilitated transport out of

the endoplasmic reticulum of chimeric proteins fused to B7 is actually associated with its structure and not to the theorized presence of an ER export motif as it was previously believed and which was proven to not be contained within the B7 cytoplasmic tail (Lin et al., 2013). In the process of presenting antigens to T cells, the protein-folding capacity of the endoplasmic reticulum is disrupted, leading to what is defined as a "ER stress" cellular state, a process that interferes with cell metabolism, restricting their capacity of antigen presentation (Salvagno & Cubillos-Ruiz, 2019). Furthermore, dendritic cells phagocytize pathogens before processing and presenting the antigens in the MHC I/II molecules in the form of peptide fragments (Eiz-Vesper & Schmetzer, 2020). This could be an alternative explanation to the stark difference in protein synthesis that can be seen when comparing the surface display of CTH522 in Cloudman infected cells or infected BMDCs, since APCs display antigens in the surface of the cell as peptides after protein degradation (Stagg et al., 2020). However, the actual reason behind this apparent disparity in both primary and immortalized dendritic cells when compared to non-antigen-presenting-cells would need further study in order to ascertain the biochemical characteristics of CTH522:B7 in these cells. Nonetheless, it is of vital importance to perform a thorough characterization of recombinant viral vectors *in vitro*, as the individual biological features of the viral constructs exhibited in these series of characterizing experiments may help to define criteria to use these constructs and to interpret the data obtained in future studies. While certain characteristics such as the virus stability, its functionality or even protein localization within the cell can only be analyzed in *in vitro* assays, it is also of interest to not only perform these studies in immortalized cell lines, but also in primary ones such as BMDCs, despite the arduous work they demand, as they may give a window of information into future *in vivo* analysis.

In order to further characterize the presence of CTH522 both intracellularly and on the surface of the cell, confocal microscopy was performed on Cloudman cells infected with MVA-CTH522:B7 or MVA-CTH522, the latter to be used as a control to ensure that any colocalization between the plasma membrane and CTH522 is caused by the B7 transmembrane domain and cytoplasmic tail and not to the vaccine antigen itself. While there doesn't seem to be any data available in confocal microscopy analysis of MVA infection in Cloudman cells, research studies have previously analyzed MVA infection in HeLa cells through confocal microscopy, showing that HeLa cells exhibited a bipolar morphology with minimal cytopathic effect, something seemingly unique to MVA when compared to other vaccinia strains such as WR or NYCBH (Gallego-Gómez et al., 2003). The methodology used for the confocal microscopy work in this experimental context

could be further improved in order to minimize the analysis of apoptotic cells, which limit the inferences drawn from them. A shorter infection window, such as 12 or 16 hours post infection instead of 24 hours post infection could prove beneficial in the future. Nonetheless, infection of Cloudman cells with MVA did not seem to elicit any immediate morphological changes in the cell at 0 hour post infection after 1 hour of viral inoculum adsorption by the cells (**Figure 20**). However, there was some minimal protein production in cells infected with both MVA-CTH522 and MVA-CTH522:B7 in cellular compartments that the assay was unable to determine. It is reasonable to say they are not what has been previously described as viral factories, membrane-like structures that are involved in the sequestration of antigens upon VACV infection (Tewalt et al., 2009) where genome replication, protein synthesis and virion assembly occur at later time points (Katsafanas & Moss, 2007). However, despite the fact that 1 hour of inoculation at room temperature is too short of a time point, the presence of a positive signal indicates that within that single hour of adsorption, protein synthesis is occurring within compartments to a certain degree. A previous study shows that mature virions (MV) were detected in vesicles as early as 30 minutes after infection at 4 ºC, and that MV particles bound to HeLa cells steadily increased as the incubation temperature did, with a higher unit amount at 37 ºC and a lower one at 4 ºC (Laliberte et al., 2011), indicating the effect of the temperatures at which the viral adsorption step is performed. Additionally, a study focusing on the characterization of a recombinant MVA vaccine candidate against Dengue Virus (DENV) encoding a DENV non-structural protein antigen under the PmH5 promoter found it was detected in HeLa cells inmediately after the 1h adsorption step (Wilken et al., 2023), further supporting the hypothesis that the CTH522 detected in those cells in this work was the result of very early protein synthesis due to the strong activity of the VACV promoter. While this confocal microscopy analysis would be the only experiment in this work that depicts such early CTH522 detection, as a previous western blot (**Figure 12**) did not display protein synthesis at 0 hpi, it is essential to remark that the cases depicted in this manuscript (**Figure 20**) were exceptional and seldom occurring, as it required strenuous visual monitoring of the infected cell monolayer. Therefore, it may be concluded that the antigen production seen in those rare cases was not enough concentration to be detected by western blot analysis.

Additional visualizations of infected Cloudman cells after the adsorption period displayed little to no CTH522 synthesis (**Supplementary Figure 2**). A bright CTH522 fluorescent signal could be observed at 8 hours post infection in cloudman cells infected with both MVA-CTH522 and MVA-CTH522:B7. As expected, a more detailed

examination of the images reveals that in the cells infected with MVA-CTH522:B7 occurred a subtle colocalization of the CTH522 signal with that of the plasma membrane stained by WGA, something that is not observed in the cell infected with MVA-CTH522 (**Figure 21**). Additionally, CTH522 displays a strong and robust signal that completely colocalizes with the cell membrane of an MVA-CTH522:B7 infected cell 24 hours after the initial infection (**Figure 22**), which further supports the fact that MVA-CTH522:B7 infection leads to the expression of CTH522 on the surface of mammalian cells to the transmembrane domain and cytoplasmic tail of the B7 molecule. While the Cloudman cells infected with MVA-CTH522 lacking the B7 domain do not exhibit any expression, this is due to CTH522 being quickly degraded by the proteasome (unpublished data, Giuseppe Andreacchio). Because CTH522 was no longer visible through confocal microscopy after 24 hours of infection, an auxiliary infection with MVA-mIi:CTH522 was used to ensure the colocalization of CTH522 in the plasma membrane was due to the B7 modification in CTH522:B7. MVA-mIi:CTH522 is an additional recombinant virus generated and characterized within the scope of this work that successfully expressed the CTH522 antigen fused to a mouse invariant chain sequence. Cloudman cells infected with MVA-mIi:CTH522 exhibited a strong CTH522-specific signal after 24 hours of infection that was nonetheless delimited to the bounds of the cell, unlike those cells infected with MVA-CTH522:B7 (**Supplementary Figure 5**), which perfectly aligned with the plasma membrane signal. There are no confocal analyses that examine the expression of mIi fused to an antigen of interest in MVA in previous literature. However, because MVA-mIi:CTH522 lacks the B7 modifications that recombinant MVA-CTH522:B7 carries, it can be used as a control in comparing both viral vectors. The observation that mIi:CTH522 is not colocalized to the plasma membrane like CTH522:B7 further reinforces the hypothesis that MVA-CTH522:B7 expresses CTH522 in the surface of the cell due to the B7 TM domain.

Furthermore, while previous studies reported that HeLa cells exhibited plasma membrane protrusions after MVA virions bound to the cells (Gallego-Gómez et al., 2003), infected Cloudman cells in this study did not seem to exhibit such protrusions after careful visual monitoring, although the antibody used for confocal microscopy was specific to C. *trachomatis* and not VV. However, they seemed to display the development of filopodia-like structures, something that had been previously observed in monkey cells upon infection with MVA (Gallego-Gómez et al., 2003). In the case of this work, it is unknown if this was caused by MVA infection or not, as cells were not stained with a viral control due to assay restrictions. However, the structures can be observed in cells infected with

MVA-CTH522, MVA-CTH522:B7 (**Supplemental Figure 10**), and they do not seem to be as apparent in cells mock-infected. Since Cloudman are epithelial cells, this could be due to the especially important role that filopodia take in cell-to-cell contact (Khurana & George, 2011). This role has been further analyzed in the specific context of viral infections, suggesting that filopodia facilitates viral infection through vertical primary infections and horizontal spread from cell-cell contact (Chang et al., 2016). Nonetheless, it can be concluded that these filopodia-like structures are not an effect specific to the B7 molecule or to the CTH522 antigen, as they can also be found in those cells infected with MVA-WT. While cellular stress due to viral infection might be a factor, cell death upon MVA infection might be a plausible explanation to the observed effect. These findings would necessitate for further studies that would include a lower MOI and shorter time points in order to analyze precisely the development of these filopodia-like structures.

Altogether, both the FACS analysis and confocal microscopy examining the surface display of CTH522 confirm that the presence of the B7 transmembrane domain and cytoplasmic domain fused to the CTH522 antigen enhanced its surface expression in mammalian cells. Something that would hopefully lead to an optimal humoral-mediated immune response. Antibodies have proven to be essential for conferring immunity to chlamydial reinfections (Morrison & Morrison, 2005) and they are now considered to be necessary in a two-arm immune response along with $CD4^+$ T cells. Confirming the enhanced presence of CTH522 expression in the surface of the cell is the first step before recognizing whether or not MVA-CT522:B7 would be capable of inducing an antibody response *in vivo* and, therefore, establish itself as a favorable vaccine candidate against C. *trachomatis*.

5.5. Two novel CTH522 peptides discovered via ex vivo overlapping peptide screening

Through a thorough characterization, MVA-CTH522:B7 has proved to not only efficiently express vaccine antigen CTH522:B7, but also to successfully target the chimeric protein at the surface of mammalian cells due to the presence of the signal sequence of Igk, the B7 transmembrane domain and cytosolic tail. In order to analyze results from cellular immune responses in future animal model assays in a cost-effective manner, it was crucial to investigate the presence of potential immunogenic peptides. This would allow for the establishment of multiple assays capable of analyzing the immune response of the vaccine vector of interest or to identify target structures for monitoring

infections with the pathogen. In the case of this study, the immunodominant peptides could be used to pulse splenocytes of immunized animals, which would then be stained and analyzed through FACS to determine the $CD4^+$ T cell response of the mice to the vaccination.

To achieve this, the CTH522 sequence was broken down *in silico* into peptide fragments of 15 amino acids, allowing for the design of a total of 138 overlapping peptides (**Supplementary Table 1**). Since a single-peptide analysis of all peptide candidates would have been extremely strenuous and labor-intensive, they were pooled in 14 groups of 9-10 peptides each (**Supplementary Table 2**) that would be analyzed in initial mice studies before analyzing the single peptides within the pools that would elicit the highest IFN-γ activation. The peptides were grouped in a simple assortment where they were placed in pools numbered 1-14, containing 8-10 peptides each. However, a more efficient way of peptide pool testing would've been to plan a higher number of pools and design the testing in a manner where they would "cross-match" each other in a table composed of both column pools and row pools. Hence, if twenty pools were designed, ten of them would have their peptides listed from top to bottom in a column manner and ten of them would have their peptides listed from left to right in a row manner. This way, each peptide could be found in two different pools and, therefore, if those pools elicited the highest IFN-γ activation, it could in theory be postulated that this specific peptide was the reason that those two pools had a higher IFN-γ response than the others. This was the strategy followed by the University of Basel when analyzing the responses to the peptides (Ciancaglani, M, unpublished data). However, while this could allow for a more specific determination of positive peptide candidates at an earlier stage in the research, there would still be a need to repeat the assay and study the individual peptides, as the response could also be additive from the other peptides present in the pools.

Results from the peptide pools 1 to 14 testing showed a consistently high response in pools 5, 6 and 12 (**Figure 23**). This data remained consistent in splenocytes that had been isolated from both, mice immunized in homologous prime/boost MVA-MVA vaccination regimens and mice immunized in priming only vaccination regimens. It is of note that B5, a VACV viral protein necessary in actin tail formation within extracellular enveloped virus at the surface of the cells (Doceul et al., 2012) and intracellular envelope virus formation (Earley et al., 2008), has previously been used in EEV visualization via electron microscopy (Spehner & Drillien, 2008) and in ICS assays to induce IFN-γ activation in $CD4^+$ T cell ICS assays in Prof. Dr. Drexler's lab (Thiele et al., 2015). In this case, B5 was used as a viral antigen control because of the previous information

supporting its use in *ex vivo* assays, but it was unable to display a consistent IFN-γ expression through the experiments in this work.

Moving forward with the peptide pool work, the study focused on the two pools with the strongest signal. Consequently, pools 6 and 12 were decided upon to continue with the search of a peptide candidate capable of eliciting IFN-γ^+ $CD4^+$ T cells.

Pool 6 showed a significant response with peptide #49 (6-4) when compared to the negative peptide control (NP) in those mice that were vaccinated with MVA-CTH522:B7, while mice vaccinated with MVA-CTH522 showed a higher response in peptide #77 (6-6) (**Figure 24**). These results stayed consistent through three independent experiments and were also supported by findings from the University of Basel (unpublished data) where they tested the same peptides in different group assortments in splenocytes isolated from mice vaccinated with arenavirus vectors expressing CTH522. Since this peptide does not seem to have been previously described as a candidate for cellular immune responses against C. *trachomatis*, it was run through an MHC-II binding prediction software (IEDB recommended 2.22) with additional in frame upstream and downstram aminoacids on the N-terminal and the C terminal in order to test whether further epitopes with a higher adjusted rank would be attributed to peptide #49 or peptide #69. The final input sequence of peptide #49 was QSVVELYTDTTFAWSVGARAALWECGC, where the underlined sequence is that of peptide 49. The software provided adjusted ranks, where a low adjusted rank was equivalent to the binding capacity of the peptide of choice. Interestingly, despite the significant IFN-γ activation in the $CD4^+$ T cell population found in immunized mice splenocytes, peptide 49 did not have a substantially low adjusted rank, with a 4.35 percentile rank (**Supplementary Figure 6**). Nonetheless, the experimentally determined threshold of the percentile rank for MHC II immunogenicity is less than or equal to 10.0, as opposed to the 1.0 expected for MHC I. this would mean that peptide 49 was found well within the desired percentage of the predicted peptides (Fleri et al., 2017). The sequence coding for peptide 49 is found within the initial 240 base pairs of the CTH522 antigen and has not been previously described in literature as an immunogenic epitope, but these results prove its capacity to activate CD4+ T cells of mice immunized with MVA-CTH522:B7.

On the other hand, pool 12 had a strong IFN-γ activation in the $CD4^+$ T cell population due to peptide 69 (12-5) with a statistically high significance when compared to the negative peptide control (**Figure 25**). A corresponding peptide fragment was run through the same previously mentioned MHC-II binding prediction software. It contained additional amino acids on the N and C terminals, with a final sequence of

DASIDYHEWQASLALSYRLNMFT, with peptide 69 having its sequence underlined. Peptide 69, unlike the other analyzed peptide, did appear in a noteworthy low percentile, with an adjusted rank of 1.96 (**Supplementary Figure 7**). A study investigating a MOMP multi-epitope vaccine selected two strings of amino acids in the epitope-rich immunodominant region of MOMP following predictions from SYFPEITHI program, one of which, namely $MOMP_{271–290}$ (WQASLALSYRLNMFTPYIGV) included a partial sequence of peptide 69 (WQASLALSYRL). The prediction was used to screen for cytotoxic T-cells (CTL), but also for B cell and Th cell epitopes, and the immunization led to a robust IgG humoral immune response as well as a high IFN-γ concentration in serum (Tu et al., 2014). Interestingly, peptides 70 and 71 also included larger conserved regions of the sequence chosen by that study, and pools 13 and 14 displayed a high IFN-γ activation, with the former having an overall stronger expression and the latter lacking such expression in the prime/boost protocol (**Figure 23**). However, pool 6 and 12 remained as the superior ones and, therefore, the individual peptides in pools 13 and 14 were not further analyzed. Even though it can be postulated that the IFN-γ expression seen in the $CD4^+$ T cell population is caused by peptides 70 and 71 respectively, further analysis would be required in order to reach that conclusion. Nonetheless, given the results in previous literature (Tu et al., 2014) and the robust IFN-γ^+ $CD4^+$ T cell response obtained after pulsing splenocytes with peptide 69, it can definitely be theorized that since the predicted peptides in both the aforementioned study and this current work elicited a cellular immune response, epitopes found within those sequences are highly immunogenic. Furthermore, a hypothesis can be made where those highly immunogenic peptides could be considered immunological hotpots, clusters of T-cell epitopes that bind to multiple alleles of an antigen and that have been the target of vaccine studies before (G. L. Zhang et al., 2008). It would be of interest for future studies to design a peptide with a shorter sequence, perhaps the region that is conserved in both this work and the previous study. Although peptides that range in 15-20 amino acids in length have shown to have comparable results (Draenert et al., 2003), it is also believed that, while longer peptides can bind to MHCI for $CD8^+$ T cell activation, mainly peptides 8-10 amino acids in length are presented to MHCI (Rist et al., 2013). Therefore, if future studies required $CD8^+$ T cell analysis, a definite peptide candidate to be included in such analysis would be the shortened version of peptide 69.

Peptide 49 and peptide 69 do not share amino acid sequences, nor are they found close to one another, with the sequence for peptide 49 found relatively close to the N-terminus of the CTH522 sequence, while the peptide 69 sequence sits approximately

halfway through the entirety of the CTH522 antigen. Interestingly, however, both peptide sequences are found withing the $rMOMP^{D}_{34-259}$ domain leading CTH522. While the VD4 region has been described to contain unspecified epitopes for T cells and B cells (Olsen et al., 2015), this study proposes both peptide epitope 49 and 60 as promising peptide candidates for $CD4^{+}$ T cells for the first time so far.

Additionally, the C. *trachomatis* core conserved TTLNPTIAG antibody epitope is found in MOMP VD-4 and has shown to elicit neutralizing activity across the urogenital serovars (Collar et al., 2022). This epitope is found within the following peptides grouped in several of the experimental pools: 80, 81, 97, 98, 114, 115, 132 (**Supplementary Table 1**). Although some pools where this neutralizing epitope can be found did not elicit any IFN-γ expression, such as pools 1, 2, 9 and 10 (where peptides 114, 115, 80 and 81 were placed, respectively), some pools including the epitope did display a higher T cell response, such as pools 12 and 3 (where peptides 97 and 98 were allocated). Pool 13 has been mentioned before, where the observed response was attributed to epitope WQASLALSYRLNMFT (peptide 70), but pools were not tested for antibody activity, instead used in T cell response assays. Pool 12 did include the TTLNPTIAG epitope in peptide 97, and this group was thoroughly tested in further assays, where peptide 97 (12-7), while exhibiting a certain degree of IFN-γ expression, did not appear to be significant enough to warrant its characterization as a successful peptide candidate to be used in *ex vivo* assays. Expectedly, the peptides including the conserved antibody epitope shown to induce neutralizing activity against C. *trachomatis* did not seem to be involved in T cell activation within the context of this work.

Another peptide was reported to be a primary T-cell epitope after it elicited a cellular immune response in C3H and BALB/c mice immunized with the TINKPKGYVGKE peptide sequence (Knight et al., 1995). This epitope was conserved in peptide 60 of this current study (TINKPKGYVGKEFPL), which was analyzed in pool 3. However, pool 3 did not seem to induce a cellular response in this work and, while further studies would be needed for a decisive conclusion, it is possible that this epitope is not immunogenic in C57BL/6 mice. Studies found that different strains of mice that were immunized with the same peptide did not only trigger different immune responses among them, but induced antibodies of different specificities to the peptide (Su & Caldwell, 1992; Velge-Roussel et al., 1997), making it highly likely that some peptides are immunogenic in specific mice strains as opposed to others. One of these works immunized six different mouse strains with a chimeric peptide including a conserved MOMP T helper cell epitope and a serovar A residue. Researchers found that mouse strains of the same H-2 haplotype produced

antibodies of various specifity to the VDI residue and that the Th cell epitope portion was recognized by multiple MHC haplotypes, concluding that their neutralizing site response was not dependent on MHC haplotypes (Su & Caldwell, 1992).

Further analysis should include the other pools that proved to be immunogenic such as pool 5, in order to study whether or not more peptides found in the CTH522 sequence are capable of triggering a $CD4^+$ T cell response. In order to improve the monitoring of the response that has been observed in these studies, however, it could be possible to increase the concentration of peptide used in the step where the splenocytes are pulsed, but the vaccination regimen should remain the same. Nonetheless, peptides 49 and 69 were able to recall a statistically significant CD4+ T cell response *ex vivo* in this mouse model. This study proposes for the first time their use in future preclinical assays aiming to analyze IFN-γ expression in $CD4^+$ T cell populations of C57BL/6 mice.

5.6. Heterologous DNA/MVA vaccination approach enhances immune response against C. *trachomatis*

Heterologous prime/boost vaccination regimens have been investigated for decades now, proving themselves to be a highly favorable strategy to elicit cellular immune responses and protection against infection in several animal models (Gherardi et al., 2003; S. Li et al., 1993b). The main advantage in heterologous immunization strategies in the MVA context is that using a different vector as a priming agent prevents an initial anti-MVA response that would be observed in a homologous MVA/MVA vaccination regimen and that would consequently inhibit the response against the antigen of choice (Pérez et al., 2021).

While other priming agents such as peptides, proteins, viral vectors or VLPs have been used before (Gherardi et al., 2003), DNA vectors have shown to significantly increase the immune response as the priming agent when included in heterologous prime/boost protocols along with a poxvirus boost (Chapman et al., 2017), examplified by a study applying a DNA/MVA heterologous prime/boost protocol against HIV capable of eliciting long-term memory T cells that persisted in NHPs three and a half years after the last immunization (Chege et al., 2017). Moreover, DNA vaccines are cost-effective, easy to produce immunization candidates, making them an excellent choice to be included in vaccination regimens, as it does not involve any virulence or anti-vector immunity risks (Chapman et al., 2017). Heterologous DNA/MVA prime/boost regimen strategies have been used in human clinical trials against viral pathogens such as HIV, HCV, EBV and

RSV before, but also against the *Plasmodium falciparum* bacterium responsible for malaria infection, triggering cellular and humoral immune responses (Pérez et al., 2021). Additionally, they have proven to be safe when in said heterologous immunization regimens along MVA in phase 1 clinical trials (Bailón et al., 2022).

Therefore, a study was designed in order to compare the cellular and humoral immune response of mice vaccinated using a heterologous DNA/MVA prime/boost strategy or a homologous MVA/MVA prime/boost regimen (**Figure 26**). There doesn't seem to be a single consensus in regards to immunization schedules, with different research groups following different time tables in both immunizations and animal sacrifice. A group that characterized the immune response in a heterologous DNA/MVA prime/boost regimen against ZIKV boosted the mice 25 days after priming and sacrificed them 41 days later (Pérez et al., 2021). Another study analyzing the immunogenicity of another heterologous prime/boost protocol against HIV boosted the mice 28 days after priming and sacrificed the animals in a different variety of dates, ranging from 12 days to 68 days after priming (Chapman et al., 2017), and another study involving a heterologous prime/boost DNA/MVA immunization regimen also chose to boost the mice 28 days after priming (Fan et al., 2020). An additional work aiming to compare the immune response of a heterologous DNA/MVA prime/boost and a homologous MVA/MVA prime/boost protocol boosted the mice 14 days after priming and sacrificed then 11 days later (García-Arriaza et al., 2021). Based on the needs and limitations of this work, an immunization schedule was determined where mice were primed once with MVA and thrice with DNA in 3-day intervals before being boosted 28 days after the first priming and sacrificed 35 days after the first priming. A study aiming to analyze the early memory phase of the immune response in mice after MVA vaccination used a similar timeframe, choosing to sacrifice the animals 36 days after their initial immunization for their T cell response and 42 days after their initial immunization for the antibody response (Baur et al., 2010). Furthermore, previous studies do show that heterologous DNA/MVA immunization regimens excel as the most immunogenic when compared to its homologous counterparts, in both adaptive and memory antigen-specific T-cell response (Pérez et al., 2021).

While MVA has been previously administered via different vaccination routes such as mucosally (intranasally or orally), it has been thoroughly used via the systemic route of vaccination, successfully inducing protection against several pathogens (Gherardi et al., 2003). A study analysis also reported that mice that had been vaccinated simultaneously viathe intrauterine and parenteral routes had only elicited memory Th1/Th17 T cells before an infection with C. *trachomatis*, while mice that were only

vaccinated with the parenteral route displayed long-lived Th1/Th17 T cells after the infection as well (Nguyen et al., 2021). Because the intraperitoneal route has been described to have a low stress impact on mice and to be suitable for proof-of concept studies (Al Shoyaib et al., 2019), it was the route of choice in this study as it is a practical and viable route of MVA immunization in regards to the study parameters and expectations in this work, including lower animal stress and its immunogenicity studies. While DNA immunizations have been used other administration routes, such as mucosal routes, and still have been able to induce local humoral response and cellular cytotoxic response (Maeto et al., 2014), mice were vaccinated intradermally with DNA vectors within this work in a collaboration with the University of Utrecht. Intradermal tattooing has also been successfully used for peptide-based vaccines but it did not seem to yield positive results as an administration route for adenoviral vectors (Oosterhuis et al., 2012). Furthermore, animals immunized by DNA tattooing showed comparable long-lasting immunity to mice immunized via the intramuscular route and induced a significant humoral antigen-specific immune response (Kulkarni et al., 2014). Additionally, DNA tattooing has proved to outperform intramuscular DNA injections in several animal models, as well as other dermal administration routes such as electroporation-mediated gene transfer or particle-mediated epidermal delivery (Oosterhuis et al., 2012).

Upon animal sacrifice and the consequent splenectomy, the isolated splenocytes were pulsed with either the designated controls of choice ($CD3^+CD28$, B5 and NP), the peptides previously designed, analyzed and decided upon in 4.4.1, a combination of both of them or the purified CTH522 protein. While, except for the splenocytes pulsed with peptide 49, there did not seem to be a significant difference between the homologous DNA/DNA immunization regimen and the homologous MVA/MVA regimen, there was a significant difference found between the homologous DNA/DNA and the heterologous DNA/MVA, as well as between the homologous MVA/MVA and the heterologous DNA/MVA. Overall, results are consistent with previous research that has found heterologous DNA/MVA prime/boost regimens to generally induce a stronger and broader immune response than homologous prime/boost protocols or prime-only strategies (Chapman et al., 2017; Chege et al., 2017).

It is not the first time that immune responses against C. *trachomatis* were analyzed after a heterologous DNA/MVA prime/boost protocol. A recent study evaluated the immunogenicity and protection of different prime/boost strategies including protein vaccines (with vaccine antigen CTH522), and DNA-, MVA- and adenovirus-based vectors encoding MOMP and claimed to prove that the groups vaccinated with the

proteins elicited a higher antigen-specific antibody levels than those immunized with DNA or vector vaccines, but failed to recognize that the comparative was performed between different antigens, as the protein vaccines encoded solely the artificially engineered CTH522, and the vectors encoded the consensus MOMP (Lorenzen et al., 2022). In order for a more accurate conclusion to be drawn, a study would necessitate the comparison of groups immunized with the CTH522 antigen against DNA and vector-based vaccines encoding the same CTH522 antigen. However, comparing different vector systems encoding different antigens (be it the artificial CTH522 or the consensus MOMP) is not an accurate analysis to investigate, and any conclusions drawn from it in regards to which vector systems outperform which are tainted by a skewed bias.

However, the results obtained from this work are very promising when arguing for a C. *trachomatis* vaccination regimen. It has been shown that clinical subjects are prone to a secondary infection and that C. *trachomatis* protective immunity against reinfection in women requires antigen-specific IFN-γ activation in $CD4^+$ T cell populations, as women who displayed this kind of response were considerably less inclined to suffer a reinfection (Bakshi et al., 2018). This has been supported in animal models as well. $CD4^+$ T cell activation was not only sufficient, but clearly necessary in order to clear the infection. Furthermore, mice lacking the IFN-γ receptor have exhibited a delay in infection clearance, indicating that the Th1 T cells producing the cytokine are essential for protection (Helble & Starnbach, 2019). Not only has the secretion of IFN-γ been proven to be necessary for improving protection against C. *trachomatis* infection, but it seems that other immune mediators exhacerbate the bacterial burden. Additionally, it seems that Th2 response leads to the increase of bacterial burden in mice lacking IFN-γ receptor, thus highlighting the central role of IFN-γ in the clearance of the infection(Gondek et al., 2009). Results in this current study definitely show a antigen-specific IFN-γ production in the $CD4^+$ T cell populations found in splenocytes of mice immunized with both the homologous MVA/MVA regimen and the heterologous DNA/MVA regimen, which suggests that both vaccine protocol candidates could confer protection mediated by Th1 $CD4^+$ T cells. Previous research proved that the murine model for C. *trachomatis* needs a Th1 IFN-γ response in order to clear primary chlamydial infections and to provide additional immunity to protect against reinfection (Bakshi et al., 2018), further supporting the use of MVA-CTH522:B7 as a vaccine against C. *trachomatis*.

5.7. Enhanced surface cell expression of CTH522:B7 leads to increase humoral response encompassing neutralizing activity

Precisely because of the scarce research aiming to develop an MVA vaccine against C. *trachomatis*, it becomes imperative to look at the performance of MVA as a vaccine candidate against other infectious pathogens, such as HCV (Marín et al., 2018)or HIV (Gómez et al., 2007), which have been intensely researched in the context of MVA itself. As a delivery vector of chimeric antigens, MVA has proven itself as an ideal candidate in triggering antibody responses in several animal models. When compared to plasmid DNA or recombinant vesicular stomatitis virus (strain Indiana), MVA induced higher antibody binding titers and a stronger neutralizing activity in a single priming vaccination regimen in NHPs, which was found to be related to the observed increase in the population of germinal center and antigen-specific B cells (Eslamizar et al., 2021). While that was a analysis of the immune response after primimg, homologous prime/boost protocols of MVA against SARS-CoV-2 also induced a robust antibody response characterized mainly by IgG antibodies, and a high neutralizing activity against the live pathogen in rhesus macaques. Generally speaking, MVA triggers an immune response characterized by its robust, broad and long-lasting protective capacity because of the B cell and T cell activation after a homologous prime/boost vaccination regimen (Mooij et al., 2022).

It is difficult to hypothesize a conclusive timeline for when exactly an antibody response starts, as it depends highly on variables such as the vector used in the study, the vaccination regimen and the antigen of interest. Research around MVA immunization schedules seems to be conflictive, as one trial immunizing healthy adults with MVA argued against compressed schedules with less than 21 days between immunizations, showing that it impaired the antibody response (Jackson et al., 2017). However, another study analyzed the difference between two vaccination schedules that lasted 21 and 56 days respectively and did not find any difference in the triggered humoral response (Kalodimou et al., 2023). Therefore, there were uncertain expectations in regards to the antibody response triggered in mice barely eight days after the boosting, but a study was performed in any case in order to gain some preliminary results on humoral immune responses upon MVA-CTH522:B7 immunization and to ensure the thorough use of laboratory animals that were sacrificed for *ex vivo* cellular immune response studies. Results do show a strong antibody response characterized by IgG and IgM antibodies in serum of mice immunized with a prime/boost of MVA-CTH522:B7, as opposed to the mice that were vaccinated with MVA-CTH522, therefore lacking the B7 antigen fused to

the CTH522 sequence (**Figure 28**). This supports the hypothesis that was theorized in the early stages of this study, where the presence of the B7 transmembrane domain and cytoplasmic tail would enhance the surface display of CTH522 on the plasma membrane of the cells, therefore increasing the humoral response. Ongoing research in Prof. Dr. Drexler's group indicates that the CTH522 antigen without the B7 modification is highly unstable and quickly degraded by the ubiquitin-proteosome system, which may further elucidate the lack of humoral response in mice immunized with MVA-CTH522. Antibodies are produced by B-cells, which have been extensively documented to acquire antigens anchored to the surface of target cells, especially antigen-presenting cells (Ciechomska et al., 2011). This was further established upon a second study where a proper immunization schedule was designed around antibody responses. While it has been previously stated that it is necessary to allow a minimum of four weeks between priming and boosting, a three-week interval between MVA priming and MVA-boosting has been analyzed before, granting comparable humoral immune responses to longer time periods such as eight weeks (Kalodimou et al., 2023). For this work, mice were immunized with thirty days between MVA priming and MVA boosting, which triggered a highly significant robust antibody response characterized by IgG and IgM antibodies (**Figure 29**). Mice with a homologous MVA-CTH522/MVA-CTH522 vaccination regimen did not show any statistically significant IgG and IgM antibody response in serum obtained after priming or boosting. They also failed to produce any significant IgG antibody responses when the sera were analyzed solely for IgG. Samples from mice immunized with the homologous MVA-CTH522:B7/MVA-CTH522:B7 regimen did show a strong IgG antibody response (**Figure 30**). An analysis has determined IgG as the predominant seromarker for *C. trachomatis,* with IgM and IgA running second and third most prevalent (Ajani et al., 2019). While the variance between the results obtained from examining the IgG and the IgG+IgM titers from two different experimental setups was not statistically analyzed (**Figure 29**, **Figure 30**), the difference that can be seen between both figures can be due to IgM antibodies found in serum even two weeks after boosting. IgM is the first class of immunoglobulins that is produced by plasma cells after B cell activation, and it has a half-life of ten days in serum, making it highly likely that low concentrations of it could be found within the mice serum (as it was tested fourteen days after boosting). On the other hand, since most of the IgG immunoglobulins have an average half-life of twenty days (Murphy et al., 2017), most of the humoral response observed in the analysis is IgG dependent. Comparison of the antibody titers of serum obtained from mice immunized with MVA-CTH522:B7 and MVA-CTH522 conclusively

showed that mice immunized with MVA-CTH522:B7 had a much humoral response. This is due to the B7 modification increasing the surface display of CTH522, which allows for the antigen to be recognized by B cells before they mediate the antibody response. While it has been previously established that there is a correlation between the levels of membrane-bound chimeric proteins and the concentration of specific secreted antibodies, there does not seem to be any previous studies analyzing the antibody response to antigens fused to the B7. Therefore, this dissertation presents for the first time the conclusion that fusion of the transmembrane domain and cytosolic tail of the murine B7-1 molecule to the antigen of interest is able to drastically enhance the antigen-specific antibody response.

Patients that exhibited a strong antibody response against C. *trachomatis* serovars D, E or K were not prone to a secondary infection, which could be correlated to the neutralizing level of 60-90% that was observed against serovar D in the study (Gupta et al., 2017). Generally, neutralizing activity has an inverse correlation to production of infectious units in immunized subjects (Mooij et al., 2022). Interestingly, a previous study has shown neutralizing activity and a strong $CD4^+$ T cell response against *C*. *trachomatis*, protecting the animals against genital challenge and encouraging research to include neutralizing antibodies in studies that aim to control the infection (Olsen et al., 2017). Since the future outlook of this study is for it to infer protection against a *C*. *trachomatis* challenge in mice, sera obtained from mice immunized with homologous prime/boost protocols was included in a neutralizing antibody assay. *Ex vivo* visual monitoring displayed a substantial difference in the number of inclusion bodies stained in a co-culture of serum:bacteria and HaK cells (**Figure 31**). HaK cells that were co-cultured with the serum from MVA-WT immunized mice exhibited a high number of chlamydial inclusion bodies, while those cells co-cultured with serum from MVA-CTH522:B7 immunized mice showed a considerable decrease in visible inclusion bodies. Further analysis led to highly promising results, with mice vaccinated with two doses of MVA-CTH522:B7 displaying a statistically significant neutralizing activity as opposed to mice vaccinated with MVA-CTH522 (**Figure 32**). A favorable 65% neutralization of chlamydial infection was observed at serum dilution 1:25, with an exponential curve leading to the hypothesis that a higher neutralization activity would be visible if a lower serum titer was analyzed. A neutralization activity of 38% has shown to be insufficient in providing protection against *C*. *trachomatis* (Degn et al., 2023). Whether or not a neutralization of 65% would be adequate to prevent the infection itself is yet to be seen, although previous studies

support the hypothesis that a sufficient neutralization is necessary for chlamydial clearance (Lorenzen et al., 2022; Olsen et al., 2017).

On the other hand, priming with DNA plasmids and boosting with recombinant MVA encoding the antigen of interest is a strategy that has been used for decades when aiming to develop an immunization regimen capable of eliciting protection against infectious pathogens, and it has been shown to trigger immune responses in both viral and parasitical diseases such as influenza or malaria (Dégano et al., 1999; McConkey et al., 2003). This kind of immunization regimen has also been analyzed in humans, previously triggering a broad and robust antibody response against HIV in healthy adults (Joachim et al., 2015). Mice that were vaccinated following a heterologous DNA/MVA prime/boost protocol did trigger a humoral response characterized by IgG antibodies, but it was outperformed by the homologous MVA/MVA regimen (**Figure 34**). This could be due to the DNA plasmid encoding a CTH522 variant containing a tetanus toxoid fragment C (TTFC) upstream of the CTH522 gene and lacking the transmembrane domain and cytoplasmic tail of the B7 molecule that has been proven throughout this work to not only enhance the surface display of CTH522 itself, but to consequently increase the antibody response in immunized mice. This would warrant an additional study analyzing the antibody response in serum of mice immunized via a heterologous prime/boost regimen where the priming agent would be a DNA plasmid encoding CTH522 with the B7 modifications comparable to the recombinant MVA in this work.

Despite the initial beliefs regarding $CD4^+$ T cells being the ones to provide protection against reinfection, antibodies have also been proven to grant it. It is now known that not only are $CD4^+$ T cells involved in protection, but the humoral response also plays a role in the triggered immune response against *C. trachomatis* (Morrison & Morrison, 2005). Therefore, considering that $CD8^+$ T cells have been proven not to be necessary for infection protection against *C. muridarum* in C57BL/6J mice (Yu et al., 2019), while $CD4^+$ T cells and antibody responses have shown to be crucial, MVA-CTH522:B7 is a promising vaccine vector, as it is capable of triggering both immune responses.

5.8. Conclusion

C. *trachomatis* is an obligate intracellular pathogen that infects humans and is currently causing the most predominant sexually transmitted bacterial infection (Wan et al., 2023), making it a worldwide issue that affects millions of people every year (World Health Organization, 2023).Its prevalence has not made a sign of progressively decreasing despite the existence of antibiotics to treat and clear the infection. The lack of success in controlling the transmission is theorized to be due to the fact that C. *trachomatis* is mainly asymptomatic in people of all genders. This makes the consolidation of routine screenings as a method of prevention ineffective and futile if those who are infected remain asymptomatic and, therefore, untested. This has led researchers to believe its control and possible eradication lies in preventive strategies such as vaccines. (Woodhall et al., 2018).

Among vaccine candidates, MVA stands out as a platform that has already shown to be safe, cost-effective and stable, all while inducing a robust immune response characterized by both T cells and antibodies. Precisely because both $CD4^+$ T cells and antibodies have proven to be essential for chlamydial clearance and inferring protection against the infection (Morrison & Morrison, 2005), this study was designed to generate and characterize a vaccine vector capable of inducing both. This approach centered around CTH522, a vaccine antigen consisting of heterologous immunorepeats from a variable domain of the MOMP protein in four different serovars previously studied in a phase 1, first-in-human, double-blind, parallel, randomized, placebo-controlled trial where it was deemed safe and immunogenic in healthy adults(Abraham et al., 2019). Precisely because the antibody response against the bacterium had proven to be crucial, CTH522 was additionally modified by fusing a signal sequence of Igk and the transmembrane domain and cytoplasmic tail of the murine B7 molecule. These sequences and domains have previously proven to enhance intracellular transport and surface display of chimeric proteins on the plasma membrane of mammalian cells (Liao et al., 2001; Pan et al., 2012), something that would in theory enhance the B cell mediated humoral response.

The novel MVA-CTH522:B7 was successfully generated and characterized, efficiently expressing CTH522:B7 through Western Blot analysis, and remaining genetically stable after 10 stability serial sub-passages in a permissive cell line. Additionally, its replication behavior and capacity followed the same pattern as MVA-WT, concluding that the insertion of CTH522:B7 into the MVA genome did not induce

any kind of detrimental effect on its replication. Moreover, infection with MVA-CTH522:B7 did resulted in a higher CTH522 surface density when compared to a recombinant MVA-CTH522 lacking the B7 modification.

The theoretical idea at the start of the study that the B7 modification eventually would lead to an enhanced humoral response was proved when mice immunized with MVA-CTH522:B7 showed a staggering antibody response characterized by both IgG and IgM antibodies, as opposed to those mice immunized with MVA-CTH522 lacking the B7 modification. A homologous MVA/MVA prime/boost immunization regimen vaccinating mice also outperformed a heterologous DNA/MVA protocol in terms of antibody responses. Moreover, even though the heterologous DNA/MVA prime/boost protocol displayed higher $CD4^+$ T cell responses that the homologous MVA/MVA, they both induced a significantly higher response than the homologous DNA/DNA, indicating that the integration of MVA-CTH522:B7 in a vaccination regimen is sufficient to elicit $CD4^+$ T cell-mediated IFN-γ activation. Additionally, sera obtained after MVA-CTH522:B7vaccination were able to have a neutralizing effect upon chlamydial infection in an *ex vivo* assay, indicating that MVA-CTH522:B7 is an ideal candidate capable of inducing robust humoral immune responses.

Overall, MVA-CTH522:B7 has proven itself as a promising vaccine candidate against *C. trachomatis*, capable of inducing a strong two-arm immune response characterized by $CD4^+$ T cell activation and antibody production, something that is essential for chlamydial clearance and protection. It has shown to have the strongest antibody response among the different immunization regimens in this study and a robust $CD4^+$ T cell response. Precisely because a favorable vaccine should be able to clear and prevent the pathogen it is intended for, MVA-CTH522:B7 presents itself as an ideal candidate that should be studied in further preclinical analysis before moving on to clinical trials.

LIST OF REFERENCES:

Abraham, S., Juel, H. B., Bang, P., Cheeseman, H. M., Dohn, R. B., Cole, T., Kristiansen, M. P., Korsholm, K. S., Lewis, D., Olsen, A. W., McFarlane, L. R., Day, S., Knudsen, S., Moen, K., Ruhwald, M., Kromann, I., Andersen, P., Shattock, R. J., & Follmann, F. (2019). Safety and immunogenicity of the chlamydia vaccine candidate CTH522 adjuvanted with CAF01 liposomes or aluminium hydroxide: a first-in-human, randomised, double-blind, placebo-controlled, phase 1 trial. *The Lancet Infectious Diseases*, *19*(10), 1091–1100. https://doi.org/10.1016/S1473-3099(19)30279-8

Ajani, T. A., Elikwu, C. J., Nwadike, V., Babatunde, T., Anaedobe, C. G., Shonekan, O., Okangba, C., Oluwasola, T., Omeonu, A., Faluyi, B., Thompson, T. E., Ebeigbe, E., Ajani, M. A., Joshua, A. K., Kolawole, T., Kristilere, H., Meremikwu, C. M., Mgbemena, L., Nwaejike, C. S., … Coker, A. O. (2019). Assessment of Serological Markers of Genital Chlamydia trachomatis Infection Among the Gynaecology Patients attending Babcock University Teaching Hospital, Ilishan-Remo, Ogun State, Nigeria. *African Journal of Reproductive Health*, *23*(4), 54–62. https://doi.org/10.29063/AJRH2019/V23I4.7

Al Shoyaib, A., Archie, S. R., & Karamyan, V. T. (2019). Intraperitoneal Route of Drug Administration: Should it Be Used in Experimental Animal Studies? *Pharmaceutical Research*, *37*(1), 12. https://doi.org/10.1007/S11095-019-2745-X

Badamchi-Zadeh, A., McKay, P. F., Holland, M. J., Paes, W., Brzozowski, A., Lacey, C., Follmann, F., Tregoning, J. S., & Shattock, R. J. (2015). Intramuscular Immunisation with Chlamydial Proteins Induces Chlamydia trachomatis Specific Ocular Antibodies. *PloS One*, *10*(10). https://doi.org/10.1371/JOURNAL.PONE.0141209

Badamchi-Zadeh, A., McKay, P. F., Korber, B. T., Barinaga, G., Walters, A. A., Nunes, A., Gomes, J. P., Follmann, F., Tregoning, J. S., & Shattock, R. J. (2016). A Multi-Component Prime-Boost Vaccination Regimen with a Consensus MOMP Antigen Enhances Chlamydia trachomatis Clearance. *Frontiers in Immunology*, *7*(APR). https://doi.org/10.3389/FIMMU.2016.00162

Bailón, L., Llano, A., Cedeño, S., Escribà, T., Rosás-Umbert, M., Parera, M., Casadellà, M., Lopez, M., Pérez, F., Oriol-Tordera, B., Ruiz-Riol, M., Coll, J., Perez, F., Rivero, À., Leselbaum, A. R., McGowan, I., Sengupta, D., Wee, E. G., Hanke, T., … Puig, J. (2022). Safety, immunogenicity and effect on viral rebound of HTI vaccines in early treated HIV-1 infection: a randomized, placebo-controlled phase 1 trial. *Nature Medicine 2022 28:12*, *28*(12), 2611–2621. https://doi.org/10.1038/s41591-022-02060-2

Bakshi, R. K., Gupta, K., Jordan, S. J., Chi, X., Lensing, S. Y., Press, C. G., & Geisler, W. M. (2018). An Adaptive Chlamydia trachomatis-Specific IFN-γ-Producing CD4+ T Cell Response Is Associated With Protection Against Chlamydia Reinfection in Women. *Frontiers in Immunology*, *9*(SEP). https://doi.org/10.3389/FIMMU.2018.01981

Barishak, R., Wellings, S. R., & Siegel, B. V. (1961). Cytologic Studies of Cultured Cells of the Cloudman S-91 Mouse Melanoma. *The American Journal of Pathology*, *38*(3), 371. https://www.ncbi.nlm.nih.gov/pmc/articles/PMC1942339/

Barnowski, C., Ciupka, G., Tao, R., Jin, L., Busch, D. H., Tao, S., & Drexler, I. (2020). Efficient Induction of Cytotoxic T Cells by Viral Vector Vaccination Requires STING-Dependent DC

Functions. *Frontiers in Immunology*, *11*, 1458. https://doi.org/10.3389/FIMMU.2020.01458/FULL

Baur, K., Brinkmann, † Kay, Schweneker, † Marc, Pätzold, J., Meisinger-Henschel, C., Hermann, J., Steigerwald, R., Chaplin, P., Suter, M., & Hausmann, J. (2010). Immediate-Early Expression of a Recombinant Antigen by Modified Vaccinia Virus Ankara Breaks the Immunodominance of Strong Vector-Specific B8R Antigen in Acute and Memory CD8 T-Cell Responses. *JOURNAL OF VIROLOGY*, *84*(17), 8743–8752. https://doi.org/10.1128/JVI.00604-10

Bayramova, F., Jacquier, N., & Greub, G. (2018). Insight in the biology of Chlamydia-related bacteria. *Microbes and Infection*, *20*(7–8), 432–440. https://doi.org/10.1016/J.MICINF.2017.11.008

Bockstal, V., Shukarev, G., McLean, C., Goldstein, N., Bart, S., Gaddah, A., Anumenden, D., Stoop, J. N., de Groot, A. M., Pau, M. G., Hendriks, J., De Rosa, S. C., Cohen, K. W., McElrath, M. J., Callendret, B., Luhn, K., Douoguih, M., & Robinson, C. (2022). First-in-human study to evaluate safety, tolerability, and immunogenicity of heterologous regimens using the multivalent filovirus vaccines Ad26.Filo and MVA-BN-Filo administered in different sequences and schedules: A randomized, controlled study. *PloS One*, *17*(10). https://doi.org/10.1371/JOURNAL.PONE.0274906

Borel, N., Leonard, C., Slade, J., & Schoborg, R. V. (2016). *Chlamydial Antibiotic Resistance and Treatment Failure in Veterinary and Human Medicine*. https://doi.org/10.1007/s40588-016-0028-4

Borges, A., Pollock, K., Stoey, L. S., Tingskov, P. N., & Dohn, R. B. (n.d.). *Safety and Immunogenicity of a Chlamydia Vaccine CTH522*. ClinicalTrials.Gov. Retrieved October 24, 2023, from https://classic.clinicaltrials.gov/ct2/show/NCT03926728?term=cth522&draw=2&rank=2

Brown, T. H. T., David, J., Acosta-Ramirez, E., Moore, J. M., Lee, S., Zhong, G., Hancock, R. E. W., Xing, Z., Halperin, S. A., & Wang, J. (2012). Comparison of immune responses and protective efficacy of intranasal prime-boost immunization regimens using adenovirus-based and CpG/HH2 adjuvanted-subunit vaccines against genital Chlamydia muridarum infection. *Vaccine*, *30*(2), 350–360. https://doi.org/10.1016/J.VACCINE.2011.10.086

Buonaguro, F. M., Tornesello, M. L., & Buonaguro, L. (2011a). New adjuvants in evolving vaccine strategies. *Expert Opinion on Biological Therapy*, *11*(7), 827–832. https://doi.org/10.1517/14712598.2011.587802

Buonaguro, F. M., Tornesello, M. L., & Buonaguro, L. (2011b). New adjuvants in evolving vaccine strategies. *Expert Opinion on Biological Therapy*, *11*(7), 827–832. https://doi.org/10.1517/14712598.2011.587802

Carroll, M. W., & Moss, B. (1997). Host Range and Cytopathogenicity of the Highly Attenuated MVA Strain of Vaccinia Virus: Propagation and Generation of Recombinant Viruses in a Nonhuman Mammalian Cell Line. *Virology*, *238*(2), 198–211. https://doi.org/10.1006/VIRO.1997.8845

Centers for Disease Control and Prevention. (2021, July 22). *STI Treatment Guidelines*. https://www.cdc.gov/std/treatment-guidelines/chlamydia.htm

Chang, K., Baginski, J., Hassan, S. F., Volin, M., Shukla, D., & Tiwari, V. (2016). Filopodia and Viruses: An Analysis of Membrane Processes in Entry Mechanisms. *Frontiers in Microbiology*, *7*(MAR), 300. https://doi.org/10.3389/FMICB.2016.00300

Chapman, R., Jongwe, T. I., Douglass, N., Chege, G., & Williamson, A. L. (2017). Heterologous prime-boost vaccination with DNA and MVA vaccines, expressing HIV-1 subtype C mosaic Gag virus-like particles, is highly immunogenic in mice. *PLoS ONE*, *12*(3). https://doi.org/10.1371/JOURNAL.PONE.0173352

Chea, L. S., Wyatt, L. S., Gangadhara, S., Moss, B., & Amara, R. R. (2019). Novel Modified Vaccinia Virus Ankara Vector Expressing Anti-apoptotic Gene B13R Delays Apoptosis and Enhances Humoral Responses. *Journal of Virology*, *93*(5). https://doi.org/10.1128/JVI.01648-18

Chege, G. K., Burgers, W. A., Müller, T. L., Gray, C. M., Shephard, E. G., Barnett, S. W., Ferrari, G., Montefiori, D., Williamson, C., & Williamson, A. L. (2017). DNA-MVA-protein vaccination of rhesus macaques induces HIV-specific immunity in mucosal-associated lymph nodes and functional antibodies. *Vaccine*, *35*(6), 929. https://doi.org/10.1016/J.VACCINE.2016.12.060

Chou W., Liao, K., Lo, Y., Jiang. S. Y., Yeh, M. Y., & Roffler, S. R. (1999). Expression of Chimeric Monomer and Dimer Proteins on the Plasma Membrane of Mammalian Cells. *Biotechnology and Engineering*, *65*(2), 160–169.

Chuang, K. H., Hsieh, Y. C., Chiang, I. S., Chuang, C. H., Kao, C. H., Cheng, T. C., Wang, Y. T., Lin, W. W., Chen, B. M., Roffler, S. R., Huang, M. Y., & Cheng, T. L. (2014). High-Throughput Sorting of the Highest Producing Cell via a Transiently Protein-Anchored System. *PLoS ONE*, *9*(7). https://doi.org/10.1371/JOURNAL.PONE.0102569

Ciechomska, M., Lennard, T. W. J., Kirby, J. A., & Knight, A. M. (2011). B lymphocytes acquire and present intracellular antigens that have relocated to the surface of apoptotic target cells. *European Journal of Immunology*, *41*(7), 1850–1861. https://doi.org/10.1002/EJI.201141472

Clark, R. H., Kenyon, J. C., Bartlett, N. W., Tscharke, D. C., & Smith, G. L. (2006). Deletion of gene A41L enhances vaccinia virus immunogenicity and vaccine efficacy. *J Gen Virol* . https://doi.org/10.1099/vir.0.81417-0

Collar, A. L., Linville, A. C., Core, S. B., & Frietze, K. M. (2022). Epitope-Based Vaccines against the Chlamydia trachomatis Major Outer Membrane Protein Variable Domain 4 Elicit Protection in Mice. *Vaccines*, *10*(6). https://doi.org/10.3390/VACCINES10060875/S1

Collier, L. H., & Smith, A. (1967). Dissemination and immunogenicity of live TRIC agent in baboons after parenteral injection. *American Journal of Ophthalmology*, *63*(5 PART 2), 1589–1602. https://doi.org/10.1016/0002-9394(67)94153-0

Collins, J. M., Donahue, R. N., Tsai, Y., Manu, M., Palena, C., Gatti-Mays, M. E., Marté, J. L., Madan, R. A., Karzai, F., Heery, C. R., Strauss, J., Abdul-Sater, H., Cordes, L., Schlom, J., Gulley, J. L., & Bilusic, M. (2020). Phase I Trial of a Modified Vaccinia Ankara Priming Vaccine Followed by a Fowlpox Virus Boosting Vaccine Modified to Express Brachyury and Costimulatory Molecules in Advanced Solid Tumors. *The Oncologist*, *25*(7), 560. https://doi.org/10.1634/THEONCOLOGIST.2019-0932

Cottingham, M. G., Andersen, R. F., Spencer, A. J., Saurya, S., Furze, J., Hill, A. V. S., & Gilbert, S. C. (2008). Recombination-Mediated Genetic Engineering of a Bacterial Artificial

Chromosome Clone of Modified Vaccinia virus Ankara (MVA). *PLoS ONE*, *3*(2). https://doi.org/10.1371/JOURNAL.PONE.0001638

Cottingham, M. G., & Gilbert, S. C. (2010). Rapid generation of markerless recombinant MVA vaccines by en passant recombineering of a self-excising bacterial artificial chromosome. *Journal of Virological Methods*, *168*(1–2), 233–236. https://doi.org/10.1016/J.JVIROMET.2010.04.012

Dai, P., Wang, W., Cao, H., Avogadri, F., Dai, L., Drexler, I., Joyce, J. A., Li, X. D., Chen, Z., Merghoub, T., Shuman, S., & Deng, L. (2014). Modified Vaccinia Virus Ankara Triggers Type I IFN Production in Murine Conventional Dendritic Cells via a cGAS/STING-Mediated Cytosolic DNA-Sensing Pathway. *PLoS Pathogens*, *10*(4), 1003989. https://doi.org/10.1371/JOURNAL.PPAT.1003989

De La Maza, L. M., Zhong, G., & Brunham, R. C. (2017). *Update on Chlamydia trachomatis Vaccinology*. https://doi.org/10.1128/CVI.00543-16

Dégano, P., Schneider, J., Hannan, C. M., Gilbert, S. C., & Hill, A. V. S. (1999). Gene gun intradermal DNA immunization followed by boosting with modified vaccinia virus Ankara: Enhanced CD8+ T cell immunogenicity and protective efficacy in the influenza and malaria models. *Vaccine*, *18*(7–8), 623–632. https://doi.org/10.1016/S0264-410X(99)00278-9

Degn, L. L. T., Bech, D., Christiansen, G., & Birkelund, S. (2023). Lack of neutralization of Chlamydia trachomatis infection by high avidity monoclonal antibodies to surface-exposed major outer membrane protein variable domain IV. *Molecular Immunology*, *163*, 163–173. https://doi.org/10.1016/J.MOLIMM.2023.09.015

Doceul, V., Hollinshead, M., Breiman, A., Laval, K., & Smith, G. L. (2012). Protein B5 is required on extracellular enveloped vaccinia virus for repulsion of superinfecting virions. *The Journal of General Virology*, *93*(Pt 9), 1876. https://doi.org/10.1099/VIR.0.043943-0

Donati, M., Sambri, V., Comanducci, M., Di Leo, K., Storni, E., Giacani, L., Ratti, G., & Cevenini, R. (2003). DNA immunization with pgp3 gene of Chlamydia trachomatis inhibits the spread of chlamydial infection from the lower to the upper genital tract in C3H/HeN mice. *Vaccine*, *21*(11–12), 1089–1093. https://doi.org/10.1016/S0264-410X(02)00631-X

Draenert, R., Altfeld, M., Brander, C., Basgoz, N., Corcoran, C., Wurcel, A. G., Stone, D. R., Kalams, S. A., Trocha, A., Addo, M. M., Goulder, P. J. R., & Walker, B. D. (2003). Comparison of overlapping peptide sets for detection of antiviral CD8 and CD4 T cell responses. *Journal of Immunological Methods*, *275*(1–2), 19–29. https://doi.org/10.1016/S0022-1759(02)00541-0

Drexler, I., Heller, K., Wahren, B., Erfle, V., & Sutter, G. (1998). Highly attenuated modified vaccinia virus Ankara replicates in baby hamster kidney cells, a potential host for virus propagation, but not in various human transformed and primary cells. *Journal of General Virology*, *79*(2), 347–352. https://doi.org/10.1099/0022-1317-79-2-347/CITE/REFWORKS

Dunachie, S. J., & Hill, A. V. S. (2003). Prime-boost strategies for malaria vaccine development. *Journal of Experimental Biology*, *206*(21), 3771–3779. https://doi.org/10.1242/JEB.00642

Earley, A. K., Chan, W. M., & Ward, B. M. (2008). The Vaccinia Virus B5 Protein Requires A34 for Efficient Intracellular Trafficking from the Endoplasmic Reticulum to the Site of Wrapping and Incorporation into Progeny Virions. *Journal of Virology*, *82*(5), 2161. https://doi.org/10.1128/JVI.01971-07

Eiz-Vesper, B., & Schmetzer, H. M. (2020). Antigen-Presenting Cells: Potential of Proven und New Players in Immune Therapies. *Transfusion Medicine and Hemotherapy*, *47*(6), 429–431. https://doi.org/10.1159/000512729

Elwell, C., Mirrashidi, K., & Engel, J. (2016). Chlamydia cell biology and pathogenesis. *Nature Reviews. Microbiology*, *14*(6), 385. https://doi.org/10.1038/NRMICRO.2016.30

Eslamizar, L., Petrovas, C., Leggat, D. J., Furr, K., Lifton, M. L., Levine, G., Ma, S., Fletez-Brant, C., Hoyland, W., Prabhakaran, M., Narpala, S., Boswell, K., Yamamoto, T., Liao, H. X., Pickup, D., Ramsburg, E., Sutherland, L., McDermott, A., Roederer, M., … Santra, S. (2021). Recombinant MVA-prime elicits neutralizing antibody responses by inducing antigen-specific B cells in the germinal center. *NPJ Vaccines*, *6*(1). https://doi.org/10.1038/S41541-020-00277-1

Esposito, I., Cicconi, P., D'Alise, A. M., Brown, A., Esposito, M., Swadling, L., Holst, P. J., Bassi, M. R., Stornaiuolo, M., Mori, F., Vassilev, V., Li, W., Donnison, T., Gentile, C., Turner, B., von Delft, A., Del Sorbo, M., Barra, F., Contino, A. M., … Woods, E. (2020). MHC class II invariant chain-adjuvanted viral vectored vaccines enhances T cell responses in humans. *Science Translational Medicine*, *12*(548). https://doi.org/10.1126/SCITRANSLMED.AAZ7715

Fan, W., Wan, Y., & Li, Q. (2020). Interleukin-21 enhances the antibody avidity elicited by DNA prime and MVA boost vaccine. *Cytokine*, *125*. https://doi.org/10.1016/J.CYTO.2019.154814

Farris, C. M., Morrison, S. G., & Morrison, R. P. (2010). CD4+ T Cells and Antibody Are Required for Optimal Major Outer Membrane Protein Vaccine-Induced Immunity to Chlamydia muridarum Genital Infection. *Infection and Immunity*, *78*(10), 4374. https://doi.org/10.1128/IAI.00622-10

Fleri, W., Paul, S., Dhanda, S. K., Mahajan, S., Xu, X., Peters, B., & Sette, A. (2017). The Immune Epitope Database and Analysis Resource in Epitope Discovery and Synthetic Vaccine Design. *Frontiers in Immunology*, *8*(MAR), 278. https://doi.org/10.3389/FIMMU.2017.00278

Fournillier, A., Frelin, L., Jacquier, E., Ahlén, G., Brass, A., Gerossier, E., Holmström, F., Broderick, K. E., Sardesai, N. Y., Bonnefoy, J. Y., Inchauspé, G., & Sällberg, M. (2013). A Heterologous Prime/Boost Vaccination Strategy Enhances the Immunogenicity of Therapeutic Vaccines for Hepatitis C Virus. *The Journal of Infectious Diseases*, *208*(6), 1008. https://doi.org/10.1093/INFDIS/JIT267

Freund, Y. R., Mirsalis, J. C., Fairchild, D. G., Brune, J., Hokama, L. A., Schindler-Horvat, J., Tomaszewski, J. E., Hodge, J. W., Schlom, J., Kantor, J. A., Tyson, C. A., & Donohue, S. J. (2000). Vaccination with a recombinant vaccinia vaccine containing the B7-1 co-stimulatory molecule causes no significant toxicity and enhances T cell–mediated cytotoxicity. *J. Cancer*, *85*, 508–517. https://doi.org/10.1002/(SICI)1097-0215(20000215)85:4

Gallego-Gómez, J. C., Risco, C., Rodríguez, D., Cabezas, P., Guerra, S., Carrascosa, J. L., & Esteban, M. (2003). Differences in Virus-Induced Cell Morphology and in Virus Maturation between MVA and Other Strains (WR, Ankara, and NYCBH) of Vaccinia Virus in Infected Human Cells. *Journal of Virology*, *77*(19), 10606. https://doi.org/10.1128/JVI.77.19.10606-10622.2003

Garber, D. A., O'Mara, L. A., Zhao, J., Gangadhara, S., An, I. C., & Feinberg, M. B. (2009). Expanding the repertoire of Modified Vaccinia Ankara-based vaccine vectors via genetic complementation strategies. *PloS One*, *4*(5). https://doi.org/10.1371/JOURNAL.PONE.0005445

García-Arriaza, J., Arnáez, P., Gómez, C. E., Sorzano, C. Ó. S., & Esteban, M. (2013). Improving Adaptive and Memory Immune Responses of an HIV/AIDS Vaccine Candidate MVA-B by Deletion of Vaccinia Virus Genes (C6L and K7R) Blocking Interferon Signaling Pathways. *PLoS ONE*, *8*(6). https://doi.org/10.1371/JOURNAL.PONE.0066894

García-Arriaza, J., & Esteban, M. (2014). Enhancing poxvirus vectors vaccine immunogenicity. *Human Vaccines & Immunotherapeutics*, *10*(8), 2235–2244. https://doi.org/10.4161/HV.28974

García-Arriaza, J., Garaigorta, U., Pérez, P., Lázaro-Frías, A., Zamora, C., Gastaminza, P., Fresno, C. del, Casasnovas, J. M., Sorzano, C. Ó. S., Sancho, D., & Esteban, M. (2021). COVID-19 Vaccine Candidates Based on Modified Vaccinia Virus Ankara Expressing the SARS-CoV-2 Spike Protein Induce Robust T- and B-Cell Immune Responses and Full Efficacy in Mice. *Journal of Virology*, *95*(7). https://doi.org/10.1128/JVI.02260-20

García-Arriaza, J., Gómez, C. E., Sorzano, C. Ó. S., & Esteban, M. (2014). Deletion of the Vaccinia Virus N2L Gene Encoding an Inhibitor of IRF3 Improves the Immunogenicity of Modified Vaccinia Virus Ankara Expressing HIV-1 Antigens. *Journal of Virology*, *88*(6), 3392. https://doi.org/10.1128/JVI.02723-13

García-Arriaza, J., Marín, M. Q., Merchán-Rubira, J., Mascaraque, S. M., Medina, M., Ávila, J., Hernández, F., & Esteban, M. (2020). Tauopathy Analysis in P301S Mouse Model of Alzheimer Disease Immunized with DNA and MVA Poxvirus-Based Vaccines Expressing Human Full-Length 4R2N or 3RC Tau Proteins. *Vaccines*, *8*(1). https://doi.org/10.3390/VACCINES8010127

García-Arriaza, J., Nájera, J. L., Gómez, C. E., Sorzano, C. O. S., & Esteban, M. (2010). Immunogenic Profiling in Mice of a HIV/AIDS Vaccine Candidate (MVA-B) Expressing Four HIV-1 Antigens and Potentiation by Specific Gene Deletions. *PLoS ONE*, *5*(8). https://doi.org/10.1371/JOURNAL.PONE.0012395

García-Arriaza, J., Nájera, J. L., Gómez, C. E., Tewabe, N., Sorzano, C. O. S., Calandra, T., Roger, T., & Esteban, M. (2011). A Candidate HIV/AIDS Vaccine (MVA-B) Lacking Vaccinia Virus Gene C6L Enhances Memory HIV-1-Specific T-Cell Responses. *PLoS ONE*, *6*(8), 24244. https://doi.org/10.1371/JOURNAL.PONE.0024244

Gherardi, M. M., Nájera, J. L., Pérez-Jiménez, E., Guerra, S., García-Sastre, A., & Esteban, M. (2003). Prime-Boost Immunization Schedules Based on Influenza Virus and Vaccinia Virus Vectors Potentiate Cellular Immune Responses against Human Immunodeficiency Virus Env Protein Systemically and in the Genitorectal Draining Lymph Nodes. *Journal of Virology*, *77*(12), 7048. https://doi.org/10.1128/JVI.77.12.7048-7057.2003

Giotis, E. S., Montillet, G., Pain, B., & Skinner, M. A. (2019). Chicken Embryonic-Stem Cells Are Permissive to Poxvirus Recombinant Vaccine Vectors. *Genes*, *10*(3). https://doi.org/10.3390/GENES10030237

Gómez, C. E., Nájera, J. L., Jiménez, V., Bieler, K., Wild, J., Kostic, L., Heidari, S., Chen, M., Frachette, M. J., Pantaleo, G., Wolf, H., Liljeström, P., Wagner, R., & Esteban, M. (2007). Generation and immunogenicity of novel HIV/AIDS vaccine candidates targeting HIV-1

Env/Gag-Pol-Nef antigens of clade C. *Vaccine*, *25*(11), 1969–1992. https://doi.org/10.1016/J.VACCINE.2006.11.051

Gondek, D. C., Roan, N. R., & Starnbach, M. N. (2009). T cell responses in the absence of IFNγ exacerbate uterine infection with Chlamydia trachomatis. *Journal of Immunology (Baltimore, Md. : 1950)*, *183*(2), 1313. https://doi.org/10.4049/JIMMUNOL.0900295

Gottlieb, S. L., Xu, F., & Brunham, R. C. (2013). Screening and treating Chlamydia trachomatis genital infection to prevent pelvic inflammatory disease: Interpretation of findings from randomized controlled trials. *Sexually Transmitted Diseases*, *40*(2), 97–102. https://doi.org/10.1097/OLQ.0B013E31827BD637

Gupta, V. K., Waugh, C. A., Ziklo, N., Huston, W. M., Hocking, J. S., & Timms, P. (2017). Systemic antibody response to Chlamydia Trachomatis infection in patients either infected or reinfected with different Chlamydia serovars. *Indian Journal of Medical Microbiology*, *35*(3), 394–401. https://doi.org/10.4103/IJMM.IJMM_17_1

Hadad, R., Marks, E., Kalbina, I., Schön, K., Unemo, M., Lycke, N., Strid, Å., & Andersson, S. (2016). Protection against genital tract Chlamydia trachomatis infection following intranasal immunization with a novel recombinant MOMP VS2/4 antigen. *APMIS*, *124*(12), 1078–1086. https://doi.org/10.1111/APM.12605

Han, J. J., Hu, Y. A., Nan, Y., Chen, Y., & Yang, Y. L. (2023). Decreased expression of HBV surface antigen (HBsAg) with sK122R and sV96A co-mutation is associated with an ineffective antibody response in a chronic hepatitis B patient. *Infection, Genetics and Evolution : Journal of Molecular Epidemiology and Evolutionary Genetics in Infectious Diseases*, *111*. https://doi.org/10.1016/J.MEEGID.2023.105431

Helble, J. D., & Starnbach, M. N. (2019). A Chlamydia trachomatis Strain Expressing Ovalbumin Stimulates an Antigen-Specific CD4+ T Cell Response in Mice. *Infection and Immunity*, *87*(7). https://doi.org/10.1128/IAI.00837-18

Holgado, M. P., Falivene, J., Maeto, C., Amigo, M., Pascutti, M. F., Vecchione, M. B., Bruttomesso, A., Calamante, G., Del Médico-Zajac, M. P., & Gherardi, M. M. (2016). Deletion of A44L, A46R and C12L Vaccinia Virus Genes from the MVA Genome Improved the Vector Immunogenicity by Modifying the Innate Immune Response Generating Enhanced and Optimized Specific T-Cell Responses. *Viruses*, *8*(5). https://doi.org/10.3390/V8050139

Horner, P. J. (2012). Azithromycin antimicrobial resistance and genital Chlamydia trachomatis infection: duration of therapy may be the key to improving efficacy. *Sex Transm Infect*, *88*(3).

Isshiki, M., Zhang, X., Sato, H., Ohashi, T., Inoue, M., & Shida, H. (2014). Effects of different promoters on the virulence and immunogenicity of a HIV-1 Env-expressing recombinant vaccinia vaccine. *Vaccine*, *32*(7), 839–845. https://doi.org/10.1016/J.VACCINE.2013.12.022

Jackson, L. A., Frey, S. E., El Sahly, H. M., Mulligan, M. J., Winokur, P. L., Kotloff, K. L., Campbell, J. D., Atmar, R. L., Graham, I., Anderson, E. J., Anderson, E. L., Patel, S. M., Fields, C., Keitel, W., Rouphael, N., Hill, H., & Goll, J. B. (2017). Safety and immunogenicity of a modified vaccinia Ankara vaccine using three immunization schedules and two modes of delivery: A randomized clinical non-inferiority trial. *Vaccine*, *35*(13), 1675–1682. https://doi.org/10.1016/J.VACCINE.2017.02.032

Joachim, A., Nilsson, C., Aboud, S., Bakari, M., Lyamuya, E. F., Robb, M. L., Marovich, M. A., Earl, P., Moss, B., Ochsenbauer, C., Wahren, B., Mhalu, F., Sandström, E., Biberfeld, G., Ferrari, G., & Polonis, V. R. (2015). Potent functional antibody responses elicited by HIV-I DNA priming and boosting with heterologous HIV-1 recombinant MVA in healthy Tanzanian adults. *PloS One*, *10*(4). https://doi.org/10.1371/JOURNAL.PONE.0118486

June, C. H., Bluestone, J. A., Nadler, L. M., & Thompson, C. B. (1994). The B7 and CD28 receptor families. *Immunology Today*, *15*(7), 321–331. https://doi.org/10.1016/0167-5699(94)90080-9

Kalodimou, G., Jany, S., Freudenstein, A., Schwarz, J. H., Limpinsel, L., Rohde, C., Kupke, A., Becker, S., Volz, A., Tscherne, A., & Sutter, G. (2023). Short- and Long-Interval Prime-Boost Vaccination with the Candidate Vaccines MVA-SARS-2-ST and MVA-SARS-2-S Induces Comparable Humoral and Cell-Mediated Immunity in Mice. *Viruses*, *15*(5). https://doi.org/10.3390/V15051180/S1

Kane, J. L., Woodland, R. M., & Forsey, T. (1984). Chlamydia trachomatis and infertility. *Lancet (London, England)*, *1*(8379), 736–737. https://doi.org/10.1016/S0140-6736(84)92247-5

Karsten Tischer, B., Smith, G. A., & Osterrieder, N. (2010). En passant mutagenesis: A Two Markerless red recombination system. *Methods in Molecular Biology*, *634*, 421–430. https://doi.org/10.1007/978-1-60761-652-8_30/COVER

Karunakaran, K. P., Yu, H., Jiang, X., Chan, Q., Moon, K. M., Foster, L. J., & Brunham, R. C. (2015). Outer membrane proteins preferentially load MHC class II peptides: Implications for a Chlamydia trachomatis T cell vaccine. *Vaccine*, *33*(18), 2159–2166. https://doi.org/10.1016/J.VACCINE.2015.02.055

Katsafanas, G. C., & Moss, B. (2007). Linkage of Transcription and Translation within Cytoplasmic Poxvirus DNA Factories Provides a Mechanism to Coordinate Viral and Usurp Host Functions. *Cell Host & Microbe*, *2*(4), 221. https://doi.org/10.1016/J.CHOM.2007.08.005

Kaynarcalidan, O., Moreno Mascaraque, S., & Drexler, I. (2021). Vaccinia Virus: From Crude Smallpox Vaccines to Elaborate Viral Vector Vaccine Design. *Biomedicines*, *9*(12). https://doi.org/10.3390/BIOMEDICINES9121780

Khurana, S., & George, S. P. (2011). The role of actin bundling proteins in the assembly of filopodia in epithelial cells. *Cell Adhesion and Migration*, *5*(5), 409–420. https://doi.org/10.4161/CAM.5.5.17644

Knight, S. C., Iqball, S., Woods, C., Stagg, A., Ward, M. E., & Tuffreyt Antigen, M. (1995). A peptide of Chlamydia trachomatis shown to be a primary T-cell epitope in vitro induces cell-mediated immunity in vivo. *Immunology*, *85*(1), 8. /pmc/articles/PMC1384018/?report=abstract

Kugler, F., Drexler, I., Protzer, U., Hoffmann, D., & Moeini, H. (2019). Generation of recombinant MVA-norovirus: a comparison study of bacterial artificial chromosome- and marker-based systems. *Virology Journal*, *16*(1). https://doi.org/10.1186/S12985-019-1212-Y

Kulkarni, V., Rosati, M., Jalah, R., Ganneru, B., Alicea, C., Yu, L., Guan, Y., Labranche, C., Montefiori, D. C., King, A. D., Valentin, A., Pavlakis, G. N., & Felber, B. K. (2014). DNA vaccination by intradermal electroporation induces long-lasting immune responses in rhesus macaques. *Journal of Medical Primatology*, *43*(5), 329. https://doi.org/10.1111/JMP.12123

Laliberte, J. P., Weisberg, A. S., & Moss, B. (2011). The Membrane Fusion Step of Vaccinia Virus Entry Is Cooperatively Mediated by Multiple Viral Proteins and Host Cell Components. *PLoS Pathogens*, *7*(12), 1002446. https://doi.org/10.1371/JOURNAL.PPAT.1002446

Lane, A. B., & Decker, C. F. (2016). Chlamydia trachomatis infections. In *Disease-a-Month* (Vol. 62, Issue 8, pp. 269–273). Mosby Inc. https://doi.org/10.1016/j.disamonth.2016.03.010

Langenmayer, M. C., Luelf-Averhoff, A. T., Marr, L., Jany, S., Freudenstein, A., Adam-Neumair, S., Tscherne, A., Fux, R., Rojas, J. J., Blutke, A., Sutter, G., & Volz, A. (2023). Newly Designed Poxviral Promoters to Improve Immunogenicity and Efficacy of MVA-NP Candidate Vaccines against Lethal Influenza Virus Infection in Mice. *Pathogens*, *12*(7). https://doi.org/10.3390/PATHOGENS12070867/S1

Lau, A., Kong, F. Y. S., Fairley, C. K., Templeton, D. J., Amin, J., Phillips, S., Law, M., Chen, M. Y., Bradshaw, C. S., Donovan, B., McNulty, A., Boyd, M. A., Timms, P., Chow, E. P. F., Regan, D. G., Khaw, C., Lewis, D. A., Kaldor, J., Ratnayake, M., … Hocking, J. S. (2021). Azithromycin or Doxycycline for Asymptomatic Rectal Chlamydia trachomatis . *New England Journal of Medicine*, *384*(25), 2418–2427. https://doi.org/10.1056/NEJMOA2031631/SUPPL_FILE/NEJMOA2031631_DATA-SHARING.PDF

Leung-Theung-Long, S., Gouanvic, M., Coupet, C. A., Ray, A., Tupin, E., Silvestre, N., Marchand, J. B., Schmitt, D., Hoffmann, C., Klein, M., Seegren, P., Huaman, M. C., Cristillo, A. D., & Inchauspé, G. (2015). A Novel MVA-Based Multiphasic Vaccine for Prevention or Treatment of Tuberculosis Induces Broad and Multifunctional Cell-Mediated Immunity in Mice and Primates. *PloS One*, *10*(11). https://doi.org/10.1371/JOURNAL.PONE.0143552

Li, S., Rodrigues, M., Rodriguez, D., Rodriguez, J. R., Esteban, M., Palese, P., Nussenzweig, R. S., & Zavala, F. (1993a). Priming with recombinant influenza virus followed by administration of recombinant vaccinia virus induces CD8+ T-cell-mediated protective immunity against malaria. *Proceedings of the National Academy of Sciences of the United States of America*, *90*(11), 5214. https://doi.org/10.1073/PNAS.90.11.5214

Li, S., Rodrigues, M., Rodriguez, D., Rodriguez, J. R., Esteban, M., Palese, P., Nussenzweig, R. S., & Zavala, F. (1993b). Priming with recombinant influenza virus followed by administration of recombinant vaccinia virus induces CD8+ T-cell-mediated protective immunity against malaria. *Proceedings of the National Academy of Sciences of the United States of America*, *90*(11), 5214. https://doi.org/10.1073/PNAS.90.11.5214

Li, W., Murthy, A. K., Lanka, G. K., Chetty, S. L., Yu, J. J., Chambers, J. P., Zhong, G., Forsthuber, T. G., Guentzel, M. N., & Arulanandam, B. P. (2013). A T Cell Epitope-Based Vaccine Protects Against Chlamydial Infection in HLA-DR4 Transgenic Mice. *Vaccine*, *31*(48), 5722–5728. https://doi.org/10.1016/J.VACCINE.2013.09.036

Liao, K. W., Chou, W. C., Lo, Y. C., & Roffler, S. R. (2001). Design of transgenes for efficient expression of active chimeric proteins on mammalian cells. *Biotechnology and Bioengineering*, *73*(4), 313–323. https://doi.org/10.1002/BIT.1064

Lin, Y. C., Chen, B. M., Lu, W. C., Su, C. I., Prijovich, Z. M., Chung, W. C., Wu, P. Y., Chen, K. C., Lee, I. C., Juan, T. Y., & Roffler, S. R. (2013). The B7-1 Cytoplasmic Tail Enhances Intracellular Transport and Mammalian Cell Surface Display of Chimeric Proteins in the Absence of a Linear ER Export Motif. *PLoS ONE*, *8*(9), 75084. https://doi.org/10.1371/JOURNAL.PONE.0075084

Lohr, V., Rath, A., Genzel, Y., Jordan, I., Sandig, V., & Reichl, U. (2009). New avian suspension cell lines provide production of influenza virus and MVA in serum-free media: studies on growth, metabolism and virus propagation. *Vaccine*, *27*(36), 4975–4982. https://doi.org/10.1016/J.VACCINE.2009.05.083

Lorenzen, E., Contreras, V., Olsen, A. W., Andersen, P., Desjardins, D., Rosenkrands, I., Juel, H. B., Delache, B., Langlois, S., Delaugerre, C., Joubert, C., Dereuddre-Bosquet, N., Bébéar, C., De Barbeyrac, B., Touati, A., McKay, P. F., Shattock, R. J., Le Grand, R., Follmann, F., & Dietrich, J. (2022). Multi-component prime-boost Chlamydia trachomatis vaccination regimes induce antibody and T cell responses and accelerate clearance of infection in a non-human primate model. *Frontiers in Immunology*, *13*. https://doi.org/10.3389/FIMMU.2022.1057375

Maeto, C., Rodríguez, A. M., Holgado, M. P., Falivene, J., & Gherardi, M. M. (2014). Novel Mucosal DNA-MVA HIV Vaccination in Which DNA-IL-12 Plus Cholera Toxin B Subunit (CTB) Cooperates to Enhance Cellular Systemic and Mucosal Genital Tract Immunity. *PLoS ONE*, *9*(9). https://doi.org/10.1371/JOURNAL.PONE.0107524

Magee, D. M., Williams, D. M., Smith, J. G., Bleicker, C. A., Grubbs, B. G., Schachter, J., & Rank, R. G. (1995). Role of CD8 T cells in primary Chlamydia infection. *Infection and Immunity*, *63*(2), 516–521. https://doi.org/10.1128/IAI.63.2.516-521.1995

Mahnel, H., & Mayr, A. (1994). Erfahrungen bei der Schutzimpfung gegen Orthopocken von Mensch und Tier mit dem Impfstamm MVA [Experiences with immunization against orthopox viruses of humans and animals using vaccine strain MVA]. *Berliner Und Munchener Tierarztliche Wochenschrift*, *107*(8), 253–256.

Marín, M. Q., Pérez, P., Gómez, C. E., Sorzano, C. Ó. S., Esteban, M., & García-Arriaza, J. (2018). Removal of the C6 Vaccinia Virus Interferon-β Inhibitor in the Hepatitis C Vaccine Candidate MVA-HCV Elicited in Mice High Immunogenicity in Spite of Reduced Host Gene Expression. *Viruses*, *10*(8). https://doi.org/10.3390/V10080414

Mbow, M. L., De Gregorio, E., Valiante, N. M., & Rappuoli, R. (2010). New adjuvants for human vaccines. *Current Opinion in Immunology*, *22*(3), 411–416. https://doi.org/10.1016/J.COI.2010.04.004

McConkey, S. J., Reece, W. H. H., Moorthy, V. S., Webster, D., Dunachie, S., Butcher, G., Vuola, J. M., Blanchard, T. J., Gothard, P., Watkins, K., Hannan, C. M., Everaere, S., Brown, K., Kester, K. E., Cummings, J., Williams, J., Heppner, D. G., Pathan, A., Flanagan, K., … Hill, A. V. S. (2003). Enhanced T-cell immunogenicity of plasmid DNA vaccines boosted by recombinant modified vaccinia virus Ankara in humans. *Nature Medicine*, *9*(6), 729–735. https://doi.org/10.1038/NM881

Meisinger-Henschel, C., Späth, M., Lukassen, S., Wolferstätter, M., Kachelriess, H., Baur, K., Dirmeier, U., Wagner, M., Chaplin, P., Suter, M., & Hausmann, J. (2010). Introduction of the Six Major Genomic Deletions of Modified Vaccinia Virus Ankara (MVA) into the Parental Vaccinia Virus Is Not Sufficient To Reproduce an MVA-Like Phenotype in Cell Culture and in Mice. *Journal of Virology*, *84*(19), 9907–9919. https://doi.org/10.1128/JVI.00756-10/ASSET/7138A431-1A08-4407-9EB9-B503119008F6/ASSETS/GRAPHIC/ZJV99909374400T1.JPEG

Meyer, H., Sutter, G., & Mayr, A. (1991). Mapping of deletions in the genome of the highly attenuated vaccinia virus MVA and their influence on virulence. *Journal of General*

Virology, *72*(5), 1031–1038. https://doi.org/10.1099/0022-1317-72-5-1031/CITE/REFWORKS

Mooij, P., García-Arriaza, J., Pérez, P., Lázaro-Frías, A., Verstrepen, B. E., Böszörményi, K. P., Mortier, D., Fagrouch, Z., Kiemenyi-Kayere, G., Niphuis, H., Acar, R. F., Meijer, L., Stammes, M. A., Kondova, I., Verschoor, E. J., GeurtsvanKessel, C. H., de Bruin, E., Sikkema, R. S., Luczkowiak, J., … Esteban, M. (2022). Poxvirus MVA Expressing SARS-CoV-2 S Protein Induces Robust Immunity and Protects Rhesus Macaques From SARS-CoV-2. *Frontiers in Immunology*, *13*. https://doi.org/10.3389/FIMMU.2022.845887

Morrison, S. G., & Morrison, R. P. (2005). A Predominant Role for Antibody in Acquired Immunity to Chlamydial Genital Tract Reinfection. *Journal of Immunology (Baltimore, Md. : 1950)*, *175*(11), 7536. https://doi.org/10.4049/JIMMUNOL.175.11.7536

Morrison, S. G., Su, H., Caldwell, H. D., & Morrison, R. P. (2000). Immunity to Murine Chlamydia trachomatis Genital Tract Reinfection Involves B Cells and CD4+ T Cells but Not CD8+ T Cells. *Infection and Immunity*, *68*(12), 6979. https://doi.org/10.1128/IAI.68.12.6979-6987.2000

Moss, B., Carroll, M. W., Wyatt, L. S., Bennink, J. R., Hirsch, V. M., Goldstein, S., Elkins, W. R., Fuerst, T. R., Lifson, J. D., Piatak, M., Restifo, N. P., Overwijk, W., Chamberlain, R., Rosenberg, S. A., & Sutter, G. (1996). Host range restricted, non-replicating vaccinia virus vectors as vaccine candidates. *Advances in Experimental Medicine and Biology*, *397*, 7. https://doi.org/10.1007/978-1-4899-1382-1_2

Murphy, K., Weaver, C., & Janeway, C. (2017). *Janeway's Immunobiology* (9th ed.). Garland Science.

Murray, S. M., & McKay, P. F. (2021). Chlamydia trachomatis: Cell biology, immunology and vaccination. *Vaccine*, *39*(22), 2965–2975. https://doi.org/10.1016/J.VACCINE.2021.03.043

Nangpal, P., Bahal, R. K., & Tyagi, A. K. (2017). Boosting with recombinant MVA expressing M. tuberculosis α-crystallin antigen augments the protection imparted by BCG against tuberculosis in guinea pigs. *Scientific Reports*, *7*(1). https://doi.org/10.1038/S41598-017-17587-5

Nguyen, N. D. N. T., Guleed, S., Olsen, A. W., Follmann, F., Christensen, J. P., & Dietrich, J. (2021). Th1/Th17 T cell Tissue-Resident Immunity Increases Protection, But Is Not Required in a Vaccine Strategy Against Genital Infection With Chlamydia trachomatis. *Frontiers in Immunology*, *12*. https://doi.org/10.3389/FIMMU.2021.790463/FULL

Nogueira, C. V., Zhang, X., Giovannone, N., Sennott, E. L., & Starnbach, M. N. (2015). Protective immunity against Chlamydia trachomatis can engage both CD4+ and CD8+ T cells and bridge the respiratory and genital mucosae. *Journal of Immunology (Baltimore, Md. : 1950)*, *194*(5), 2319. https://doi.org/10.4049/JIMMUNOL.1402675

O'Hagan, D. T., & De Gregorio, E. (2009). The path to a successful vaccine adjuvant – 'The long and winding road.' *Drug Discovery Today*, *14*(11–12), 541–551. https://doi.org/10.1016/J.DRUDIS.2009.02.009

Okeke, M. I., Nilssen, Ø., & Traavik, T. (2006). *Modified vaccinia virus Ankara multiplies in rat IEC-6 cells and limited production of mature virions occurs in other mammalian cell lines*. https://doi.org/10.1099/vir.0.81479-0

Olivares-Zavaleta, N., Whitmire, W. M., Kari, L., Sturdevant, G. L., & Caldwell, H. D. (2014). CD8+ T Cells Define an Unexpected Role in Live-Attenuated Vaccine Protective Immunity against Chlamydia trachomatis infection. *Journal of Immunology (Baltimore, Md. : 1950)*, *192*(10), 4648. https://doi.org/10.4049/JIMMUNOL.1400120

Olsen, A. W., Follmann, F., Erneholm, K., Rosenkrands, I., & Andersen, P. (2015). Protection Against Chlamydia trachomatis Infection and Upper Genital Tract Pathological Changes by Vaccine-Promoted Neutralizing Antibodies Directed to the VD4 of the Major Outer Membrane Protein. *The Journal of Infectious Diseases*, *212*(6), 978–989. https://doi.org/10.1093/INFDIS/JIV137

Olsen, A. W., Lorenzen, E. K., Rosenkrands, I., Follmann, F., & Andersen, P. (2017). Protective effect of vaccine promoted neutralizing antibodies against the intracellular pathogen Chlamydia trachomatis. *Frontiers in Immunology*, *8*(DEC). https://doi.org/10.3389/FIMMU.2017.01652/FULL

Olsen, A. W., Rosenkrands, I., Holland, M. J., Andersen, P., & Follmann, F. (2021). A Chlamydia trachomatis VD1-MOMP vaccine elicits cross-neutralizing and protective antibodies against C/C-related complex serovars. *NPJ Vaccines*, *6*(1). https://doi.org/10.1038/S41541-021-00312-9

Oosterhuis, K., Van Den Berg, J. H., Schumacher, T. N., & Haanen, J. B. A. G. (2012). DNA vaccines and intradermal vaccination by DNA tattooing. *Current Topics in Microbiology and Immunology*, *351*(1), 221–250. https://doi.org/10.1007/82_2010_117

Paes, W., Brown, N., Brzozowski, A. M., Coler, R., Reed, S., Carter, D., Bland, M., Kaye, P. M., & Lacey, C. J. N. (2016). Recombinant polymorphic membrane protein D in combination with a novel, second-generation lipid adjuvant protects against intra-vaginal Chlamydia trachomatis infection in mice. *Vaccine*, *34*(35), 4123. https://doi.org/10.1016/J.VACCINE.2016.06.081

Pal, S., Cruz-Fisher, M. I., Cheng, C., Carmichael, J. R., Tifrea, D. F., Tatarenkova, O., & de la Maza, L. M. (2020). Vaccination with the recombinant major outer membrane protein elicits long-term protection in mice against vaginal shedding and infertility following a Chlamydia muridarum genital challenge. *NPJ Vaccines*, *5*(1). https://doi.org/10.1038/S41541-020-00239-7

Pal, S., Peterson, E. M., & De La Maza, L. M. (2003). Induction of protective immunity against a Chlamydia trachomatis genital infection in three genetically distinct strains of mice. *Immunology*, *110*(3), 368–375. https://doi.org/10.1046/J.1365-2567.2003.01748.X

Pal, S., Peterson, E. M., & De La Maza, L. M. (2005). Vaccination with the Chlamydia trachomatis Major Outer Membrane Protein Can Elicit an Immune Response as Protective as That Resulting from Inoculation with Live Bacteria. *INFECTION AND IMMUNITY*, *73*(12), 8153–8160. https://doi.org/10.1128/IAI.73.12.8153-8160.2005

Pal, S., Tatarenkova, O. V., & de la Maza, L. M. (2015). A vaccine formulated with the major outer membrane protein can protect C3H/HeN, a highly susceptible strain of mice, from a Chlamydia muridarum genital challenge. *Immunology*, *146*(3), 432–443. https://doi.org/10.1111/IMM.12520

Pan, W. Y., Lo, C. H., Chen, C. C., Wu, P. Y., Roffler, S. R., Shyue, S. K., & Tao, M. H. (2012). Cancer Immunotherapy Using a Membrane-bound Interleukin-12 With B7-1 Transmembrane and

Cytoplasmic Domains. *Molecular Therapy*, *20*(5), 927. https://doi.org/10.1038/MT.2012.10

Panzetta, M. E., Valdivia, R. H., & Saka, H. A. (2018). Chlamydia Persistence: A Survival Strategy to Evade Antimicrobial Effects in-vitro and in-vivo. *Frontiers in Microbiology*, *9*(DEC), 3101. https://doi.org/10.3389/FMICB.2018.03101

Pérez, P., Marín, M. Q., Lázaro-Frías, A., Óscar, C., Sorzano, S., Pilato, M. Di, Gómez, C. E., Esteban, M., & García-Arriaza, J. (2019). *An MVA Vector Expressing HIV-1 Envelope under the Control of a Potent Vaccinia Virus Promoter as a Promising Strategy in HIV/AIDS Vaccine Design*. https://doi.org/10.3390/vaccines7040208

Pérez, P., Marín, M. Q., Lázaro-Frías, A., Sorzano, C. Ó. S., Gómez, C. E., Esteban, M., & García-Arriaza, J. (2020). Deletion of Vaccinia Virus A40R Gene Improves the Immunogenicity of the HIV-1 Vaccine Candidate MVA-B. *Vaccines*, *8*(1). https://doi.org/10.3390/VACCINES8010070

Pérez, P., Martín-Acebes, M. A., Poderoso, T., Lázaro-Frías, A., Saiz, J. C., Sorzano, C. Ó. S., Esteban, M., & García-Arriaza, J. (2021). The combined vaccination protocol of DNA/MVA expressing Zika virus structural proteins as efficient inducer of T and B cell immune responses. *Emerging Microbes & Infections*, *10*(1), 1441. https://doi.org/10.1080/22221751.2021.1951624

Peuchant, O., Lhomme, E., Martinet, P., Grob, A., Baïta, D., Bernier, C., Gibaud, S. A., Le Hen, I., Le Naour, E., Trignol-Viguier, N., Lanotte, P., Lefebvre, P., Vachée, A., Girard, T., Loubinoux, J., Bébéar, C., Ghezzoul, B., Roussillon, C., Kret, M., … Galet, J. (2022). Doxycycline versus azithromycin for the treatment of anorectal Chlamydia trachomatis infection in women concurrent with vaginal infection (CHLAZIDOXY study): a multicentre, open-label, randomised, controlled, superiority trial. *The Lancet. Infectious Diseases*, *22*(8), 1221–1230. https://doi.org/10.1016/S1473-3099(22)00148-7

Phillips, S., Quigley, B. L., & Timms, P. (2019). *Seventy Years of Chlamydia Vaccine Research – Limitations of the Past and Directions for the Future*. https://doi.org/10.3389/fmicb.2019.00070

Postlethwaite, R., & Maitland, H. B. (1960). The eclipse phase of vaccinia virus growing in chick embryo cell monolayers and some technical procedures which affect its demonstration. *The Journal of Hygiene*, *58*(2), 133. https://doi.org/10.1017/S0022172400038213

Raman, S. C., Mejías-Pérez, E., Gomez, C. E., García-Arriaza, J., Perdiguero, B., Vijayan, A., Pérez-Ruiz, M., Cuervo, A., Santiago, C., Sorzano, C. O. S., Sánchez-Corzo, C., Moog, C., Burger, J. A., Schorcht, A., Sanders, R. W., Carrascosa, J. L., & Esteban, M. (2019). The Envelope-Based Fusion Antigen GP120C14K Forming Hexamer-Like Structures Triggers T Cell and Neutralizing Antibody Responses Against HIV-1. *Frontiers in Immunology*, *10*. https://doi.org/10.3389/FIMMU.2019.02793/FULL

Rehm, K. E., & Roper, R. L. (2011). Deletion of the A35 Gene from Modified Vaccinia Virus Ankara Increases Immunogenicity and Isotype Switching. *Vaccine*, *29*(17), 3276. https://doi.org/10.1016/J.VACCINE.2011.02.023

Richert, L., Lelièvre, J.-D., Lacabaratz, C., Hardel, L., Hocini, H., Wiedemann, A., Lucht, F., Poizot-Martin, I., Bauduin, C., Diallo, A., Rieux, V., Rouch, E., Surenaud, M., Lefebvre, C., Foucat, E., Tisserand, P., Guillaumat, L., Durand, M., Hejblum, B., … Group, on behalf of the A. V. S. (2022). T Cell Immunogenicity, Gene Expression Profile, and Safety of Four Heterologous

Prime-Boost Combinations of HIV Vaccine Candidates in Healthy Volunteers: Results of the Randomized Multi-Arm Phase I/II ANRS VRI01 Trial. *The Journal of Immunology*, *208*(12), 2663–2674. https://doi.org/10.4049/JIMMUNOL.2101076

Rist, M. J., Theodossis, A., Croft, N. P., Neller, M. A., Welland, A., Chen, Z., Sullivan, L. C., Burrows, J. M., Miles, J. J., Brennan, R. M., Gras, S., Khanna, R., Brooks, A. G., McCluskey, J., Purcell, A. W., Rossjohn, J., & Burrows, S. R. (2013). HLA peptide length preferences control CD8+ T cell responses. *Journal of Immunology (Baltimore, Md. : 1950)*, *191*(2), 561–571. https://doi.org/10.4049/JIMMUNOL.1300292

Rollier, C. S., Verschoor, E. J., Verstrepen, B. E., Drexhage, J. A. R., Paranhos-Baccala, G., Liljeström, P., Sutter, G., Arribillaga, L., Lasarte, J. J., Bartosch, B., Cosset, F. L., Inchauspe, G., & Heeney, J. L. (2016). T- and B-cell responses to multivalent prime-boost DNA and viral vectored vaccine combinations against hepatitis C virus in non-human primates. *Gene Therapy*, *23*(10), 753. https://doi.org/10.1038/GT.2016.55

Rose, F., Karlsen, K., Jensen, P. R., Jakobsen, R. U., Wood, G. K., Rand, K. D., Godiksen, H., Andersen, P., Follmann, F., & Foged, C. (2018). Unusual Self-Assembly of the Recombinant Chlamydia trachomatis Major Outer Membrane Protein-Based Fusion Antigen CTH522 Into Protein Nanoparticles. *Journal of Pharmaceutical Sciences*, *107*(6), 1690–1700. https://doi.org/10.1016/J.XPHS.2018.02.005

Salvagno, C., & Cubillos-Ruiz, J. R. (2019). The impact of endoplasmic reticulum stress responses in dendritic cell immunobiology. *International Review of Cell and Molecular Biology*, *349*, 153–176. https://doi.org/10.1016/BS.IRCMB.2019.08.004

Sánchez-Sampedro, L., Perdiguero, B., Mejí As-Pé Rez, E., Garcí A-Arriaza, J., Pilato, M. Di, & Esteban, M. (2015). The Evolution of Poxvirus Vaccines. *Viruses*, *7*, 1726–1803. https://doi.org/10.3390/v7041726

Sasso, E., D'Alise, A. M., Zambrano, N., Scarselli, E., Folgori, A., & Nicosia, A. (2020). New viral vectors for infectious diseases and cancer. *Seminars in Immunology*, *50*, 101430. https://doi.org/10.1016/J.SMIM.2020.101430

Schröter, W., Stickl, H., Idel, H., & Schlipköter, H. W. (1980). MVA-Stufenimpfung bei Pockenschutz-Erstimpfungen nach dem dritten Lebensjahr [MVA-vaccine in primovaccination against smallpox after the age of three (author's transl)]. *Zentralblatt Fur Bakteriologie, Mikrobiologie Und Hygiene*, *171*(4–5), 309–319.

Shen, X., Basu, R., Sawant, S., Beaumont, D., Kwa, S. F., LaBranche, C., Seaton, K. E., Yates, N. L., Montefiori, D. C., Ferrari, G., Wyatt, L. S., Moss, B., Alam, S. M., Haynes, B. F., Tomaras, G. D., & Robinson, H. L. (2017). HIV-1 gp120 and Modified Vaccinia Virus Ankara (MVA) gp140 Boost Immunogens Increase Immunogenicity of a DNA/MVA HIV-1 Vaccine. *Journal of Virology*, *91*(24). https://doi.org/10.1128/JVI.01077-17

Sixt, B. S., & Valdivia, R. H. (2016). Molecular Genetic Analysis of Chlamydia Species. *Https://Doi.Org/10.1146/Annurev-Micro-102215-095539*, *70*, 179–198. https://doi.org/10.1146/ANNUREV-MICRO-102215-095539

Spehner, D., & Drillien, R. (2008). Extracellular vesicles containing virus-encoded membrane proteins are a byproduct of infection with modified vaccinia virus Ankara. *Virus Research*, *137*(1), 129–136. https://doi.org/10.1016/J.VIRUSRES.2008.07.003

Spencer, A. J., Cottingham, M. G., Jenks, J. A., Longley, R. J., Capone, S., Colloca, S., Folgori, A., Cortese, R., Nicosia, A., Bregu, M., & Hill, A. V. S. (2014). Enhanced vaccine-induced CD8+

T cell responses to malaria antigen ME-TRAP by fusion to MHC class ii invariant chain. *PloS One*, *9*(6). https://doi.org/10.1371/JOURNAL.PONE.0100538

Stagg, A. J., Hornsby, E., & Knight, S. C. (2020). Antigen-Presenting Cells. *ELS*, *1*, 1–12. https://doi.org/10.1002/9780470015902.A0029138

Staib, C., Kisling, S., Erfle, V., & Sutter, G. (2005). Inactivation of the viral interleukin 1β receptor improves CD8+ T-cell memory responses elicited upon immunization with modified vaccinia virus Ankara. *Journal of General Virology*, *86*(7), 1997–2006. https://doi.org/10.1099/VIR.0.80646-0/CITE/REFWORKS

Stary, G., Olive, A., Radovic-Moreno, A. F., Gondek, D., Alvarez, D., Basto, P. A., Perro, M., Vrbanac, V. D., Tager, A. M., Shi, J., Yethon, J. A., Farokhzad, O. C., Langer, R., Starnbach, M. N., & Von Andrian, U. H. (2015). A mucosal vaccine against Chlamydia trachomatis generates two waves of protective memory T cells. *Science (New York, N.Y.)*, *348*(6241), aaa8205. https://doi.org/10.1126/SCIENCE.AAA8205

Stickl, H. A. (1974). Smallpox vaccination and its consequences: First experiences with the highly attenuated smallpox vaccine "MVA." *Preventive Medicine*, *3*(1), 97–101. https://doi.org/10.1016/0091-7435(74)90066-8

Stickl, H., Hochstein-Mintzel, V., Mayr, A., Huber, H. C., Schäfer, H., & Holzner, A. (1974). MVA-Stufenimpfung gegen Pocken: Klinische Erprobung des attenuierten Pocken-Lebendimpfstoffes, Stamm MVA. *Deutsche Medizinische Wochenschrift*, *99*(47), 2386–2392. https://doi.org/10.1055/s-0028-1108143

Sturd, N., & Rucks, E. A. (2023). Chlamydia trachomatis. *Trends in Microbiology*, *31*(5), 535–536. https://doi.org/10.1016/j.tim.2022.11.002

Su, H., & Caldwell, H. D. (1992). Immunogenicity of a chimeric peptide corresponding to T helper and B cell epitopes of the Chlamydia trachomatis major outer membrane protein. *The Journal of Experimental Medicine*, *175*(1), 227. https://doi.org/10.1084/JEM.175.1.227

Sutter, G., & Moss, B. (1992). Nonreplicating vaccinia vector efficiently expresses recombinant genes. *Proceedings of the National Academy of Sciences of the United States of America*, *89*(22), 10847. https://doi.org/10.1073/PNAS.89.22.10847

Taylor-Robinson, D. (2017). The discovery of Chlamydia trachomatis. *Sexually Transmitted Infections*, *93*(1), 10–10. https://doi.org/10.1136/SEXTRANS-2016-053011

Tewalt, E. F., Grant, J. M., Granger, E. L., Palmer, D. C., Heuss, N. D., Gregerson, D. S., Restifo, N. P., & Norbury, C. C. (2009). Viral Sequestration of Antigen Subverts Cross Presentation to CD8+ T Cells. *PLoS Pathogens*, *5*(5). https://doi.org/10.1371/JOURNAL.PPAT.1000457

Thiele, F., Tao, S., Zhang, Y., Muschaweckh, A., Zollmann, T., Protzer, U., Abele, R., & Drexler, I. (2015). Modified Vaccinia Virus Ankara-Infected Dendritic Cells Present CD4+ T-Cell Epitopes by Endogenous Major Histocompatibility Complex Class II Presentation Pathways. *Journal of Virology*, *89*(5), 2698. https://doi.org/10.1128/JVI.03244-14

Tischer, B. K., Von Einem, J., Kaufer, B., & Osterrieder, N. (2006). Two-step Red-mediated recombination for versatile high-efficiency markerless DNA manipulation in Escherichia coli. *BioTechniques*, *40*(2), 191–197. https://doi.org/10.2144/000112096/ASSET/IMAGES/LARGE/FIGURE3.JPEG

Tu, J., Hou, B., Wang, B., Lin, X., Gong, W., Dong, H., Zhu, S., Chen, S., Xue, X., Zhao, K. N., & Zhang, L. (2014). A multi-epitope vaccine based on Chlamydia trachomatis major outer membrane protein induces specific immunity in mice. *Acta Biochimica et Biophysica Sinica*, *46*(5), 401–408. https://doi.org/10.1093/ABBS/GMU016

Ullah, I., Bibi, S., Ul Haq, I., Safia, Ullah, K., Ge, L., Shi, X., Bin, M., Niu, H., Tian, J., & Zhu, B. (2020). The Systematic Review and Meta-Analysis on the Immunogenicity and Safety of the Tuberculosis Subunit Vaccines M72/AS01E and MVA85A. *Frontiers in Immunology*, *11*. https://doi.org/10.3389/FIMMU.2020.01806

Vázquez, M.-I., & Esteban, M. (1999). Identification of functional domains in the 14-kilodalton envelope protein (A27L) of vaccinia virus. *Journal of Virology*, *73*(11), 9098–9109. https://doi.org/10.1128/JVI.73.11.9098-9109.1999

Velge-Roussel, F., Moretto, M., Buzoni-Gatel, D., Dimier-Poisson, I., Ferrer, M., Hoebeke, J., & Bout, D. (1997). Differences in immunological response to a T. gondii protein (SAG1) derived peptide between two strains of mice: Effect on protection in T. gondii infection. *Molecular Immunology*, *34*(15), 1045–1053. https://doi.org/10.1016/S0161-5890(97)00133-8

Ventura, J. D., Nkolola, J. P., Chandrashekar, A., Borducchi, E. N., Liu, J., Mercado, N. B., Hope, D. L., Giffin, V. M., McMahan, K., Geleziunas, R., Murry, J. P., Yang, Y., Lewis, M. G., Pau, M. G., Wegmann, F., Schuitemaker, H., Fray, E. J., Kumar, M. R., Siliciano, J. D., … Barouch, D. H. (2022). Therapeutic efficacy of an Ad26/MVA vaccine with SIV gp140 protein and vesatolimod in ART-suppressed rhesus macaques. *NPJ Vaccines*, *7*(1). https://doi.org/10.1038/S41541-022-00477-X

Vijayan, A., García-Arriaza, J., Raman, S. C., Conesa, J. J., Chichón, F. J., Santiago, C., Sorzano, C. Ó. S., Carrascosa, J. L., & Esteban, M. (2015). A Chimeric HIV-1 gp120 Fused with Vaccinia Virus 14K (A27) Protein as an HIV Immunogen. *PLoS ONE*, *10*(7). https://doi.org/10.1371/JOURNAL.PONE.0133595

Walker, A. S., Lourenço, J., Hill, A. V. S., & Gupta, S. (2015). Modeling Combinations of Pre-erythrocytic Plasmodium falciparum Malaria Vaccines. *The American Journal of Tropical Medicine and Hygiene*, *93*(6), 1254–1259. https://doi.org/10.4269/AJTMH.14-0767

Wan, W., Li, D., Li, D., & Jiao, J. (2023). Advances in genetic manipulation of Chlamydia trachomatis. *Frontiers in Immunology*, *14*, 1209879. https://doi.org/10.3389/FIMMU.2023.1209879/BIBTEX

Wang, S. A., Rapp, J. R., Stamm, W. E., Peeling, R. W., Martin, D. H., & Holmes, K. K. (2005). Evaluation of antimicrobial resistance and treatment failures for Chlamydia trachomatis: a meeting repor. *J Infect Dis*, *191*(6), 917–923.

Wang, Y. (2023). Rendezvous with Vaccinia Virus in the Post-smallpox Era: R&D Advances. *Viruses*, *15*(8). https://doi.org/10.3390/V15081742

Wilken, L., Stelz, S., Agac, A., Sutter, G., Prajeeth, C. K., & Rimmelzwaan, G. F. (2023). Recombinant Modified Vaccinia Virus Ankara Expressing a Glycosylation Mutant of Dengue Virus NS1 Induces Specific Antibody and T-Cell Responses in Mice. *Vaccines*, *11*(4). https://doi.org/10.3390/VACCINES11040714

Woodhall, S. C., Gorwitz, R. J., Migchelsen, S. J., Gottlieb, S. L., Horner, P. J., Geisler, W. M., Winstanley, C., Hufnagel, K., Waterboer, T., Martin, D. L., Huston, W. M., Gaydos, C. A., Deal, C., Unemo, M., Dunbar, J. K., & Bernstein, K. (2018). Advancing the public health

applications of Chlamydia trachomatis serology. *The Lancet. Infectious Diseases*, *18*(12), e399. https://doi.org/10.1016/S1473-3099(18)30159-2

World Health Organization. (2022, October 5). *Trachoma*. Trachoma. https://www.who.int/en/news-room/fact-sheets/detail/trachoma

World Health Organization. (2023, July 17). *Chlamydia*. https://www.who.int/news-room/fact-sheets/detail/chlamydia

Wyatt, L. S., Carroll, M. W., Czerny, C. P., Merchlinsky, M., Sisler, J. R., & Moss, B. (1998). Marker Rescue of the Host Range Restriction Defects of Modified Vaccinia Virus Ankara. *Virology*, *251*(2), 334–342. https://doi.org/10.1006/VIRO.1998.9397

Yu, H., Karunakaran, K. P., Jiang, X., & Brunham, R. C. (2014). Evaluation of a multisubunit recombinant polymorphic membrane protein and major outer membrane protein T cell vaccine against Chlamydia muridarum genital infection in three strains of mice. *Vaccine*, *32*(36), 4672. https://doi.org/10.1016/J.VACCINE.2014.06.002

Yu, H., Lin, H., Xie, L., Tang, L., Chen, J., Zhou, Z., Ni, J., & Zhong, G. (2019). Chlamydia muridarum Induces Pathology in the Female Upper Genital Tract via Distinct Mechanisms. *Infection and Immunity*, *87*(8). https://doi.org/10.1128/IAI.00145-19

Zhang, G. L., Khan, A. M., Srinivasan, K. N., Heiny, A., Lee, K., Kwoh, C. K., August, J. T., & Brusic, V. (2008). Hotspot Hunter: a computational system for large-scale screening and selection of candidate immunological hotspots in pathogen proteomes. *BMC Bioinformatics*, *13*(9).

Zhang, X., Cassis-Ghavami, F., Eller, M., Currier, J., Slike, B. M., Chen, X., Tartaglia, J., Marovich, M., & Spearman, P. (2007). Direct Comparison of Antigen Production and Induction of Apoptosis by Canarypox Virus- and Modified Vaccinia Virus Ankara-Human Immunodeficiency Virus Vaccine Vectors. *Journal of Virology*, *81*(13), 7022. https://doi.org/10.1128/JVI.02654-06

SUPPLEMENTARY MATERIAL

Name	Sequence
1	MKKLLKSVLVFAALS
2	LKSVLVFAALSSASS
3	LVFAALSSASSLQAL
4	ALSSASSLQALPVGN
5	ASSLQALPVGNPAEP
6	QALPVGNPAEPSLMI
7	VGNPAEPSLMIDGIL
8	AEPSLMIDGILWEGF
9	LMIDGILWEGFGGDP
10	GILWEGFGGDPCDPC
11	EGFGGDPCDPCATWC
12	GDPCDPCATWCDAIS
13	DPCATWCDAISMRVG
14	TWCDAISMRVGYYGD
15	MGDAISMRVGYYGDF
16	DAISMRVGYYGDFVF
17	MRVGYYGDFVFDRVL
18	YYGDFVFDRVLKTDV
19	FVFDRVLKTDVNKEF
20	RVLKTDVNKEFQMGA
21	TDVNKEFQMGAKPTT
22	KEFQMGAKPTTDTGN
23	MGAKPTTDTGNSAAP
24	PTTDTGNSAAPSTLT
25	TGNSAAPSTLTAREN
26	AAPSTLTARENPAYG
27	TLTARENPAYGRHMQ
28	RENPAYGRHMQDAEM
29	AYGRHMQDAEMFTNA
30	HMQDAEMFTNAACMA

31	AEMFTNAACMALNIW
32	TNAACMALNIWDRFD
33	CMALNIWDRFDVFCT
34	NIWDRFDVFCTLGAT
35	RFDVFCTLGATSGYL
36	FCTLGATSGYLKGNS
37	GATSGYLKGNSASFN
38	GYLKGNSASFNLVGL
39	GNSASFNLVGLFGDN
40	SFNLVGLFGDNENQK
41	VGLFGDNENQKTVKA
42	GDNENQKTVKAESVP
43	NQKTVKAESVPNMSF
44	VKAESVPNMSFDQSV
45	SVPNMSFDQSVVELY
46	MSFDQSVVELYTDTT
47	QSVVELYTDTTFAWS
48	ELYTDTTFAWSVGAR
49	DTTFAWSVGARAALW
50	AWSVGARAALWECGC
51	GARAALWECGCATIL
52	ALWECGCATILGASF
53	CGCATILGASFQYAQ
54	TILGASFQYAQSKPK
55	ASFQYAQSKPKVEEL
56	YAQSKPKVEELNVLC
57	KPKVEELNVLCNAAE
58	EELNVLCNAAEFTIN
59	VLCNAAEFTINKPKG
60	AAEFTINKPKGYVGK
61	TINKPKGYVGKEFPL
62	PKGYVGKEFPLDLTA
63	VGKEFPLDLTAGTDA
64	FPLDLTAGTDAATGT

65	LTAGTDAATGTKDAS
66	TDAATGTKDASIDYH
67	TGTKDASIDYHEWQA
68	DASIDYHEWQASLAL
69	DYHEWQASLALSYRL
70	WQASLALSYRLNMFT
71	LALSYRLNMFTPYIG
72	YRLNMFTPYIGVKWS
73	MFTPYIGVKWSRASF
74	YIGVKWSRASFDADT
75	KWSRASFDADTIRIA
76	ASFDADTIRIAQPKS
77	ADTIRIAQPKSATAI
78	RIAQPKSATAIFDTT
79	PKSATAIFDTTTLNP
80	TAIFDTTTLNPTIAG
81	DTTTLNPTIAGAGDV
82	LNPTIAGAGDVKTGA
83	IAGAGDVKTGAEGQL
84	GDVKTGAEGQLGDTM
85	TGAEGQLGDTMQIVS
86	GQLGDTMQIVSLQLN
87	DTMQIVSLQLNNMFT
87	DTMQIVSLQLNNMFT
88	IVSLQLNNMFTPYIG
89	QLNNMFTPYIGVKWS
90	MFTPYIGVKWSRASF
91	YIGVKWSRASFDADT
92	KWSRASFDADTIRIA
93	ASFDADTIRIAQPKS
94	ADTIRIAQPKSATAI
95	RIAQPKSATAIFDTT
96	PKSATAIFDTTTLNP
97	TAIFDTTTLNPTIAG

98	DTTTLNPTIAGAGDV
99	LNPTIAGAGDVKASA
100	IAGAGDVKASAEGQL
101	GDVKASAEGQLGDTM
102	ASAEGQLGDTMQIVS
103	GQLGDTMQIVSLQLN
105	IVSLQLNNMFTPYIG
106	QLNNMFTPYIGVKWS
107	MFTPYIGVKWSRASF
108	YIGVKWSRASFDSDT
109	KWSRASFDSDTIRIA
110	ASFDSDTIRIAQPRL
111	SDTIRIAQPRLVTPV
112	RIAQPRLVTPVVDIT
113	PRLVTPVVDITTLNP
114	TPVVDITTLNPTIAG
115	DITTLNPTIAGCGSV
116	LNPTIAGCGSVAGAN
117	IAGCGSVAGANTEGQ
118	GSVAGANTEGQISDT
119	GANTEGQISDTMQIV
120	EGQISDTMQIVSLQL
121	SDTMQIVSLQLNNMF
122	QIVSLQLNNMFTPYI
123	LQLNNMFTPYIGVKW
124	NMFTPYIGVKWSRAS
125	PYIGVKWSRASFDSN
126	VKWSRASFDSNTIRI
127	RASFDSNTIRIAQPK
128	DSNTIRIAQPKLAKP
129	IRIAQPKLAKPVVDI
130	QPKLAKPVVDITTLN
131	AKPVVDITTLNPTIA
132	VDITTLNPTIAGCGS

133	TLNPTIAGCGSVVAA
134	TIAGCGSVVAANSEG
135	CGSVVAANSEGQISD
136	VAANSEGQISDTMQI
137	SEGQISDTMQIVSLQ
138	GQISDTMQIVSLQLN

Supplementary Table 1. List of peptides used in *ex vivo* assays for IFN-γ $^{+}$ CD4+ T cell analysis. Peptides were designed by Giuseppe Andreacchio to be overlapping by 5 amino acids (aa) with the previous and the next ones and made of 15 aa each. Peptides were produced by peptides & elephants GmbH (Hennigsdorf, Germany) and dissolved in dimethyl sulfoxide (DMSO) at a stock concentration of 1 ug/uL unless otherwise specified.

Pool	Peptides
1	1, 16, 30, 44, 58, 72, 86, 100, 114, 128
2	2, 17, 31, 45, 59, 73, 87, 101, 115, 129
3	3, 18, 32, 46, 60, 74, 88, 102, 116, 130
4	4, 19, 33, 47, 61, 75, 89, 103, 117, 131
5	5, 20, 34, 48, 62, 76, 90, 87*, 118, 132
6	6, 21, 35, 49, 63, 77, 91, 88, 119, 133
7	7, 22, 36, 50, 64, 78, 92, 106, 120, 134
8	8, 23, 37, 51, 65, 79, 93, 107, 121, 135
9	9, 24, 38, 52, 66, 80, 94, 108, 122, 136
10	10, 25 39, 53, 67, 81, 95, 109, 123, 137
11	11, 26, 40, 54, 68, 82, 96, 110, 124, 138
12	12, 27, 41, 55, 69, 83, 97, 111, 125, 15
13	13, 28, 42, 56, 70, 84, 98, 112, 126
14	14, 29, 43, 57, 71, 85, 99, 113, 127

Supplementary Table 2. List of peptide pools used in *ex vivo* assays to determine CTH522-specific IFN-γ $^{+}$ CD4+ T cell populations. Each pool was formed by diluting 9-10 peptides as listed in equal concentration. Pools were stored at -80 ºC and underwent a maximum of three freeze-thaw cycles.
Peptides 87 and 104 shared the same sequence.

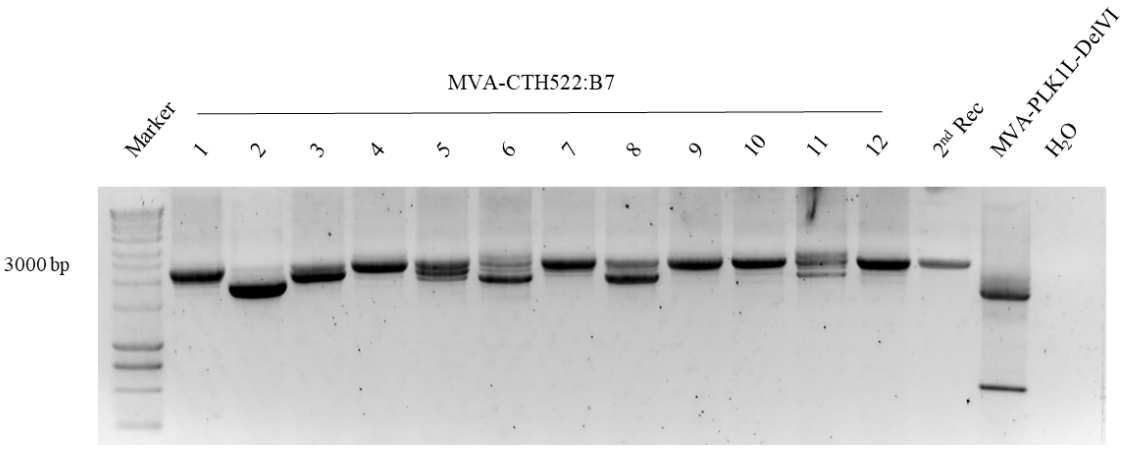

Supplementary Figure 1. Single MVA-CTH522:B7 clones generated after viral progeny rescue and by limiting dilution. Agarose gel containing PCR-amplified DNA fragments obtained by a screening PCR performed with purified DNA generated from single viral clones obtained after limiting dilution. Verification of the integrity of CTH522:B7 within the flanks of Deletion VI of MVA after three sub-passages in DF-1 cells. Positive control was DNA obtained after the second recombination, negative controls were RNAse-free H_2O as primer control and recombinant MVA-PK1L-DelVI. Primers annealed at the flanking regions of deletion VI where MVA-CTH522:B7 was inserted. Twelve clones were tested. The marker ladder of 1 kb is on the left.

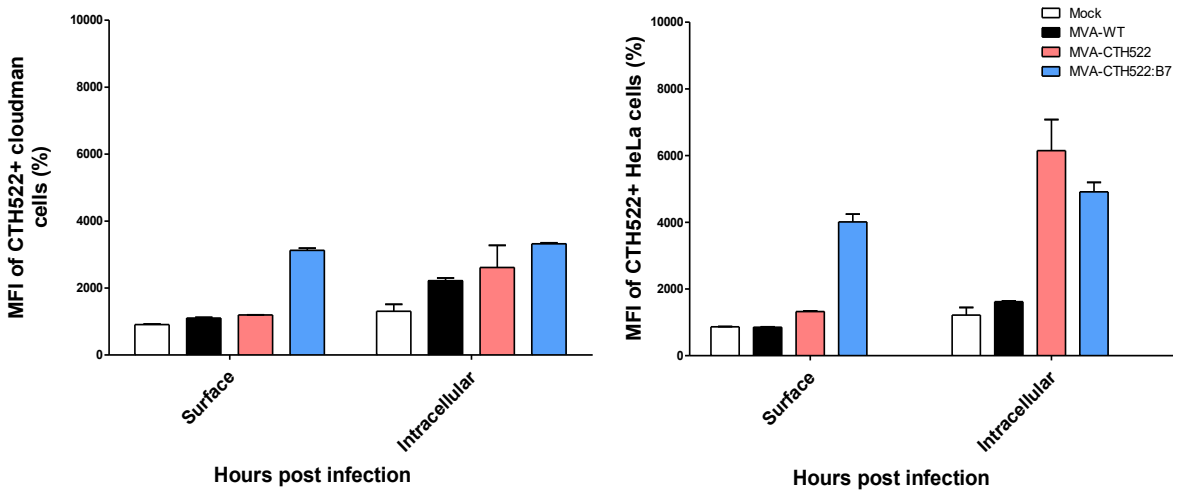

Supplemental Figure 2. MFI of CTH522:B7 poduced by MVA-CTH522:B7 exhibits an enhancement on the surface rather than intracellular accumulation in mammalian cells. FACS analysis of CTH522 expression. Cells were infected at MOI=5 overnight and harvested via scraping. Samples stained for living or dead cells with Fixable Visability Dye eFluor 660, for CTH522:B7 with C. *trachomatis* species-specific MOMP mononuclear primary antibody and fragment Goat Anti-Mouse IgG-PE secondary antibody. **(A)** Cloudman cells and **(B)** HeLa cells. Results represent 2 independent experiments shown with means ±SEM.

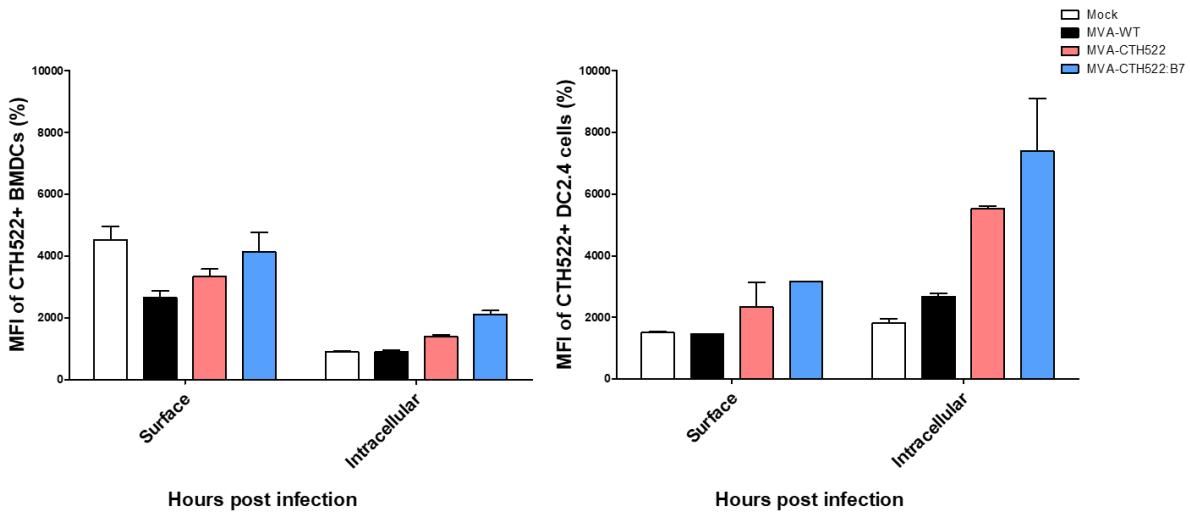

Supplemental Figure 3. MFI of CTH522:B7 poduced by MVA-CTH522:B7 exhibits an enhancement on the surface rather than intracellular accumulation in dendritic cells. FACS analysis of CTH522 expression. Cells were infected at MOI=5 overnight and harvested via scraping. Samples stained for living or dead cells with Fixable Visability Dye eFluor 660, for CTH522:B7 with C. *trachomatis* species-specific MOMP mononuclear primary antibody and fragment Goat Anti-Mouse IgG-PE secondary antibody. **(A)** BMDCs and **(B)** DC2.4 cells infected at MOI = 5 overnight. Results represent 2 **(B)** or 3 **(A)** independent experiments shown with means ±SEM.

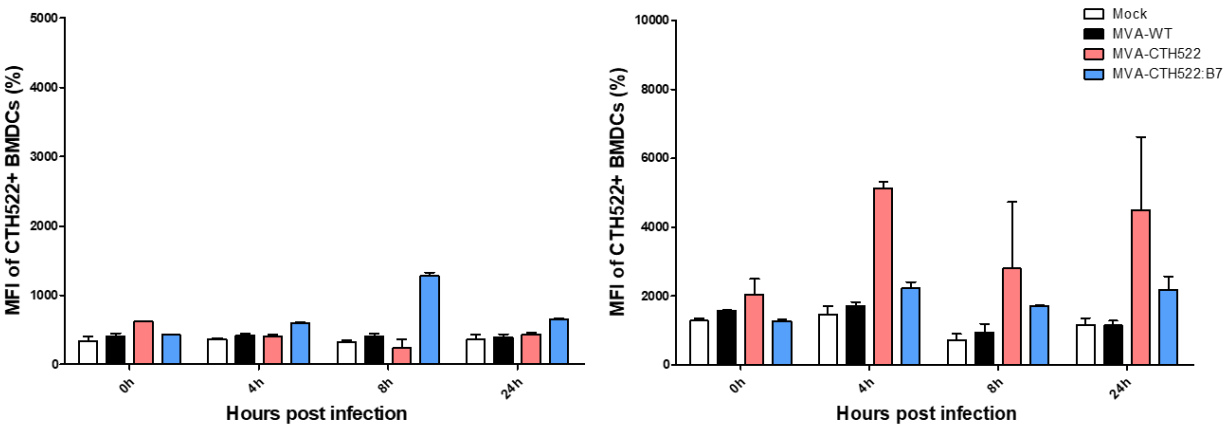

Supplemental Figure 4. MFI of CTH522:B7 distribution in BMDCs from 0hpi to 24hpi. FACS analysis of CTH522 and CTH522:B7 localisation in BMDCs **(A)** at the surface or (**B)** intracellularly. Cells were infected at MOI=5 for 0, 4, 8 and 24 hours and harvested via Ethylenediaminetetraacetic acid (EDTA) treatment. Samples were stained for living or dead cells with Fixable Visability Dye eFluor 660, for CTH522:B7 with C. *trachomatis* species-specific MOMP mononuclear primary antibody and fragment Goat Anti-Mouse IgG-PE secondary antibody. Results represent 3 independent experiments shown with means ±SEM.

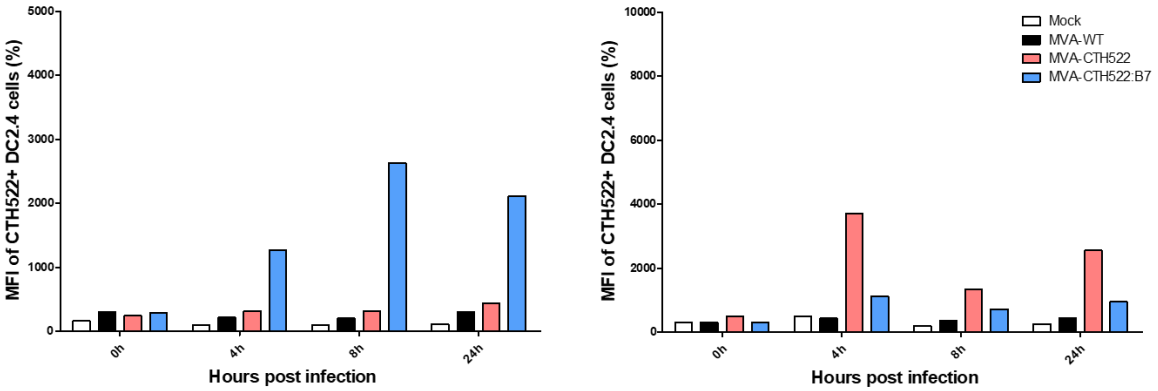

Figure 5. MFI of CTH522:B7 in DC2.4 infected with recombinant MVA from 0hpi to 24hpi . FACS analysis of CTH522 expression on DC2.4 cells analyzing the **(A)** surface and **(B)** intracellular expression. Samples were stained for living or dead cells with Fixable Visability Dye eFluor 660, for CTH522:B7 with C. *trachomatis* species-specific MOMP mononuclear primary antibody and fragment Goat Anti-Mouse IgG-PE secondary antibody. Results represent 1 independent experiment.

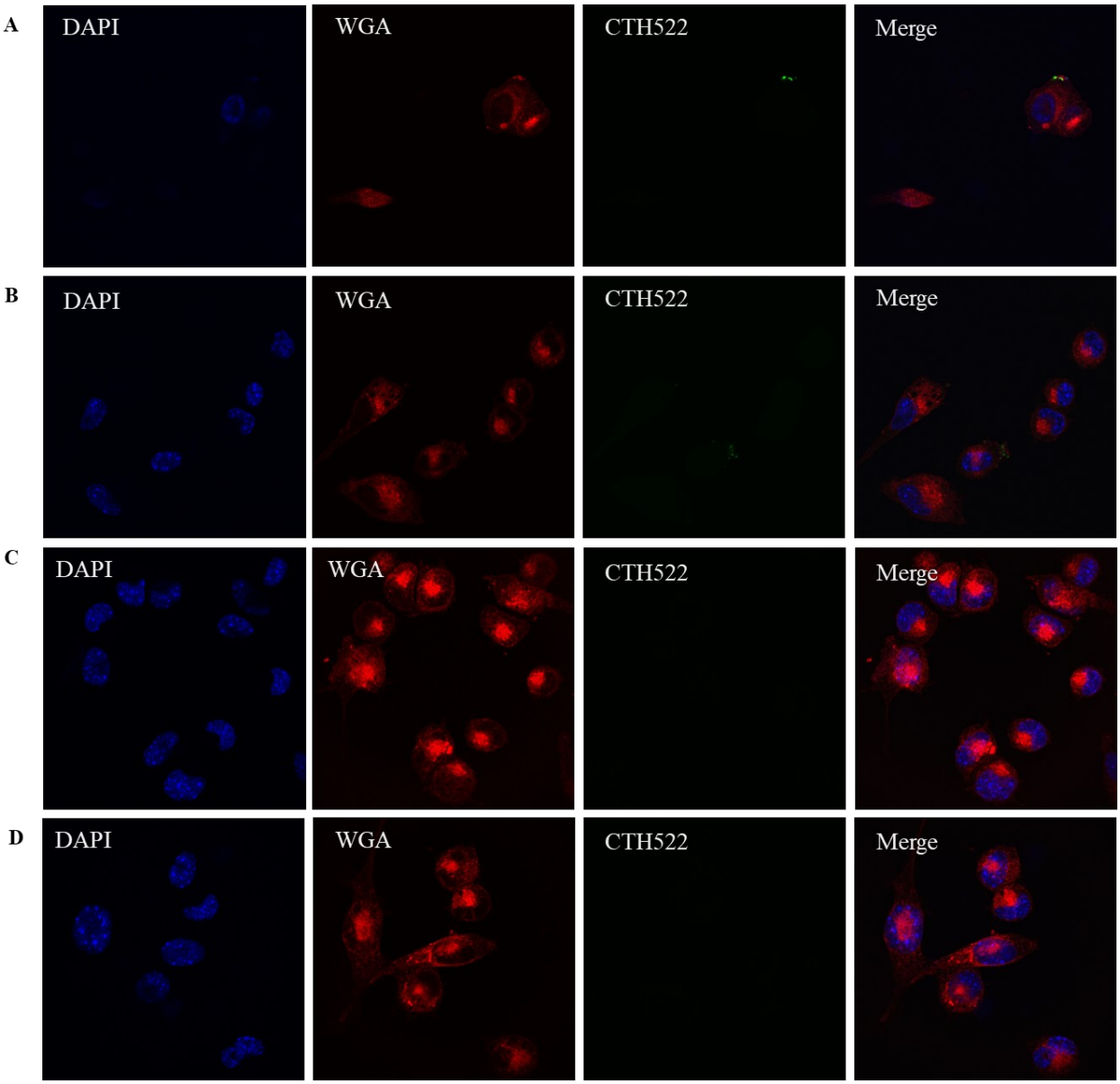

Supplemental Figure 6. Confocal microscopy images show a CTH522 positive signal detected at 0 hpi in cells infected with MVA-CTH522:B7 or MVA-CTH522. Confocal microscopy imaging showing Cloudman cells infected with **A.** MVA-CTH522:B7. **B.** MVA-CTH522. **C.** MVA-WT. **D.** Mock. Cells were fixed at 0 hpi (1 hour after inoculum was placed on cells at room temperature) after an infection at MOI=5 and stained with DAPI for the nucleus and viral factories, WGA for the cell surface, C. trachomatis species-specific MOMP monoclonal antibody and anti-mouse IgG Alexa Fluor 647. Multiple images were taken and results display the best representatives of each group (n = 3)

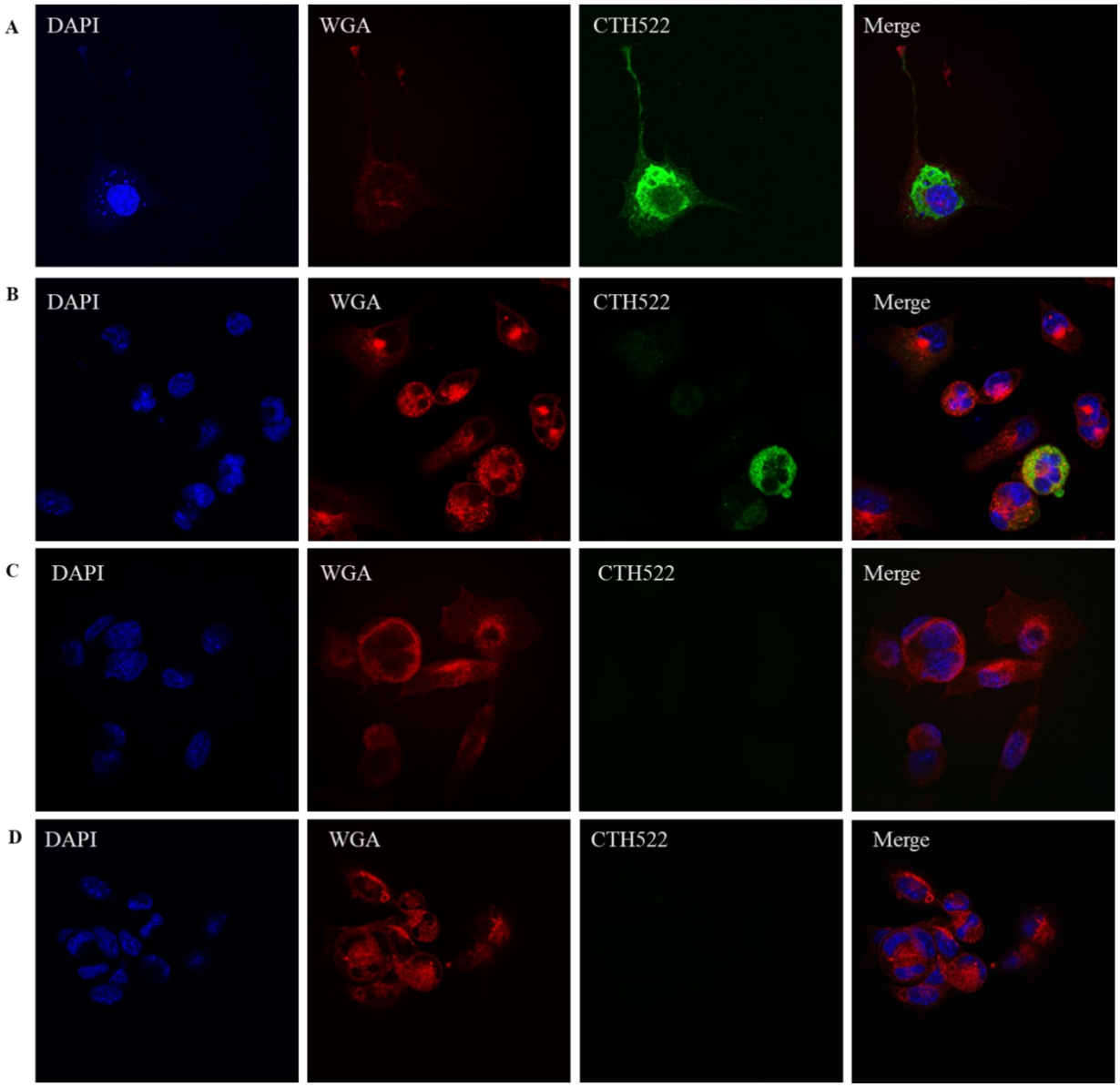

Supplemental Figure 7. Additional confocal microscopy images show CTH522 is found both within the cell and on the cell surface in cells infected with MVA-CTH522:B7 at 8hpi. Confocal microscopy imaging showing Cloudman cells infected with **A.** MVA-CTH522:B7. **B.** MVA-CTH522. **C.** MVA-WT. **D.** Mock. Cells were fixed at 8 hpi after an infection with MOI=5 and stained with DAPI for the nucleus and viral factories, WGA for the cell surface, C. trachomatis species-specific MOMP monoclonal 1st antibody and anti-mouse IgG Alexa Fluor 647 2nd antibody. Multiple images were taken and results display the best representatives of each group (n = 3)

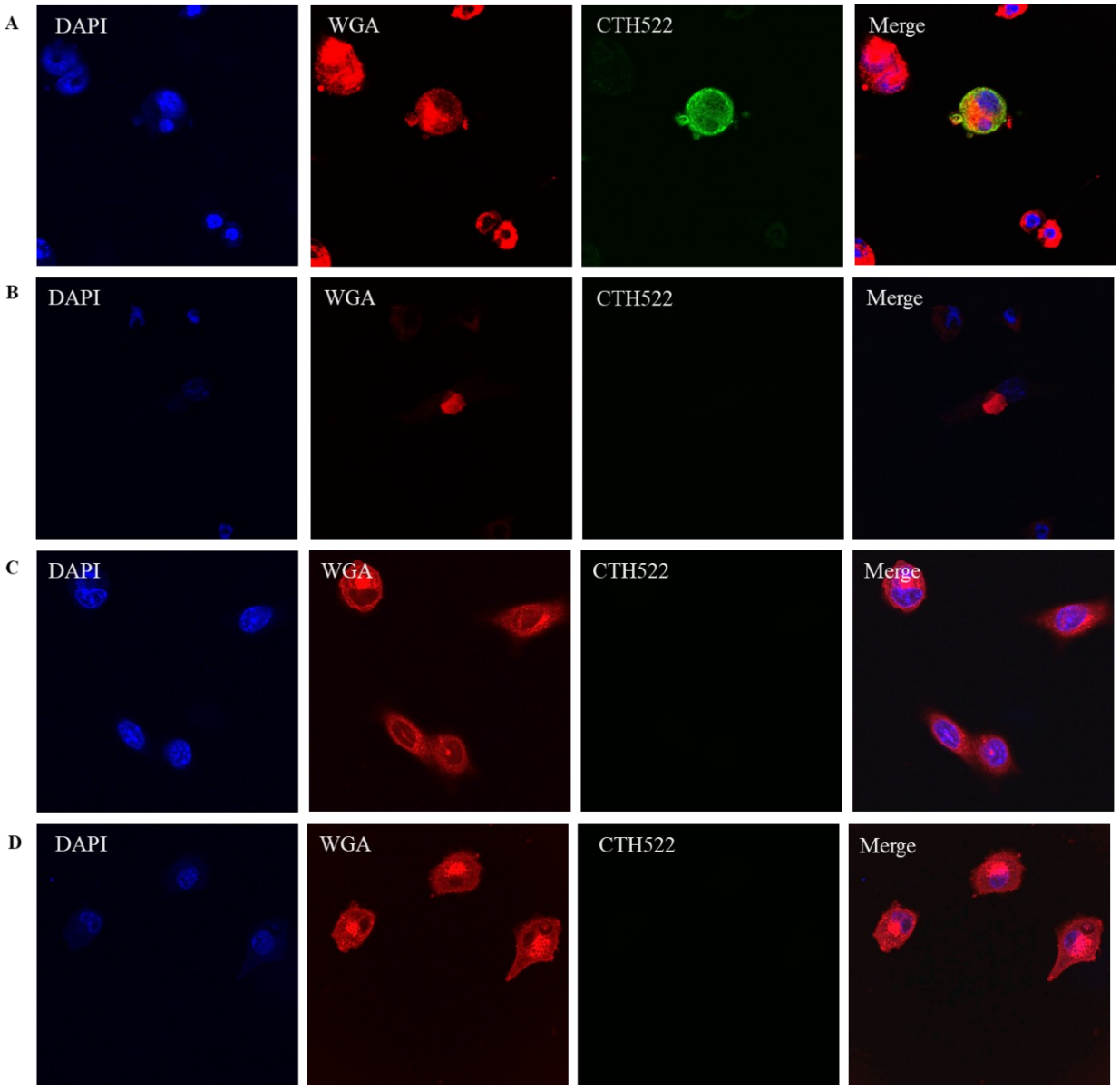

Supplemental Figure 8. Additional confocal microscopy images of CTH522 found on the cell surface of cells infected with MVA-CTH522:B7 at 24hpi. Confocal microscopy imaging showing Cloudman cells infected with **A.** MVA-CTH522:B7. **B.** MVA-CTH522. **C.** MVA-WT. **D.** Mock. Cells were fixed at 24 hpi (1 hour after inoculum was placed on cells at room temperature) after an infection with MOI=5 and stained with DAPI for the nucleus and viral factories, WGA for the cell surface, C. trachomatis species-specific MOMP monoclonal 1st antibody and anti-mouse IgG Alexa Fluor 647 2nd antibody. Multiple images were taken and results display the best representatives of each group (n = 3).

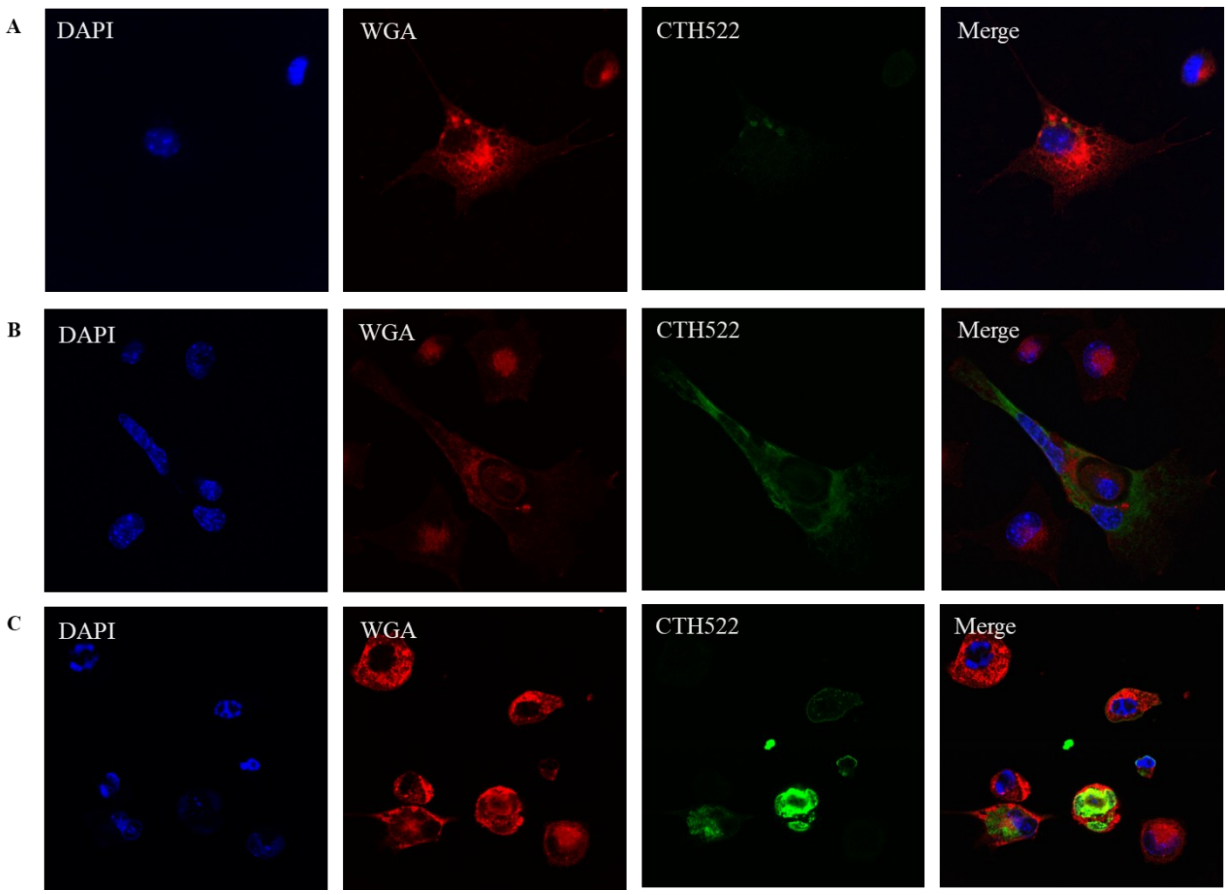

Supplemental Figure 9. Additional confocal microscopy images of CTH522 found within cloudman cells infected with mIi:MVA-CTH522. Confocal microscopy imaging showing Cloudman cells infected with recombinant MVA encoding mouse invariant chain segment fused to the CTH522 antigen and stained at **A.** 0 hours post infection. **B.** 8 hours post infection. **C.** 24 hours post infection. Cells were fixed after an infection at MOI=5 and stained with DAPI for the nucleus and viral factories, WGA for the cell surface, C. trachomatis species-specific MOMP monoclonal 1st antibody and anti-mouse IgG Alexa Fluor 647 2nd antibody. Multiple images were taken and results display the best representatives of each group (n = 3)

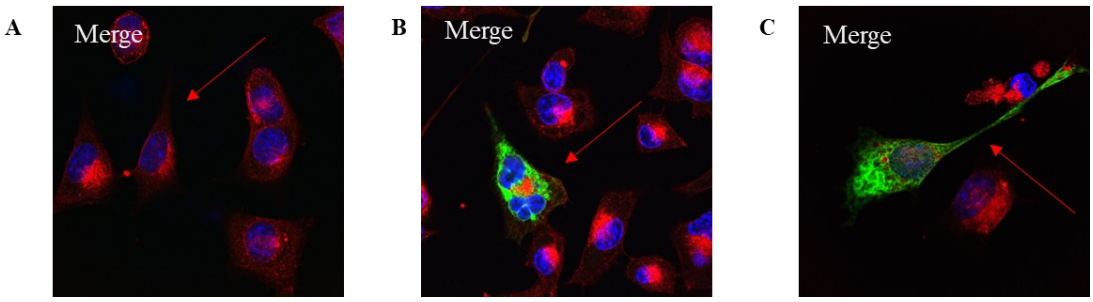

Supplemental Figure 10. Confocal microscopy images of CTH522 in MVA-infected cloudman cells that display filopodia-like structures. Confocal microscopy imaging showing Cloudman cells infected with **A.** recombinant MVA-CTH522:B7 at 24 hours post infection (hpi). **B.** MVA-CTH522 at 8 hpi. **C.** MVA-WT at 8 hpi. Cells were fixed after an infection at MOI=5 and stained with DAPI for the nucleus and viral factories, WGA for the cell surface, C. *trachomatis* species-specific MOMP monoclonal 1st antibody and anti-mouse IgG Alexa Fluor 647 2nd antibody. Multiple images were taken and results display the best representatives of each group (n = 3). Red arrows indicate cells exhibiting the filopodia-like structure.

Allele	#	Start	End	Length	Method used	Peptide	Percentile Rank	Adjusted rank
H2-IAb	1	9	22	14	Consensus (smm/nn)	DTTFAWSVGARAAL	3.30	3.55
H2-IAb	1	10	23	14	Consensus (smm/nn)	TTFAWSVGARAALW	3.40	3.66
H2-IAb	1	10	22	13	Consensus (smm/nn)	TTFAWSVGARAAL	2.45	3.82
H2-IAb	1	8	21	14	Consensus (smm/nn)	TDTTFAWSVGARAA	3.80	4.09
H2-IAb	1	8	22	15	Consensus (smm/nn)	TDTTFAWSVGARAAL	4.10	4.10
H2-IAb	1	9	23	15	Consensus (smm/nn)	DTTFAWSVGARAALW	4.35	4.35
H2-IAb	1	10	24	15	Consensus (smm/nn)	TTFAWSVGARAALWE	4.60	4.60
H2-IAb	1	9	21	13	Consensus (smm/nn)	DTTFAWSVGARAA	3.00	4.68
H2-IAb	1	7	21	15	Consensus (smm/nn)	YTDTTFAWSVGARAA	4.80	4.80
H2-IAb	1	11	24	14	Consensus (smm/nn)	TFAWSVGARAALWE	5.10	5.49
H2-IAb	1	11	23	13	Consensus (smm/nn)	TFAWSVGARAALW	3.60	5.61
H2-IAb	1	10	21	12	Consensus (smm/nn)	TTFAWSVGARAA	1.95	5.78
H2-IAb	1	7	22	16	Consensus (smm/nn)	YTDTTFAWSVGARAAL	5.55	6.41
H2-IAb	1	8	23	16	Consensus (smm/nn)	TDTTFAWSVGARAALW	5.65	6.52
H2-IAb	1	11	25	15	Consensus (smm/nn)	TFAWSVGARAALWEC	6.65	6.65
H2-IAb	1	11	22	12	Consensus (smm/nn)	TFAWSVGARAAL	2.25	6.67

Supplemental Figure 11. MHC-II Binding Prediction Results for peptide #49. The used sequence was peptide 49 (previously referred to as 6-4) with additional amino acids on the N and C terminals (QSVVELYTDTTFAWSVGARAALWECGC). Peptide 49 is shown in a blue square. Low adjusted rank is an indicator of good MHC II binders. More peptides below 3.00 adjusted rank were predicted (data not shown). Prediction method: IEDB recommended 2.22 (https://tools.iedb.org/mhcii/).

Allele	#	Start	End	Length	Method used	Peptide	Percentile Rank	Adjusted rank
H2-IAb	1	4	17	14	Consensus (smm/nn)	IDYHEWQASLALSY	0.98	1.06
H2-IAb	1	4	18	15	Consensus (smm/nn)	IDYHEWQASLALSYR	1.33	1.33
H2-IAb	1	3	17	15	Consensus (smm/nn)	SIDYHEWQASLALSY	1.33	1.33
H2-IAb	1	5	17	13	Consensus (smm/nn)	DYHEWQASLALSY	0.97	1.50
H2-IAb	1	5	18	14	Consensus (smm/nn)	DYHEWQASLALSYR	1.49	1.61
H2-IAb	1	4	16	13	Consensus (smm/nn)	IDYHEWQASLALS	1.09	1.70
H2-IAb	1	3	16	14	Consensus (smm/nn)	SIDYHEWQASLALS	1.65	1.77
H2-IAb	1	5	19	15	Consensus (smm/nn)	DYHEWQASLALSYRL	1.96	1.96
H2-IAb	1	2	16	15	Consensus (smm/nn)	ASIDYHEWQASLALS	2.15	2.15
H2-IAb	1	4	19	16	Consensus (smm/nn)	IDYHEWQASLALSYRL	1.98	2.29
H2-IAb	1	2	15	14	Consensus (smm/nn)	ASIDYHEWQASLAL	2.15	2.32
H2-IAb	1	2	17	16	Consensus (smm/nn)	ASIDYHEWQASLALSY	2.02	2.34
H2-IAb	1	3	15	13	Consensus (smm/nn)	SIDYHEWQASLAL	1.50	2.34
H2-IAb	1	3	18	16	Consensus (smm/nn)	SIDYHEWQASLALSYR	2.02	2.34
H2-IAb	1	6	21	16	Consensus (smm/nn)	YHEWQASLALSYRLNM	2.20	2.54
H2-IAb	1	5	20	16	Consensus (smm/nn)	DYHEWQASLALSYRLN	2.21	2.55
H2-IAb	1	4	15	12	Consensus (smm/nn)	IDYHEWQASLAL	0.93	2.76
H2-IAb	1	1	15	15	Consensus (smm/nn)	DASIDYHEWQASLAL	2.90	2.90

Supplemental Figure 12. MHC-II Binding Prediction Results for peptide #69. The used sequence was peptide 49 (previously referred to as 12-5) with additional amino acids on the N and C terminals (DASIDYHEWQASLALSYRLNMFT). Peptide 69 is shown in a blue square. Low adjusted rank is an indicator of good MHC II binders. Prediction method: IEDB recommended 2.22 (https://tools.iedb.org/mhcii/)

ACKNOWLEDGEMENTS:

This study has been performed at the Institute of Virology in the group of Prof. Dr. Ingo Drexler and it has been supported by the Vacpath Project funded by the European Union's Horizon 2020 research and innovation program under the Marie Skłodowska-Curie grant agreement No 812915.

First of all, I would like to express my gratitude to my supervisor Prof. Dr. Ingo Drexler for giving me the opportunity to be a part of Vacpath and for letting me learn and grow both as a scientist and as a person in his research group. I am also greatly thankful to Prof. Dr. Alice Sijts and her entire team in Utrecht University for giving me such a warm welcome and making me feel part of the team, specially Emmanuele Nolfi, a friend with whom I have shared many adventures inside and outside the lab.

I am incredibly thankful to Noèmi Vago and Cornelia Barnowski for their advice and guidance at the beginning of my project, who took the time to teach me new techniques and show me new concepts while working on their own PhDs. Their patience and readiness to help accompanied me for the time we shared at work, and will do so as I move on to new chapters in my life.

I would like to thank Ylenia Longo, for being an unwavering support throughout my entire PhD and the time after. Every late night, long day and difficult morning was better because of you. I will forever cherish the memories and the time we shared in the lab; the dinners in the kitchen during the early night while it was dark out and we ate every fifteen minutes between infections and staining, the walks to the university campus at sunrise with a cup of coffee at hand talking about BMDCs and FACS, the long weekends in the lab sharing meals and thoughts, and so many more. A special thanks to Giuseppe Andreacchio, who always had an answer to a question and was willing to share and discuss just about any topic. Your help and camaraderie made my way through the PhD lighter and allowed me to overcome the impasses I had to come across, helping me move forward when the obstacles made it hard to do so. Both of you have been a cornerstone of my PhD experience and provided me with such comfort and motivation that you made this project not only possible but enjoyable as well.

A deeply heartfelt thank you to my family and friends, who have always and will always support me. The small windows of time I could travel back to Spain provided me

with a boundless comfort that I can never thank them enough for. I want to specially thank my parents, for their continuous encouragement and belief in every single new endeavor I have taken part in, as well as their endless patience and understanding even at times when I was not at my best. When challenges rose, they rose right along with them, and anchored me down to earth. Gracias.

Gracias mi abuela, ayuda siempre. Amor mucho.

Overall, this thesis and the years I worked in Heinrich-Heine University have been made possible by the collective support of everyone around me, both academically and personally. There are so many people who helped, supported and believed in me and for that I will be forever grateful.

DECLARATION:

I hereby declare that this thesis, submitted for the degree of Doctor of Philosophy (PhD) at the Heinrich-Heine-University Düsseldorf, has been entirely planned, written and produced independently by me without any undue assistance by any third parties and taking into consideration the principles of "Good Scientific Practice". No Artificial Intelligence tools were used in the writing or planning of this dissertation.

Düsseldorf, 17.11.23 Sara Moreno Mascaraque